Hydrogeological assessment for evaluating the feasibility of managed aquifer recharge in Northeastern Ghana

A thesis approved by the Faculty of Environment and Natural Sciences at the Brandenburg University of Technology Cottbus – Senftenberg in partial fulfilment of the requirement for the award of the academic degree of Doctor of Philosophy (PhD) in Environmental Sciences

by

Master of Science

Louis Boansi Okofo

from

Old Tafo, Kumasi – Ghana

Supervisor: Prof. Dr. habil. Marion Martienssen

Supervisor: Prof. Dr. Ralf Merz

Date of oral examination: 07.02.2023

DOI: https://doi.org/10.26127/BTUOpen-6244

Copyright and Ownership

Declaration

I hereby declare that I have never had any permission to the final examination for a doctoral degree cancelled nor I have had a doctoral degree disqualified as a result of an attempt to deceive. I never made any attempt of deceit after entering the International PhD Programme ERM at the BTU Cottbus-Senftenberg.

Louis Boansi Okofo

Dedication

This thesis is dedicated to my parents Mr Martin Asiedu Mensah and Mrs Grace Ocansey, and my good friend Martin Fordjour of blessed memory.

Acknowledgements

I would like to thank my supervisor Prof. Dr. habil. Marion Martienssen, head of Biotechnology and Water Treatment Chair. I am very much grateful to her for offering me the chance to work with her group and for her support throughout my entire PhD work. I appreciate her time and effort, the numerous discussions, and the support of all kinds in making this thesis successful. I am grateful to my second supervisor Prof. Dr Ralf Merz, the head of Catchment Hydrology, UFZ Halle for his time and help.

My sincere gratitude goes to the German Academic Exchange Service (DAAD) for awarding me a scholarship, which has helped me to pursue this program at the Brandenburg University of Technology in Cottbus. Without this support, the study would have not been possible. I would like to thank the Graduate Research School in BTU Cottbus for the travel grant given to present some of the thesis findings at the ISMAR Conference in Long Beach, California, USA.

I would like to extend my greetings to Dr Birte Seffert, the former PhD coordinator for her immense help and guidance throughout my PhD work. Special thanks go to Dr Stella Gypser, the current coordinator of the ERM PhD programme for her guidance throughout the submission and defense of my PhD thesis.

Special thanks go to Dr Tino Rödiger at the Department of Catchment Hydrology, UFZ Halle, Germany, for the introduction to groundwater modelling. I am grateful to Dr Melvin-Guy Adonadaga for his unflinching support given for my PhD work. My sincere thanks go to Mr Solomon Affi and Emmanuel Nkrumah at Cardinal Resources, Bolgatanga for their assistance given during data collection in Ghana. I am grateful to Mr Evans, head of the water quality lab at Ghana Water Company Limited, Bolgatanga for providing me with the Hach digital titrator for my fieldwork. The same appreciation goes to Mr Anderson Nana Akyerefi of Bauer Ghana Limited for providing me with the Multi-Probe Meter to carry out my fieldwork.

Mrs Zahra Neumann, Mrs Stefanie Schmidt and Mrs Claudia Cosma thank you very much for the technical assistance during the preparation and laboratory analysis of hydrochemical and isotopic water samples at the Institute of Geoscience, Technical University of Darmstadt, Germany. I am also grateful to Professor Dr Christoph Schüth and AOR Dr Thomas Schiedek for allowing me to analyse my samples at the hydrogeochemistry laboratory, TU Darmstadt.

I would like to thank Frau Dr Ing. Ramona Kuhn for her occasional advice and inspiration given to me and also for translating my summary into German Version.

I thank Herr Dr Joerg Boellmann for taking me through the laboratory procedure at BTU Cottbus. I am grateful to Frau Perch and Frau Krahl for the technical support given during my tracer gas analysis at the Biotechnology Laboratory, BTU Cottbus. I am thankful to Herr Erwin Banscher and Dip. Ing Ralf Regel for the continuous help given to me anytime I had a challenge with my computer and GMS software.

I wish to express my profound gratitude to Dr Millicent Addai of University Education Winneba, Ghana for her guidance in my groundwater modelling work. I also thank Mr Musah Saeed Zango for his guidance and inspiration provided throughout my PhD work. Special thanks go to Mrs Afrakoma Ekua at CSIR Industrial Research, Accra and Mr Joseph Ayer at CWSA, Accra and Mr Nat Antwi of BioAgilytix Europe Gmbh, Hamburg for their input on my PhD thesis. I am grateful to my former office colleagues Dr Bryant Isaac and Dr Samuel Dido for the numerous discussions we held together and for not forgetting Abdul Rahaman Afitiri.

Kind help and support were obtained from my Ghanaian PhD colleagues in Cottbus (Kenneth Bernard Frimpong, Fredrick Gyasi, Samuel Osei, Bernard Effah, Ampadu, Martha and Valentina) with whom I shared many research experiences, joys, and suffering during the periods of our PhD works. The journey was ups and downs but we managed to complete it. Special thanks go to Kobby, Abeiku, Adoma Kwadwo, Joe, Julia, Reggae, Daniella, Fiona, Linda, Pearl, Phillip and Ferdinand and Pique) for their warm friendship in Cottbus and Akua Ampem Of Rhine-Waal University and her husband Desmond, Evans Manu of GFZ Potsdam, Kennedy Owusu of Phillips-University Marburg and Kwaku Boadi of Hamburg.

Finally, I thank my siblings Charles, Matilda, Mavis, Joe, Anas, Ama and Afia for their motivations and cover my back for the past years.

Abstract

In the Garu-Tempane area and Tamne River basin of north-eastern Ghana, granitic aquifers supply nearly 80% of annually abstracted groundwater. Rapid and diffuse recharge enters the fractured and weathered Tamnean Plutonic Suite aquifers mainly granitoid, which are the dominant rock types in the study area. However, a greater challenge to the water supply in the area is posed by global climatic changes and overexploitation due to population growth. The semi-arid nature of the area together with the factors mentioned earlier has caused water scarcity, particularly in the dry season and these have affected the livelihoods of the farmers who depend mostly on the groundwater for irrigation and domestic purposes. A promising way to balance water resources in the region is using engineering technology such as managed aquifer recharge (MAR). MAR augments water levels in water-scarce areas and represents a key tool in water supply management.

For this reason, a comprehensive hydrogeological characterization involving the hydrochemistry of the groundwater, groundwater recharge process and residence time using multi-environmental tracers, and a numerical groundwater flow model was developed.

Based on the hydrochemistry results, the water quality index showed that the groundwater is very suitable for drinking. However, about 10.5 % out of the 38 groundwater samples had elevated nitrate concentrations exceeding the permissible WHO drinking water limit. These are mainly agricultural areas, which might have influenced the elevated nitrate concentrations.

Groundwater age dating using sulphur hexafluoride (SF6) and chlorofluorocarbons (CFCs) was used to date shallow groundwater in Ghana for the first time. The results proved that the mean residence time of groundwater was around 30 years, an indication of young groundwater and rapid groundwater renewability. The findings also showed different groundwater ages implying diffused flow systems occurring in the fractured granitic aquifer.

Investigation of the groundwater recharge using stable isotopes of deuterium and oxygen-18 revealed that the main source of groundwater recharge is of meteoric origin. There were little or no contributions from the stream and ponds as they were subjected to evaporative fractionation during the dry season. The White Volta River samples and samples from two big rivers were depleted in heavy isotopes, which suggested a hydraulic connection between them and the groundwater.

The numerical groundwater flow model was used to assess the feasibility of MAR and determine the maximum recharge and abstraction rates. The results showed that the aquifer had enough storage to accommodate enough volumes of floodwater without causing

groundwater mounding. This shows that MAR is feasible in augmenting the water levels in the area when irrigation and domestic withdrawals are regulated.

Keywords: Northeastern Ghana, Managed aquifer recharge, SF6, CFCs, Numerical modelling, Water chemistry, Garu-Tempane, Tamne River basin, Hydrogeology

Zusammenfassung

Im Garu-Tempane-Gebiet und im Tamne River basin im Nordosten Ghanas liefern Granitgrundwasserleiter fast 80 % des jährlich aufkommenden Grundwassers. In beiden Gebieten tritt eine schnelle und diffuse Wiederanreicherung des Grundwasserleiters vor allem durch Granitoide als dominierende Gesteinstypen auf. Eine große Herausforderung für die Wasserversorgung in der Region stellen globale klimatische Veränderungen und die Übernutzung des Grundwasserleiters durch das aktuelle Bevölkerungswachstum dar. Hinzu kommt die charakteristische Trockenheit des Gebiets, die die Wasserknappheit insbesondere in der Trockenzeit immens verstärken. Dies beeinträchtigt wiederum erheblich die Lebensgrundlage der Bauern, die für Bewässerungs- und Haushaltszwecke hauptsächlich vom Grundwasser abhängig sind. Alternativen für die regionale Wasserversorgung wie Oberflächengewässer trocknen in der Trockenzeit in aller Regel schnell aus und stehen somit nicht zur Verfügung. Aus diesem Grund wurde für die ausgewählte Region eine umfassende hydrogeologische Charakterisierung unter Einbeziehung der Hydrochemie des Grundwassers, des Grundwasserneubildungsprozesses und der Verweilzeit unter Verwendung von „Multi-Umwelttracern“ sowie ein numerisches Grundwasserströmungsmodell entwickelt.

Basierend auf den Daten der Hydrochemie zeigt der sogenannte Wasserqualitätsindex, dass das Grundwasser sehr gut zum Trinken geeignet ist. Allerdings weisen etwa 10,5 % der Grundwassersproben aus insgesamt 38 Messstellen erhöhte Nitratkonzentrationen auf, die den zulässigen WHO-Trinkwassergrenzwert überschreiten. Die erhöhten Nitratwerte werden hauptsächlich durch Landwirtschaft verursacht.

Die Datierung des Grundwasseralters mit Multi-Umwelt-Tracers (SF6, FCKW) wurde erstmals von flachem Grundwasser in Ghana verwendet. Die Ergebnisse belegen, dass die Durchschnittsverweildauer des Grundwassers bei etwa 30 Jahren liegen. Dies ist ein Hinweis auf junges Grundwasser, d.h. der Grundwasserleiter kann „zügig“ mit Grundwasser angereichert werden. Die Ergebnisse zeigen auch unterschiedliche Grundwasseralter, was auf diffuse Strömungssysteme hindeutet, die im zerklüfteten Granitaquifer vorkommen.

Die Untersuchung der Grundwasserneubildung mit stabilen Isotopen von Deuterium und Sauerstoff-18 zeigt, dass die Hauptquelle der Grundwasserneubildung meteorischen Ursprungs ist. Es gab nur geringe oder keine Wassereinträge aus den kleineren Oberflächengewässer da keine Isotopen aus diesen Quellen im Grundwasser nachweisbar waren. Der Grund dafür liegt im Austrocknen dieser Gewässer während der Trockenzeit. Aus den größeren Oberflächengewässern wie dem White Volta River konnten hingegen schweren Isotopen im Grundwasser nachgewiesen werden, was wiederum ein Hinweis auf eine hydraulische Verbindung zwischen ihnen ist.

Das numerische Grundwasserströmungsmodell wurde verwendet, um die Machbarkeit von MAR zu bewerten und die maximalen Neubildungs- und Entnahmeraten zu bestimmen. Die Ergebnisse zeigen, dass der Aquifer über genügend Stauraum verfügt, um genügend Hochwassermengen aufzunehmen ohne Grundwasseranhäufungen zu verursachen. MAR ist somit realisierbar, um die Wasserstände in dem Gebiet zu erhöhen, wenn Bewässerung und häusliche Entnahmen reguliert werden.

Keywords: Nordosten Ghana, Schwefelhexafluorid (SF6), Fluorchlorkohlenwasserstoffen (FCKW), Garu-Tempane, Tamne River basin, Grundwasserströmungsmodell, Hydrochemie, Hydrogologie

Table of Contents

List of Figures

List of Tables

List of abbreviations

MAR = Managed aquifer recharge

SF6 = Sulphur hexafluoride

CFCs = Chlorofluorocarbons

HCFC = Hydrochlorofluorocarbons

WQI = Water Quality Index

CMB = Chloride mass balance

MARSOL = Manged aquifer recharge solutions

BC = Boundary Conditions

CWSA = Community Water and Sanitation Agency

WRC = Water Resources Commission

SVD = Single value decomposition

GMS = Groundwater modelling system

RMSE = Root mean square error

CSIR = Council of Scientific & Industrial Research

EC = Electrical conductivity

PPT = Parts Per Trillion

GMWL = Global Meteoric Water Line

VSMOW = Vienna Standard Mean Ocean Water

LMWL = Local Meteoric Water Line

ECD = Electron capture detector

GC = Gas Chromatography

MFC = Mass flow meter

FID = Flame ionization detector

IAEA = Internation Atomic Energy Agency

NAOO = National Oceanic and Atmospheric Administration

LPM = Lumped parameter model

PFM = Piston floe model

EMM = Exponential mixing model

BMM = Binary mixing model

GHB = General Head Boundary

LPF = Layer Property Flow

TDS= Total dissolved solids

PCA = Principal component analysis

HCA = Hierarchical cluster analysis

WHO = World Health Organization

CAI = Chloro alkaline indices

SI = Saturation indices

IGRAC = International Groundwater Resources Assessment Center

GWCL= Ghana water Company Limited

Meg/L = Milli equivalence per liter

NGO = Non-Governmental Organization

GIS = Geographic Information system

SICalib = Stable Isotopes Calibration

CHAPTER 1

Introduction

1.0 Background

In many regions of the world where surface waters are limited, groundwater has been the reliable and alternative water source to meet domestic, industrial, and agricultural needs (Ebrahim et al., 2016). Groundwater is used to support the well-being of humans and the social development of many countries (Jasechko et al., 2014). For instance, in Saudi Arabia, groundwater has contributed to about 80 % of the country´s water supply needs (Mallick et al., 2021). Groundwater use in Africa is mainly for drinking water purposes, and irrigation to combat the increasing food insecurity. The groundwater volume in Africa is estimated at around 0.66 million km^3 square, which exceeds the yearly freshwater renewability by 100 times (MacDonald et al., 2012). However, the availability and quantity of groundwater resources are depleting at a faster rate due to increasing water demand from the ever-growing population and the pronounced global climate changes. In the same way, the impacts of human activities have deteriorated groundwater quality leading to contamination problems at a local and regional scale (Zango et al., 2021). A typical example of groundwater depletion is an episodic decrease in the high plains and central valley aquifers of California, which is restricted largely to droughts and overexploitation. This has accounted for about 50% of groundwater reductions in the United States of America and presents an unequal distribution of water resources (Scanlon et al., 2012).

A promising way to balance groundwater resources in a catchment is through the application of an emerging technology known as managed aquifer recharge (MAR) (Dillon, 2005). This involves, collecting water when there is a surplus during the rainy season, infiltrating it into the aquifers as a means of storage, and later recovering this water for use during the dry season when demand is high. Different structures such as rainwater harvesting, riverbank infiltration recharge wells, infiltration basins, and subsurface dams are widely used to address MAR technologies (Fig.1). The successful application of MAR depends on a complete understanding of the hydrogeological site conditions such as land availability, water quality, aquifer types, and storage capacity (Dillon et al., 2019; Gale, 2005). Water types ranging from wastewater, floodwater, rainwater, surface water, and other groundwater are used as a source of water for the MAR. These waters contain high concentrations of suspended solids and excessive algal growth from organic matter that can accelerate and cause clogging of the wells (Dillon et al., 2009). Therefore, the injected water is usually analysed and pre-treated before use.

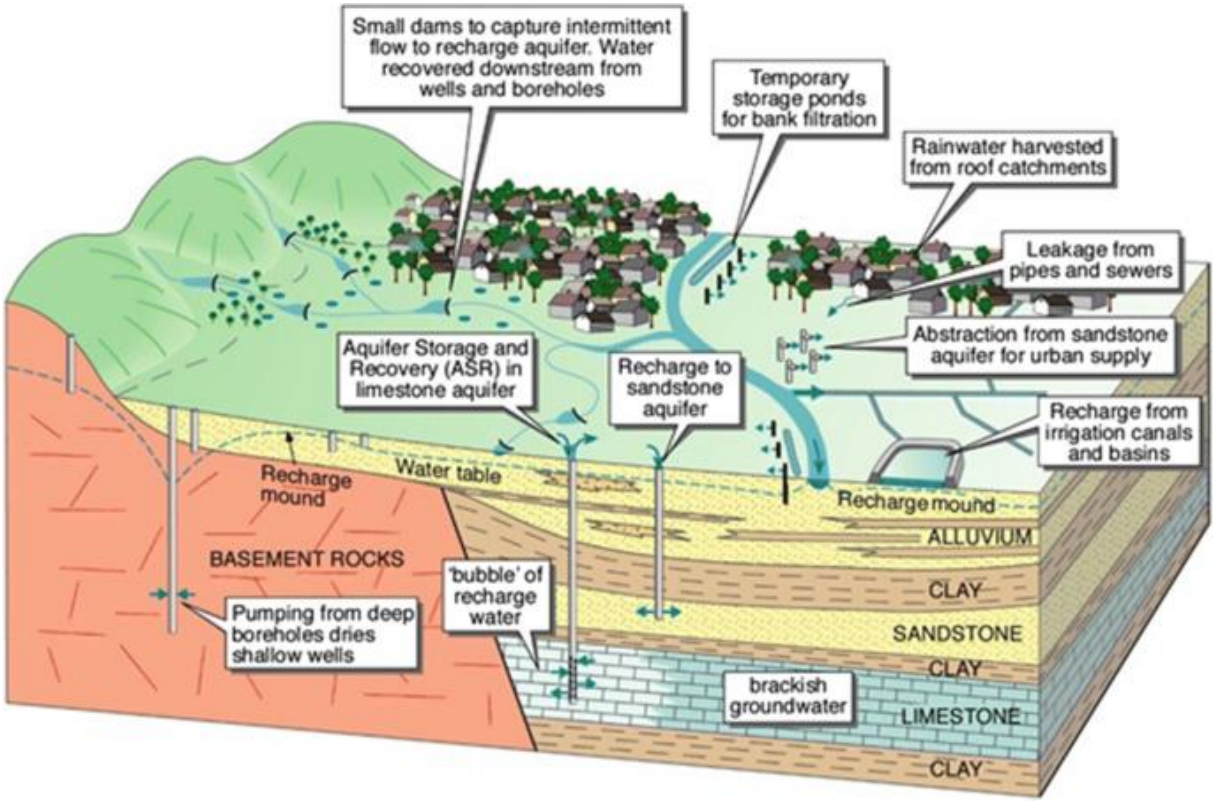

Fig. 1 *Different structures and water types are used to address MAR technologies. Source: (Dillon et al., 2019; Gale, 2005)*

Similarly, the native groundwater may contain elevated nitrate, arsenic concentrations, and salinity problems, which pose threats to humankind. These factors may limit the effort in accomplishing the United Nations Sustainable Development goal 6 (ensuring clean water). For this, hydrochemical studies are usually investigated to determine the water types, major ions, and trace metals of the groundwater. In addition, isotopic studies are needed to determine the recharge rates and sources of groundwater recharge. The recharge rate will help to establish the water balance component in the catchment and plan for effective MAR implementation. Since storage is an important component of any MAR system, groundwater age dating is a very useful tool to determine how long the water has resided in an aquifer. Knowledge of groundwater dating helps in understanding the groundwater mixing dynamics, storage within the aquifer, and renewability rate (IAEA, 2006). Furthermore, numerical groundwater flow models (MODFLOW) are extensively used in conjunction with optimization tools to design, optimize and plan MAR systems (Bekele et al., 2011; Lacher et al., 2014). They are also used to evaluate the feasibility of MAR by testing different injection and abstraction scenarios (Ebrahim et al., 2016).

In northern Ghana, groundwater is the main source of water supply for the inhabitants. There are documented cases of declining groundwater levels and this has caused water scarcity, especially during the dry season-irrigation farming (Ghana Statistical Service, 2013). To

properly manage this situation, it is essential to have detailed MAR and hydrogeologic studies to augment aquifer storage and declining water levels.

1.1 Problem statement

Groundwater is an essential resource used to meet the demands of agricultural food production and drinking water supplies in arid and semi-arid regions (Dennehy et al., 2015a). However, the excessive utilization of groundwater for irrigation has given rise to a drastic decrease in aquifer volume. This, in turn, has caused the drying of farmlands with the consequence that irrigation wells have to be deepened and the cost of abstracting water has become expensive. In addition, human endeavours over the past years have caused unparalleled groundwater overdrafts (Dillon et al., 2019).

The Garu-Tempane area is a typical case study of groundwater overdraft due to the extreme irrigation practices, high evapotranspiration, and low erratic rainfall. The hydrogeological catchment is a sub-basin of the White Volta River basin of Ghana. As high as 95 % of households are engaged in livestock production and farming, which is highly focused on onion cultivation, watermelons, and tomatoes (Ghana statistical service, 2010). This serves as the main income for the people. The main sources of water used for agricultural irrigation are rainwater, boreholes, hand-dug wells, and surface waters, especially from Bugri and Gagbiri dams. The catchment experiences only one short rainy season between May and September and is accompanied by a long dry season (Asamoah & Ansah-Mensah, 2020; Issahaku et al., 2016). Due to this, the hand-dug wells quickly dry out during the dry season, and the rainfall reaching the catchment experiences evaporation. These factors have contributed to low groundwater recharge and water scarcity during the dry season-irrigation farming.

In response to these unfavourable climatic conditions, the Bugri and Gagbiri dams were designed purposely to provide alternative water supply during the dry season irrigation-farming. However, challenges such as inadequate water to fill the dam, high evaporation losses, high water demand for irrigation, and broken and choked canals have rendered the irrigation scheme ineffective (Jonah & Dawda, 2014a). For better management of groundwater resources and sustainable agricultural livelihoods, the area represents a typical case study to explore the opportunities of MAR using alternative waters. While it is evident that many MAR studies have been done across the globe, very few MAR sites can be found in Africa. In Ghana, MAR technology is currently gaining attention and emerging MAR schemes can be found in Northern Ghana (Conservative Alliance, 2015). Other studies are related to the institutional feasibility of MAR (Kwoyiga & Stefan, 2019) and the GIS land feasibility of MAR (Owusu et al., 2017). No detailed hydrogeological investigations have been done to assess the feasibility of MAR in Ghana. To address the research paucity in the area, the study seeks to

assess the feasibility of MAR and to provide avenues for all-year-round water for irrigation and domestic purposes.

1.2 Research aim

The main aim of the study is to conduct hydrogeological investigations to assess the feasibility of MAR in northeastern Ghana. Some of the specific objectives set are as follows:

1. To determine the hydrochemical facies and pollution sources of the groundwater.
2. To examine the residence times and recharge processes of the groundwater using multi-environmental tracers such as sulphur hexafluoride (SF6), chlorofluorocarbon (CFCs) and stable isotopes of oxygen-18 and deuterium.
3. To develop a 3D numerical groundwater flow model and obtain relevant information on the maximum recharge and abstraction rate.

To achieve the above-mentioned objectives would be sought for the following questions.

a. Is the groundwater suitable for drinking and irrigation purposes?
b. What are the sources of groundwater recharge and how long does the water reside in the aquifer?
c. Will the aquifer receive and store the infiltrated water or is there enough source of water for the MAR scheme in the area?

1.3 Dissertation structure

The structure of the thesis is arranged into six chapters. Repetitions of the description of the study area, geology, hydrogeology, and soil types occur in some of the chapters. A brief introduction of the chapters is as follows:

Chapter 1 begins with the research background, problem statement, study objectives, and research questions.

Chapter 2 consists of a comprehensive literature review detailing the state-of-art information regarding managed aquifer recharge in Europe, Asia, and Africa. It addresses the European MAR catalogue along with some case studies. The different MAR types and sources of water are also discussed. Additionally, knowledge gaps were identified and addressed.

Chapter 3 describes the study area and some physical features such as the vegetation cover and soil types. The groundwater sampling methods, laboratory analysis as well as the various instruments used are described in detail.

Chapter 4 describes the hydrochemistry and pollution patterns of the groundwater. Here, multivariate statistics and conventional graphical methods explain the factors affecting groundwater chemistry and the natural baseline chemistry of water. The water quality index (WQI) and Wilcox diagram are presented to elucidate the suitability of the groundwater for drinking water and irrigation purposes.

Chapter 5 presents groundwater age dating using SF6 and CFCs and the groundwater residence time of the aquifer. It also discusses the recharge patterns of the area using $\delta^{18}O$ and δD. The chloride mass balance is presented to determine the recharge rate. Numerical groundwater flow was developed to simulate flow under steady-state conditions and provide key aquifer properties such as hydraulic conductivity, and recharge rates.

Chapter 6 presents a 3D numerical groundwater model to evaluate the feasibility of MAR in the Tamne River basin. This area was selected because of the historical water levels for transient simulation. The Tamne River basin covers Garu-Tempane areas and some parts of Bawku Municipality. MAR scenarios are presented to obtain information on the aquifer response of the injection and abstraction.

Chapter 7 synthesises all the results discussed in the various chapters. Conclusions are presented as well as recommendations for future research. Chapters 4, 5, and 6 have been published in peer-reviewed journals.

CHAPTER 2

Managed aquifer recharge – A review

2.1 General Overview

Water scarcity in the world; caused by global climatic changes and increasing population; has posed a serious threat to freshwater resources. Due to this, there is always a deficit of water resources on an annual basis on a catchment scale. The fluctuations of water resources are imperative for decision-makers in the water sector to enhance and provide available and quality water to the people in water-scarce areas. As a response, managed aquifer recharge (MAR) has become a unique technique for collecting and storing water in aquifers during availability and later using it when there is a scarcity (IGRAC, 2007; Maliva and Missimer, 2012).

To date, many international water researchers, and national and local organizations have used MAR techniques to augment the supply of groundwater water in the world, especially in drought-prone areas (Gale, 2005a). In such areas, where there has been a prolonged drought due to the shortage of rainfall and high evaporation, managed aquifer recharge techniques have provided an alternative means to address the predicted water shortages over the long period. Apart from increasing the volume of water in aquifer systems, MAR applications can play a vital role in combating seawater intrusions into coastal aquifers, reducing poverty, increasing economic returns, and increasing agricultural yield from available water for irrigation (Gale, 2005a).

Several publications and books have discussed MAR techniques and their contributions to improving water availability in various regions of the world. Managed Aquifer Recharge – An introduction (Dillon et al., 2009); documented that MAR has significantly improved irrigation water supply (45GL/yr) and urban water supply in Australia (75GL/yr) in the year 2008. The publication also presented the new Australia MAR guidelines that tackle hazards exposed to the environment and the health of humankind. Another book titled “Strategies for managed aquifer recharge (MAR) in semi-arid – UNESCO’s International Hydrological Programme” (IHP) edited by (Gale, 2005a), outlines various MAR schemes used in the different semi-arid terrains. IGRAC (2007) documented several other case studies from various regions using different methods: watershed management in Rajasthan, India; aquifer recharge using a spreading system in Kaftari, Iran; inter-dune recharge in Atlantis, South Africa; sub-surface water storage in Kenya and recharging fractured quartzites in Windhoek, Namibia. Recently, a special issue “Managed Aquifer Recharge for Water Resilience” which comprises about 23 selected papers from the 10th International Symposium on Managed Aquifer Recharge (ISMAR) done in Madrid 2019 has been published in the MDPI water journal. The papers

address the scientific advancement of different MAR schemes, their relevance, and constraints across the globe (Dillon et al., 2020).

In Europe, Sprenger et al. (2017) compiled an inventory of managed aquifer recharge sites and the various MAR applications and types. The catalogue consists of 224 active MAR sites presently found in 23 European countries. In this catalogue, Germany has 64 active MAR sites; followed by the Netherlands (41), France (21); Sweden (11), Switzerland (10); Spain (10), and the rest are in different countries that have fewer MAR sites less than 10. The most common MAR methods used are induced bank infiltration (n=127); the second most widespread MAR method is the surface spreading method (n=77), and the third is the well injection method. All these data are incorporated into the Global MAR Inventory portal, which is constantly being compiled by the “International Groundwater Resources Assessment Centre” (IGRAC) in the Netherlands and a team of researchers from TU Dresden (INOWAS), Germany. The Inventory contains the different MAR schemes across the globe under varying hydrogeological and climatic conditions. This could prove vital in the planning and establishing MAR projects for irrigation water supplies, water security, and improvement of water quality in semi-arid areas such as Northern Ghana.

2.2 Definitions and Concepts of Managed Aquifer Recharge

Managed aquifer recharge can be defined as the deliberate recharge of aquifers with water sources that would otherwise be wasted. It is also the process of infiltrating water into the ground to be stored in the underlying aquifers for later abstraction or environmental benefits (Dillon et al., 2009). According to Dillon (2005), MAR is the ‘‘intentional banking and treatment of aquifer waters.’’ The term has been a substitute for the previously used term “artificial recharge” because of the connotations that community participation in water use has become common and unnatural (Dillon, 2005; Maliva and Missimer, 2012).

The basic concept of MAR is simply collecting water when there is too much, treating it, storing it in drinking water aquifers, and later using it when demands are high (dry season. The subsurface storage where influent water flows depends on natural attenuation processes such as sorption and biodegradation (Sprenger et al., 2017). As future water security is under constant threat due to climate change and increasing urbanization, surface storage dams have been used to store water in different places around the world in water-scarce terrains. However, surface water dams offer several disadvantages such as high evaporation losses, displacement of people due to the large surface area needed, structural failures, and increasing contamination (Bouwer, 2002; Maliva and Missimer, 2012). Managed aquifer recharge over the past decades, has been an alternative means to store water underground, primarily to augment the storage of aquifers. It has provided a seasonal water balance in areas

having declining water yields. The MAR technique, if utilized and managed well, can offer advantages such as: meeting industrial and agricultural water supply demands, reduced poverty and risk; increased economic returns, improved water quality; reduced vulnerability to droughts, and emergency plans to augment the natural volume in aquifers (Gale, 2005a). Other advantages also include a barrier to combat saline intrusions in overexploited aquifers, sustaining environmental flows, and phreatophyte vegetation in stressed surface water or groundwater systems (Dillon et al., 2014).

In general, managed aquifer recharge provides two main end-member types of technologies namely: the temporal water storage method and the water treatment method (Dillon, 2005). MAR water sources such as wastewater and saline water are treated for “aquifer recharge and recovery” (ARR) — the term describing recharging in local and regional aquifers for later recovery and use (Maliva and Missimer, 2012).

Augmenting the natural rate of groundwater recharge using MAR techniques in rural and urban areas should address the source and quality of water, aquifer storage space, demand, economics, and monitoring in pre-feasibility studies (Steinel, 2012). In urban areas, where a considerable amount of run-off is generated, harvesting structures such as infiltration and storm-water retention ponds, porous pavements, and grassed areas are recommended in the planning and optimization of any MAR watershed areas (Murray and Tredoux, 1998). Stormwater runoff containing a mixture of highly variable contaminants from areas such as animal waste sites, industrial areas, construction sites, and seepage tank leakages, is thus directed for treatment before recharging it into the groundwater systems (Gale, 2005a). Poor water quality sources can deteriorate existing groundwater, and clog a recharge basin, or well. The treatment of most urban stormwaters used to recharge brackish limestone aquifers is a passive treatment method — water is treated and passed through a granular activated carbon tank and consequently filtered using microfiltration means (Dillon et al., 2009).

2.3 Classification of MAR techniques

Several MAR techniques have been described in the literature and are classified depending on their purposes (Gale, 2005a; IGRAC, 2007; Maliva and Missimer, 2012). Depending on the local conditions, a wide range of MAR techniques is designed with the basic aim of enhancing the recharge (Gale, 2005a). Usually, five main techniques and fourteen sub-types are distinguished based on the classification system of the International Groundwater Resources Assessment Centre as shown in Table 1. The five main techniques are spreading methods, in-channel modifications, induced bank infiltration, runoff harvesting, and well-shaft and borehole recharge (Gale, 2005a). These MAR techniques are selected in relation to getting water

infiltrated, or used to intercept the water. The subtypes, on the other hand, are engineering techniques that are applied to the main methods (IGRAC, 2007). The different MAR techniques are illustrated in (Fig 2.1).

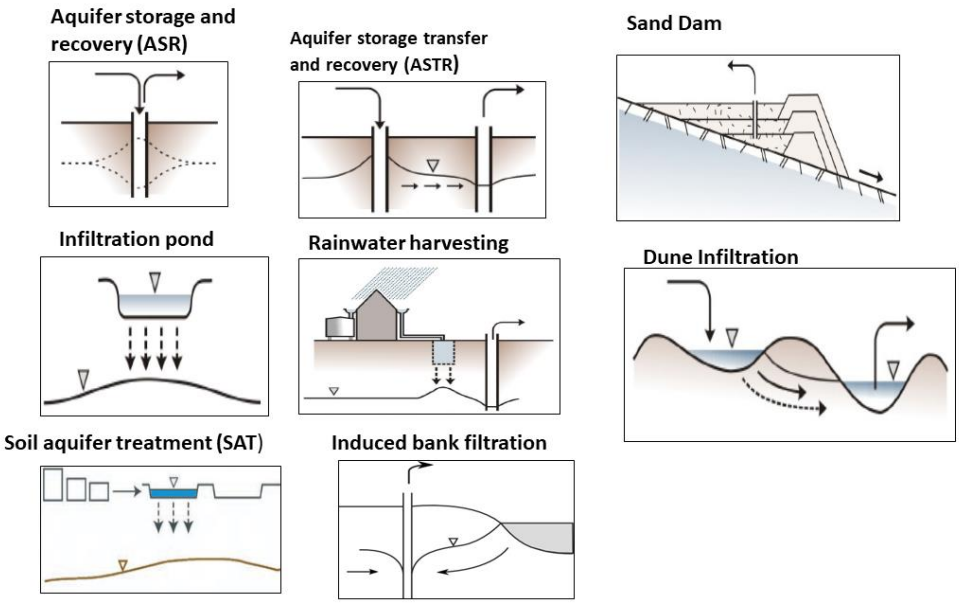

Fig.2.1 *Illustrations showing the different MAR types after Gale, (2005a)*

Table 2.1 Overview of MAR techniques and sub-techniques (IGRAC, 2007)

<table>
<tr><th></th><th>Technology</th><th colspan="2">Subtypes</th></tr>
<tr><td rowspan="6">Techniques referring primarily to getting water infiltrated</td><td rowspan="4">Spreading methods</td><td colspan="2">Infiltration ponds & basins</td></tr>
<tr><td colspan="2">flooding</td></tr>
<tr><td colspan="2">Ditch, furrow, drains</td></tr>
<tr><td colspan="2">Irrigation, Soil Aquifer treatment</td></tr>
<tr><td colspan="3">Induced bank infiltration</td></tr>
<tr><td rowspan="3">Well, Shaft and borehole recharge</td><td rowspan="2">Deep well injection</td><td>Aquifer storage (Transfer & recovery) AS(TR)</td></tr>
<tr><td>ASR (Aquifer storage recovery)</td></tr>
<tr><td colspan="2">Shallow well/shaft/pit infiltration</td></tr>
<tr><td rowspan="5">Techniques referring primarily to intercepting the water</td><td rowspan="4">In-Channel modifications</td><td colspan="2">Recharge dams</td></tr>
<tr><td colspan="2">Sub-surface Dams</td></tr>
<tr><td colspan="2">Sand Dams</td></tr>
<tr><td colspan="2">Channel spreading</td></tr>
<tr><td rowspan="2">Runoff and Rainwater Harvesting</td><td colspan="2">Barriers and bunds</td></tr>
<tr><td colspan="2">trenches</td></tr>
</table>

2.3.1 Spreading method

The spreading method is a low-tech, cost-efficient, and widely used MAR technique (Steinel, 2012). This method is mostly applied in areas where there are unconfined aquifers and recharge is at the ground surface (Gale, 2005a). Here, the source water is conveyed by the use of pipes, ditches, or banks to the spreading area, and the water to be infiltrated is spread over a permeable material into the unsaturated zone. The factors that govern successful spreading techniques and infiltration rate are; gentle slope, large surface areas, soils with good hydraulic conductivities, and the absence of saline layers (Asano, 2016). In areas where the source water is of good quality, the spreading methods are applied for varying soil textures with yearly hydraulic loadings such as 500m/yr for coarse clean sands, 300m/yr for medium clean sands, 100m/yr for loamy soils and 30m/yr for sandy loam soils (Herman Bouwer, 2002; Gale, 2005a). Where the water source is of highly suspended solids, a highly regulated recharge structure or strategy is required to overcome the potential clogging (Asano, 2016).

Based on several kinds of literature, Maliva and Missimer (2012) postulated that surface spreading systems of an infiltrated area differ in terms of never flooded, permanently, and occasionally flooded areas. The total volume of water infiltrated is expressed by multiplying the land area infiltrated, the period infiltration took place and the amount of water infiltrated (infiltration rate). Based on water infiltrating into the ground, it can be assumed that the infiltration rate decreases with time until a more or less constant value is reached. The total volume of water infiltrated is an integral function of the infiltration capacity and a time curve, in which the infiltration rate decreases exponentially from an initial maximum value as shown in (Fig. 2.2). This method or approach described above is in line with the Horton equation, and as such, locations with higher infiltration and percolation rates — vertical hydraulic conductivities are required in the selection of suitable surface spreading systems. However, it was argued that high vertical hydraulic conductivities as a result of secondary porosities can surpass the natural attenuation processes (Maliva and Missimer, 2012).

The basin or pond infiltration is a type of surface spreading frequently applied in semi-arid areas. This is constructed by excavating a ground surface, or an area enclosed by a bank where continuous recharge water is infiltrated through the bottom of the basin (Gale, 2005a). The underlying aquifer materials can experience rapid clogging if it consists of fine texture. In such cases, the basin floor and sides of the basin should be covered with medium sand of 0.5 m thickness (Huisman & Olsthoorn, 1983). Furthermore, the clogging effect can be minimized by intermittent wetting and drying, as this changes the redox conditions that are necessary for the removal of nutrients in wastewater systems (Maliva and Missimer, 2012).

The design of an infiltration basin for surface spreading systems often involves a comprehensive understanding of hydrogeological processes with the fundamental aim of maximizing the infiltration rate for a constant recharge over some time. Hydrogeological characterizations both at the surface and at vadose conditions are very useful in the selection of suitable surface spreading designs at a given location. The site characterization often includes an integrated method for a successful basin design. Infiltration tests often determine the hydraulic properties of the soil and this is done by the use of a double-ring infiltrometer. Additionally, test borehole/ core drillings usually provide the geological properties of the unsaturated media and the saturated aquifers. Haimerl et al. (2002), cited in Maliva and Missimer (2012) carried out an infiltration test in the Sultanate of Oman. The test site demonstrating a surface spreading method was installed with 11 tensiometers at different depths. Water level measurements were done in adjacent boreholes and it was concluded that dry soils have the greatest infiltration rates, but recharge was greater in pre-wetted soils. Generally, dry soils have a high matrix potential (water suction) and tend to draw water into the soil and therefore, evaporate with little or no recharge. Pre-wetted soils often have smaller

infiltration volumes and recharge usually occurs when the area is smaller, allowing longer application time for greater recharge rates. Hence, large basins should be divided into smaller sub-basins during the design of surface infiltration basins (Haimerl et al., 2002).

Modelling techniques can be used to select and evaluate feasible sites for the application of surface spreading systems (Ringleb et al., 2016). The groundwater flow models such as MODFLOW are widely used to design, optimize and manage surface spreading basins (Bekele et al., 2011; Lacher et al., 2014; Legg and Sagstad, 2002). Other modelling tools such as MT3DMS, PHREEQC, MARTHE, and CXTFTIT are also used to identify and evaluate the water quality changes and geochemical processes during surface spreading methods (Ringleb et al., 2016).

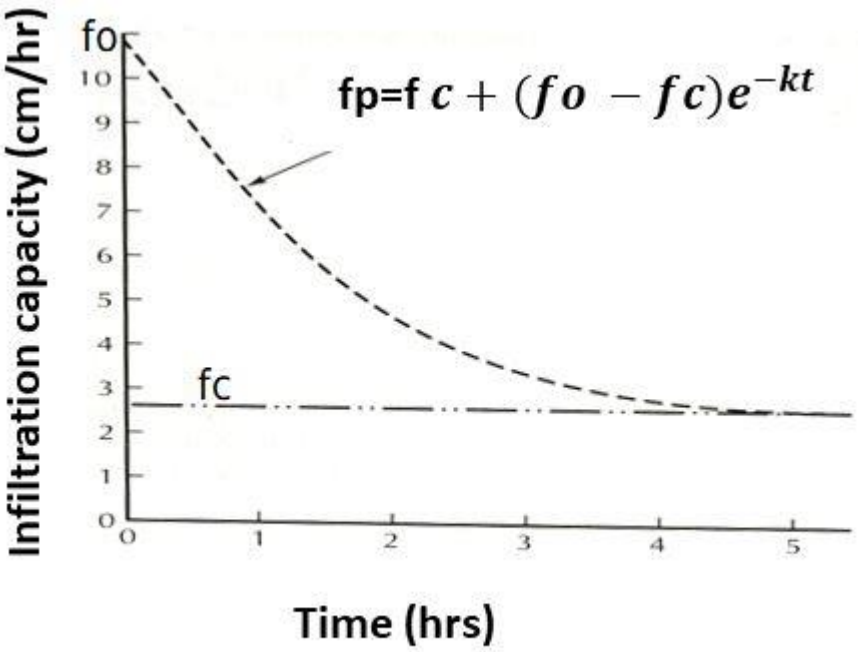

Fig. 2.2 *Relationship between infiltration capacity against time, where infiltration rate decreases exponentially from an initial, maximum value Fo (L/m) to a final constant rate Fc (L/m). This relation describes an exponential function and with this function, the infiltration rate F_p (L/T) can be calculated at each time. K (1/T) is the rate constant that describes the decline in infiltration. (Fetter, 2004) adapted from the Horton equation.*

2.3.2 Soil Aquifer Treatment (SAT)

For water quality improvements, the SAT is a specific type of surface spreading system designed to allow reclaimed water to infiltrate a recharge basin to the underlying aquifers. This process contributes to the treatment and removal of organic contaminants, biological oxygen demand (BOD), viruses, and nitrogen from partially treated wastewater by means of natural attenuation processes. Again, SAT systems can mitigate saltwater or contaminants intrusion

by displacing salty water intruding into coastal aquifers with freshly injected water. The water recovered can be disinfected with chlorine if it is intended for non-potable use. Similarly, if the recovered water is for potable water supply, post-treatment methods such as “granulated activated carbon and reverse osmosis” is often used (Maliva and Missimer, 2012).

A key to good SAT system performance depends on the local hydrogeology with granular soils (sandy loam, fine sand) having sufficient permeability and a high infiltration rate. Soils with fine sands are usually underlain with coarse grain materials, where the unsaturated zone and underlying aquifer should be devoid of an impermeable layer such as clay, as this slows down the vertical flow of the water (Maliva and Missimer, 2012). Sites with less unsaturated zone depth and shallow water tables are to be avoided in preference to sites with thick unsaturated zone and high-water tables that can manage infiltration and natural attenuation process effectively.

Where wastewater is intended as an influent water source for the SAT system, pre-treatment is recommended in regulating the oxidation and reducing condition (redox potential). Wastewater containing a considerable amount of organic carbon contents can lead to higher concentrations of oxygen loads and this may eventually create an anaerobic situation in the vadose system (Fox et al., 2001). On the other hand, high concentrations of suspended solids and excessive algal growth from organic matter can accelerate and cause clogging in the SAT system. Hence, SAT system should be designed to cater for clogging issues, and remove nitrates and nitrogen compounds by employing denitrification. In this case, microorganisms are used to degrade nitrate to nitrogen gas under anaerobic conditions. Substances that have very slow rates of biodegradation can be reduced by absorption (activated carbon filter). Harmful microorganisms are removed by ultraviolet disinfection, through the use of ozone or chlorine. Removal of nitrogen compounds from high concentrated water in SAT system usually depends on the periodic flooding and drying as well as the hydraulic loadings of the infiltration basin. Longer flooding and drying periods of the SAT system usually create anaerobic conditions, whereas the short period of flooding and drying leads to aerobic processes which convert nitrification of ammonium to nitrate (Maliva and Missimer, 2012). Bouwer (1991), postulated some specific factors needed in the periodic flooding and drying of SAT system and these factors include the following:

- The cation exchange capacity of the soil
- Exchangeable ammonium percentage in the soil
- Depth of oxygen penetration into the soil during the drying period

- Ammonium and carbon concentrations in the sewage effluent
- Soil and effluent temperature
- Infiltration rate

An example of an SAT system is the Shafdan treatment plant in Israel. The plant uses biological secondary effluent to infiltrate a series of open ponds into the underlying aquifers. This contributes to a recharge rate of 70-210 m/year. The treatment plant removes 90 % of total suspended solids (TSS), biological oxygen demand (BOD), nitrogen, and ammonia (Jiménez, & Asano 2008)

2.3.3 Induced Bank infiltration

Induced bank infiltration consists of several boreholes constructed at a short interval from each other that is in line, or parallel to the bank of a surface water body. During pumping, the water table is lowered adjacent to the river bed, inducing the surface water to infiltrate the aquifer system (Gale, 2005a). The factors that govern some induced bank filtration schemes are perennial streams or lakes with unconsolidated bottom deposits, and of acceptable quality that is hydraulically connected to an aquifer system (Gale, 2005a; IGRAC, 2007). Induced bank infiltration schemes often improve water quality issues. With this, dissolved and suspended contaminants are removed from the passage water through the riverbed by biological, physical, and chemical processes. In some parts of the world, this scheme is being supported by infiltration ponds or recharge shafts to increase recharge and improve the water quality (IGRAC, 2007).

A large variety of induced bank infiltration schemes is used in the world to increase groundwater recharge and improve water quality issues. In Hungary, Simonffy (2002), applied an induced bank infiltration scheme on the Csepel Island of Budapest. The island consists of sandy- gravel deposits with several wells oriented parallel to the Danube River. The infiltration system capacity was 400 Mm^3/day with an actual abstraction rate of 250 Mm^3 /yr in 2002. This scheme supplies drinking water to 1.7 million inhabitants of Budapest with a backup system for future abstraction.

Dillon et al. (2014) also documented induced bank infiltration at Palla on the Yamuna River, New Delhi. The Palla well fields are situated along the western bank of river Yamuna, where recharge usually occurs through the riverbed in response to well abstraction adjacent to the river. The Yamuna River can be turbid during high flows and consists of fertilizers, animal waste, and faecal materials from the high agricultural area close to the catchment. The drinking

water supply from the groundwater wells via 90 tube wells in the Palla sector is treated by chlorination means. However, treatment is often interrupted by power failures.

For the improvement of water quality issues, some guidelines suggested by IHE - Delft Institute for water education are generally adopted to evaluate and determine the fate of water treated in an induced bank filtration system. The four methods include (i) “hydraulic simulation using MODFLOW” (ii) the NASRI-BF simulator, to predict “the share of bank filtrate” (iii) the water quality guidelines for predicting water quality from a bank filtration system (iv) the costs of bank filtration system compare with current “conventional surface treatment” options usually applied in treating water (Sharma et al., 2012). The NASRI-BF simulating tool usually provides an optimal position of wells and also gives an estimate of the bank filtration in any pre-feasibility studies and this has been applied in countries such as Malawi and Germany (Holzbecher et al., 2008; Ringleb et al., 2016). The major advantages of induced bank infiltration schemes are that bacteria, viruses, and parasites are removed during the infiltration process. Again, there are no serious effects on the groundwater table further inland, since groundwater in large quantities is always abstracted from several boreholes. The disadvantages are that long-term clogging of the river due to large amounts of suspended loads requires the surface to be scraped during periods of low water level. Also, rivers with considerable amounts of persistent organic compounds such as pharmaceuticals and pesticides when infiltrated may contaminate the groundwater (Gale, 2005a; IGRAC, 2007).

2.3.4 Well, Shaft, and borehole recharge

Generally, recharge of groundwater via well is of two main technologies and these are shallow depth well recharge and deep well recharge. The open wells and shafts are applied in shallow phreatic aquifers; where recharge takes place in areas of low permeability surface layers where spreading methods are not applicable (Gale, 2005a). The main purpose of this method is to restore groundwater wells that have a declining water table or yields. Thus, surface structures are excavated approximately 5 m to 15 m deep to penetrate the low permeability strata, usually called recharge pits and trenches (Gale, 2005a). The recharge trench is made by filling it with a mixture of coarse sand and fine gravel materials and water is infiltrated through the formations into the aquifer.

Wells or borehole recharge represents a deep recharge method; in which low permeable strata overlie target aquifers and recharge of water is directed into the aquifer. In a broad sense, well or borehole recharge is the direct recharge of wells where surface infiltration is practically not possible. This is usually applied in deep confined aquifers and preferred in areas where land is scarce. It is also preferred in areas where there is a high evaporation loss of surface infiltration basins (Pyne,1995). The injection of water via a well can be performed either through the

aquifer by pressure, or under gravity into the unsaturated media. Thus, injecting water into a well forces a significant amount of water through the borehole wall. Various factors such as quality of the influent water, pre-treatment, the design of injection well scheme and set-up, and lastly program to restore or renovate the injection well are essential in the optimization and maintenance of the well injection system (Maliva and Missimer, 2012). However, a review conducted by Maliva & Missimer (2010), recommended that the design of wells for water injection ought not to be similar to extraction wells or production wells. Again, the wells should be designed in a manner to allow for good rehabilitation, and the efficiency should be maximized to control or minimize the clogging rate. Generally, there are two main applications of the deep well recharge. These are Aquifer Storage and Recovery (ASR) and Aquifer Storage Transfer and Recovery (ASTR).

2.3.5 Aquifer Storage and Recovery (ASR)

The aquifer storage and recovery is the injection of water into a well and recovery from the same well (Dillon, 2005). It is one of the common deep well recharge methods used to store and recover treated water for communities and towns during a period of high demand. According to (Pyne, 2005), aquifer storage and recovery are defined as the "storage of water in a suitable aquifer through a well during times when water is available, and the recovery of the water in the same well during times when it is needed ". Three essential components of ASR can be noted. These are (a) water is temporarily stored in the aquifers (b) the aquifer embraces the water using the wells (c) the water is abstracted from the same well as in the case of the emplacement. A modification of Pyne`s (2005) concept of ASR by Maliva & Missimer, (2010), defined ASR as "*the storage of water in a suitable aquifer through a well during times when water is available, and recovery of the same or similar quality water using a well during times when it is needed"*.

The ASR technique involves the injection of water sources such as stormwater, desalinated water, treated surface water, and treated wastewater, storage of the water, and recovery of the same water for later use. During injection, a buffer zone is created between injected water and ambient water already in the well. Similarly, in times of recovery, the injected water stored, together with the surrounding ambient groundwater is abstracted through the aquifer storage and recovery well (Maliva and Missimer 2012). The advantages of this method include (i) no evaporation losses of surface water, (ii) less prone to contamination of the stored water, and (iii) fewer costs of land required compared with the surface storage method. The main drawback of this method is that there are low and poor water quality changes in the stored water recovered during unfavourable hydrogeological conditions such as metal leaching (Maliva and Missimer, 2012; Pyne, 2005).

The aquifer storage and recovery technique are based on three different types of storage systems that are used to store the injected water. The three storage systems described by (Maliva and Missimer (2012) are as follows:

(a) The recovery efficiency (RE), which is chemically bonded, is used to evaluate the functioning of an ASR system and this is the ratio of the volume of injected water (Vinj) and that of water recovered (Vrec) at a quality appropriate for its anticipated use or purpose'' expressed as a percentage as shown in equation 2.1 (Maliva & Missimer 2010)

RE (%) = 100 (Vrec/Vinj) …… (2.1)

This method is very useful in restoring large amounts of brackish water in a well by pumping fresh water into the same well. When freshwater is injected into a well containing brackish water, a buffer zone is created dividing a mixture of native brackish water and freshwater. These may be drawn from the well at the quality saline level, appropriate for its intended use.

(b) The physical storage system is the injection of freshwater into a well containing native groundwater. The injection causes a significant increase in the aquifer volume and a corresponding increase in the pressure head or water level. Net storage is always paramount to the increase of water head, and the latter must be constant until a recovery time is reached. Physical storage of the ASR system is generally evaluated using water quality criteria and groundwater model tools that best describe or quantify the water levels that are likely to occur at a recovery time when there is no recharge or pumping. This is because in evaluating a proper baseline of physical storage system recharge, pumping or recharge should be absented as this induces changes in the storage volume. An example of a physical storage system is an overexploited unconfined aquifer that has available storage space (Maliva & Missimer 2010).

(c) The third storage system of an ASR method is the regulatory storage system, which describes the injection of water that allows the system owner to pump additional water, which is practically not allowed. The main goal of this method is to control over-drafted aquifers, which in other words means, the injection and recovery provide a balance and do not adversely affect long-term water levels in aquifers. This system is practised mostly in some parts of the United States and it may have an impact on the water levels if a long dry period persists where water is constantly being withdrawn.

Aquifer storage systems have been used in many parts of the world to increase the total volume of aquifers using varying water sources and storage periods (Maliva and Missimer, 2012). In Australia, urban stormwater from Andrews's farm and Regent Gardens were collected, treated, and injected into aquifers via wells. The typical recharge rates per year were 150 million litres/yr and 60 million litres/yr, respectively (Gerges et al., 2020). In Abu Dhabi, the

domestic water supply is mainly desalinated seawater, consisting of a total water volume of 26 million m^3. This can supply 182,000 m^3/day for 90 days In case of a breakdown of the desalinated plants, the ASR system is used as an alternative water supply to meet the city's drinking water needs (Schüth, 2014).

2.3.6 Aquifer Storage Transfer and Recovery (ASTR)

The Aquifer Storage Transfer and Recovery (ASTR) is the injection of water into a well for storage and recovery from a different well, generally some few meters apart to increase the groundwater residence time, thereby treating the water in the aquifer (IGRAC, 2007; Murray, 2017). The rationale behind the ASTR system is to serve as a treatment option for the water in the well—aquifer quality is enhanced through natural attenuation processes (biological, chemical, and physical means) (Maliva and Missimer 2012).

The ASTR system is usually practised in areas where the terrain is hilly and the injection of water is in deep aquifers (Dillon, 2005). Again, it is practised to have information on the residence time of the water. Therefore, accurate determination of the residence time between the injection and recovery wells is very necessary to check the travel and recovery times of the water. Gas tracers such as SF6 and CFCs are widely used to assess the groundwater residence time in the aquifer. Conservative tracers such as chloride and bromide are useful in obtaining information on the mixing influence of the injected water and the native groundwater. Where there is a minor difference in the salinity level between the native groundwater and the injected water, a run on the recovery wells using a time series of resistivity logs is necessary to obtain information on the exact flow paths between the injected and recovery wells (Maliva and Missimer, 2012).

2.3.7 In-Channel Modification

In-channel modifications are structures that are constructed in streams or rivers to detain or capture river flow via a natural drainage channel, to enhance groundwater recharge. In-channel modification has the following technological applications (IGRAC, 2007):

- Groundwater recharge dams - are constructed dams with built-in stream beds to collect stream runoff water.
- Subsurface dams - are structures constructed to detain underground flow from a natural aquifer.
- Sand storage dams - are designed above ground in an ephemeral river bed.

- Mini earthen check dams and permeable rock dams – are gullies and ravines, transformed into small streams at the base of the hills.
- Channel spreading techniques- involve the use of “L”- shaped levees to slow the pattern and surface flow of a river. This provides more time for infiltration.
- Streamflow augmentation - this is applied in areas, where streams fed by groundwater have dried up in their upper reaches. In this case, a stream channel close to the head of its drainage head is used to recharge the groundwater through the stream bed.

2.3.8 Sand Storage Dam

A sand storage dam is a special type of in-channel modification made of impermeable barrier and constructed across a sandy ephemeral river bed. The sand storage dam also known as a trap dam detains sudden flash floods or high ephemeral flow and this is designed usually across the breadth or width of the streambed, thus creating artificial recharge. During flooding events, coarser grain materials are trapped behind the walls of the dam; and the surface runoff can easily penetrate the soil formations forming the upstream aquifer of the dam. The height of the dam wall that determines the storm flow and sediment accumulation can be raised after a heavy rainfall event. Sand dams are normally preferred in areas where the land is undulating and sufficient runoff is generated as flash floods (Gale, 2005a).

Sand storage dam has shown to be a major contributor to small-scale water supply in developing countries. Besides, it has contributed to the domestic and irrigation water supply of small towns and villages (Maliva and Missimer, 2012).

Van Haveren (2004), Agarwal & Narain (1997) cited in Maliva and Missimer (2012), documented several advantages of sand storage dams and they include the following: (a) high evaporation losses are reduced during the prolonged dry season as compared to surface dams (b) water quality is significantly improved when the infiltrated water passes through the sand dam (c) It controls flood as the sand dam serves as a barrier and a spillway (d) It increases the natural volume of regional and local aquifers from a cascade of dams.

The evaporation of water contained in a sand storage dam depends on the geological materials (grain size) of an area. Coarse grain gravels and sands are more permeable and have a greater infiltration capacity than clay and fine sands. The high infiltration rate, allows more rapid artificial recharging thus reducing the evaporation of water contained in the sand dam. In terms of recovery water, the amount depends on the volume of sediment accumulation, the specific yield, the baseflow, and the net inflow and outflow from the aquifers.

Aerts et al., (2007) presented an equation to estimate the amount of extractable water (Ve) which is given as follows:

$$Ve = (X * W * D * S_y) + B - L_v - L_{out} + L_{in} \quad (2.2)$$

X is the river segment length (m) (ft)
W is the average width of the river segment (m) (ft)
D is the average thickness of riverbed sediments (m) (ft)
B is the base flow into river sediments from riverbanks (m^3) (ft^3)
Lv is the vertical leakage out of the bottom of the aquifer (m^3) (ft^3)
Lout is the leakage out of the horizontal aquifer downstream of the dam (m^3) (ft^3)
Li is the leakage into the horizontal aquifer from upstream of the dam (m^3) (ft^3)

Sand storage dams are less expensive to construct and usually, they are a village infrastructure-based project (Maliva and Missimer, 2012; Van Haveren, 2004). The largest and greatest density sand dam in the world is in the Kitui District of Kenya. This is a community-based project financed by "Sahelian Solution Foundation, SASAOL", an NGO to solve domestic water scarcity problems. The heights of the sand dams are 1.5 m to 2 m and some up to 4m. The quantity of water annually captured from an average sand dam is 5300 m^3 (IGRAC, 2007).

2.3.9 Wadi Dams

A wadi is a bed or valley of a stream that is intermittent due to the nature of rainfall events in arid areas and preserves its water during the rainy season, generally forming an oasis. During the rainy season, flood retention or recharge dams can be constructed from the wadi. Wadi dams are commonly found in the regions of the Middle East and North Africa (MENA) (Maliva and Missimer, 2012).

Wadi dams, constructed in the Middle East countries such as Oman and UAE offer two main end-users, namely: aquifer recharge and flood control. For the flood control program, intense flash floods can cause destruction of the dam as well as loss of lives, and therefore requires the construction of wadi dams to be able to control the flooding. The waters retained during flood events are thus used in recharging the aquifers (Maliva and Missimer, 2012).

Owing to the high evapotranspiration demand in the MENA countries, the amount of water infiltrated as a result of wadi development can be estimated using methods such as water balance, groundwater modelling, and Darcian flow nets. Natural recharge estimation of wadis in these regions is quite complicated to measure due to scarce data such as groundwater levels and meteorological data. Hence, water circulation through the fractured rock and

channel losses methods are commonly used to estimate the natural wadi recharge during flood events. (Maliva and Missimer, 2012).

Al-Turbak & Al-Muttair (1989) investigated recharge estimation for two reservoirs in Central Saudi Arabia using the water balance method. The recharge rates were very high (82% and 94.5%) and this is because of the high volume of water contained in the wadi reservoirs that percolate through the soil into the underlying aquifers. Comparative studies by Missimer et al., (2012) using channel loss and fractured rock methods in western Saudi Arabia, revealed recharge between 3- 11% based on annual precipitation.

2.3.10 Rainwater Harvesting (RWH)

From a storage point of view, rainwater harvesting can be considered as a storage system, where roof rainwater is harvested, and diverted into existing wells via drainage pipes or storage tanks. Roof rainwater harvesting is commonly applied in urban and rural areas and the water harvested can be used directly in the household or for aquifer recharge.

Roof-top rainwater harvested can be poor in microbial quality or other pathogens. Hence, roof rainwater harvesting for direct household consumption is usually allowed to run for some time to clean the dirt on the rooftop. The water collected needs to be disinfected before usage (Gale, 2005a; NRMMC-EPHC-AHMC, 2006). Apart from the microbial quality issues of rainwater harvesting, other disadvantages of rainwater harvesting include the leaching of metals and chemicals from galvanized steel and asphalt roof shingles. The leaching may cause contamination of the water and thus, the best rooftop to consider for rooftop harvesting is a “stainless steel or enamel-coated steel” (Maliva and Missimer, 2012).

According to NRMMC EPHC (2009), typical water projects for rainwater harvesting as shown in (Fig. 2.3) consist of seven elements namely: zone of capture, techniques for pre-water treatment, water recharge, subsurface storage, recovery, post-treatment, and end-use.

Rooftop rainwater harvesting has been successfully applied in many parts of India to augment the natural storage of aquifers. In India, rainwater was harvested from the rooftops of the Indian Institute of Technology and this was conducted by the Central Ground Water Board, India. The rainwater collected was used to recharge two wells, which are slotted and wrapped with geotextile. The rooftop surface area was 1660 m^2 and the annual recharge volume of the underlying alluvial unconfined aquifer was estimated at around 830 m^3 (Dillon et al., 2014 2014).

In the city of Coimbatore in India, rapid population growth and copious industries resulted in an extreme depletion and pollution of the groundwater. In 1980, the city was declared a drought-prone area by studies conducted by the United Nation Development Program. In the year

2003, groundwater levels were as low as 1000 feet and drinking water was scarce at an aberrant rate. This necessitated Siruthuli, an NGO based in Coimbatore, to provide an alternative drinking water source for the people. In 2004, hydrogeological investigations were piloted to assess the feasibility of rainwater harvesting in the area. Based on that, 154 rainwater-harvesting structures were constructed between 2004 and 2005. The harvested water was used to recharge the aquifers and the water levels subsequently rose between 15 ft and 60 ft. Furthermore, an additional 215 rainwater harvesting structures were constructed by the Central Groundwater Board, Ministry of Water Resources (IDEP Foundation, 2007)

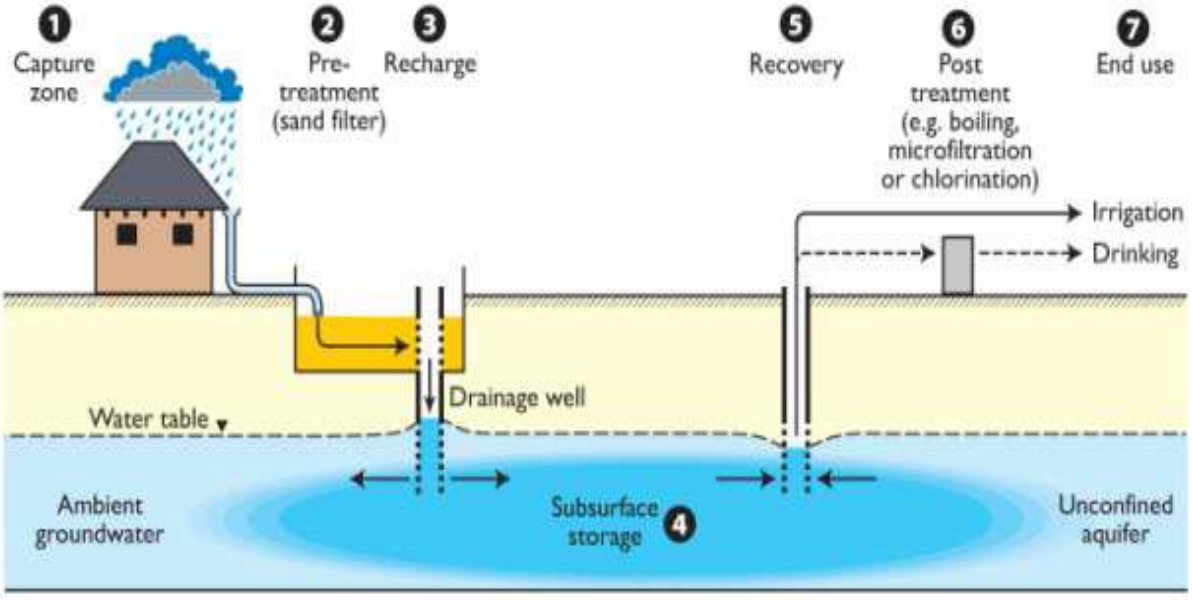

Fig. 2.3 *Sequence and elements of rainwater harvesting (NRMMC EPHC (2009)*

2.4 Historical development and current perspective of managed aquifer recharge sites in Europe

In Europe, pioneering work of managed aquifer recharge was started in 1890 in Scotland-Glasgow, where the first MAR site was constructed by the Glasgow Waterworks Company (Hannappel et al., 2014; Sprenger et al., 2017). A perforated collected pipe was constructed parallel to the Clyde River (Ray et al., 2003) and abstracted bank filtrated water (BMI, 1985). The scheme was therefore replicated in many other urban cities in the U.K such as Newark, Derby, Perth, and Nottingham. The pinnacle of this was very much evident in the 1860s as “naturally filtered water’’ in the U.K. However, there were drawbacks, as many of the sites were abandoned in the subsequent years due to decrease well performance (BMI, 1985; Hannappel et al., 2014). Notwithstanding this, the “naturally filtered water’’ method was modified and replaced with induced bank filtration schemes and this was extended to most European countries such as Germany, Netherland, Austria, Belgium, and France (Hannappel et al., 2014; Sprenger et al., 2017).

The rapid population growth, coupled with the copious industries in Europe and surface water impairment by contaminants and improper sanitation, challenged the municipal water supply to deal with the above-mentioned problems. In Germany, riverbank filtration was installed at the "River Rhine (Water Works Düsseldorf in 1870), the Ruhr River (Water Works Essen in 1875), the Elbe River (Water Works Saloppe, in 1875, Water Works Hosterwitz in1908) around Dresden and in the Berlin area (Water Works Müggelsse, changed to groundwater in 1904-1909, Water Works Tegel 1901- 1903)''. Comparative applications of riverbank filtration and basin infiltration schemes were also located in Sweden, Switzerland, and Netherlands. Stuyfzand (1989), reported that the first riverbank filtration in Netherland was started in the year 1890. Similarly, in Switzerland, riverbank filtration was found to be operational in Basel, a forest riparian town called "Langen Erlen" in the year 1912 (Hannappel et al., 2014; Sprenger et al., 2017)

The Riverbank filtration method was further spread to eastern European countries such as Hungary, where the first MAR site was found in Danube Island "Szentendre'' north of Budapest, in the year 1920. On the Csepel Island of Danube, riverbank filtration was constructed and several other sites were also found near Raba, Ipoly, Sajo, Hernad, and Drava Rivers (Homonnay, 2002; Sprenger et al., 2017). In the South-eastern European country of Romania, riverbank filtration and infiltration ponds were constructed in the year 1961, previously started in the year 1911 as the "Lasi water supply system'' at the Moldova River. Another site was constructed in the northwestern Romanian city of Cluj Napoca in the year 1935 (Hannappel et al., 2014; Sprenger et al., 2017). In the north European country of Finland, Katko et al., (2006) documented that MAR applications started in the 1960s, replacing the earlier water plant system that uses infiltration ponds to recharge groundwater in the west coast city of Vaasa in the year 1929.

Regarding well injection methods and other MAR development, (Stuyfzand et al., 2013), reported that the first ASR sites were found in the Netherland as pilot-scale projects in the 1960s. However, clogging issues had resulted in the closure of many of these ASR sites. In Barcelona, Spain, some of the aquifer storage and recovery schemes built in the early 1970s are working to date due to the high aquifer transmissivity and the low turbidity of the source water (Sprenger et al., 2017).

For the In-channel modification method, the first scheme was constructed in the Llobregat River in Barcelona in the year 1960. This technique is gradually experiencing low infiltration rates and is being managed together with other ASR and basin infiltration schemes in the Llobregat area of Barcelona (Sprenger et al., 2017). In summary, the historical development of managed aquifer recharge has increased considerably since the 1870s. There are a large number of active sites in operation with a few other abandoned sites as shown in Figure 2.4.

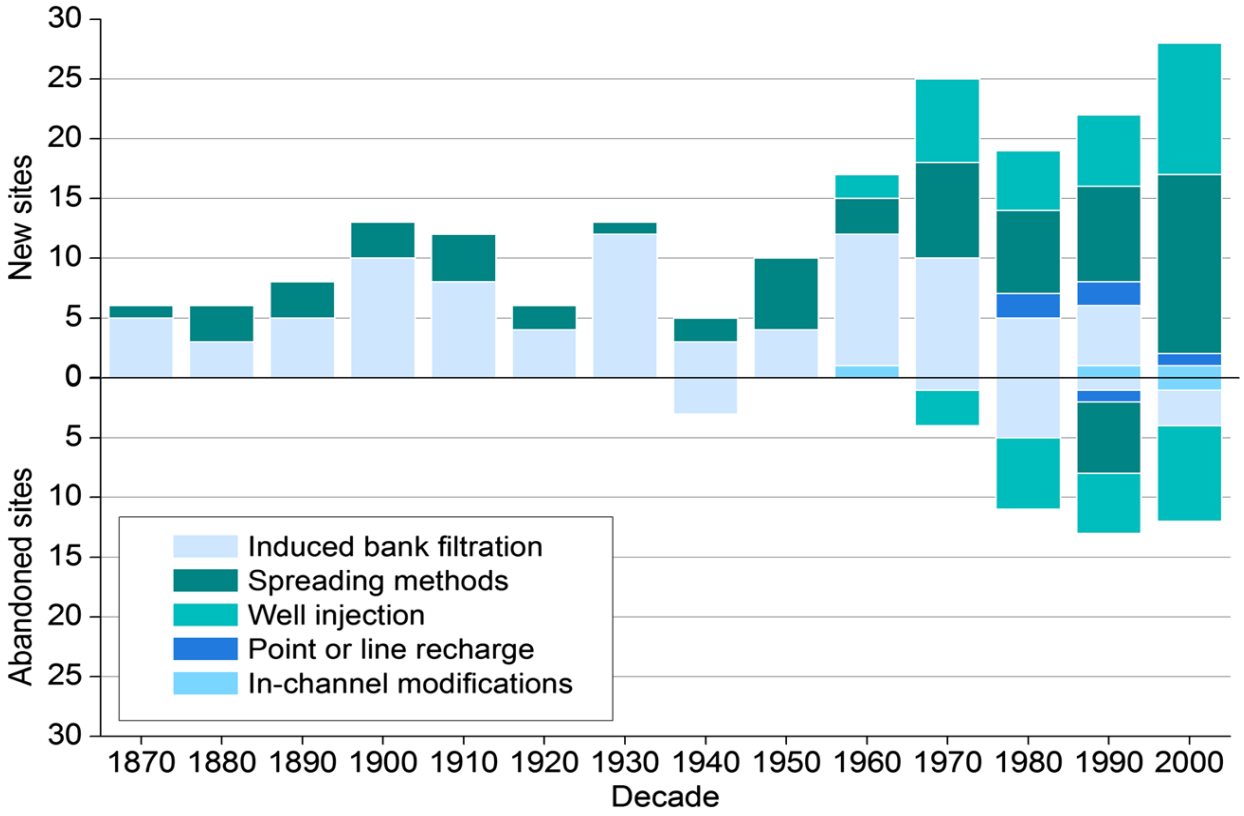

Fig. 2.4 *Summary of the old and currently managed aquifer sites in Europe between 1870 and 2000 (Sprenger et al., 2017).*

2.4.1 The Current State of MAR in Europe

The European MAR catalogue presented by Sprenger et al., (2017) comprises 224 active MAR sites that are located in 23 European countries as of 2013. The catalogue documents that Germany has 64 active MAR sites; followed by the Netherlands (41), France (21); Sweden (11), Switzerland (10); Spain (10), and the rest are in different countries, which are less than 10. The majority of the managed aquifer schemes in Europe are induced bank filtration having 127 MAR sites (57%); the second most widespread MAR method is the surface spreading method in 77 sites (34%), and the third is the well injection method in 11 active sites (5%) and 23 sites have been shut down.

In terms of geology, a large number of managed aquifer schemes are found in unconsolidated soil formations, and the majority of the schemes such as induced bank filtration and surface spreading methods exist around perennial rivers and lakes. In central Europe, most of the induced bank filtration (IBF) sites are found in unconsolidated unconfined aquifers and along major rivers. For example, in Germany and Netherlands, clusters of IBF sites are situated along the Rhine River; and in Austria, Hungary, and Slovakia, along the Danube River. A typical hydraulic conductivity of the IBF sites (n=53) is between $5.5*10^{-9}$ m/day and $5.5*10^{-3}$

m/day (Sprenger et al., 2017). Surface spreading methods are very common in Nordic countries such as Norway, Denmark, and Finland. The geology is characterized by hard rock formations and small-unconsolidated glacial deposits, which usually limit the occurrence of groundwater. In Finland, a special kind of surface spreading method called sprinkling infiltration plants (n=3) has been developed in the forest eskers of Finland (Helmisaari et al., 2006).

In terms of the potential source water, river water represents 78% and lake water 11% are the most influent water sources used for the various MAR schemes across Europe (Hannappel et al., 2014). Induced bank filtration has two main source waters: lake water and river water, as IBF usually exists along with these water bodies. Reclaimed water (treated effluent) constitutes 4% of the MAR influent water sources and is used mostly for agricultural purposes. An example is a Llobregat aquifer in Barcelona that uses reclaimed water as a source of MAR water via wells to combat seawater intrusions (Ortuño et al., 2010). Bank filtration scheme at Berlin- Tegel uses reclaimed treated water as a source of MAR water and this comes from a sewage treatment plant. The stormwater run-off was not documented in the literature as an influent source for MARs in Europe. Groundwater was virtually not used as a MAR water source in Europe because it is not considered a primary influent source (Hannappel et al., 2014; Sprenger et al., 2017).

The end use of the MAR scheme is the final usage of MAR water and this includes agricultural, domestic, industrial, and environmental purposes. MAR schemes for domestic purpose is the common end-use water in Europe (88%), next is agricultural (8%), ecological, and industrial (2%) (Hannappel et al., 2014). Industrial end-use water is located in Cologne and Duisburg in Germany, and this is operated by industrial companies using IBF schemes (Sprenger et al., 2017). Agriculture end-use is very prevalent in Spain than in any other European country (Hannappel et al., 2014). There are few cases of environmental end-use in Europe and an example can be found in Garzweiler near Cologne in Germany. In this city, a mining company that aims of protecting the natural swamps and wetlands in the area, and operated by surface spreading schemes such as infiltration wells and shafts, use groundwater as influent water to regulate the water table (Sprenger et al., 2017).

2.5 State of the art managed aquifer recharge solutions (MARSOL) in eight demonstration sites in Europe

In the quest to tackle the increasing water scarcity problems in the southern European countries and Mediterranean regions due to climate change on the available water resources and the ever-growing population; the MARSOL project aims to deal with the above-mentioned objectives. MARSOL is a consortium project involving six European countries (Greece, Germany, Italy, Malta, Portugal, and Spain) and Israel. The project comprises 21 partners from

research institutions, water institutions, universities, etc., and the overall project is coordinated at the Technical University of Darmstadt, Germany. The project was started in 2014 and received funding from the European Union with an estimated budget of 5.2 million euros (Marsol, 2014).

The MARSOL project aims to demonstrate that acute water shortages over a long period can be alleviated using managed aquifer recharge techniques. In this project, eight demonstration field sites were selected for different recharge methods and different influent water sources such as treated wastewater, desalinated water, and river water were used for recharge. The approaches adopted include site selection mapping, modelling; water quality monitoring, economics feasibility, technical risk assessment, legal issues, policy, and governance. These would form a benchmark for MAR projects as well as established state-of-the-art MAR implementation in Europe. The main objective of this project is to augment the natural storage of aquifers using different water sources during drought periods in a safe and sustainable approach (Marsol, 2014). Other objectives include (a) creating market avenues for the European industry through the application of low-tech and cost-effective MAR solutions (b) Increasing freshwater availability during drought, counteracting seawater intrusions using 8 demonstration sites as case studies, and (c) tailoring MAR advantages and programs to enable high accelerated market intimacy in Europe. The project is expected to address water scarcity problems and provide market opportunities through these state of art MAR solutions.

2.5.1 System designs at the demonstration sites

The MARSOL project was piloted in 8 sites in Europe and Israel and these sites are; Lavrion in Greece, Algarve in Portugal; Arenales in Spain, Llobregat in Spain; Brenta in Italy, Serchio (Italy); Malta South in Malta, and Menashe in Israel.

In Lavrion, an integrated method was adopted to solve the growing water scarcity problems and seawater intrusion typically of any Mediterranean region. Lavrion is a coastal town found in the south-eastern part of Attica, near Athens in Greece. The town depends on its coastal aquifer for domestic water supply (7.8 Mm^3) and irrigation (1.2 Mm^3). However, overexploitation, seawater intrusion, and a decrease in rainfall patterns have caused widespread contamination and water scarcity of the coastal alluvial and karst aquifers in Lavrion. Infiltration basins were constructed at the Lavrion Technological and Cultural Park and water sources such as treated wastewater were infiltrated into the bottom of the basins for recharging purposes. This technique also treats the aquifers thus operating as soil aquifer treatment. For continuous monitoring of the water infiltrating into the aquifer and also to check the performance of the SAT scheme, prototype sensors containing Time Domain

Reflectometry (TDR) and Frequency Domain Reflectometry (FDR) were installed. Furthermore, the Lavrion aquifer formation was hydraulically assessed using the vibrio direct probe method. Piezometer monitoring networks were installed as well as electrical conductivity logging and ad-hoc sensors for data transmission. Geophysical investigations were taken to assess and locate the boundary of the SAT aquifer system. Hydrogeochemical and isotopic analyses of the water samples were also conducted to determine the water quality and general recharge of the area. The groundwater flow model using Modflow was used to assess the feasibility of the SAT system under different scenarios (Protonotarios et al., 2016).

In the Menashe site, Israel, a two-stage MAR method (Infiltration basin and ASR) was used to store water in the aquifers. In the first stage, an infiltration basin was constructed on a sandy dune, where excess amounts of desalinated seawater were infiltrated into the basin. The desalinated seawater is treated with chlorine at the Hedera desalinated plant. Site characterization was conducted and with this, the soil was excavated to the vadose zone and a gallery of monitoring networks was installed to monitor the unsaturated zone. The monitoring networks include; a volumetric water content probe, Decagon 5TE, and GS3 soil sensors; 5 silicon-carbide suction cups installed at different depths, and electrical conductivity probe, and a temperature probe. Results indicate that after two hours of regulated infiltration (1.7 cm/min infiltration rate), water was found to be in the suction cup at depths between 0.5 m and 2 m. Furthermore, aquifer properties and groundwater sampling were tested in the two observation wells and electrical conductivities and temperature values were found to be 330 µS/cm and 21.3°C, respectively. A demo column experiment using desalinated seawater and sandy soil from the Menashe site was demonstrated at the lab to mimic the conditions that would occur in the vadose zone during the long and short periods. The column setup was made up of 3 processes (a) groundwater flow saturation in dry sand for two-pore volumes (b) desalinated water flow through the soil for five pore volumes and (c) groundwater replacing the desalinated water for three pore volumes. Results indicate that during the first stage (a), the groundwater did not receive any ion concentration from the column setup. This is probably due to the mixing effect of the desalinated water with the soil before it was taken from the site. In the second stage (b) there was a higher enrichment of bicarbonate (HCO_3^-) measured under the assumption that mixing has occurred. The high concentration of bicarbonate ions could be a result of calcium carbonate dissolution. The enrichment of bicarbonate is thus associated with a high level of hydraulic conductivity, confirming a possible formation of a bicarbonate dissolution (Kurtzman et al., 2014).

2.6 General Overview of Managed Aquifer Sites in Africa

The development of managed aquifer sites in Africa shown in (Table 2.2), has been abstracted from the web-based global inventory of the MAR portal (IGRAC, 2020). The portal contains 46 MAR sites in Africa as of 2021 and includes data types such as MAR main types, specific MAR types, influent source, final use, and the year of operations. Based on the Africa MAR data, it can be assumed that information on the first MAR site in Africa started in the Northern Cape Town of South Africa in the year 1959. It can be added that South Africa is the major MAR hot spot in Africa with 13 MAR sites; followed by Kenya with 10 MAR sites, Tunisia with 7 MAR sites, Algeria with 5 MAR sites, Egypt has 4 MAR sites; Morocco, Nigeria, Namibia has 2 MAR sites each, and Ethiopia has 1 MAR site as shown in (Fig.2.5). The commonest MAR type in Africa is the spreading method (n=17), the second-most used method is In-channel modification (n=15), well, shaft and borehole recharge is the third (n=11) and induced bank filtration (n=3).

The predominant influent source of MARs in Africa is river water with 24 case studies. Reclaimed wastewater is the next influent water source with 9 case studies, third is stormwater with 5 case studies. Groundwater and lake water is rarely used with 4 and 2 case studies, respectively. The final MAR used in Africa shows 71% for domestic purposes, 26% for agricultural purposes, and 3% for industrial purposes (IGRAC, 2020).

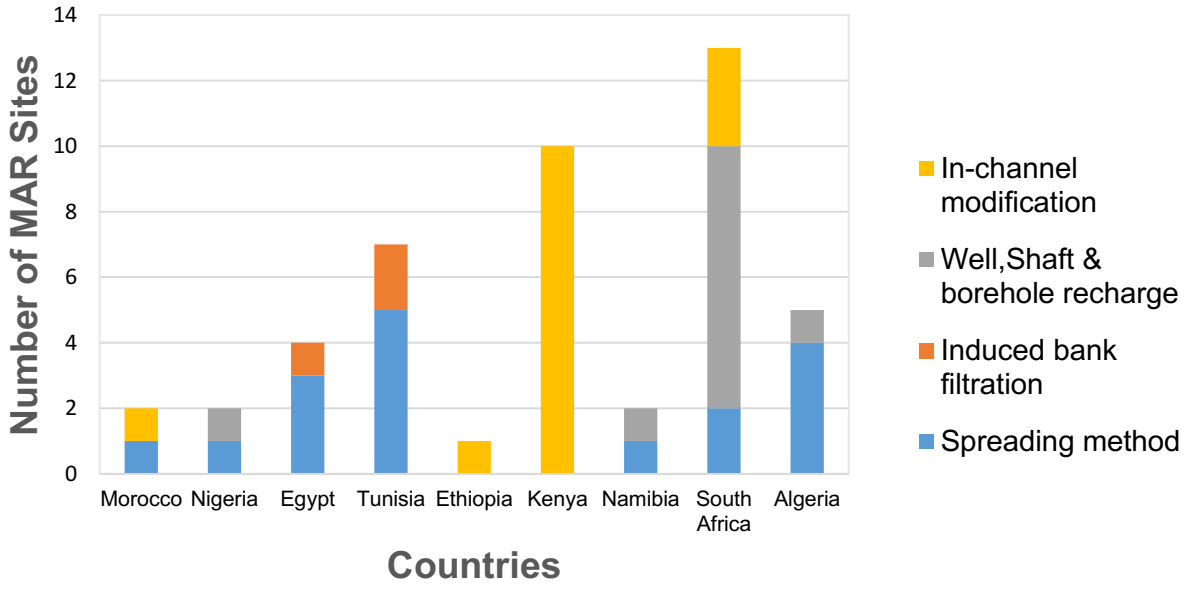

Fig. 2.5 *Distribution of managed aquifer sites in Africa.*

Table 2.2 Managed aquifer recharge sites in Africa abstracted from the web-based global MAR Inventory (2020)

Country	Year Started	Site	Main MAR Type	Specific MAR type	Source water	Final Use
Morocco	1989	Ben Sergao	Spreading method	Infiltration Ponds	Reclaimed wastewater	
Morocco	2012	Souss-Maasa	In-Channel Modification	Channel spreading	River water	Agricultural
Nigeria	2009	Kano river Irri. Project.	Spreading method	Excess Irrigation	River water	Agricultural
Nigeria	2011	Michael Okpara Univ	Borehole Recharge	Dug well/Shaft	Stormwater	Domestic
Ethiopia	2009	Koraro- 01	In-Channel Modification	Subsurface dam	Groundwater	Domestic
Egypt	2001	Toushka Khoure	Spreading method	Infiltration Ponds	River water	Natural storage
Egypt	2004	Sidifa Riverbank Filtration	Induced bank filtration	Induced bank filtration	River water	Domestic
Egypt	2011	Abu Rawash	Spreading method	Infiltration Ponds	Reclaimed wastewater	-
Egypt	1995	El Bustan Ext. Area	Spreading method	Infiltration Ponds	River water	-
Namibia	2000	Windhoek	Borehole Recharge	Dug well/Shaft	Lake water	Domestic
Namibia	1997	Omaruru Delta	Spreading method	Infiltration Ponds	River water	Domestic
South Africa	2009.	Polokwane	In-Channel Modification	Channel spreading	Reclaimed wastewater	Agricultural
South Africa	2007	Eland Platinum Mine	In-Channel Modification	Sand Storage Dam	No data	Industrial
South Africa	1959	Northern Cape	Borehole Recharge	Dug well/Shaft	River water	Agricultural
South Africa	2010.	Sedgefield	Spreading method	Infiltration Ponds	Reclaimed wastewater	-
South Africa	2007	Prince Albert	Borehole Recharge	Dug well/Shaft	No data	Agricultural
South Africa	2007	Plettenberg Bay	Borehole Recharge	Dug well/Shaft	River water	Domestic
South Africa	1994	Atlantis water Resour.	Spreading method	Infiltration Ponds	Reclaimed wastewater	Domestic
South Africa	2008	Langebaan	Borehole Recharge	Dug well/Shaft	River water	No data
South Africa	2010	Hermanus	In-Channel Modification	Subsurface dam	Stormwater	Domestic
South Africa	2010.	Loeriesfontein	Borehole Recharge	Dug well/Shaft	stormwater	Domestic
South Africa	2015	Calvinia	Borehole Recharge	ASR/ASTR	Lake water	Domestic
South Africa	2010.	Williston	Borehole Recharge	ASR/ASTR	Groundwater	Domestic

South Africa	2009	Kharkams	Borehole Recharge	ASR/ASTR	River water	Domestic
Tunisia	1994	Mahdia Ksour Essef	Induced bank filtration	Induced bank filtrat	Stormwater	-
Tunisia	2002	Korba	Spreading method	Infiltration Ponds	Reclaimed wastewater	-
Tunisia	1991	Khlidia	Spreading method	Infiltration Ponds	River water	-
Tunisia	2003	Boumerdes Aquifer	Induced bank filtration	Induced bank filtrat	Stormwater	-
Tunisia	1965	Soukra	Spreading method	Flooding	Reclaimed wastewater	Agricultural
Tunisia	1986	Nabeul-Hammamet	Spreading method	Infiltration Ponds	Reclaimed wastewater	-
Tunisia	1989	El- Hajeb Sidi Abid	Spreading method	Flooding	Reclaimed wastewater	-
Algeria	-	Oued Biskra	Spreading method	Recharge Dam	River water	Agricultural
Algeria	-	Oued Beshes	Borehole Recharge	Dug well/Shaft	River water	Agricultural
Algeria	2000	La Mitidja Legros	Spreading method	Infiltration Ponds	River water	Agricultural
Algeria	2000	La Mitidja basin	Spreading method	Infiltration Ponds	River water	Agricultural
Algeria	2002	La Mitidja Big Bag	Spreading method	-	River water	Agricultural
Kenya	-	Kitui District	In-Channel Modification	Sand Storage Dam	Groundwater	Domestic
Kenya	-	Kitui District	In-Channel Modification	Subsurface dam	Groundwater	Domestic
Kenya	-	Kiindu Dam 3	In-Channel Modification	Subsurface dam	River water	Domestic
Kenya	-	Kiindu Dam 4	In-Channel Modification	Subsurface dam	River water	Domestic
Kenya	-	Kiindu Dam 5	In-Channel Modification	Subsurface dam	River water	Domestic
Kenya	-	Kiindu Dam 6	In-Channel Modification	Subsurface dam	River water	Domestic
Kenya	-	Kiindu Dam	In-Channel Modification	Subsurface dam	River water	Domestic
Kenya	-	Anna catchment 1	In-Channel Modification	Subsurface dam	River water	Domestic
Kenya	-	Anna catchment 2	In-Channel Modification	Subsurface dam	River water	Domestic
Kenya	-	Anna catchment 3	In-Channel Modification	Subsurface dam	River water	Domestic

2.7 Some selected state of the art managed aquifer recharge case studies in Africa

2.7.1 Large scale borehole injection scheme using Aquifer Storage and Recovery(ASR) and Aquifer Storage Transfer and Recovery (ASTR): The case of Windhoek in Namibia.

Windhoek is the largest city and the capital of the Republic of Namibia. The average annual potential evapotranspiration is 2170 mm and this exceeds the average annual precipitation of 360 mm, making Windhoek the driest city in sub-Saharan Africa. The city has inhabitants of about 326,000 and the main water supply is from the Windhoek aquifer and three dams. The ever-growing population has caused pressure on the existing water wells as there are no perennial rivers. In the early 1950s, water levels started declining, and have decreased about 40 m in the micaceous quartzite, which is fractured and faulted, and constitute the main geological formation where groundwater flow. In the year 2004, managed aquifer recharge was considered the cost-effective method to counteract the growing drought in the area and with this, four boreholes were used for the aquifer recharge and an additional two boreholes in the year 2011 contributing to a recharge capacity of 420 m^3/hr (Murray, 2017).

2.7.2 System structure and design

The ASTR technique involves transferring a mixture of treated wastewater and dam water into 6 injection boreholes between 2005 and 2012. The total volume of water injected was 3.3 million m^3. The influent source water was stored in a carbon tank, where it was passed through a granular activated carbon to reduce dissolved oxygen concentrations (DOC) and also to minimize bacteria growth in the water. The water was filtered and disinfected with chlorine before injection. After injection, the water level rose about 50 m and the Windhoek aquifer was fully replenished as shown in (Fig 2.6). Currently, 34 equipped abstraction boreholes with a total capacity of 954m^3/hr are being recovered to supply the inhabitants of Windhoek (Murray, 2017). In the year 2017, geophysical and hydrogeological studies were conducted to identify and construct an additional 20 injection and abstraction wells to meet future water demands. The cost of the Windhoek ASR scheme including the completed scheme and future scheme is estimated at around USD 52.4million. An estimated amount of USD 8.4 has been spent by Windhoek city out of the required USD 52.4 million and a further USD 9.6 million are in place to finance additional schemes (Murray, 2017).

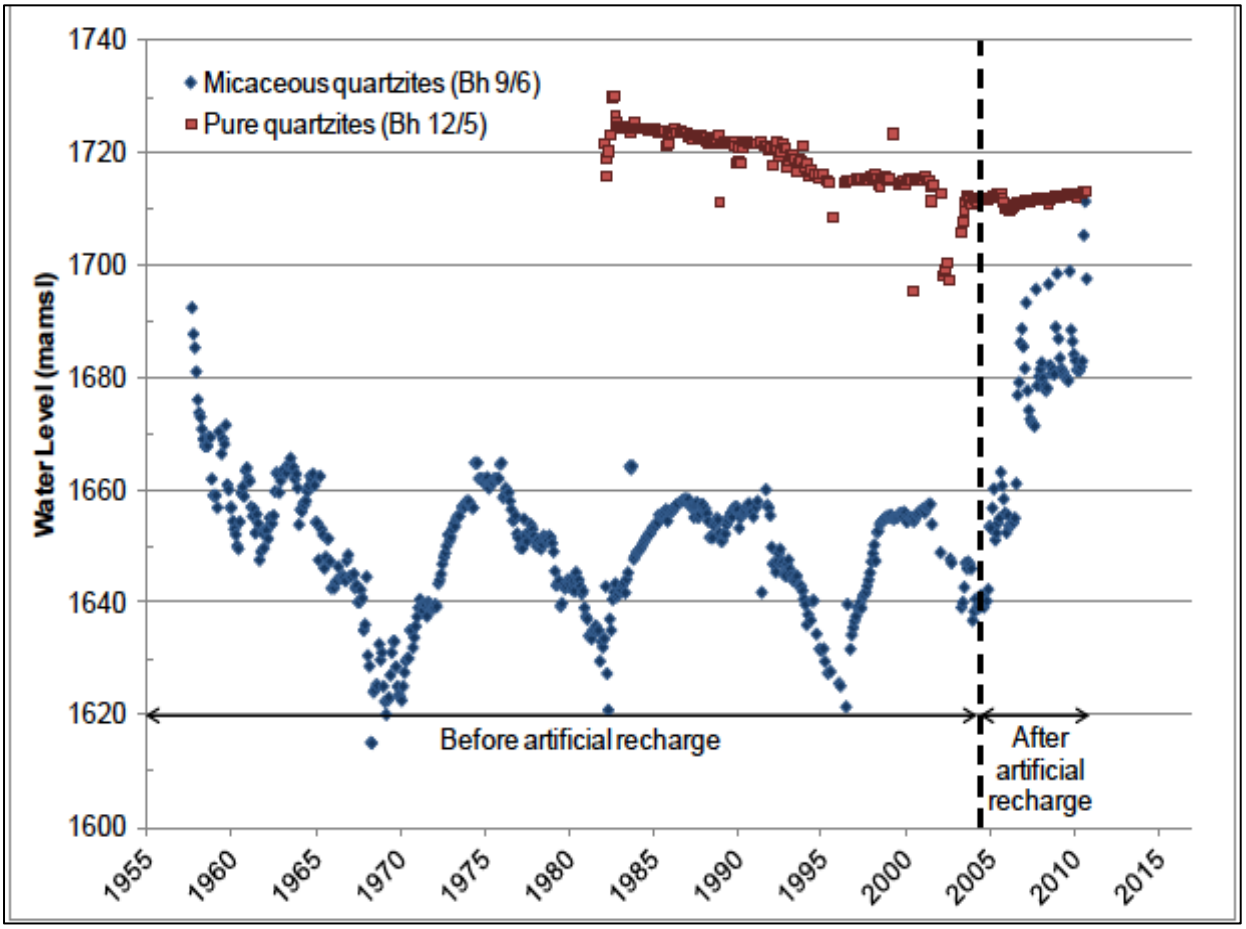

Fig. 2.6 *Water level changes in the Windhoek aquifer before artificial recharge and after recharge (Murray, 2017)*

2.7.3 A low-level technology of Sand dam in the Kitui District, Kenya

Kitui district is one of the semi-arid lands in Kenya experiencing limited rainfall and high evaporation. The district has an age-long practise of using sand dam technology for irrigation and domestic water purpose, but it has not been applied on a large scale. Furthermore, overpopulation and low erratic rainfall coupled with surface run-off losses and high irrigation potential in the district have compelled an NGO called Sahelian Solution Foundation (SASOL) in co-operation with the community to construct sand dams as a means of community- based community-based water conservation program to tackle the domestic and irrigation water problems. The sand dam, which is constructed in a stream or river aims to harvest rainwater and surface runoff during high flow. This creates artificial recharge in the aquifers and is subsequently abstracted to be used for domestic and irrigation purposes (Mutiso, 2002).

2.7.4 System structure and design

The sand storage dam in the Kitui district consists of a masonry check dam constructed in streams and rivers that abound in the district. The dams are positioned above the ground of an ephemeral river bed. The sand dam is sited in geological terrains having high storage capacity. The area selected is thus excavated to reach the base rock or impermeable layer such as clay; acting as a basement layer of the dam. During high flow events, runoff water containing sediments and gravels are trapped against the walls of the dam forcing the water to infiltrate the permeable soil. The accumulated sand behind the dam, therefore, holds water or stores a greater percentage of its total groundwater volume. However, Gathuru, (1990), contended that high volumes of water can be found in the dam than in the accumulated sand of the wall. This is because the water flowing through the dam reaches a horizontal distance of 200 m on the banks and up to 500 m upstream of the dam. Over 200,000 households in the district have benefited from this sand dam technology with clean and accessible water for domestic use. This technology has increased economic activities and improved their livelihoods. There have been many monitoring and evaluation programs conducted by SASOL to see the effectiveness of the sand dam technology as well as the socio-economic impacts. Some of the observations gathered include (a), during high peak flow, a considerable amount of water is harvested in the riverbanks and the dams are filled to the brim (b) there is no adverse effect on the people downstream of the dam because water balance results indicate that less than 5% of the total surface run-off is intercepted and (c) during drought periods, the communities can get water for use from the dams, reducing the amount of time spent on collecting water from distant areas. The only problem with this technology is that yield of the water is sometimes determined by the quality of the sand and soil properties. The cost of a dam in the Kitui district with a capacity of 60 m^3 and a design lifetime of 50 years is estimated to be 6000 euros (Mutiso, 2002).

2.7.5 Full-scale coastal recharge basin in Atlantis, South Africa

Atlantis is one of the semi-arid towns found along the west coast of South Africa and has been relying on groundwater since its initiation in 1976. The mean annual average precipitation in Atlantis is 450 mm. Most of the areas are underlain by sandy soil formation limiting 70% of the natural recharge and the highest recharge occurs in dune areas where there is no vegetation. An infiltration pond, as a means of groundwater recharge, was constructed in the dune areas to infiltrate water into the local aquifers. The water used for artificial recharge consists of stormwater from the residential areas and reclaimed wastewater from the industrial areas. During the 1970s apartheid in South Africa, the city of Atlantis was divided into industrial and residential areas. Many industries were seen in Atlantis after the apartheid because of the government policy to give tax incentives to an industrialist for relocation to Atlantis. Based on

this fact, much wastewater generated from the industries is treated and combined with urban stormwater to augment the storage of the coastal aquifers. The geology of Atlantis is made up of unconsolidated Cenozoic sediments with an average thickness of 25 m that is situated on bedrock strata mainly phyllitic shale and greywacke. Groundwater occurrence can be found in the bedrock and has a moderately steep gradient towards the coast. Groundwater abstractions are generally taken at a depth of 35 m, but they can vary from place to place. (Tredoux et al., 2020).

2.7.6 System structure and design

The infiltration pond in Atlantis is practised around the southern Witzand wellfield due to its favourable geological and topographical terrain as shown in (Fig. 2.7). The infiltration area is made up of 12 retention and detention basins with connecting pipes. The connecting pipes carry treated wastewater and urban stormwater with varying salinity and regulated flows into the basins (Tredoux et al., 2020). Water having a high salinity level is pumped into the coastal basins or in the River Donkergat, whiles waters with low salinity flows are used for recharging the aquifers up gradient — the water is diverted into two large spreading basins around the Witzand wellfield. The capacity of the recharge basin during storm-water discharges in Atlantis can be as high as 72,000 m^3/day. Similarly, during times of no rainfall or in the summer, groundwater baseflow can reach an average of 2160 m^3/day. The average recharge from the storm-water and wastewater infiltration in the Witzand wellfield is 1.5×10^6 to 2.5×10^6 m^3/yr. As a means of controlling seawater intrusion into the Witzand wellfield aquifers and also reducing its salinity level, the treated wastewater, urban storm-water and softening plant regenerant brine are together discharged into the coastal recharge basins and this can also be high as 2 million m^3/yr. Artificial basin recharge in Atlantis has proven to be a cost-effective method over the last 20 years serving domestic and industrial purposes. However, water quality issues arising from the salinity levels in the water supply of Atlantis have been a major challenge. It is reported that salinity in the Atlantis aquifer originates from sources such as marine origin, shale leaching into the soil and water bodies and also salt aerosols that are blown from the Atlantic Ocean. Another issue is the decline of borehole yield in the Atlantis aquifer due to clogging. Over-pumping of the boreholes in Atlantis has permitted oxygen into the aquifers and subsequent biofouling problems causing extensive biological clogging of the production boreholes (Tredoux et al., 2020).

Fig. 2.7 *Coastal dune infiltration basin in Atlantis, South Africa (Tredoux et al., 2020)*

2.8 Water resources in Ghana

In Ghana, water supply to the inhabitants can be classified into two folds: the urban water supply and the rural water supply. The Ghana Water Company Limited (GWCL) is a government-owned utility agency established in 1965 under the parliament act (Act 310) to provide water supply and the construction of sewerage works to urban communities across the 16 regions of Ghana. Presently, 88 urban water supply systems are operational and the daily water production is estimated at around 871, 496 m^3/ day. The water supply coverage by GWCL is around 77%. This coverage is within some selected geographical areas and therefore is inadequate. In addition, with the increasing calls to extend coverages to other areas due to pressure on existing water resources, the water supply in the future remains uncertain (Cobbinah et al., 2016).

The Community Water and Sanitation Agency (CWSA) was established in 1998 under the parliament act (Act 564) to provide sustainable safe drinking water and sanitation services in rural communities and small towns in Ghana. The CWSA has also extended its mandate in the direct management of water supply systems. It operates in all 16 regions of Ghana and so far has provided over 30,000 boreholes fitted with hand pumps and hand-dug wells. In addition,

from 1994 to 2021, the delivery of pipe systems for small community systems (n=71), small towns piped schemes (n= 504) and mechanised systems (n=125) have been done across the country. Boreholes installed with solar pumps (n=18,009) and a rainwater catchment harvesting system (n=110) have been completed and added to the existing schemes (CWSA, 2021).

All the boreholes are situated in the crystalline basement igneous and metamorphic rocks, the sedimentary Voltaian rocks and the Mesozoic rocks of Ghana (Dapaah-Siakwan & Gyau-Boakye, 2000). These host important groundwater resources and are used exclusively for domestic and irrigation water supply. The groundwater quality is very good except in some places in Greater Accra and Central regions where saline waters have intruded the aquifers making the water unsafe for drinking (Kortatsi & Jorgensen, 2001). In northern Ghana, agricultural farming and livestock rearing are the main occupations of the people. The people use groundwater to irrigate their farms ranging from small, and medium to large size. Government and Non-Government Organizations (NGOs) are implementing several irrigation schemes. The irrigation schemes used are smallholder and large-scale irrigation. The small scale irrigation uses buckets or irrigation cans to take water from hand-dug wells for irrigation usually up to 0.5 ha (Kortatsi, 1994). However, during the dry season, most of the farmers do not get sufficient water for irrigation mainly due to water scarcity. There are reported cases of declining water levels in Northern Ghana due to unfavourable weather conditions (Martin, 2006). These have some repercussions for dry season -irrigation farming (Kwoyiga & Stefan, 2019).

2.8.1 Managed aquifer recharge (MAR) in Ghana

Considering the relevance of agricultural irrigation farming to the people of Northern Ghana, and taking a clue from other successful MAR schemes in Africa, it is imperative to employ MAR technology to provide all-year-round water for sustainable farming. Gradually, there is a paradigm shift from water supply management to a demand-driven approach and this requires a holistic MAR investigation to address water scarcity.

In Ghana, MAR is gaining attention and emerging MAR schemes can be found in northern Ghana. One of the schemes is being piloted in the Jagsi and Kpasenkpe communities in Northern Ghana and the Weisi community in the Upper East region of Ghana by the International Water Management Institute (Owusu et al., 2017). These are flood-prone areas that employ Bhungroo Irrigation Technology (widely used in India for floodwater harvesting) to secure water for vegetable production. This technology is akin to the artificial recharge and recovery (ASR) method, which harvests excess floodwater, stores the water in the unsaturated zone and later abstracts the water for use. The design of the Bhungroo scheme consists of a

rectangular infiltration bed of depth of 3 m, a borehole connected with a pipe of a diameter of 5 m and a length of 40 – 60 cm above the ground surface (Owusu et al., 2017). The borehole depth ranges from 18 m to 39 m based on the geology of the three communities. The infiltration bed receives the raw stormwater and consists of materials such as gravels, coarse sediments and activated charcoal to purify the odour quality issue, especially in the Weisi community. The pipes serve as a medium for conveying the stored water and the water to be abstracted. The scheme additionally has an overhead storage and distribution tank and a sprinkler system to irrigate crop farms. Hydrogeological investigations conducted indicated that transmissivity values of the borehole ranged between 6.32 m^2/day and 7.60 m^2/day. The pumping test results further indicated that there were high water recovery rates and generally the boreholes have a success rate of 50% to 85% (Owusu et al., 2017).

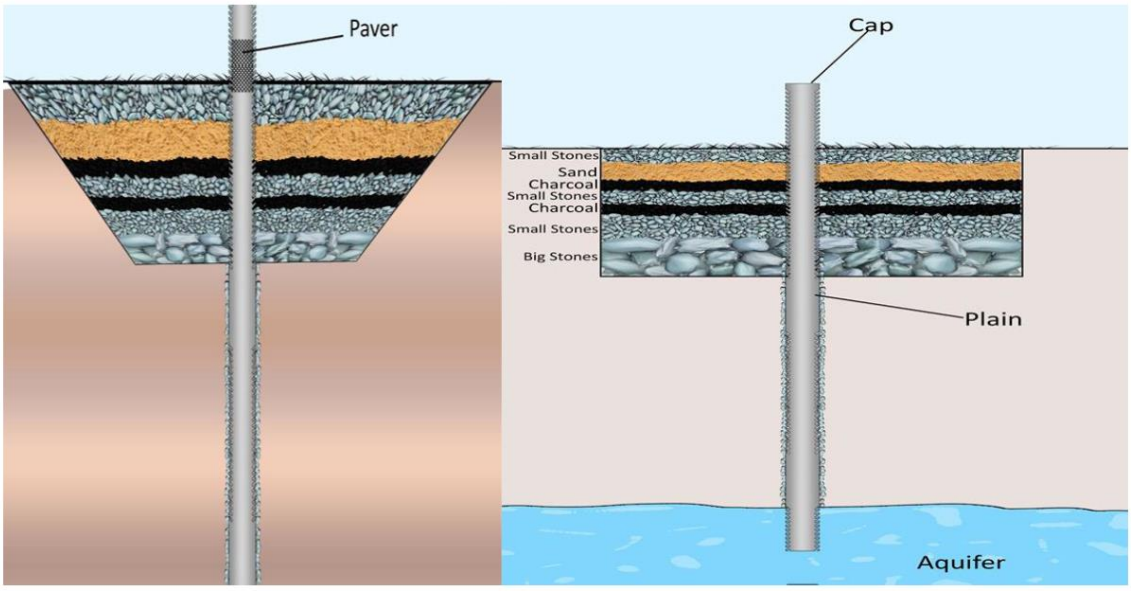

Fig. 2.8 *Pave irrigation technology and infiltration system consisting of different materials (Conservative Alliance, 2015).*

The PAVE irrigation technology (PIT) is also another MAR scheme found in communities such as Talensi, Karaga, Savelungu Nanton, and Tolon Kumbungu of Northern Ghana. This scheme ensures that the small–scale farmers have enough water for vegetable production during the dry season. The PIT harvests excess rainwater or flood water, filters and infiltrates it into the aquifer for storage. The design of the PIT scheme consists of a vertically drilled borehole installed with PAVE pipes and an infiltration system around the borehole to purify and treat the raw water injected into the aquifer as shown in (Fig. 2.8). The infiltration system is made up of different local and carbonization materials that purify the water for acceptable quality. Solar or

motorized pumps are installed to distribute and lift water for agricultural farming. The PIT can accommodate 4- 40 million litres of water (Conservative Alliance, 2015).

2.9 Knowledge gaps

In Africa, the current water management situation has necessitated the use of MAR technology to augment the shortfall in the water supply. A large part of the problem is a result of climatic change and the pressure on existing water resources. The majority of the MAR sites can be found in some arid cities in South Africa and North Africa, with little discussed about West Africa. Considering the arid nature and climatic condition of North African countries such as Morocco, Tunisia and Egypt which have had successful MAR applications, an important question is “can MAR application be replicated in Northern Ghana having similar climate conditions to the above-mentioned countries? The knowledge gaps are elaborated below

a. Even though emerging MAR schemes (Bhungroo and the PAVE irrigation technology) and MAR studies such as site selection mapping and institutional feasibility have been conducted in Ghana. There is growing evidence that the people of Northern Ghana are still experiencing water scarcity during the dry season. The reports on MAR studies and hydrogeological characterization are very limited and as such are not recognized by IGRAC which managed the global MAR portal.

b. There is little insight in the groundwater modelling studies in Africa to assess the feasibility of managed aquifer recharge and to obtain information on the maximum recharge and recovery rate.

c. There is no insight into the water quality guidelines for MAR implementation in Africa. In Asia, India has Indian Guidelines for MAR and this is applied only when data on water qualities are sporadic (Dillon et al.,2014). There are also Australia MAR guidelines and Water Framework Directive and Groundwater Directive (2006/118/EC) used in Australia and Europe, respectively but water quality guidelines about Africa are lacking.

CHAPTER 3

3.1 Study area, climate, materials and methods

The study area (Garu-Temapane) is located in the northeastern part of the Upper East region of Ghana (Fig. 3.1). The region is one of the 16 administrative regions of Ghana with Bolgatanga as its regional capital (Fig. 3.2). It shares an international border with the Republic of Togo to the east, to the south by East Mamprusi district, to the north by Burkina Faso and to the west by Bawku Municipality. The area has a total land size of 1230 square km and marks the highest point in the Upper East region of Ghana (Ghana statistical service, 2010). The topography of the area is flat, especially in areas close to the White Volta River, with heights ranging between 120 m and 150 m above sea level. The other parts of the area comprise a series of plateau surfaces of an average height of 400 m and with isolated peaks of 430 m above sea level. The study area falls under the White Volta River basin of West Africa and comprises three sub-basins: the Tamne River basin, Morago River and Biankuri River basins, and the White Volta River and Nahau River basins (SNC-Lavalin/INRS, 2011). Several rivers and streams drain the catchment of which the dominant one is the Tamne River, which lies in the northern part, and is a tributary of the White Volta River in the southwestern part (Fig 3.3).

Fig.3.1 *Map of Ghana showing all the sixteen administrative regions and the study area (Garu-Tempane district) located in the northeastern part of the Upper East region.*

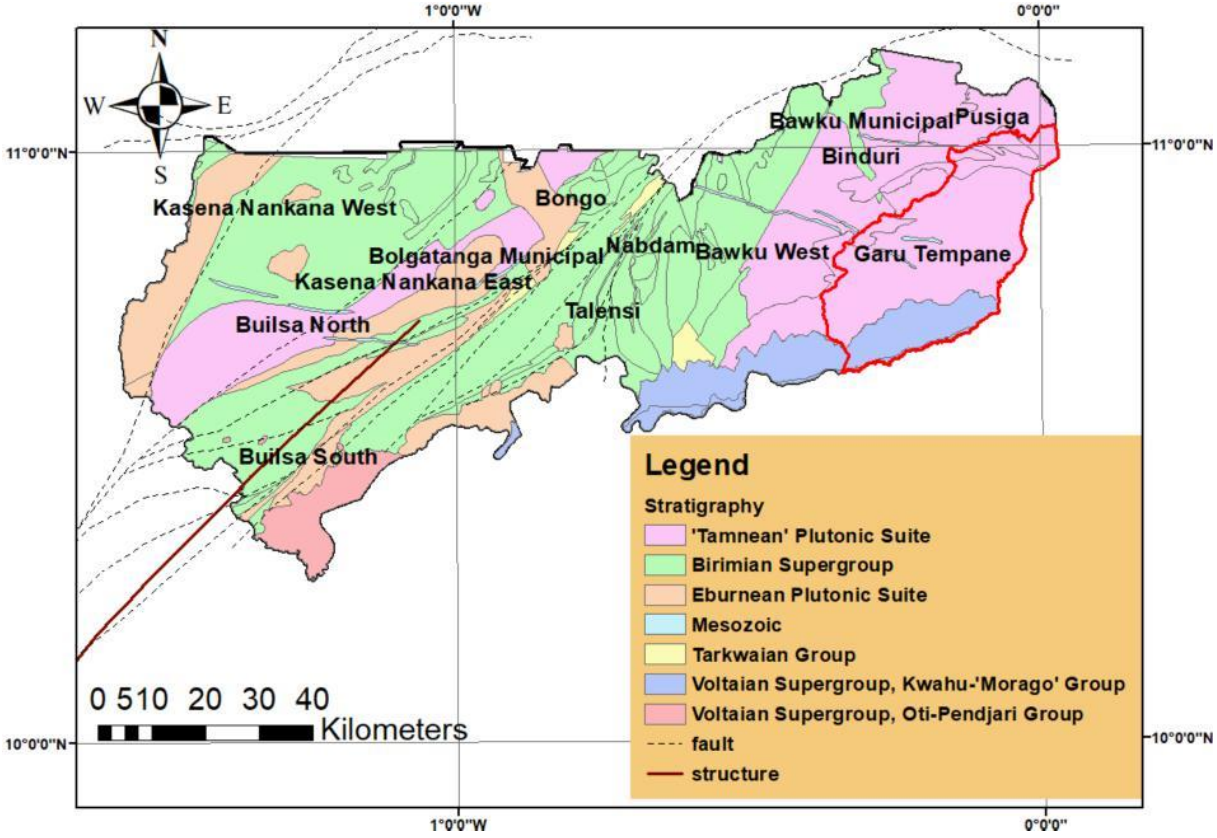

Fig.3.2 *Map of Upper East region of Ghana showing the various districts including the study area (Garu-Tempane). (Generated from the database of SNC-Lavalin/INRS, 2011)*

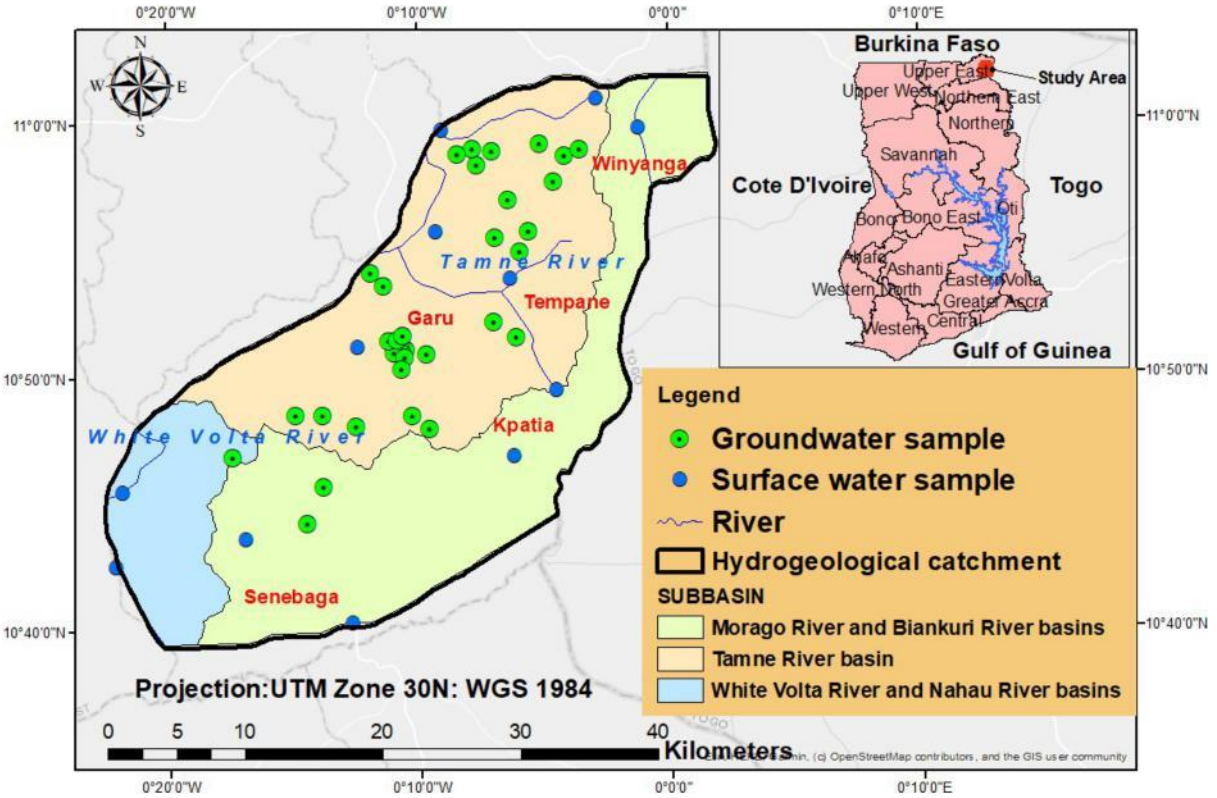

Fig. 3.3*. Location of the study area showing the sampling points and the sub-basins.*

3.2 Climate condition

The circulation of the Intertropical Convergence Zone (ITCZ) that brings dry northeast trade winds (Harmattan) and moist southwest monsoon winds mainly controls the climate of the area. The ITCZ affects the rainfall amounts and intensity of an area (Obuobie, 2008). The rainy season is unimodal, which occurs from May to September, followed by a prolonged dry season that extends from October to April (Issahaku et al., 2016). The rainfall amount ranges between 669.8 mm and 1339.4 mm, with an annual mean of 935 mm. In contrast, the highest temperature of 45° is recorded in March and April, and the lowest temperature of 12°C is recorded around December with an annual mean temperature of 28.7°C (Asamoah & Ansah-Mensah, 2020). The potential evapotranspiration rate in the White Volta River basin has been reported at around 910 mm/yr, and this exceeds almost all the monthly rainfall rates except in June, July, and August, where the highest rainfall amounts are recorded (WRC, 2008). Figure 3.4 shows the long-term rainfall and potential evapotranspiration of the regional capital (Bolgatanga) which has the same climatic conditions as the study area.

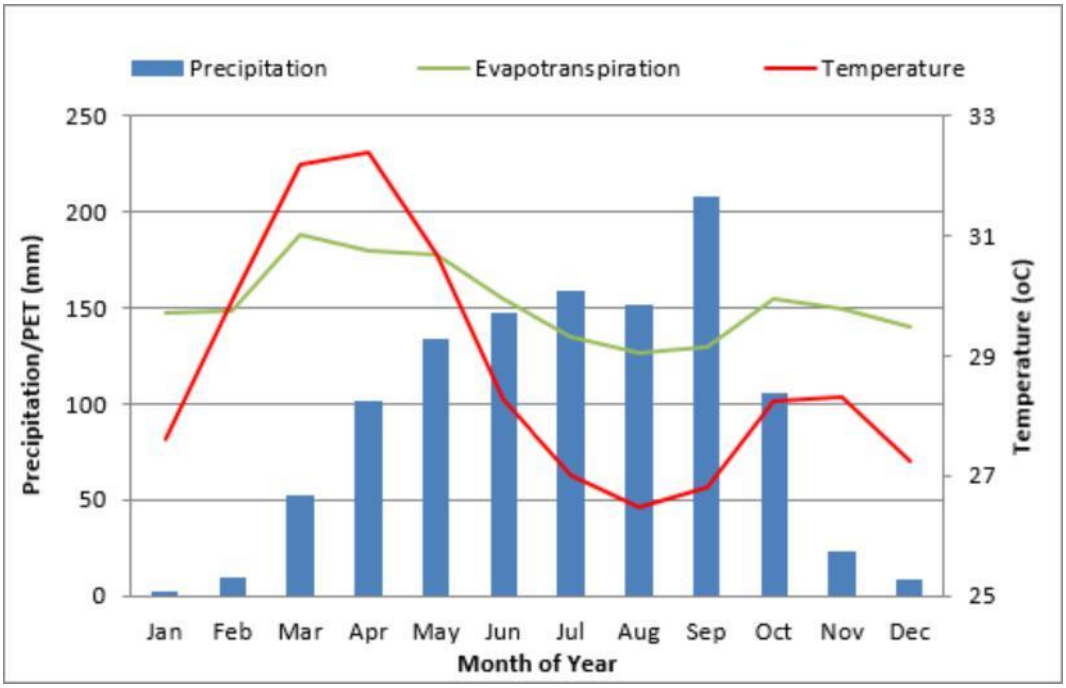

Fig. 3.4 Potential evapotranspiration and rainfall patterns of the regional capital (Bolgatanga) (source Amgraf 2017)

3.3 Vegetation and Soil

The vegetation in the study area consists mainly of widely open-cultivated and open cultivated savannah woodlands (Fig.3.5a). The main economic trees in the study area are *Parkia biglobosa* (dawadawa tree), *Adansonia digitata* (baobab tree) and *Vitellaria paradoxa* (shea

butter tree). During the dry season, the grasses and herbs in the savannah woodlands are exposed to bush burning and these leave traces of unclassified bushfire vegetation separated by deciduous trees. There are protected vegetative forest reserves that serve as sites for livestock production in the area, and these are Denugu, Kpatua, Karateshie and Tarivargo forest reserves. The riverine vegetation is found along the White Volta River in the southwestern part of the district (Ghana statistical service, 2010).

The soils in the district are formed because of the chemical weathering of the underlying rocks. Four soil types overlie the area: Gleysols, Leptosols, Lixisols and Fluvisols (Fig. 3.5b). The lixisols are predominant in the district and they consist of reddish-brown sandy loam and clays that support crop production. Lithic leptosols and dystic leptosols are found in the northern and southern part of the district respectively and comprise a pale brown coarse sandy loam with biotic granite. Eutric gleysols are mostly saturated with water and are sparsely scattered in the district. Limestone deposits, which serve as the raw materials for the economic production of chalk and paint, are reportedly found in the western part of the study area at a location called the Worikambo area. (Ghana statistical service, 2010).

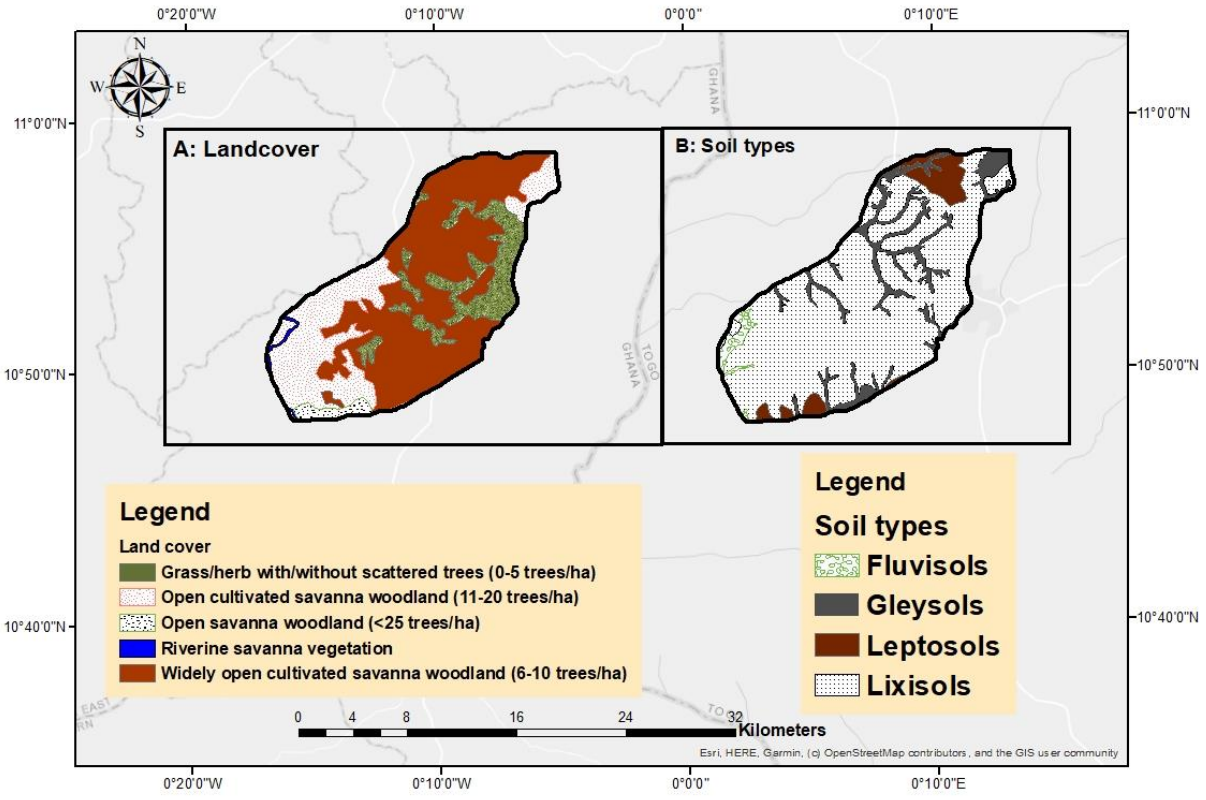

Fig.3.5 *(a) Landuse cover (b) Soil types in the study area (Generated from the database of SNC-Lavalin/INRS, 2011)*

3.4 Methodology

The methods employed can be categorized into three main groups (1) hydrochemistry and stable isotopes geochemistry (2) groundwater age dating and (3) numerical groundwater modelling as shown in (Fig. 3.6). Fieldwork was conducted for the groundwater and surface water sampling earmarked for hydrochemical, stable isotopes and groundwater age dating analyses. Laboratory analysis was performed within two months after collection and the results were processed using ArcMap 10.8.1, SPSS Version 26.0, Excel, PHREEQC, AQUACHEM and USGS TracerLPM. For the groundwater modelling, a desk study was conducted to know the hydrogeological condition of the area. Secondary data such as borehole drilling logs, storage parameters, pumping tests, and topographical and geological maps were collected from Community Water and Sanitation Agency (CWSA), Water Resources Commission (WRC), and the Center for Scientific and Industrial Research (CSIR). The model was developed using Groundwater Modelling Software (GMS 10.4) whereas the borehole lithology models were developed using RockWork20 and Strater5. Shapefiles for geology, soil vegetation and study area were generated from the database of Hydrogeological Assessment of the Northern Region of Ghana Project (HAP). Digital elevation model 90 m was taken from (earthexplorer.usgs.gov).

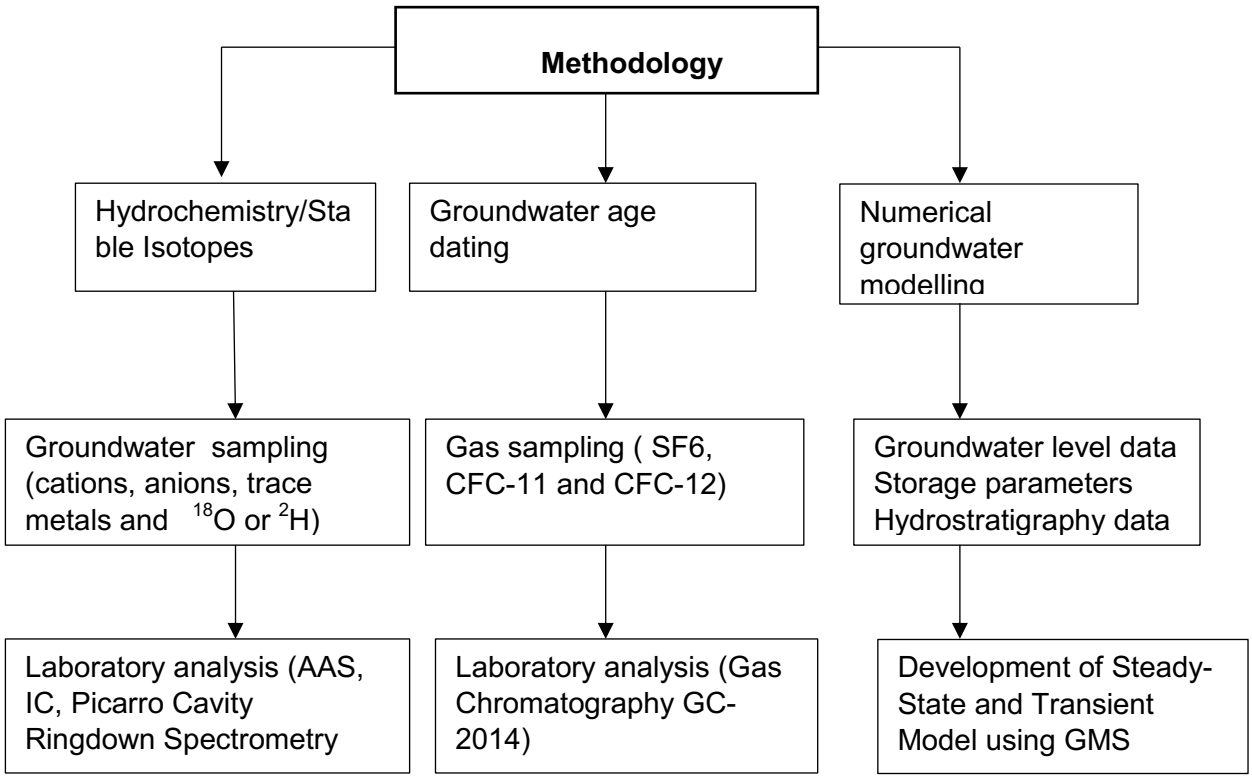

Fig .3.6 *Flowchart showing the field methods and laboratory analysis*

3.4.1 Field sampling of major ions, trace metals and stable isotopes

Thirty–eight (38) groundwater samples were collected from shallow wells between October and November 2019. Parameters such as temperature, pH and dissolved oxygen were measured directly on the field after purging the well for about 10 minutes. The in-situ parameters were measured using a well-calibrated Multi Probe Meter (PCE-1). Alkalinity was also determined on the field through the titration method using the Hach digital titration cartridge Pipette. This was done by adding a bromocresol green indicator into a flask containing 1000 mL of water. Titration with sulphuric acid (1.60 normality) was slowly done until the colour changed to pink (Fig.3.7a). The reading on the digital pipette was then expressed as equivalent concentrations of $CaCO_3$ in mg/L. Groundwater was then sampled each for cations and anions in clean 50 ml plastic bottles with rubber stoppers. The samples labelled for cations were acidified with a few drops of nitric acid (HNO_3^-) to preserve the cations and prevent bacteria and oxidation reactions. For the stable isotope, 50 samples (38 groundwater samples and 12 surface waters) were collected each in 40 mL glass vials sealed with a poly cap. The glass vials were filled with water leaving no air space to avoid isotopic exchange with the air.

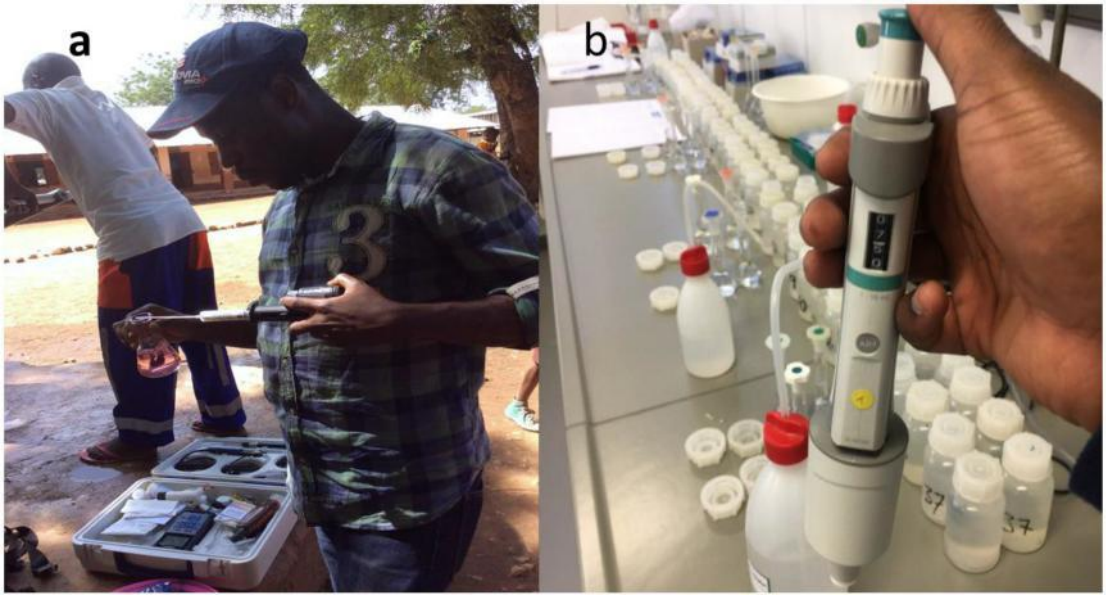

Fig. 3.7 *(a) Researcher performing a digital alkalinity titration of groundwater in the field (b) sample preparations of the groundwater samples for hydrochemical analysis*

3.4.2 Field sampling of sulphur hexafluoride (SF6) and Chlorofluorocarbons (CFCs) gases

The water was allowed to overflow the glass bottle by several litres to remove excess air in and around the glass bottle. The bottle was closed with a rubber seal cap inside the container. In

the next step, the water sample was turned down to detect any gas bubbles, and where gas bubbles were seen, the method was repeated. While the bottle was inverted, a headspace volume (approximately 0.2 L) was created by adding nitrogen gas and, at the same time, taking some of the water using a displacement syringe. The addition of nitrogen gas ensures that no outside air contaminates the sample. The sample was vigorously shaken in the closed bottle and allowed to settle for some minutes to reach equilibration between the gas headspace and the water. The gas was then extracted using two-end disposable needles: one connected to the 1L glass bottle and the other to a 22 mL glass vial containing ultra-pure water (Fig 3.8). A gas-tight syringe (30 mL) was inserted into the 22 mL glass vial to remove the water from the vial and simultaneously draw the gas from the headspace into the vial. Precautions were undertaken to avoid contamination with the outside air, and the samples were taken in triplicate at each sampling site.

Fig. 3.8 *Researcher extracting SF6 and CFCs gases from the groundwater into 22 mL glass vials (Field Photo 2019)*

3.4.3 Sample preparations and laboratory analysis

The various analytical methods and instruments were used to analyse and prepare the samples in the laboratory. Thirty-eight groundwater samples were measured for the major

cations and anions using Methrom 882 Compact Ion Chromatography Plus. Iron and manganese were also analyzed using Atomic Absorption Spectrometry ContrAA® 300 at the hydrochemistry laboratory Institute of Applied Geosciences, Technical University of Darmstadt, Germany. In the first place, the water samples were filtered through a membrane of 0.45 µm to remove larger particles and suspended materials. A volume of water was then pipetted into two sets of 25 mL measuring flasks (cation and anion flasks) and these were diluted with distilled water (Fig.3.7b). The dilution factor (DF) depends on the respective electrical conductivity of the groundwater samples. A dilution factor of 15 implies that the original sample is now contained in 15 times higher volume and is often referred to as a dilution of 1:15. It must be noted that a dilution of 1:15 always means adding 1+14 volumes. A groundwater sample with > 300 µS requires a DF of 3.33 as shown in Table 3.1. The diluted water was then poured into a vial, which was filled to the brim. The digital pipette and the measuring flask were rinsed three times with sample water after every use. For calibration, a standard solution of $A7^{+}$ was used for the analysis. A 625 µL master solution was added to both anion and cation samples with an additional 37 µmL of nitrate added to the anion samples.

Table 3.1 Dilution factors and range of conductivity used to prepare the samples

Sample Volume	**Dilution Factor**	**Conductivity**
10 mL Sample	DF 2.2	>300 µS conductivity
7.5 mL Sample	DF 3.33	>500 µS conductivity
5 mL Sample	DF 5	>850 µS conductivity
3 mL Sample	DF 8.33	>1.5 mS conductivity
2 mL Sample	DF 12.5	>2 mS conductivity
1.5 mL Sample	DF 16.67	>2.8 mS conductivity
1.0 mL Sample	DF 25	>3.5 mS conductivity
750 µL Sample	DF 33.33	>4.2 mS conductivity
500 µL Sample	DF 50	>6.5 mS conductivity
300 µL Sample	DF 83.33	>9 mS conductivity
200 µL Sample	DF 125	>18 mS conductivity
100 µL Sample	DF 250	>30 mS conductivity

3.4.4 Ion Chromatography

The concentrations of the major cations and anions were determined using Ion chromatography. This consists of an auto-sampler, pump, separator system, and detector as shown in (Fig 3.9). The auto-sampler picks the sample from the vial using a 2-µL syringe and injects it into the separator system. The machine measures the concentration of ionic species by separating them based on the charged properties of the molecule and their interaction with the resin. The sample solution passed through a column that consists of stationary phase material. This typically consists of a resin or matrix gel made up of agarose or cellulose beads.

A buffer solution (mobile phase) carries the sample through the column. The target analytes (anions or cations) are absorbed in the stationary phase where they begin to separate from it. The retention time of different species determines the ionic concentrations in the sample. The retention time also known as elution time represents the time taken by the ion to move through the column. Peaks, as shown in (Fig. 3.10), represent the concentrations of ions in the column. The detection limit of the IC is less than 1 ug/L.

Fig. 3.9 *Laboratory photo of the Ion Chromatography 882 Compact IC plus*

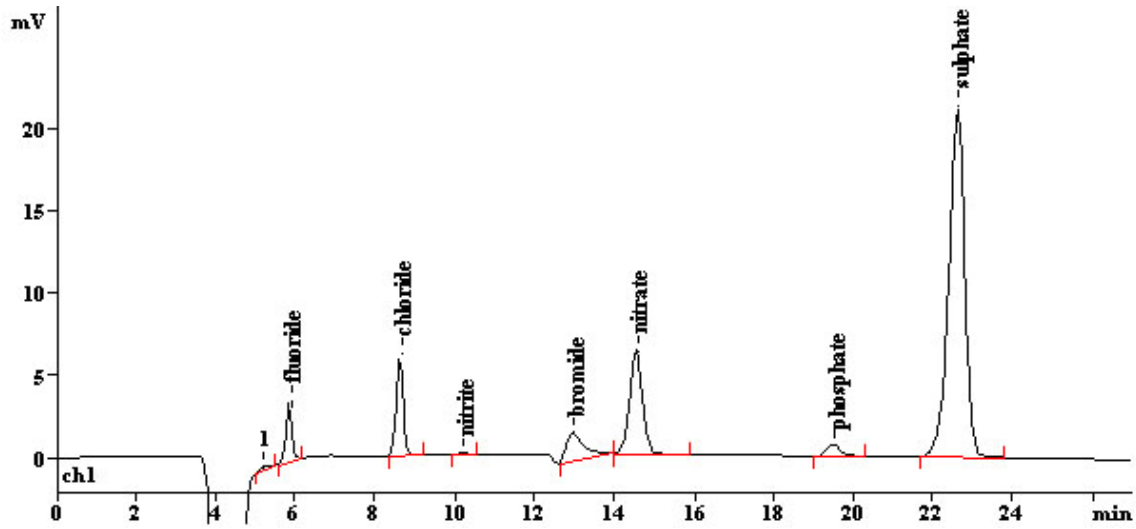

Fig. 3.10 *Graph showing anion output from an Ion chromatography. The ion concentrations were calculated from the area under each peak, where a larger area depicts a higher concentration of a specific ion species*

3.4.5 Atomic Absorption Spectrometry

The groundwater samples were also analyzed for only iron and manganese using Atomic Absorption Spectrometry ContrAA® 300 (Fig.3.11). The device works by using a flame to atomize the samples. Other atomizers such as graphite furnaces were also used. It consists of three chambers; desolvation chamber, vaporization chamber and volatilization chamber. First, the auto-sampler takes water samples from the flask with a syringe and injects them into the Hollow Cathode Lamp (HCL), which contains noble gas of neon and argon. The liquid solvent is evaporated and left the dry sample in the desolvation chamber. It is then vaporized into gas in the vaporization chamber where finally the sample is broken into free atoms in the volatilization chamber. This atom absorbs ultraviolet from characteristic wavelengths and is excited to higher energy levels. The wavelength of the light emitted is measured by a detector and compared to the original wavelength of the sample. A signal processor incorporates the changes in wavelength absorbed, which are represented as peaks of energy absorbed at discrete wavelengths. A calibration curve is used to produce and compare known quantities of elements when measuring an amount of an element present in a sample. For this curve, a specific wavelength is selected where a detector measures the wavelength of the energy transmitted. As the target atom concentration increases, there is a proportional increase in absorption in the sample. The measured absorption is then plotted at each concentration to produce a straight line between the resulting points.

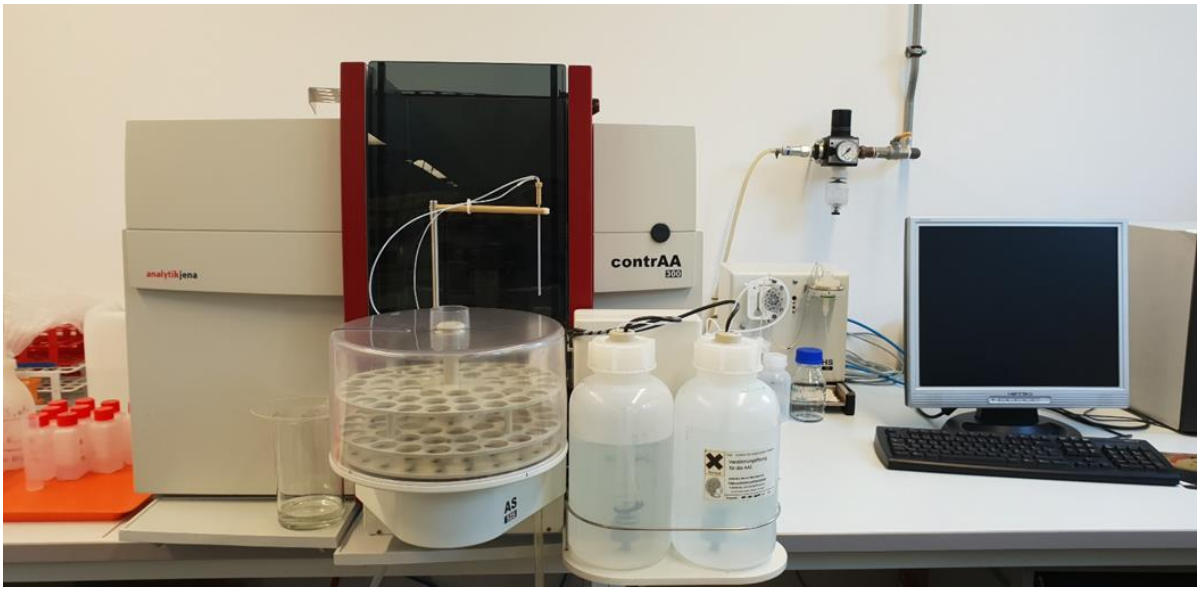

Fig. 3.11 *Laboratory photo showing the Atomic Absorption Spectrometry used in the analysis of iron and manganese*

3.4.6 Stable Isotopes Analysis

Thirty-eight groundwater samples and twelve surface waters were analyzed for $\delta^{18}O$ and $\delta^{2}H$ using Picarro Cavity Ringdown Spectrometry (Model L2130-i) equipped with a CTC auto sample (Fig. 3.12). This machine also consists of a vaporizer (110°C), a long cavity, which is 25 m long inserted into metallic hardware, and two wash stations for the pre and post cleaning of the syringe (containing ultra-pure water,18.2 MΩcm at 25°C and methyl pyrrolidone solution), and two pumps. A highly purified nitrogen gas (99.999%) was used as a carrier gas and supplied to the device at 200 SCCM and a pressure of 2.5 psi. It also has an analyzer software that regulates the measurement and displays it on a screen connected to the instrument. The pre and post-cleaning can be regulated by the user`s needs (Mariani, 2013). The samples were prepared into a glass vial and arranged into the autosampler tray with standards. The standards used are listed below in Table 3.2. The vials were arranged in a proper order into autosampler trays where the samples were pre-cleaned. A syringe embedded in the autosampler automatically injects the water samples of approximately 2 µL into a vaporizing unit held at a high temperature of 110°C and the vapour is sent to the analyzer in dry nitrogen gas. The water vapour is then flushed into the cavity, usually kept at atmospheric pressure of 67 hPa, reducing the widening of spectral lines. The cavity temperature is stabilized at 80°C and this ensures high pressure and thermal stability. The water samples were corrected for memory effect and instrumental drift. A memory effect is detected when a measurement is affected by previously unavoidable traces of the sample in the syringe and cavity. To normalise or reduce this effect, it is critical to repeat the measurements at least 6 times and use the only last injections for assessing the sample. The Picarro instrument ensures a 24-hour drift below 0.2‰ and 0.8‰ for $\delta^{18}O$ and $\delta^{2}H$, respectively. To correct this drift, it is recommended to average the last three injections. The measured stable isotope concentrations were reported in delta per mil notation (δ‰) relative to the international VSMOW (Vienna Standard Mean Ocean Water) with analytical reproducibility of 0.025 ‰ for $\delta^{18}O$ and 0.100 ‰ for $\delta^{2}H$. Stable Isotope Calibration (SICalib, version 2.14j) excel sheet was used in the calibration of the isotopic results regarding the VSMOW and the in-lab standards.

Table 3.2 Various standards used in the stable isotopes preparations

Standards	$\delta^{2}H$	Stdeviation	$\delta^{18}O$	Stdeviation
Light water (LW)	-152.18	0.87	-20.29	0.11
Rainwater(RW)	-29.27	0.45	-1.61	0.08
Heavy water (HW)	19.08	0.63	11.76	0.10
Tapwater (CS)	-61.29	0.36	-8.59	0.02

Fig 3.12 *laboratory photo of the Picarro L2130-I Cavity Ringdown Spectrometry at the hydrochemistry laboratory of TU Darmstadt.*

3.3.7 Laboratory measurements of SF6 and CFCs gases

The SF6 and CFCs concentrations in groundwater were measured by purge and trap system with electron capture detector (ECD) gas chromatography (GC Shimadzu, 2014) at the department of biotechnology of water treatment laboratory, Brandenburg University of Technology (BTU) — Cottbus. The method described by Busenberg and Plummer (2000) was adapted and used for this study. The analytical setup consists of a mass flow meter (MFC, Aalborg Orangeburg USA) and a GC composed of four integrated functions: an inlet port, a column, a detector, and an evaluation system. The inlet port is equipped with a Rheodyne 6-port valve (Supleco, USA model 7000/7010), which is connected to a stainless-steel column trap (30 cm long) from WICOM Germany GmbH and filled with Porapak T (50/80 mesh). The Rheodyne 6- port valve can be switched to position A “load” and position B “inject”. In position A, the sample is loaded into the trap, while in position B, the carrier gas flows through the trap, and the samples are thus, flushed onto the precolumn in the Gas Chromatography. The carrier gas is helium that flows at a constant rate of 30ml/min. The column is 1 m long, packed with HayeSep Q (80/100 mesh), and placed inside an oven. This allows a temperature gradient to be driven. It has a starting temperature of 80°C, which is kept for 5 mins, and the mixture can be heated up to 180°C. The GC is equipped with two detectors: an electron capture detector (ECD) for detecting specific tracer gases (CO_2, N_2O, SF6, and CFCs) and a flame ionization detector (FID) for measuring organic compounds. Before injection, the gas sample in the vial

was purged with nitrogen (N_2) using the mass flow meter and a syringe (Hamilton, Switzerland). To remove the gas impurities from the glass vials, it was fixed to a trap, which was placed in a dry ice and ethanol mixture (- 70 °C) for 5 mins and the valve was set to position A. While in the cold bath, the sample was loaded into the stainless-steel loop to be injected into the GC via the 6-port valve. Subsequently, the trap was removed and transferred into a heat bath (95°C) for 5 mins to rerelease the immobilized tracer while purging was done with N_2 gas in a reverse flow of the gas. The temperature of the hot and cold bath was measured with the Vario Mag electronic stirrer mono thermometer. Next, the batch table and detector response on the computer was started. Finally, the valve was turned to position B so that the carrier gas (helium) directed the tracer into GC. Before the experiment, the GC was calibrated with standards prepared by the Technical University of Bremen. For the preparation of the calibration, lines 11, 22, 44 and 66 ml of the standard were directly injected at a temperature of 23°C and a pressure of 1005 mbar. The analytical uncertainty for the SF6 and CFCs gases was about 2%, which corresponds to a dating error of ± 1 year.

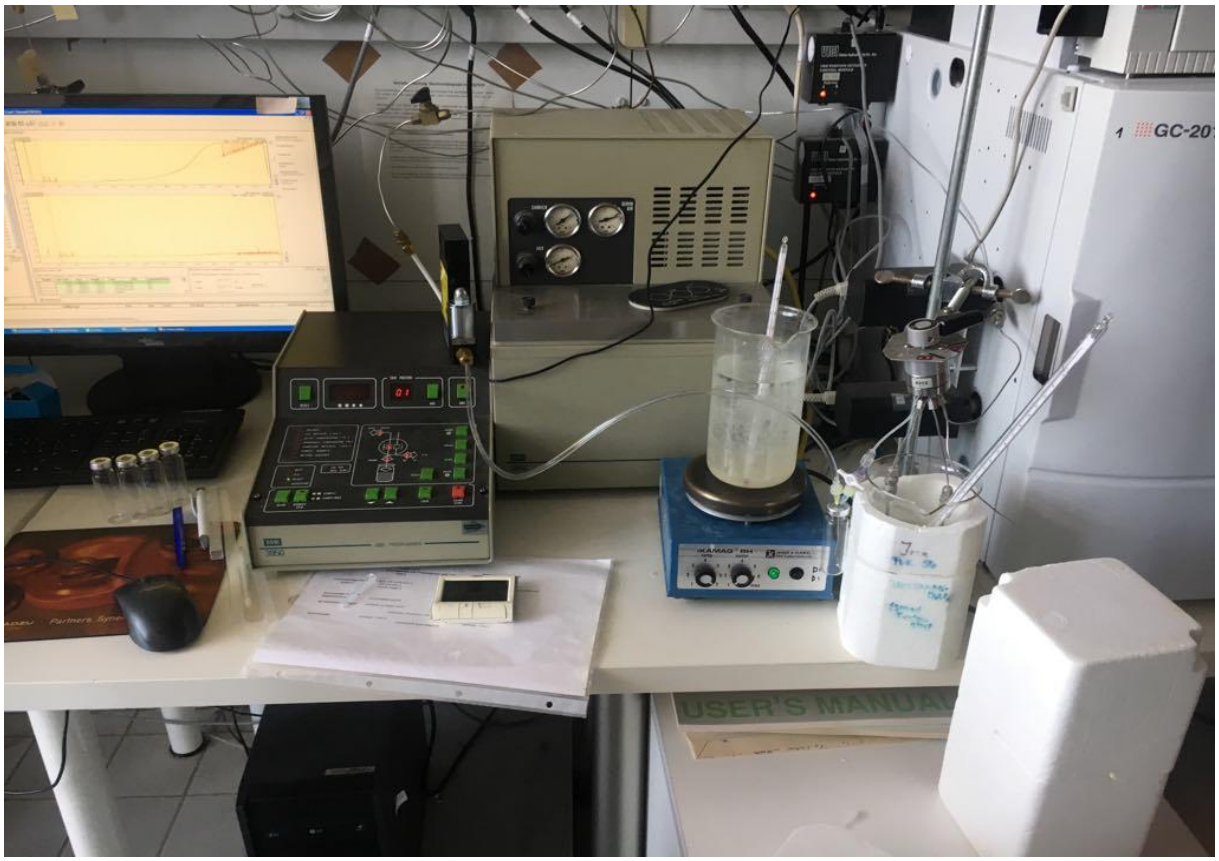

Fig 3.13 *A picture showing the analytical setup of the GC, Mass flow meter, a column and a detector. A 22ml glass vial containing a gas sample is first trapped in a cold bath for 5 mins. This was subsequently transferred to the glass warm bath and put on an electric stove. Thermometers were put in both the cold bath and warm bath to measure the temperatures of the water*

CHAPTER 4

Characterization of groundwater in the `Tamnean`Plutonic Suite aquifers using hydrogeochemical and multivariate statistical evidence: a study in the Garu- Tempane District, Upper East Region of Ghana

Reproduced from: Okofo, L.B., Bedu-Addo, K. & Martienssen, M. Characterization of groundwater in the 'Tamnean' Plutonic Suite aquifers using hydrogeochemical and multivariate statistical evidence: a study in the Garu-Tempane District, Upper East Region of Ghana. *Appl Water Sci* **12,** 22 (2022). https://doi.org/10.1007/s13201-021-01559-2

Abstract

The 'Tamnean' Plutonic Suite aquifer is the main public water used for the people of the Garu-Tempane District. Thus, hydrogeochemical characterization is essential to provide valuable insights into pollution sources and the main controls on groundwater chemistry. In this regard, multivariate statistical methods, conventional hydrochemical graphical methods and various ionic ratios complemented with PHREEQC geochemical modelling were carried out using 38 groundwater samples collected from the Tamnean Plutonic Suite aquifers, Ghana. The ionic ratio plots, the chloro-alkaline indices and the graphical diagrams indicate that the major sources of groundwater chemistry are silicate mineral dissolution and cation exchange coupled with the leaching of domestic solid waste and nitrogen-based fertilizers. The Q–mode hierarchical cluster analysis reveals three spatial groundwater zones. Groundwater from recharge areas consists of Ca —Na—HCO_3 water types in cluster 1. The intermediate zone is characterized by Ca—Mg—Na—HCO_3 water types of moderate ionic compositions in cluster 2; and this evolves into a discharge zone in cluster 3 mainly of Ca—Mg—Na—HCO_3—NO_3 water types. The principal component analysis (PCA) reveals three factors, which account for 81% of the total variance, and this suggests most of the groundwater chemistry had longer interaction with the lithological materials. The PHREEQC geochemical modelling consisting of mineral saturation index suggests that groundwater is supersaturated with respect to albite and undersaturated with respect to calcite, fluorite, gypsum and halite. Based on the Wilcox diagram and water quality index, the groundwater in the district is generally suitable for irrigation and drinking water purposes. All the samples are within the World Health Organizations acceptable limits for drinking water except for elevated nitrate and bromide concentrations, which occur in some of the wells. About 10.5 % of the groundwater samples are contaminated with nitrate, which may pose a health danger to the inhabitants of the communities. The finding of this study will not only contribute to solving the research paucity regarding the Tamnean Plutonic Suite aquifers in the Garu- Tempane district but will serve as a useful document for water managers and decision-makers in Ghana.

4.1 Introduction

Sustainable and quality water to meet global demand for agricultural food production and drinking water supplies are goals the world at large is striving toward (Dennehy et al., 2015b; E. Dişli, 2018). It is estimated that around 2.5 billion people depend on groundwater as a means of drinking water in the world (Dhar, 2017; Hölting & Coldewey, 2019). Despite this huge number, approximately 783 million people, who correspond to 11% of the global population still cannot find access to safe drinking water since 2012 (WHO, 2012). Furthermore, there is a projection that by the year 2025 and beyond, an increasing number of the world population will experience water scarcity (Lautze and Hanjra, 2014; World Health Organization, 2018). This development would significantly undermine the efforts toward achieving the United Nations Sustainable Development goals 6 (ensuring clean water and sanitation for mankind) (UN, 2015). Challenges arising from the ever-growing population, and the global climatic changes have severely affected precipitation patterns and groundwater recharge, thereby affecting the available water resources (Mook and Rozanski, 2000). In addition, the steady rise in excessive agricultural- irrigation practices coupled with the abstraction of groundwater for industrial purposes has exacerbated the negative impacts of groundwater quantity and quality (Ounvichit, 2011). While the challenge of ensuring sustainable management of groundwater resources has become a universal goal for most countries, the idiosyncrasies of groundwater use warrant a holistic diagnosis and approach (Okofo et al., 2021).

Groundwater availability for irrigation and drinking water purposes is often affected by geogenic and anthropogenic pollution and these are reported in several studies (Ashraf et al., 2017; Kirschke et al., 2019; Suciu et al., 2020; Zango et al., 2019). The anthropogenic source of pollution includes activities of mining, untreated solid and liquid waste, and intensive agriculture (Hölting & Coldewey, 2019). In the absence of functional effluent and waste treatment facilities, these pollutants are usually facilitated by rainfall events and seep into the groundwater. This eventually causes an impairment of the groundwater quality (Xanke et al., 2020).

In Ghana, the zeal of the farmers to increase their agricultural yields through the use of chemical and organic fertilizers has inadvertently caused elevated nitrate concentrations in groundwaters in some agricultural communities (Anornu et al., 2017; Egbi et al., 2020). Geogenic pollution, on the other hand, includes solutes emanating from the water-bearing rocks, which change the chemistry of the groundwater in space and time (Appelo & Postma, 2005). The chemistry of groundwater is greatly affected by geology, groundwater-rock interactions, precipitation of minerals, and their compositions (Appelo & Postma, 2005; Erkan Dişli & Gülyüz, 2020; Güler et al., 2002). To safeguard groundwater quality against non-point

and point sources of pollution, there is the need to assess groundwater periodically from a hydrogeochemical perspective.

Several techniques including conventional hydrogeochemical graphical and multivariate statistical techniques have been copiously used to understand the geochemical processes in the aquifer systems (Saravanakumar and Ranjith Kumar, 2011; Sunkari and Abu, 2019; Zakaria et al., 2020). Multivariate statistical methods such as principal component analysis (PCA) and hierarchical clustering are the most applied geostatistics in hydrological studies (Loh et al., 2020). Hierarchical cluster analysis is essentially used to discuss the groupings of groundwater samples that reflect the multiple sources such as natural or anthropogenic activities in the groundwater (Güler et al., 2002). It also helps to elucidate the main factors controlling the groundwater chemistry of an area (Güler et al., 2002).

The area under investigation falls under the White Volta Basin of Ghana. The primary source of public water consumption for the inhabitants is from the 'Tamnean' Plutonic Suite aquifer. Several boreholes are situated in this unique aquifer, where the people tap groundwater exclusively for drinking and irrigation purposes. Furthermore, the district is mostly a rural setting, which has no groundwater protection zone and program. This has been a major driver of worsening groundwater quality in most rural and peri-urban areas in Sub-Saharan Africa (Nyenje et al., 2010). It is, therefore, necessary to understand the water chemistry and quality in the area for groundwater resources planning.

Different researchers have used multivariate tools to elucidate hydrogeochemical studies in the White Volta Basin of Ghana. For example, Chegbeleh et al. (2020) studied the hydrogeochemistry of groundwater using principal component analysis (PCA) and hierarchical cluster analysis (HCA) in the Talensi District of the White Volta basin, Ghana. The PCA and HCA revealed silicate and carbonate weathering as the main conspicuous minerals controlling groundwater chemistry in the Birimian rock terrain of the district. Koffi et al. (2017) also characterized the hydrochemistry of the groundwater and surface in the Vea catchment and concluded that the groundwater is suitable for drinking and irrigation purposes. The results also indicated that silicate weathering and cation exchange are the major processes controlling groundwater chemistry in the Upper Birimian and Bongo granitic terrain of the area. Similar work conducted by Anim-Gyampo et al. (2018) also studied the hydrochemistry of groundwater in the Atankwidi basin and suggested silicate weathering as the major factor influencing groundwater chemistry in the Bongo granite terrain. Despite the numerous hydrochemistry studies, in the White Volta Basin of Ghana, none to date has been written in the study and for this reason; there is a paucity of research on hydrochemistry studies in the area.

Therefore, this paper presents an approach to (1) ascertain the natural baseline chemistry in the groundwater of the area and (2) elucidate the main factors controlling groundwater hydrochemistry and its evolution using principal component analysis (PCA) and hierarchical cluster analysis (HCA). The combination of these methods will help to identify the pollution sources in the area for improved groundwater management.

4.2 Geology and Hydrogeology

The area is underlain by two main geological formations: the Precambrian basement complex and the Voltaian Supergroup (SNC-Lavalin/INRS, 2011). The Precambrian basement complex is geologically subdivided into a Birimian supergroup consisting of volcanic and sedimentary rocks. These rocks have undergone systematic deformation and metamorphism and intruded by rocks of the Tamnean Plutonic Suite (mainly granitoids) formed during the Paleoproterozoic era ca. 2150–2070 ma (Feybesse et al., 2006). The Tamnean Plutoncic Suite covers about 80% of the district and comprises mainly hornblende-biotite granitoids, alkali granite, syenite, minor granodiorite, and minor quartz diorite and biotite tonalite (Fig.4.1a). The rocks are generally exposed as tabular hills and are found in the northern and western parts of the area.

The Voltain supergroup overlies the southeastern part of the district and falls under the Morago River and Biankuri river sub-basin. The Voltaian supergroup lies unconformably on the Tamnean Plutonic Suite and consists exclusively of fine-grained and locally bedded sandstones from the Tossiego formations (SNC-Lavalin/INRS, 2011). The study area forms an extension of the Gambaga scarp along the southeastern portion and the scarps are formed as a result of erosion and faulting of the sandstone rocks. There are small pockets of Mesozoic rocks that are rich in mafic dykes and dolerite in the area.

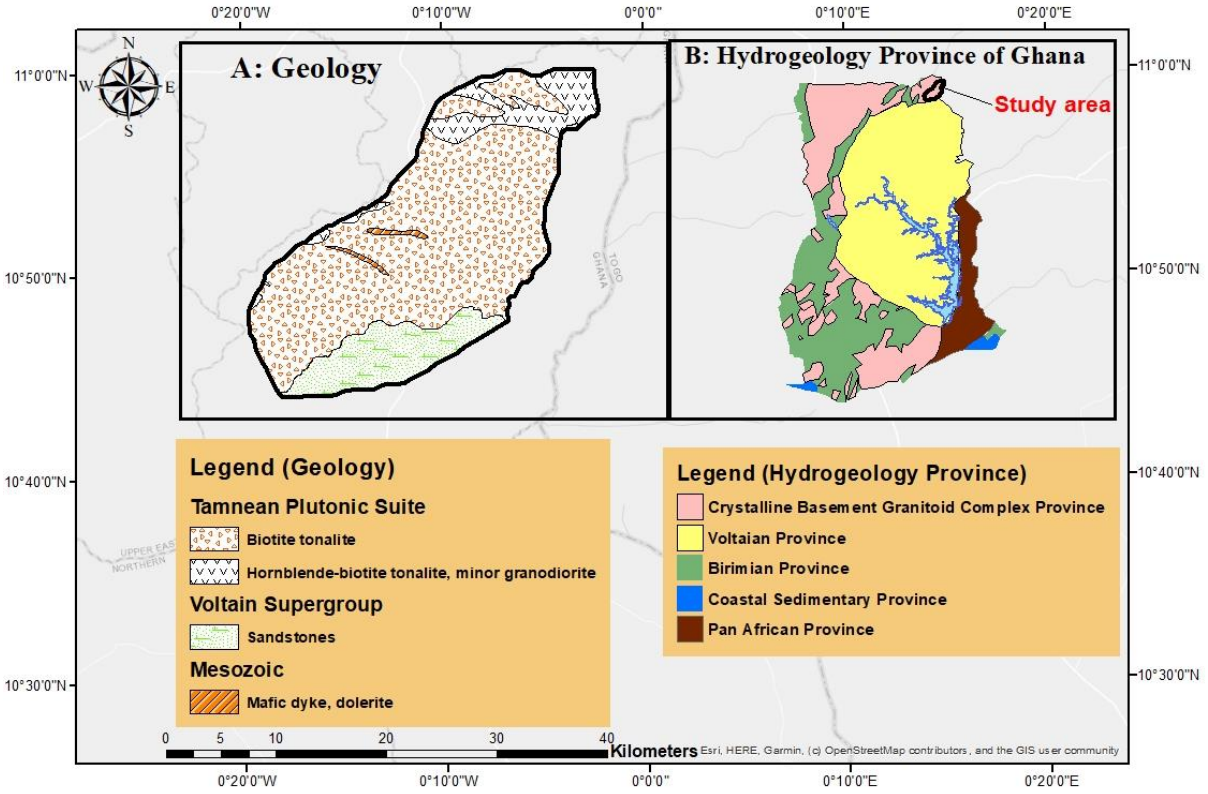

Fig.4.1 *(a) The geological map of the area (b) the hydrogeology provinces of Ghana after Banoeng-Yakubu et al. (2011)*

Hydrogeologically, the area under study is part of the Crystalline Basement Granitoid Complex Province and the Voltaian Province (Fig.4.1b) (Banoeng-Yakubu et al., 2011). The Crystalline Basement Granitoid Complex Province consists of aquifers of the Tamnean Plutonic Suites, which are considered a powerful body of groundwater. These aquifers are intrinsically low in permeability, however secondary porosity developed from chemical weathering and fracturing controls the groundwater occurrence in the area. According to Carrier et al. (2008), granitoids formations have borehole depths ranging from 35 m to 55 m with a mean depth of 50 m. Transmissivity has been reported to be in the range of 0.3 m^2/day to 114 m^2/day with an average of 6.6 m^2/day in granitoids terrains (Martin and van de Giesen, 2005).

In the Voltain Province, processes such as compaction and cementation have affected the primary porosity of the rocks and thus, groundwater generally occurs in the fracture zones and along bedding planes. (Dapaah-Siakwan and Gyau-Boakye, 2000; Carrier et al., 2008). Acheampong and Hess (1998) described the regolith thickness to be relatively thin, circa 9 m, due to the mixtures of clay, quartz and mudstone materials. This would imply that small amounts of water could be withdrawn locally in the Voltaian Province (Carrier et al., 2008). A study conducted by Acheampong (2017), in the Garu-Tempane district, using thirty-three drill

logs from the World Vision GI-WASH program indicates three main layers (Fig. 4.2). The first layer (residual soil) thickness is 6 m and consists of silty and sandy clay soil, and lateritic sandy gravels mixed with clay. The second layer (saprolite) is made up of slightly- completely weathered granite that overlies a fresh unweathered granite. The third layer comprises the saprock that overlie a fresh granitoid bedrock. The fracture zone is mostly found in the saprock under semi-confined and confined conditions. Groundwater generally occurs in the upper portion of the saprock and saprolite and the groundwater table on average ranges between 12 m –25 m (Acheampong, 2017). There is no established groundwater recharge and groundwater flow regime in the district, however, groundwater recharge in the White Volta Basin ranged between 3.4 and 18.4 % of the mean annual precipitation of 980 mm (Obuobie, 2008). The groundwater flow regime in the Upper East region is from the north to the south. The aquifers in the district have been reported to have good potential to sustain the inhabitants with yields high as 5.5 m^3/h (Gumma and Pavelic, 2013).

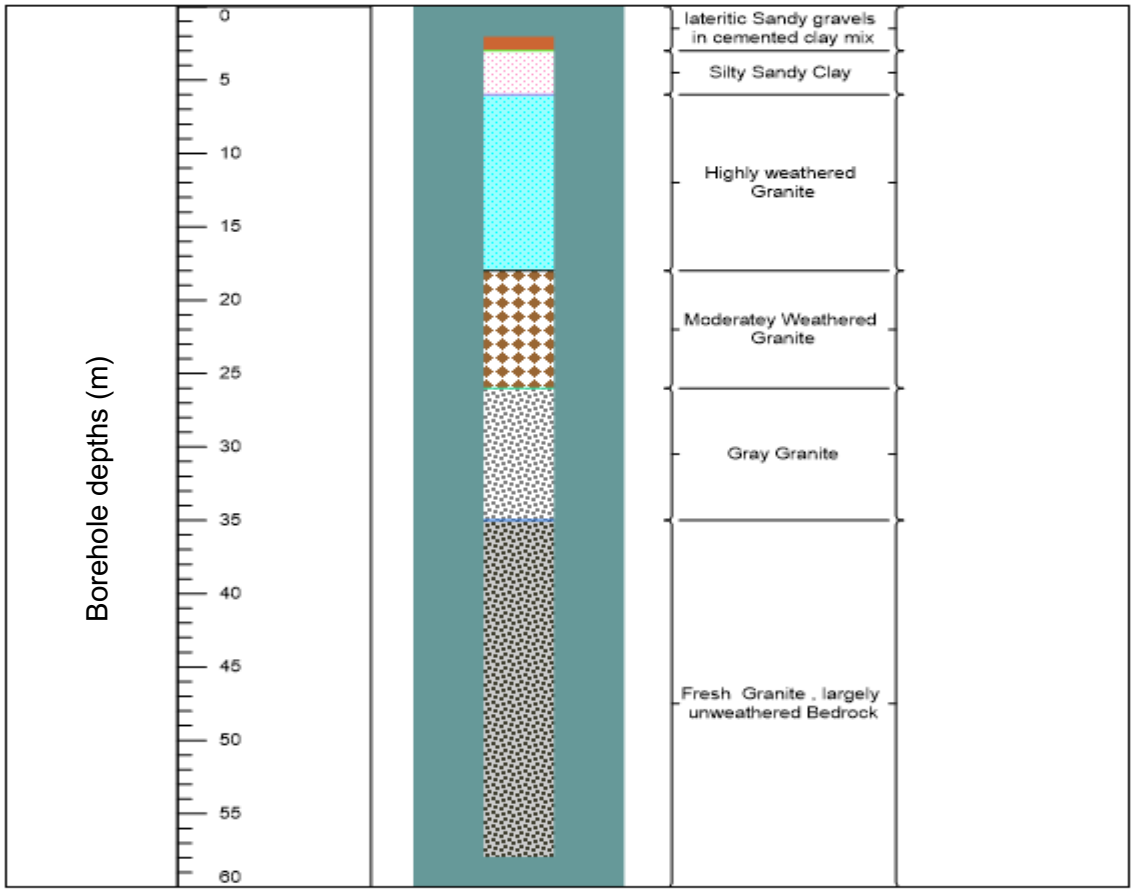

Fig. 4.2 *Hydrostratigraphy of boreholes in the study area*

4.3 Data analysis

SPSS software package version 26.0 was employed for the analytical methods to analyse the Pearson correlation, principal component analysis (PCA) and the hierarchical cluster

analysis (HCA). Pearson's correlation coefficient (r) analysis was carried out to determine the correlation and similarity between the hydrochemical parameters. The correlation coefficient between pairs of the parameters generated, and their significance was tested by the p-value (Table 2). The correlation coefficient lies between -1 and 1; where significantly correlated 30 parameter pairs have r > 0.5 and non-significant correlated pairs have r values less than 0.5 (Liu et al., 2003).

The principal component analysis method was performed to ascertain the key values in the dataset and to minimize the large datasets into a small dimensionality. This was used to explain the origin of the hydrochemical parameters and deduce geochemical meanings (Yidana et al., 2010) The dataset was first standardized and a correlation matrix was produced to determine the interrelationships between variables (R-mode analysis). To ensure that the number of components is minimized in the model, the Kaiser Criterion was adopted, which was constrained to only components greater than 1 (Kaiser, 1960). Varimax rotation technique was chosen to increase the variance of the retained components greater than 1. In the current study, some of the datasets such as PO_4^{3-}, NO_2^-, NH_4^+, and trace metals (Fe, Ni, Cr, and Mn) did have missing data, for which reason they were excluded from the statistical analysis. The HCA technique was further used to validate the results of the PCA by assembling the water samples into homogeneous clusters or groups on the assumptions of samples that are alike and at the same time unlike samples (Güler et al., 2002). To define these unique clusters, hydrochemical data were log-transformed and consequently standardised using equation 1. This was done to attain normal distribution, homogenize the variance, and ensure that there is no bias in the sampling population. This is because, during the use of Euclidean distance in hierarchical cluster analysis, the chemical variables with the greatest variance usually influence the smallest variables (Güler et al., 2002)

$$Z=\frac{X-mean}{Stdev} \quad (4.1)$$

Where Z is the standardized measurement and X is an individual sample measurement.

The Euclidean distance and Ward's linkage method were applied to generate two hierarchical cluster analysis dendrograms: R-mode and Q-mode HCAs by assembling similarity and dissimilarity clusters using 38 groundwater samples and 14 variables. These methods were chosen because of their rigidity evidence of wh is amply presented in numerous successful studies, where distinct homogenous clusters are joined such that an increase in the within-group variance is minimized (Cloutier et al., 2008).

4.3.1 Water quality index (WQI)

In this study, 15 chemical parameters were considered for the WQI. This computation is based on the premise of giving weights to each of the chemical parameters (wi) according to the relative importance of the WHO, (2017) drinking water guidelines. For example, elevated fluoride and nitrate concentrations in drinking water are of health concern, so they were assigned the highest weight of 5. The other chemical parameters such as Ca^{2+}, Mg^{2+}, TDS, and Na^{+} were given different weight values between 1–5 according to their importance. The computed WQI is expressed below in equation (4.2)

$$Wi=\frac{wi}{\sum_{i=1}^{n} wi} \tag{4.2}$$

Where Wi, is the relative weight, wi, is the individual parameter of a sample at a given location, and n is the total number of parameters.

In the next step, the concentration of the individual parameter is divided by the WHO standard limit of that parameter and multiplied by 100 to obtain the quality rating (qi), in equation (3)

$$qi=\frac{Ci}{Si}\times 100 \tag{4.3}$$

Where qi, is the quality rating, Ci, is the concentration of the individual parameter and Si, is the WHO standard limit value of the individual parameter.

The water quality index (WQI) of each location is finally determined from the subindex Si in Eq. (4) and (5)

$$SIi=Wi\times qi \tag{4.4}$$

Where $SIi,_{is}$ the subindex

$$WQI=\sum SIi \tag{4.5}$$

The spatial water quality distribution map (Fig.4.10) was interpolated using the inverse distance weighted in ArcGIS software 10.7.1. IDW interpolation was used because it is effective and robust, and can deal with densely even space points (Loh et al., 2020)

4.3.2 Chloro-alkaline indices

The chloro-alkaline indices (CAI) developed by Schöeller H, (1965.) were used to determine the ion exchange process that takes between the groundwater and the geological medium

during its residence time. The chloro-alkaline indices (meq/L) were computed using the expression in equations (4.6) and (4.7).

$$CAI1 = \frac{Cl-(Na+k)}{Cl} \quad (4.6)$$

$$CAI2 = \frac{Cl-(Na+K)}{SO4+HCO3+NO3} \quad (4.7)$$

4.4. Geochemical modelling

The mineral species in the groundwater were investigated by calculating the saturation index expressed in equation 4.8 (Parkhust and Appelo, 2013).

$$SI = \log\left(\frac{IAP}{Ks(T)}\right) \quad (4.8)$$

Where K_s (T) is the solubility constant for temperature-dependent of the mineral, IAP is the ion activity product.

Si = 0 mineral is in equilibrium with the solution

Si <0 mineral is undersaturated (may reflect mineral dissolution, if present in the water)

Si >0 mineral is supersaturated (may reflect mineral precipitation and mineral formation, if present in the water)

The Wilcox diagram and Piper diagram were graphically interpreted using Aquachem software version 4.0.

4.5 Results and Discussions

The descriptive statistics of the physicochemical parameters and the trace metals are presented in Table 4.1. Some of the on-site field parameters show a wide range of variance (Fig. 4.3). The groundwater temperature lies within the range from 31.1°C to 32.9°C with a mean value of 31.9°C. The groundwater temperature was higher than the recent average annual temperature (28.7°C) of the area (Asamoah and Ansah-Mensah 2020). This suggests that the heating of the groundwater is influenced by the local geothermal gradient (Reiter, 2001). Most of the areas have dissolved-oxygen concentrations of less than 1 mg/L indicating the water is non-oxidized. The mean value of the dissolved oxygen is 0.57 mg/L and varies from 0.4 mg/L to 1 mg/L. Electrical conductivity is the measure of all ionic solutes in water and is closely related to total dissolved solids (TDS). The conductivity of water can

vary temporally and spatially because of processes such as temperature, ion exchange, dissolution and adsorption. For instance, an increase in temperature generally shows an increase in electrical conductivity (Clark 2015). In the study area, specific conductance values range from 85.5 µS/cm - 593 µS/cm with a mean value of 249.86 µS/cm implying a general dilute to slightly mineralized water. The conductance displays high variance and standard deviation attributed to the mixing of diluted and mineralized water (Plummer et al., 2012). The total dissolved solids (TDS) values are less than 1000 mg/L indicating the water is very young and fresh (Freeze and Cherry, 1979). According to Hounslow (1995), groundwater usually has a moderately acidic pH ranging between 4.0 and 6.5; neutral pH between 6.5 and 7.8; moderately alkaline pH between 7.8 and 9 and alkaline pH above 9. The groundwater in the study area is moderately acidic to moderately alkaline with pH values ranging from 6.25 – 7.93 with a mean of 7.09. This indicates that about 10.5 % of the samples have pH values that are below the WHO permissible limit of pH (6.5- 8.5). The low pH value (acidic water) in the area is ascribed to carbon dioxide and man-made factors. Carbon dioxide derived from rain reacts with the water to form a weak carbonic acid (H_2CO_3) and hydrogen ion (H^+). The hydrogen ion released into the water can decrease the pH of the water. Another source of acidity in groundwater is the reaction of oxygen with iron sulphide minerals (FeS_2) (Candela and Morell, 2009). The total alkalinity, which is expressed as the equivalent concentration of calcium carbonate ($CaCO_3$) or bicarbonate (HCO_3^-) displays a high variance. A high value of 446 mg/l was recorded around the Yaratinga area in the northern part of the district. Low to medium bicarbonate values are dominant and scattered all over the area. The primary source of bicarbonate in groundwater is attributed to carbon dioxide in the atmosphere and in soil gases that dissolve in rain and surface water (Clark, 2015).

Table 4.1 Summary of the physiochemical parameters in the study area

Parameters	Min	Max	Mean	Std dev	WHO (2017)
pH	6.25	7.93	7.09	0.42	6.5 – 8.5
Temp °C	31.1	32.9	31.91	0.48	NA
O_2 mg/L	0.4	1	0.57	0.14	NA
EC (µS/cm)	85.5	593	249.86	107.61	500–700
HCO_3^-(mg/L)	90.23	446.3	188.61	58.1	NA
Ca^{2+} (mg/L)	4.31	61.79	20.32	12.05	200
Mg^{2+} (mg/L)	1.18	30.48	9.85	6.3	150
Na^+ (mg/L)	4.06	48.6	17.7	10.72	200

K^+ (mgLl)	0.05	6.1	1.76	1.33	30
SO_4^{2-}(mg/L)	0.49	18.99	2.82	3.45	400
Cl^-(mg/L)	0.34	42.22	6.23	8.37	200 –250
F^- (mg/L)	0.19	1.61	0.59	0.35	0.5 – 1.5
NO_3^-(mg/L)	0.08	147.6	21.8	29.86	50
NO_2^- (mg/L)	0.01	0.284	0.02	0.05	3
PO_4^{3-}(mg/L)	0.01	4.146	0.67	0.76	30
Br^- (mg/L)	0.309	2.538	0.88	0.5	0.5
Li^+(mg/L)	0.01	0.091	0.03	0.02	NA
NH_4^+ (mg/L)	0.01	0.186	0.03	0.05	NA
Sr^{2+}(mg/L)	0.01	0.89	0.25	0.19	NA
Cu (mg/L)	0.03	0.06	0.04	0.01	2
Ni (mg/L)	0.08	0.06	0.013	0.03	0.7
Mn^{2+} (mg/L)	0.02	0.1	0.009	0.03	0.4
Fe (mg/L)	0.16	2.95	0.145	0.51	0.3
Cr^+(mg/L)	0.02	0.05	0.032	0.01	0.05
TDS (mg/L)	127.4	524.8	247.89	77.46	1000

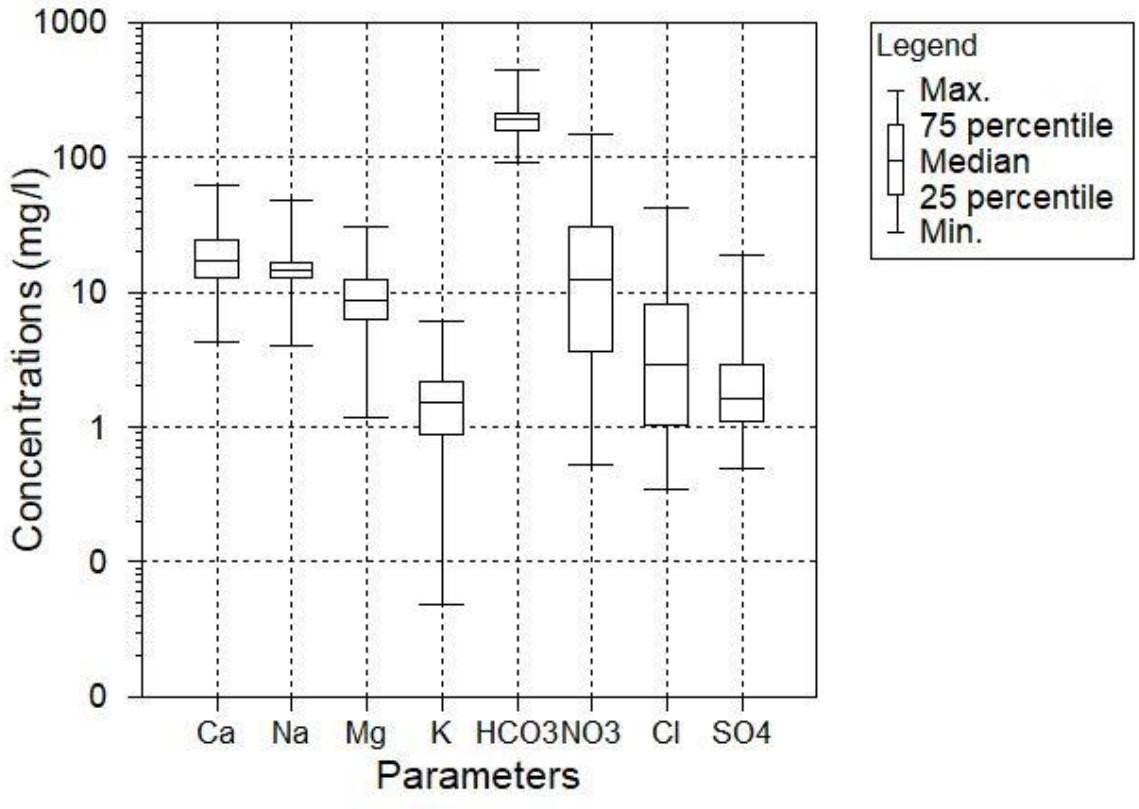

Fig. 4.3 *Box and Whisker plot of major cations and anions in the groundwater*

4.6 Major ions' chemistry and correlation

Pearson's correlation coefficient (r) between the physicochemical parameters and other trace metals is presented in (Table 4.2). Pearson's correlation coefficient reveals that the total dissolved solids (TDS) have a significant positive correlation with HCO_3^-(r=0.89), K^+(r=0.74), Ca^{2+}(r=0.68), Na^+(r=0.70), Br^-(r=0.66), NO_3^-(r=0.58), F^-(r=0.58), SO_4^2(r=0.53), Mg^{2+} (0.52), and Sr^{2+}(0.51). This suggests that the major ions originate from the same source as the total dissolved solids and they control the major groundwater chemistry in the area. A significant correlation between TDS and EC (r= 0.74) indicates that these parameters are closely related and that the water contains a relatively small amount of inorganic salts arising from domestic and agricultural waste (Rusydi 2018). The order of dominance of the cations is $Ca^{2+} > Na^+ > Mg^{2+} > K^+$ with their average concentrations of 20.32 mg/L, 17.7 mg/L, 9.8 mg/L, 1.7 mg/L, respectively.

Calcium appears to be the major cation contributor to groundwater in the area. Calcium has significant correlation with Mg^{2+} (r=0.91), Na^+(r=0.85), F^-(0.80), SO_4^2 (0.76), NO_3^-, (0.76), K^+ (0.69) and Cl^- (0.55). The significant correlation between Ca^{2+} and Mg^{2+} generally gives a clue about the hardness of the water. Water is classified as hard if the calcium carbonate concentration ranges between 120-180 mg/L (Ahn et al., 2018). Excessive water hardness can be mitigated by softening it with ion exchangers such as sodium zeolite, which displaces the Ca^{2+} and Mg^{2+}. The calcium signatures in the groundwater generally originate from the dissolution of calcite, gypsum and silicate mineral anorthite (Plummer et al., 2012). Intense agricultural activities may also introduce calcium into groundwater (Böhlke, 2002). In this study, the groundwater samples were mainly taken from the host plutonic igneous rocks, and thus the source of calcium in the groundwater could be attributed to silicate mineral dissolution.

Although sodium is not a conservative ion, it occurs abundantly in groundwater as a result of the weathering of feldspar and plagioclase minerals and to some extent cation exchange (Clark, 2015). Other sources of Na^+ in groundwaters could be attributed to the leaching of municipal solid waste and from the sea, where concentrations can be as high as 1000 mg/L (Hem, 1985). The correlation between Na^+ and Cl^- exhibits a non-significant correlation (r=0.46), which possibly indicates the dissolution of silicate mineral weathering other than halite as its origin. However, a significant correlation exists between Na^+ and F^-(r=0.89), Na^+ and Br^- (r=0.84), Na^+ and K^+ (r=0.75), Na^+ and NO_3^- (r=0.71). Na^+ and $S0_4^{2-}$ display a significant correlation (r= 0.68), which indicates a possible dissolution of sodium sulphate decahydrate $Na_2SO4.10H_2O$ (Glauber's salt) that is of health significance to the body (Zhu et al., 2007). However, there are no known deposits of Glauber salts in the area.

Magnesium concentrations in groundwater could be attributed to the leaching of igneous and magmatic minerals such as olivine, pyroxene and amphibole in the groundwater (Clark, 2015). Sedimentary origins such as dolomite and magnesite minerals may also contribute to magnesium in groundwater. There is a significant correlation between Mg^{2+} and Ca^{2+} (r=0.91) indicating the weathering and dissolution of magnesium bearing minerals such as biotite, chlorite and hornblende, which may be found in the host plutonic rocks in the catchment (Zango et al., 2021). However, there is a non-significant correlation between Mg and EC (r^2=0.36), suggesting minimum magnesium ions in solution as a single salt (Tutmez et al., 2006).

Potassium appears to be the lowest cation concentration in the groundwater of the district. Sources of potassium in groundwater are potassium feldspars, micas and synthetic fertilizers from agricultural activities (Clark, 2015). Generally, potassium concentrations in groundwater are very low due to the high resistance of potassium feldspar and biotite minerals to weathering (Appelo & Postma, 2005). Potassium correlates significantly with Ca^{2+} (r=0.69) Na^{+} (r=0.75) and F^{-} (r = 0.64), which indicates that these minerals may originate from common source in the host plutonic rock. The significant correlation between K^{+} and F^{-} is consistent with the work of Anim-Gyampo et al. (2018), who found out that these minerals are from the potassium-rich Bongo granites in the Atankwidi basin — 80 km from the study area.

The decreasing trends of the anions are $HCO_3^{-} > NO_3^{-} > Cl^{-} > S0_4^{2-} > F^{-}$ with resulting mean values of 188.61 mg/L, 21.8 mg/L, 6.23 mg/L and 0.59 mg/L, respectively. Bicarbonate appears to be the dominant anion and generally, the source may originate from silicate weathering that releases HCO_3^{-} in groundwater (Appelo & Postma, 2005). Bicarbonate correlates significantly with TDS (r= 0.899) and is non-significant with Ca^{2+} (r=0.30) and Na^{+} (r=0.37) suggesting the major source of bicarbonate is carbon dioxide in the atmosphere and in soil gases that dissolve in rain and surface water. Nitrate correlates significantly with SO_4^{2-} (r= 0.93), and Cl^{-} (r=0.82) indicating possible leaching of domestic solid waste, fertilizer and manure into the groundwater (Appelo and Postma, 2005). Nitrate is present in groundwater in the form of nitrogen organic compounds that are synthesized in the presence of oxygen (Rees, 1995). High nitrate concentrations are primarily from human and animal wastes and to a lesser extent nitrogen-based fertilizers and precipitation induced-nitrogen (Anornu et al., 2017). Fluoride concentrations in groundwater may come from the dissolution of fluorite and apatite minerals or in igneous minerals such as amphibole and mica (Hounslow, 1995). In Northern Ghana, elevated fluoride concentrations in groundwater have been of health concern to the people; and the source of fluoride was discovered in the Bongo granites (Alfredo et al., 2014; Apambire et al., 1997). Fluoride has a significant correlation with the major cations, indicating the weathering of apatite and fluorite minerals are common in the

underlying igneous rocks as has been espoused by (Alfredo et al., 2014). All the fluoride concentrations are within the WHO acceptable limit (0.5 mg/L - 1.5 mg/L) except that of the borehole situated at Holy English junior high school, which has fluoride a concentration of 1.61 mg/L.

Table 4.2 The correlation matrix for water quality parameters in the study area

	pH	EC	O2	HCO3	Ca^{2+}	Mg^{2+}	Na^{+}	K^{+}	SO_4^{2-}	Cl^{-}	F^{-}	NO_3^{-}	Br^{-}	Sr^{2+}	TDS
pH	1														
EC	0.13	1													
O_2	-0.01	-0.12	1												
HCO_3^{-}	-0.09	**0.63**	-0.25	1											
Ca^{2+}	-0.01	**0.56**	-0.09	0.30	1										
Mg^{2+}	0.017	0.36	0.06	0.17	**0.91**	1									
Na^{+}	-0.03	**0.70**	-0.11	0.37	**0.85**	**0.69**	1								
K^{+}	0.123	**0.64**	-0.18	**0.56**	**0.69**	0**.52**	0**.75**	1							
SO_4^{2-}	-0.12	0.28	-0.23	0.18	**0.76**	**0.63**	**0.68**	0.47	1						
Cl^{-}	-0.29	0.35	-0.17	0.12	**0.55**	0.38	0.46	0.17	**0.72**	1					
F^{-}	0.01	**0.57**	0.03	0.26	**0.80**	**0.74**	**0.89**	**0.64**	**0.56**	0.31	1				
NO_3^{-}	-0.12	0.35	-0.31	0.17	**0.75**	**0.56**	**0.71**	0.47	**0.93**	**0.82**	**0.55**	1			
Br^{-}	0.01	0**.70**	0.14	0.42	**0.76**	**0.72**	**0.84**	**0.73**	0.36	0.16	**0.84**	0.33	1		
Sr^{2+}	-0.15	0.42	-0.14	0.211	**0.66**	0.40	**0.72**	**0.64**	**0.74**	**0.55**	**0.53**	**0.76**	**0.51**	1	
TDS	-0.11	**0.74**	-0.24	**0.89**	**0.68**	**0.52**	**0.70**	**0.74**	**0.53**	0.41	**0.58**	**0.53**	**0.66**	**0.51**	1

Bolded values suggest a significant correlation (r >0.5)

4.7 Factor analysis

Principal component analysis (PCA) was carried out on the 38-groundwater samples and the dimensionality of the 14 parameters was reduced to three principal components, which accounted for 81% of the total variance (Table 4.3a and 4.3b). PCA 1 explains 34% of the total variance and has high positive loading for, Ca^{2+}, Mg^{2+}, Na^{+}, SO_4^{2-}, F^{-}, and Br^{-}. The strong positive loadings, especially of Ca^{2+} and Mg^{2+} in PCA1 suggest higher groundwater-rock interaction, which leaches appreciable quantities of silicate minerals such as anorthite, biotite and hornblende in the groundwaters (Sunkari and Abu, 2019). These rock-bearing minerals reflect the hydrochemical water composition of the plutonic rocks in the study area. The presence of Na^{+} can be explained as the weathering of silicate mineral albite ($NaAlSi_3O_8$) and also the cation exchange process, in which Na^{+} tends to displace Ca^{2+} in water (Freeze and Cherry 1979). PCA2 also accounts for 24% of the total variance and is dominated by high positive loadings for NO_3^{-}, SO_4^{2-}, Cl^{-} and Sr^{2+} but low negative loading for

pH. The result of the PCA2 corroborates with the findings of Cluster 1 in the R-mode HCA. The predominant chemical parameters (NO_3^-, SO_4^{2-}, Cl^-) in PCA2 suggest the application of inorganic and organic fertilizers such as animal waste, which cause elevated amounts of nitrate in the groundwaters as it is evident in places such as Baranatinga, Garu Zongo and Duadinyediga in the area. The low pH loading is attributed to the buffering activity of HCO_3^-. In a natural geochemical process, carbon dioxide derived from the atmosphere reacts with neutral water in the subsurface to form weak carbonic acid ($H_2CO_3^-$). The carbonic acid dissociates into HCO_3^-, H^+ and CO_3^{2-}. The hydroxyl ion (H^+) released in the water can decrease the pH, thus the low negative loading for pH. Besides, the movement of groundwater through the aquifer matrix will cause more reactions to decrease the carbonic acid and increase the HCO_3^- and CO_3^{2-} concentrations, thus high positive loadings of HCO_3^- for PCA3 (Clark, 2015). The third component (PCA3), loads strongly for HCO_3^-, EC, K^+, and TDS and accounts for 23% of the total variance. The presence of K^+ in the groundwater may reflect the weathering of potassium feldspar associated with the igneous rocks in the "Tamnean Plutonic Suites" (SNC-Lavalin/INRS, 2011).

Table 4.3a The total variance of the hydrochemical components

Total Variance Explained									
	Initial Eigenvalues			Extraction Sums of Squared Loadings			Rotation Sums of Squared Loadings		
Component	Total	% of Variance	Cumulative %	Total	% of Variance	Cumulative %	Total	% of Variance	Cumulative %
1	7.96	56.85	56.85	7.96	56.85	56.85	4.81	34.36	34.36
2	2.04	14.60	71.45	2.04	14.60	71.45	3.37	24.06	58.42
3	1.36	9.69	81.14	1.36	9.69	81.14	3.18	22.72	81.14
4	0.89	6.32	87.46						
5	0.58	4.13	91.58						
6	0.51	3.64	95.22						
7	0.26	1.90	97.13						
8	0.16	1.17	98.29						
9	0.08	0.54	98.84						
10	0.07	0.47	99.30						
11	0.06	0.45	99.75						
12	0.02	0.16	99.91						
13	0.01	0.09	99.99						
14	0.01	0.07	100.00						

Table 4.3b. Principal components of the hydrochemical parameters

Parameters	PCA1	PCA 2	PCA3
pH	0.36	-0.53	-0.14
EC	0.44	0.09	0.73
HCO_3^-	0.01	0.06	0.96
Ca^{2+}	0.81	0.45	0.26
Mg^{2+}	0.83	0.28	0.08
Na^+	0.78	0.37	0.40
K^+	0.62	0.11	0.60
SO_4^{2-}	0.50	0.79	0.06
Cl^-	0.16	0.88	0.08
F^-	0.84	0.20	0.27
NO_3^-	0.45	0.84	0.08
Br^-	0.79	0.00	0.49
Sr^{2+}	0.46	0.64	0.29
TDS	0.36	0.33	0.84

4.8 Hierarchical cluster analysis (HCA)

The Hierarchical cluster analysis (HCA) was further used to validate the results of the factor analysis by assembling the distinct clusters into distinct groups. Thirty-eight groundwater samples and 14 variables were used for the hierarchical cluster analysis. The HCA produced Q-mode and R-mode dendrograms. For the R-mode technique, the 14 variables/parameters were used to define their relationships and generate homogenous clusters based on a subjective assessment. A phenon line was connected at a linkage distance of about 15 to avoid the generation of fewer or greater clusters. The visual observation of the R-mode HCA displays three main clusters (Fig.4.4).

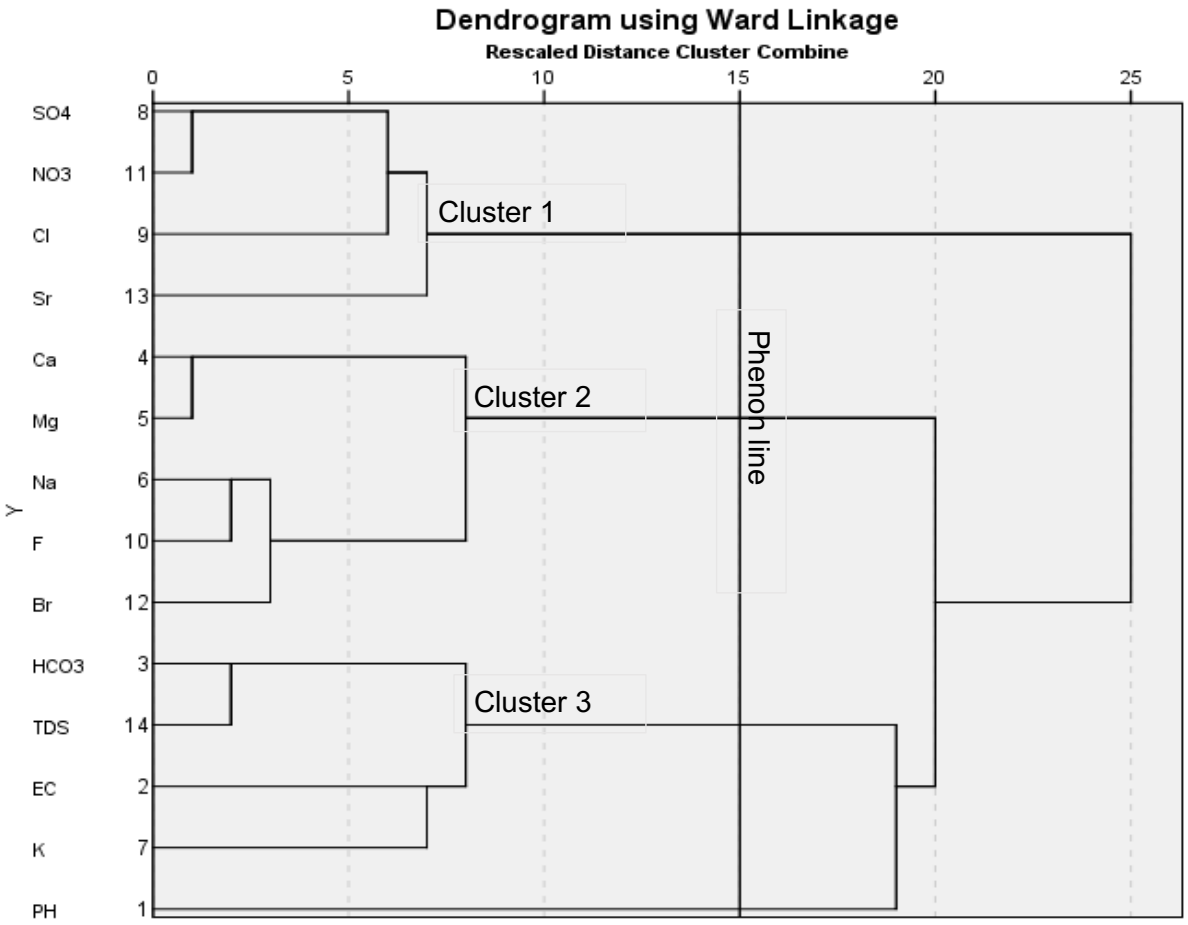

Fig. 4.4 *Dendrogram showing R-mode clusters*

Cluster 1 is characterized by SO_4^{2-}, NO_3^-, Cl^-, and Sr^{2+}, which indicates the groundwater appears to be influenced by anthropogenic activities at the near-surface groundwater such as the use of domestic wastewaters and the application of chemical and organic fertilizers in the study area (Loh et al., 2020). These pollutants may reach a considerable amount, thereby increasing nitrate and sulphate concentrations in groundwater. The results of cluster 1 confirm the results of PCA2. The second cluster consists of Ca^{2+} Mg^{2+}, Na^+, K^+, F^-, and Br^- suggesting groundwater rock interactions are largely influenced by silicate weathering in the area. The weathering of rocks tends to increase these ions from upstream to downstream in the study area and this is characteristic of a semi-arid environment (Wu et al., 2017). Strontium and calcium are very close in terms of distance, because strontium has identical physical and chemical properties to calcium, and tends to replace Ca^{2+} in mineral structures. Strontium concentrations in groundwaters are mostly found in carbonate rocks when its bearing minerals such as celestite ($SrSO_4$) and strontianite ($SrCO_3$) precipitate out from calcite solution (Skougstad and Horr, 1963). Granitic rocks showing high contents of rubidium are also characterized by strontium concentrations in groundwater (Kharaka and Hanor, 2003). It can be added that anthropogenic activities such as the burning of coal and the use of phosphate fertilizers can release strontium into the groundwater (Höllriegl and

München, 2011). The third cluster represents close associations between TDS, HCO_3^-, EC, K and pH. This cluster, especially the bicarbonate can be indicative of the dissolution of silicate minerals which is accompanied by the release of bicarbonates through carbonic acid from infiltrating recharging waters as has been espoused by previous researchers in Northern Ghana (Chegbeleh et al., 2020; Loh et al., 2020).

The Q-mode dendrogram, on the other hand, represents the relationship between groundwater parameters in the different parts of the study area. Three spatial groundwater clusters were revealed from the Q-mode dendrogram (Fig. 4.5). Cluster 1 has the lowest mineralized water with mean TDS and EC values of 207 mg/L and 186 µS/cm respectively. This is particularly found in recharge areas since precipitation usually contains low ionic composition which is in equilibrium with groundwater recharge in the area (Salifu et al., 2012). Cluster 2 can be described as a transition zone with an average TDS of 251 mg/L and EC of 271 µS/cm. Cluster 3 consists of relatively high concentrations of average TDS and EC values of 362 mg/L and 409 µS/cm respectively relative to the other clusters. The highly mineralised water of this cluster can be indicative of a discharge zone that possibly had longer residence time and greater rock interaction, thus leaching more ions into the groundwater (Appelo and Postma 2005). From Fig 4.6, cluster 1 (recharge zone) occurs in the highest elevations mostly around the northern and central parts of the study area. Cluster 2 (transition zone) is found in the northern and southern parts of the study area, whereas cluster 3 (discharge zone) is located around the northern and southern parts of the area.

4.9 Water-types or Hydrogeochemical facies

The clusters of the Q-mode hierarchical cluster analysis (HCA) were used to construct the Piper diagram (Fig 4.7). The trilinear Piper diagram consists of the relative proportion of major cations and anions. The Piper plot reveals that all three clusters are found in the no dominant cations water zone, except for two samples that are found in the $Na^+ + K^+$ zone. The anions are characterized mostly by HCO_3^- of all the three clusters. From the trilinear plot, it can be deduced that three water types exist in the area. The first type is composed of Ca—Na—HCO_3 water, indicating the freshwater type of the underlying plutonic rocks undergoing an initial stage of the hydrogeochemical evolution (Tran et al., 2020). This water type is consistent with the findings of Anim-Gyampo et al. (2018); Sunkari and Abu (2019); Zakaria et al. (2020) done in the crystalline igneous terrains of Ghana; thus implying these water types are predominately found in the igneous rocks terrains of Northern Ghana. The second type consists of Ca — Mg — HCO_3 or Mg — Ca — Na — HCO_3 mixed water types. This also highlights the greater role of the alkaline earth metals ($Ca^{2+} + Mg^{2+}$) over the alkali metals ($Na^+ + K^-$). The third type consists of Ca — Mg — Na — HCO_3 —NO_3 or Ca — Mg — HCO_3 —Cl—NO_3 water types, suggesting higher rock interaction and the effect of anthropogenic

activities on the groundwater. In the Garu-Tempane areas, the main occupation of the inhabitants is farming and cattle rearing. The use of different fertilizers such as phosphate and nitrogen on their farms may dissolve and enter the aquifers, causing anthropogenic pollution in the area.

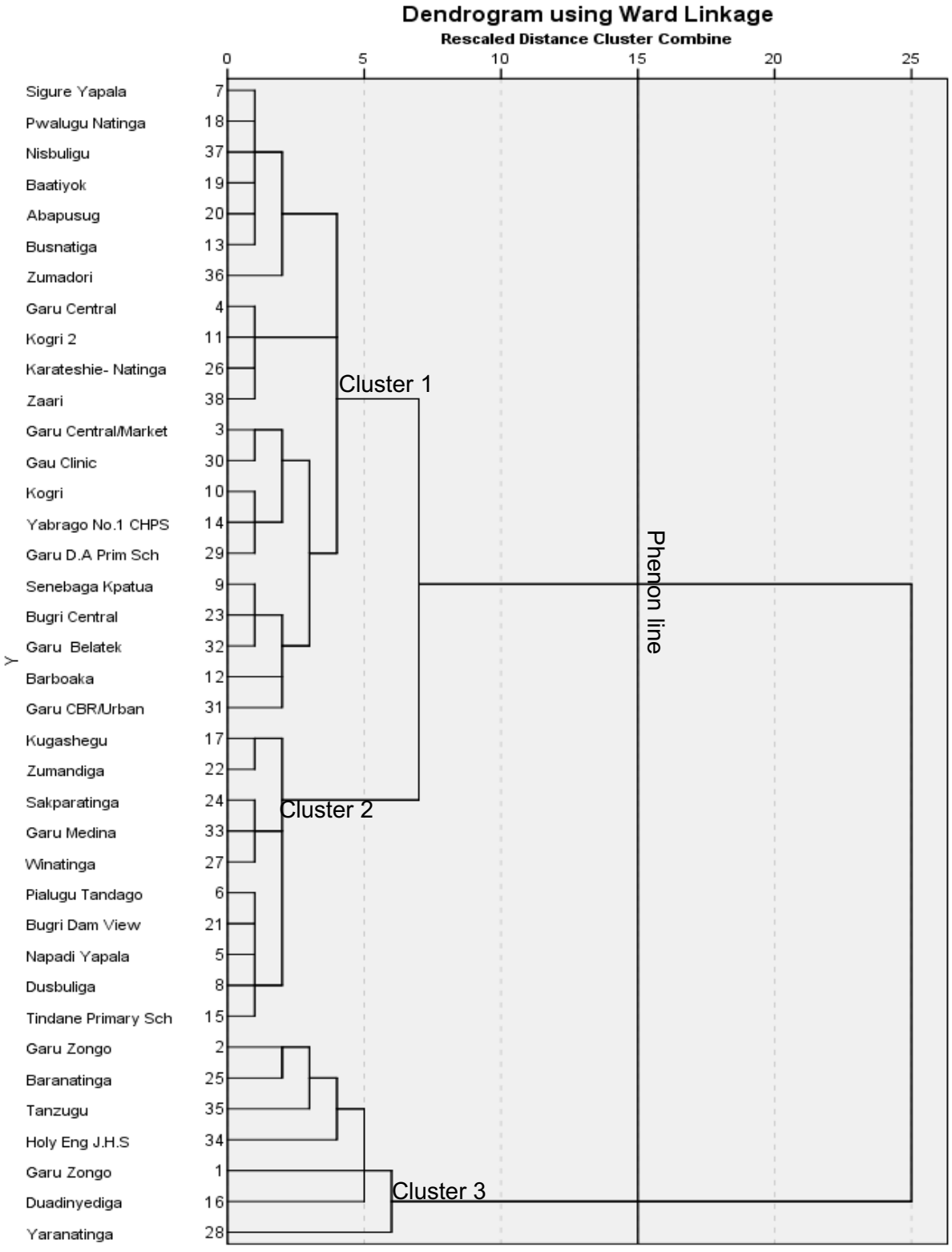

Fig. 4.5 *Dendrogram showing Q-mode clusters*

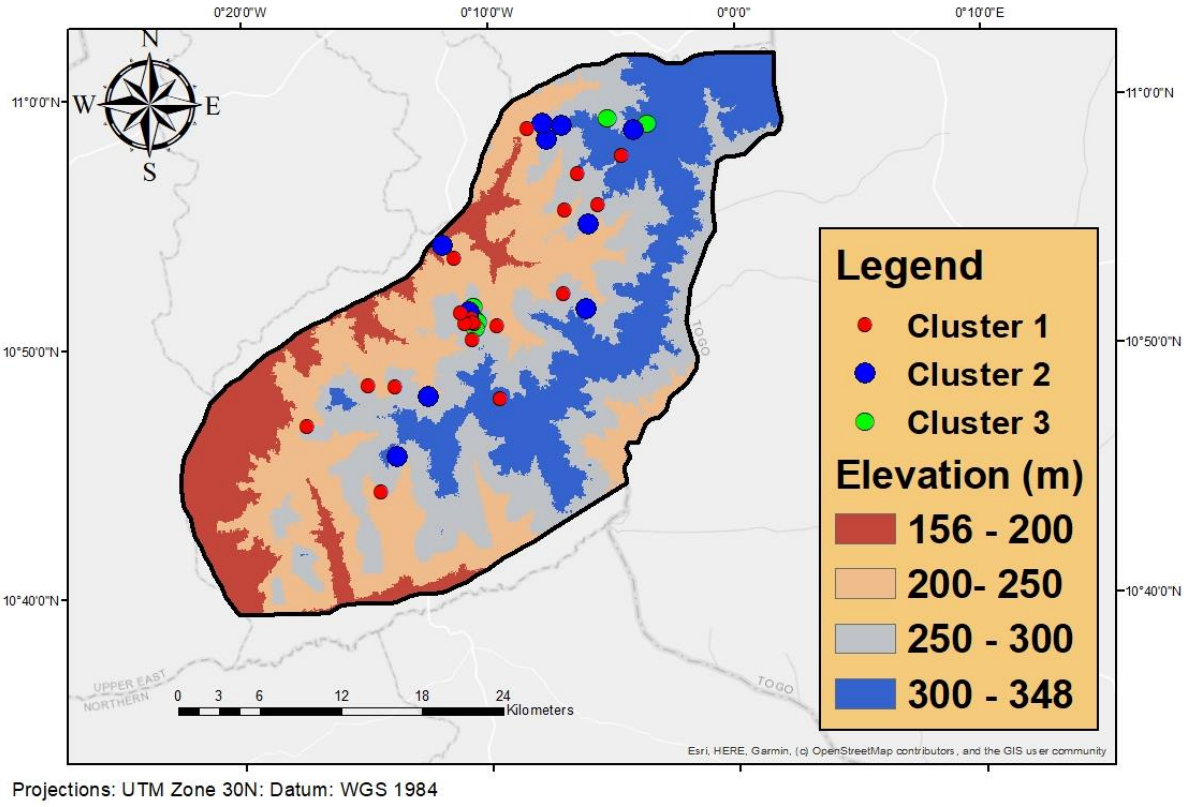

Fig. 4.6 *Spatial distribution of the clusters from the Q-mode HCA*

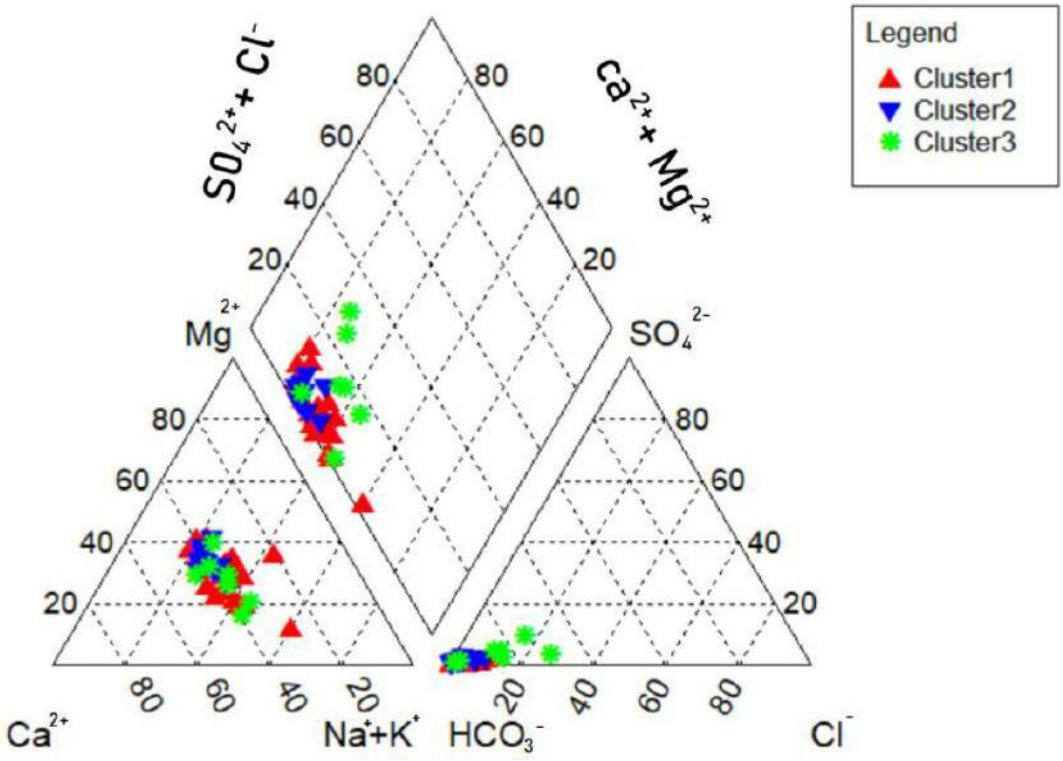

Fig. 4.7 *The Trilinear piper plot showing the major ions*

4.10 Weathering process and the mechanism controlling the evolution of groundwater chemistry

To determine the influence of major geochemical processes such as water-rock interaction, precipitation and evaporation on groundwater chemistry, the Gibbs (1970) plot was used. The Gibbs plot (Fig.4.8) shows that all the groundwater samples are within the rock dominant boomerang-shaped area, which is consistent with most ionic compositions found in the world's major aquifer bodies (Marandi and Shand, 2018). Groundwater quality evolution along its flow path typically contains freshwater enriched in Ca — HCO_3^- and evolves to Na —Cl type with increasing salinity during prolonged residence time. This evolution would move the freshwater to the evaporation domination zone due to the anthropogenic activities that may introduce Na^+ and Cl^- ions. Evaporation of minerals from groundwater usually occurs when the groundwater table is near the earth's surface and this is negligible in deep aquifers. The hydrochemistry data in the study area do not reflect this tendency, rather the ion compositions are characterized by water-rock interaction.

The genesis of groundwater chemistry requires the knowledge of aquifer forming minerals and weathering processes (Hwang et al., 2017). To understand the weathering process, the major ions are plotted against each other to deduce the important process controlling the evolution of groundwater chemistry in the area. The bivariate plot of Ca^{2+} + Mg^{2+} versus HCO_3^- + SO_4^{2-} (Fig 4.9a) should indicate ion exchange if the samples fall on the right section of the 1:1 line. On the other hand, if the samples fall on the left portion of the 1:1 line, the results should indicate a reverse ion exchange (Fisher and Mullican, 1997). In addition, the samples above the 1:1 line suggest carbonate weathering, whereas the samples below the 1:1 line indicate silicate weathering. The samples(8%) along the 1:1 line depict that the water chemistry has been influenced by both carbonate and silicate weathering (Koffi et al., 2017). From Fig 4.9a, the majority of the samples (72%) are below the 1:1 line, implying that silicate weathering and ion exchange are the controlling factors that affect the groundwater chemistry in the area. Here, there is an enrichment of HCO_3^- + SO_4^{2-} relative to Ca^{2+} + Mg^{2+} in the groundwater (Rajmohan and Elango, 2004). Few of the samples (20%) are above the 1:1 line, suggesting carbonate weathering from the Voltain formations in the study area. The carbonate rocks in the study are hydraulically linked to the crystalline basement rocks and the associated granitoids (Dapaah-Siakwan and Gyau-Boakye, 2000). The evolution of carbonate weathering begins when precipitation induced CO_2^- gets in contact with soils containing carbonate minerals, and releases HCO_3^- in the groundwater as shown in the following reaction equations below (Zaidi et al., 2015).

$$H_2O + CO_2 \rightleftharpoons H_2CO_3 \text{ (carbonic acid)} \quad (4.8)$$

$H_2CO_3 \rightleftharpoons H^+ + HCO_3^-$ (bicarbonate) (4.9)

$CaCO_3 \rightleftharpoons Ca^{2+} + CO_3^{2-}$ (dissolution of calcite) (4.10)

Silicate minerals such as anorthite and albite are formed from magma cooling and crystallization at varying temperatures (Clark, 2015). Silicate weathering is often deduced using the 1:1 molar ratios of Na/Cl to define the salinity levels in groundwater. It is generally accepted that If the data fall on the 1:1 plot, then it implies halite dissolution prevails in the groundwater (Meybeck, 1987). The plot Fig. 9b of Na (meq/L) against Cl (meq/L) is below the 1:1 line, and this suggests the dissolution of Na^+ in groundwater, in which Na^+ displaces Ca^{2+} during the cation ion exchange process. Groundwaters having high Na^+ concentrations due to silicate weathering can be indicative of water enriched in HCO_3^- and this explains the predominance of HCO_3^- in the groundwater in the area as shown in equation 4.11 (Yidana et al., 2018).

$$2NaAlSi_3O_8\,(albite) + 2H_2CO_3 + 9H_2O \rightleftharpoons Al_2Si_2O_5\,(OH)_4\,(kaolinite) + 2Na^+ + 4H_4SiO_4 + 2HCO_3^- \quad (4.11)$$

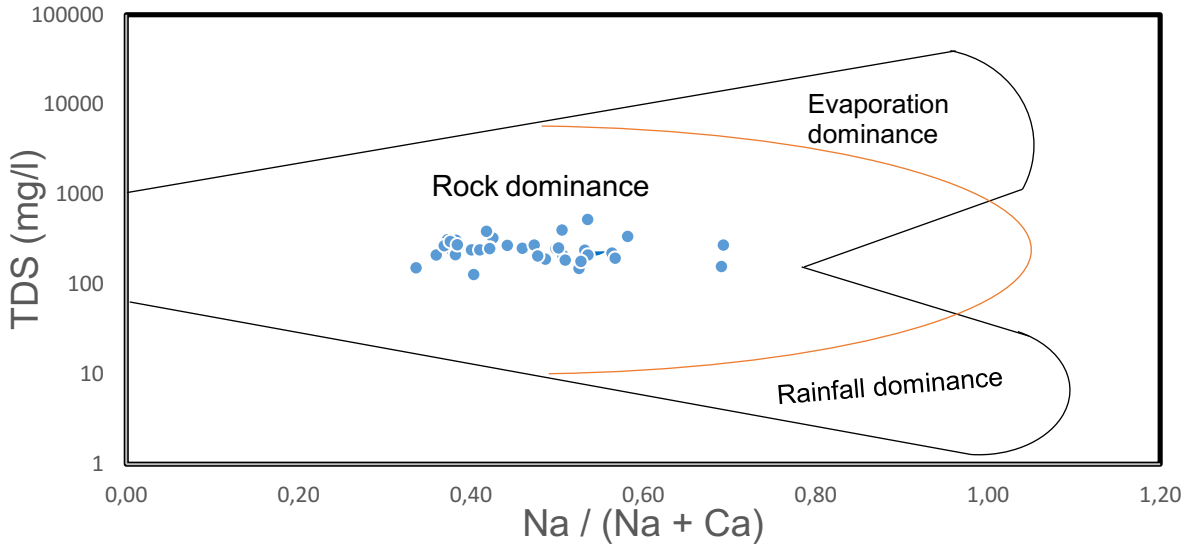

Fig. 4.8 *Gibbs diagram showing TDS versus Na/Na+Cl*

From Fig. 4.9b, three groundwater samples are above the 1:1 line, which indicates that reverse ion exchange involving sodium and chloride has taken place and that these samples are enriched in Cl^-, albeit the chloride concentrations are within the WHO acceptable limit (250 mg/L). The mechanism explaining reverse ion exchange is shown in equation 4.12.

$Na^+ (K^+)$ + Ca (Mg) — Clay = Na (K) — Clay + Ca^{2+} (Mg^{2+}) (4.12)

To further substantiate the cation ion exchange reactions during silicate weathering, the plot of (Ca^{2+} + Mg^{2+}) – (HCO_3^- + SO_4^{2-}) against Na^+ + K^+ - Cl^- (Fig.9c) was used. According to Zaidi et al. (2015), the relationship between these indices should give a slope of – 1 to confirm the active role of Ca^{2+}, Mg^{2+} and Na^+ in the cation exchange process. Accordingly, the relationships between these indices in the study area give a slope of – 1.2, indicating the majority of the water samples have undergone a cation exchange reaction (Anim-Gyampo et al., 2018). The mechanism explaining cation exchange is shown in equation 4.13.

Na (K) — Clay + Ca^{2+} (Mg^{2+}) = 2Na^+ (K^+) aq + Ca (Mg) — Clay (4.13)

Silicate and carbonate mineral weathering can be invoked using the bivariate plot of (Ca^{2+} + Mg^{2+}) versus HCO_3^- (Fig.4.9d). This is useful to determine the influence of different weathering processes in an aquifer. According to Sami (1992), the trend of groundwater samples falling along the y=2x of (Ca^2 + Mg^{2+}) versus HCO_3^- indicates that carbonate mineral dissolution is predominant in an aquifer. If the samples do not fall on that line, it could be the alteration of silicates. In this study, the bivariate plot of (Ca^{2+}+Mg^{2+}) versus HCO_3^- in Fig.4.9d shows only three samples falling on the y=2x line, indicating that carbonate weathering is not the dominant process occurring in the study area. The majority of the groundwater samples fall below the y=2x line, indicating silicate weathering is the predominant process controlling groundwater chemistry in the Garu-Tempane area.

4.11 Chloro-alkaline indices (CAI)

The chloro-alkaline indices CAI 1 and CAI 2 were computed for 38 water samples for this study to explain the type of ion exchange in the groundwater (Schöeller H, 1965). An assertion is made for positive CAI if Na^+ and K^+ ions of the water are substituted by the Ca^{2+} and Mg^{2+} of the aquifer material. Here the CAI will indicate reverse ion exchange. On the contrary, a negative CAI implies ion exchange in which the Ca^{2+} and $Mg2^+$ of the water are substituted by Na^+ and K^+ of the aquifer material. According to Srinivasamoorthy et al. (2014), the negative CAI is also widely accepted as a cation-anion-exchange reaction or chloro-alkaline disequilibrium, which is due to low salt waters. Where there is no exchange between the ions and the aquifer material, the relationship attains equilibrium and CAI becomes zero. The computed CAI-1 has 93% negative values and 7% positive values ranging between -43.26 and 0,597. The CAI-2 has 97% negative values and 3% positive values ranging between -0.245 and 0.144. The results above suggest that the majority of the groundwater samples attain a negative chloro-alkaline index and therefore, the cation

exchange process is one of the factors influencing groundwater chemistry in the area. This is consistent with the plot of (Fig. 4.9b), in which three samples attain reverse ion exchange and the majority are cation exchange.

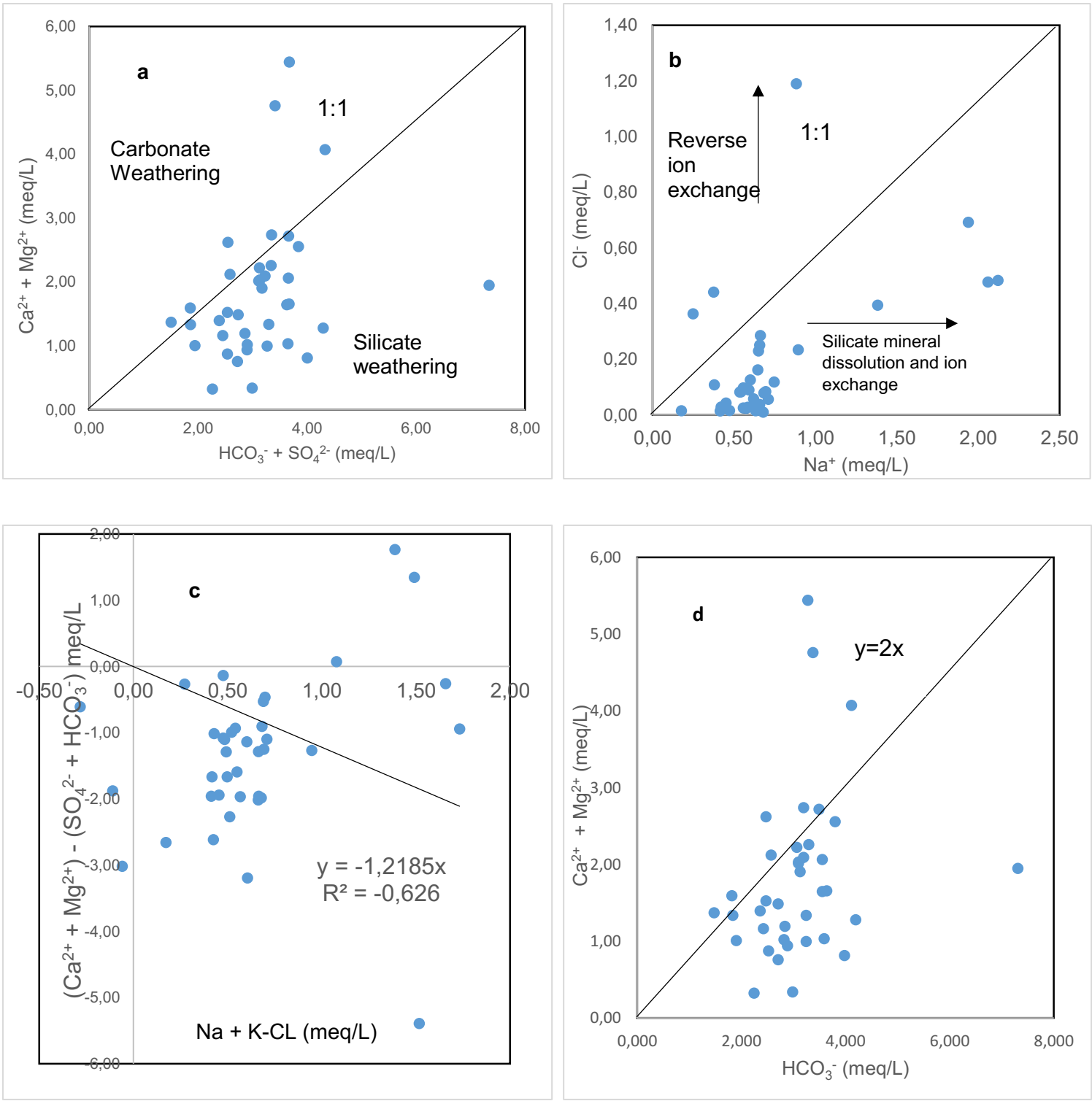

Fig .4.9. *Bivariates plots of (a) Ca^{2+} +Mg^{2+} (meq/L) against HCO_3^- (meq/L) + SO_4^{2-} (b)Na^+ (meq/L) against Cl^- (meq/L) (c) (Ca^{2+} + Mg^{2+}) – (SO_4^{2-} + HCO_3^-) meq/L against Na^++K^+-Cl^- meq/L (d) Ca^{2+} + Mg^{2+} against HCO_3 (meq/L)*

4.12 Water quality index (WQI)

Horton (1965) first used the water quality index in the USA to evaluate the suitability of drinking water and since then, various researchers have used WQI to characterize groundwater for drinking water purposes (Tyagi et al., 2017; Kawo and Karuppannan 2018; Ponsadailakshmi et al., 2018). The water quality index agglomerates large and different chemical parameters into a single variable for geochemical inferences (Tyagi et al., 2017).

Thirty-eight groundwater samples and 15 chemical parameters were used for the water quality index (WQI) assessment and their relative weights as shown in (Table 4.4). An adapted version of the WQI classification scheme postulated by Sahu and Sikdar (2008) was used for this study. The WQI classification for "excellent water" ranges from (0–50); "good water" from (51-100); "poor water" from (101-200); "very poor water" (201-300) and "unsuitable drinking water" (>300). The computed WQI ranges between 13.3 and 97.4. The WQI spatial distribution map (Fig. 4.10) shows two types of water quality in the area. Almost all groundwater samples (95%) can be described as "excellent water", whereas 5% of the samples show "good water" in the eastern part of the area. The influencing parameters of the "good water" are associated with higher NO_3^-, F^-, and Fe and TDS values. These values indicate generally that the groundwater in the 'Tamnean Plutonic Suite' aquifer is excellent for drinking.

Table 4.4 WQI values based on the assigned weights and relative weights

Parameters	WHO (2017) drinking water guidelines	Assigned Weight (wi)	Relative Weight (W)
pH	7,5	4	0.08
TDS	1000	4	0.08
Na^+ (mg/L)	200	2	0.04
K^+ (mg/L)	30	2	0.04
Ca^{2+}(mg/L)	200	2	0.04
Mg^{2+}(mg/L)	150	2	0.04
Cl^- (mg/L)	250	3	0.06
SO_4^2(mg/L)	250	3	0.06
PO_4^3(mg/L)	30	4	0.08
NO_2^-(mg/L)	3	4	0.08
NO_3^-(mg/L)	50	5	0.1
F^- (mg/L)	1.5	5	0.1
Mn^{2+}(mg/L)	0.1	4	0,08

Fe (mg/L)	0.3	4	0.08
Cu (mg/L)	2	2	0.04
		$\Sigma wi = 50$	$\Sigma Wi = 1$

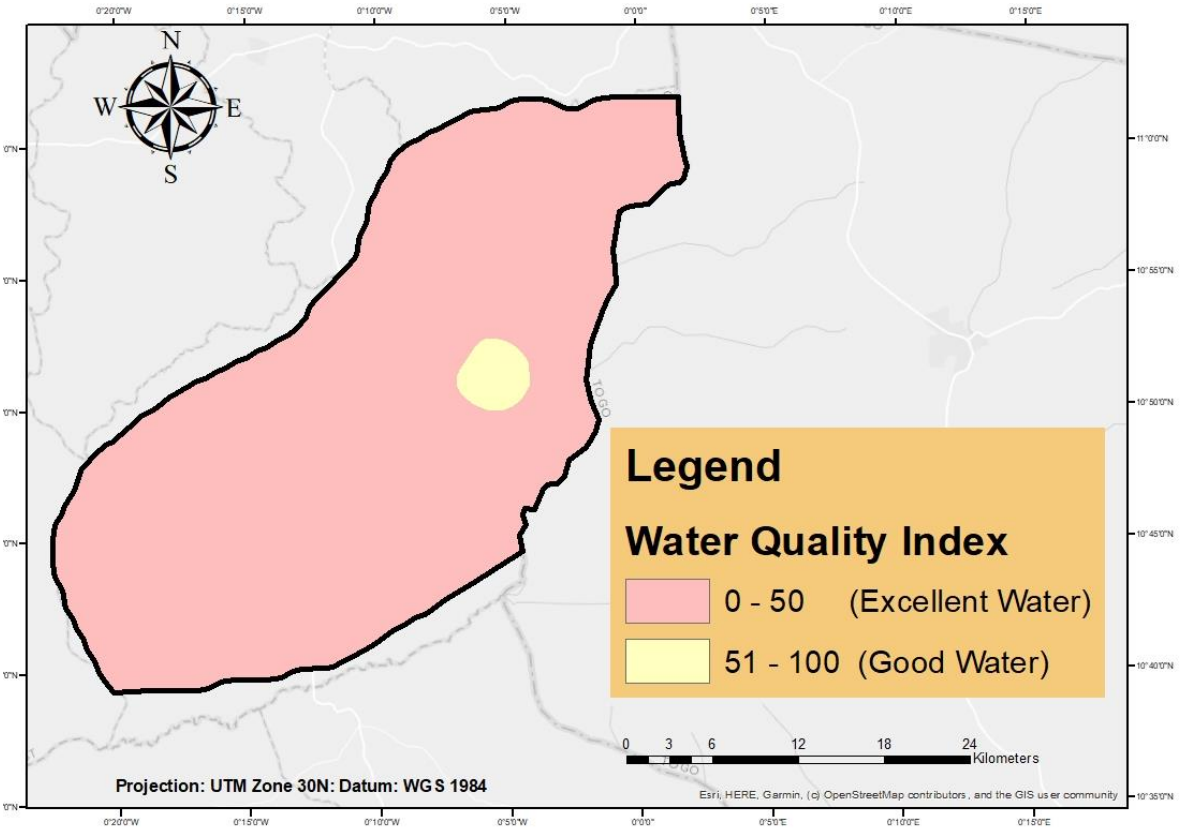

Fig.4.10 *Spatial water quality index distribution map of the study area*

4.13 Saturation index of mineral

The mineral saturation index of groundwater is very useful to determine the type of mineral present in groundwater and the precipitation and dissolution reactions (Appelo & Postma, 2005). Three types of saturation indices/states can be distinguished. A saturation index of zero implies that the groundwater is in equilibrium with the precise mineral in the water. A saturation index, less than zero implies that the groundwater is undersaturated with respect to the mineral. Here, the mineral will continue to dissolve, if that particular mineral is present in the water. A saturation index greater than zero implies the groundwater is deemed supersaturated and the mineral may precipitate from the solution. In this particular case, the mineral should be forming and the aquifer may contain a sufficient amount of minerals needed to attain an equilibrium (Appelo & Postma, 2005; Parkhust and Appelo, 2013). The plausible minerals found in the 'Tamnean Plutonic Suite aquifer' are presented in Table 4.5.

Table 4.5 Summary of the mineral saturation index statistics in the study area

Saturation Index	Min	Max	Mean	Std dev
SI Calcite	-1.874	0.092	-0.789	0.549
SI Halite	-10.204	-7.537	-8.868	0.657
SI Gpsum	-4.901	-2.446	-3.815	0.504
Si Fluorite	-3.911	-1.314	-2.656	0.627
Si Dolomite	-2.628	1.241	-0.480	1.087
Si Anhydrite	-5.034	-2.579	-3.943	0.504

From Fig.4.11, groundwater in the 'Tamnean Plutonic Suite aquifer' clearly shows undersaturation with respect to gypsum, fluorite and halite and anhydrite. These minerals indicate a shorter residence time in the groundwater, where there is the dissolution of these minerals if present. Similarly, all the 38-groundwater samples are undersaturated with respect to calcite except for two samples, which show supersaturation. The calcite supersaturation indicates that the minerals are forming and may contain enough minerals to equilibrate with the groundwater. Again, nearly 66 % of the groundwaters are supersaturated with respect to dolomite. This together with the calcite undersaturation reflect the conditions necessary for carbonate dissolution.

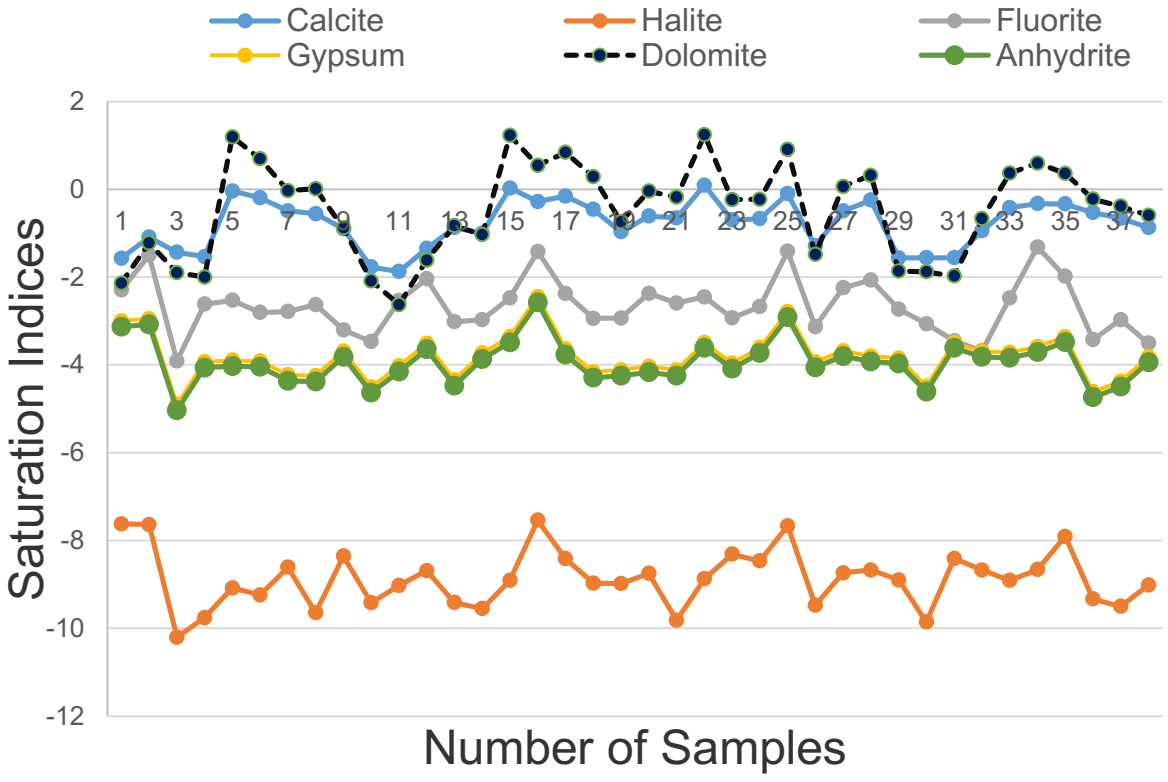

Fig. 4.11 *Mineral saturation index of groundwater in the study area*

4.14 Nitrate levels in groundwater

Several studies have linked elevated nitrate concentrations in groundwaters to anthropogenic activities (Suthar et al., 2009; Wick et al., 2012; Sajedi-Hosseini et al., 2018; Suciu et al., 2020). In the study area, nitrate concentration ranges between 0.08 mg/L and 147.6 mg/L with a mean value of 21.8 mg/L. The acceptable limit of nitrate in drinking water is 50 mg/L (WHO 2017). However, communities such as Garu Market (68.36 mg/L), Garu Zongo (77.8 mg/L), Baranatinga (85.7 mg/L) and Duadinyediga (147.6 mg/L) have nitrate levels in the groundwaters exceeding the WHO acceptable drinking water limit. The first two communities are located in the centre of the district, where there are no agricultural activities. Thus, the source of nitrate in the groundwater could be attributed to animal waste (cattle dung) and untreated household wastes (Anornu et al., 2017). The latter communities are agricultural areas and the source of nitrate in groundwater is chemical and organic fertilizers. There is a significant correlation between NO_3^- and SO_4^{2-} (r=0.93) and NO_3^- and Cl^- (r=0.82), implying that these pollutants are commonly found in agricultural areas (Loh et al., 2020). In general, about 10.5% of the groundwater samples are contaminated with nitrate and the spatial distribution is shown in (Fig. 4.12). The continuous use of water in these communities may be detrimental to people's health.

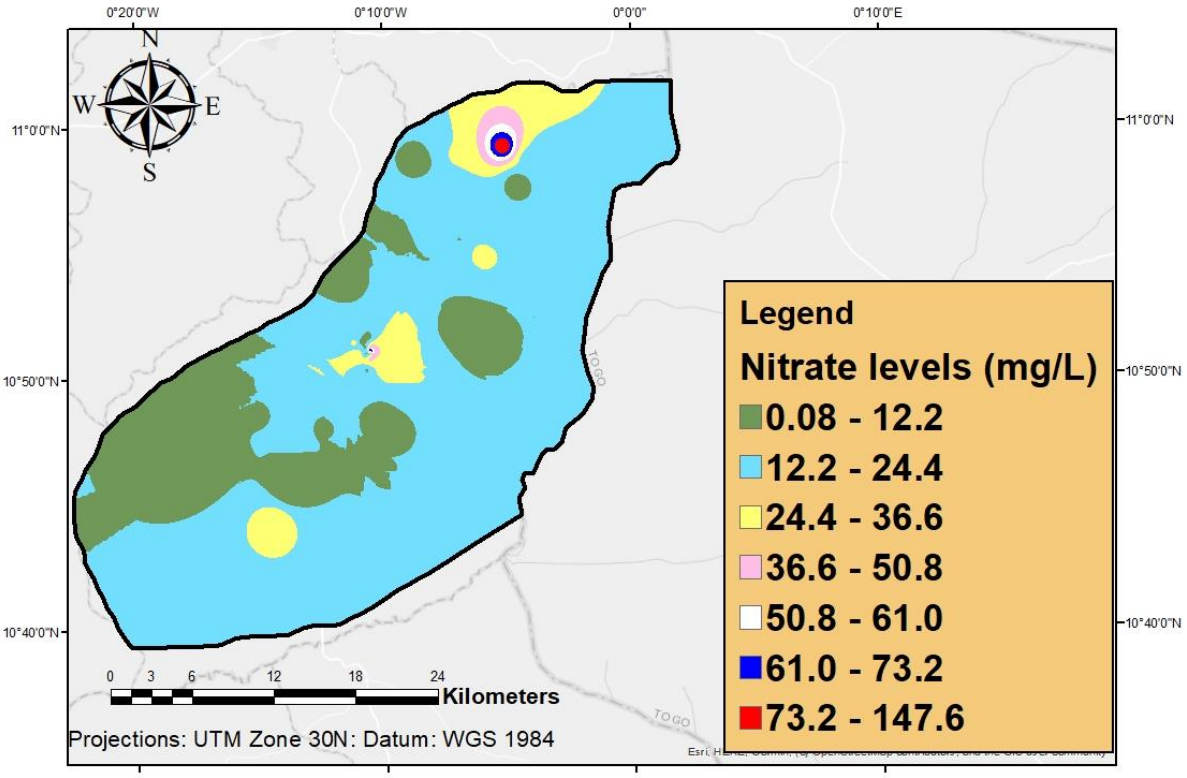

Fig. 4.12 *Spatial distribution of nitrate in groundwater in the study area*

4.15 Suitability for irrigation use

The area under study is a low-lying agricultural area, where the majority of inhabitants use shallow groundwater to irrigate their farms. Therefore, it is imperative to assess the suitability of groundwater for irrigation purposes. The slow and continuous movement of groundwater along sodium silicate rocks can cause sodium to leach into the water, and this is generally associated with chloride ions. This causes high salt content in groundwater (Hem, 1985). The high amount of sodium can initiate reverse ion exchange, in which sodium displaces calcium and magnesium ions adsorbed on clay minerals. High saline water can cause a decrease in the permeability of soil as well as swelling of the soil. The sodium salinity hazard can be assessed using the Wilcox (1955) diagram.

Figure 4.13 shows a Wilcox plot of sodium hazard (SAR) on the y-axis and the salinity hazard represented as conductivity (µS) on the x-axis. All the clusters fall within the low (S1) group and the low to medium (C1 — C2) groups. The low (C1 — S1) group is dominated by the water type of cluster 1; these contain low saline waters from recharge areas. The cluster 2 and cluster 3 water types fall within the (C2 — S2) group and are associated with moderate saline waters from discharge areas. In brief, all the three cluster water types indicate little or no danger to crops and as such suitable for irrigation.

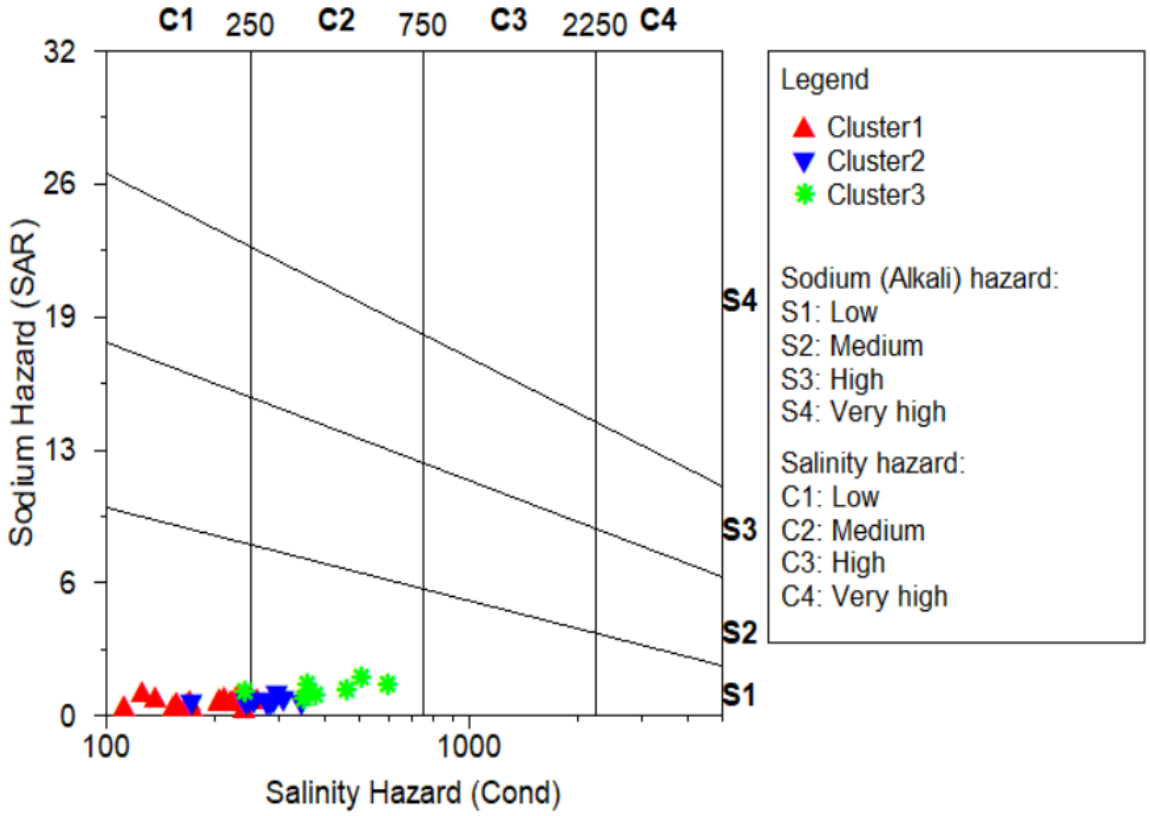

Fig 4.13 *Wilcox diagram for irrigation water quality*

4.16 Conclusions

Groundwater characterization was carried out to investigate the natural baseline chemistry and the factors controlling groundwater chemistry in the Garu- Tempane hydrogeological catchment. The methods employed are the multivariate statistical method, hydrochemical graphical method, PHREEQC geochemical modelling approach and various ionic ratio plots. The graphical methods reveal an order of ion compositions $Ca^{2+} > Na^{+} > Mg^{2+} > K^{+}$ and $HCO_3^- > NO_3^- > Cl^- > SO_4^{3-}$ in the water. All the physicochemical parameters and trace metals are within the WHO acceptable limit for drinking water except for elevated bromide and nitrate concentrations that occur in some of the wells. In addition, one borehole has a fluoride concentration (I.61 mg/L) exceeding the WHO drinking water limit (1.5 mg/L). About 10.5 % of the groundwaters are contaminated with nitrate due to anthropogenic activities in the area. The cation composition of the groundwater is predominantly of mixed types of calcium, magnesium and sodium, where the first two arise from the weathering and dissolution of silicate minerals such as pyroxene, olivine and biotite, and the latter (Na^{+}) suggests the dissolution of silicate mineral albite that are all found in crystalline basement rocks of the area. The predominant anion (HCO_3^-) is characterized by the dissolution of silicate minerals by recharging waters through a carbonic acid reaction. The various ionic ratios suggest that the groundwater chemistry is mainly influenced by silicate mineral weathering and cation exchange process and to a lesser extent by leaching of domestic solid waste and nitrogen-based fertilizers. The saturation index indicates that groundwater is undersaturated with respect to halite, calcite, anhydrite, fluorite and gypsum, but supersaturated with respect to dolomite. The Q–mode HCA reveals three spatial groundwater clusters. Cluster 1 consists of Ca—Na—HCO_3^- water type from recharge areas. Groundwater recharge inflows occur from the northern to southern parts of the area. Cluster 2 is characterized by Ca—Mg—Na—HCO_3 intermediate water types of moderate ionic compositions. The third cluster is mainly of Ca — Mg — HCO_3 —Cl—NO_3 water types and can be described as a discharge zone. Based on the water quality index (WQI), about 95% of the groundwater is excellent for drinking. The groundwater in the area is generally suitable for irrigation purposes with low to medium salinity hazards.

CHAPTER 5

Groundwater age dating using multi-environmental tracers (SF6, CFC-11, CFC-12, $\delta^{18}O$, and δD) to investigate groundwater residence times and recharge processes in Northeastern Ghana

Reproduced from: Okofo, L.B., Adonadaga Melvin-Guy, Martienssen Marion. Groundwater age dating using multi-environmental tracers (SF6, CFC-11, CFC-12, $\delta^{18}O$, and δD) to investigate groundwater residence times and recharge processes in Northeastern Ghana: Journal of Hydrology Vol 60 (2022) https://doi.org/10.1016/j.jhydrol.2022.127821

Abstract

The granitic aquifer of the area under investigation serves as an important source of water supply for the inhabitants. However, information about groundwater renewability and recharge process has not been defined. Multi-tracers were then applied to determine the residence times and recharge patterns of aquifer systems. In this study, sulphur hexafluoride (SF6) and chlorofluorocarbons (CFCs) were used to date shallow groundwater in Ghana for the first time. The tracer concentrations were measured in 38 groundwater wells from 38 sampling sites in Northeastern Ghana. A lump parameter model (LPM) describing the different age distributions reveals that the groundwater residence times are less than 50 years. The SF6 ages obtained were much younger than CFCs, an indication of terrigenous source enrichment. The young groundwater ages inferred from the dating process indicate modern recharge and, this collaborates with the results of the stable isotopes, in which there is a direct link between the isotopic composition of the rainfall and the groundwater. The results also indicate that the weathered and fractured granitic aquifer in the area enhances rapid and diffuse recharge after precipitation. In addition, a 3D numerical groundwater model has been developed to simulate groundwater flow under steady-state and obtain information on the key aquifer properties such as hydraulic conductivity and recharge rates. A comparison of the simulated and observed heads suggests a good match, and the developed model can satisfactorily describe groundwater flow in the area. A groundwater flow system has been delineated based on the multi-tracers (SF6, CFC-11, CFC-12, δ18O) and the numerical groundwater model. The findings of this study will be valuable for water managers and stakeholders to obtain relevant hydrogeological information for improved aquifer resource planning.

5.1 Introduction

Investigating which parcel of water enters a groundwater system needs a good understanding of isotopic studies and the groundwater age dating (IAEA, 2006). This is essential to know if an aquifer receives modern recharge for improved water resources planning (Beyer et al., 2014; Busenberg & Plummer, 2000; Cook & Solomon, 1997) Groundwater age dating can help to decipher dispersion, transport process, and residence time in an aquifer (Plummer et al., 1998), map the vulnerability of shallow aquifers to contamination (Beyerle et al., 1999; J.K. Böhlke et al., 1997; Haase et al., 2014) and reveal the consequences of land use patterns on water quality (Toews et al., 2016). Comprehension of groundwater age dating allows for the prevention of aquifer overexploitation and contamination before it begins (Kazemi et al., 2006). The past decades have witnessed tritium as an effective and consistent dating tool for groundwater due to its concentrations in precipitation arising from natural cosmic radiations and man-made thermonuclear tests that started in 1952 (Kazemi et al.,2006; Zuber et al., 2005) However, its application is limited due to declining concentrations in the atmosphere, which has made it very challenging to differentiate the tritium levels in groundwater generated by the artificial sources from the natural sources (IAEA, 2006).

So far, chlorofluorocarbons (CFC-11, CFC-12, and CFC-13) and Sulphur hexafluoride (SF6) have been at the forefront of dating groundwater (Busenberg & Plummer, 2000; Oster et al., 1996; Thompson et al., 1974). It is assumed that these compounds behave conservatively when they enter the saturated zone and travel in the direction of groundwater flow. The input functions of CFCs are well established and can be used to date post-1945 waters (IAEA, 2006). A fundamental problem with CFC dating is that the mixing ratios are levelling off and have been replaced temporarily by hydrochlorofluorocarbons such as HCF-22 and HCF-134a (Haase et al., 2014). To compensate for the limitation of CFCs, SF6 is often used in conjunction with CFCs to date groundwater and reduce ambiguities (Beyer et al., 2014). SF6 is an anthropogenic and stable gas used to date young groundwaters, which are less than 50 years (Busenberg & Plummer, 2000). SF6 offers advantages such as no contamination from urban and industrial areas and also unaffected by degradation in comparison with CFCs (P. G. Cook & Solomon, 1997). Furthermore, SF6 does not sorb easily on organic matter. Enrichment of SF6 from igneous and metamorphic rocks can complicate groundwater dating, which is a pitfall in using this technique (Busenberg & Plummer, 2000)

An increasing number of studies have successfully carried out groundwater dating using SF6 and CFCs (Busenberg & Plummer, 2000; Coralie et al., 2021; Friedrich et al., 2013; Gil-Márquez et al., 2020; Gooddy et al., 2006; Kagabu et al., 2017; Oster et al., 1996). These studies often used lump parameter models (LPMs) to explain the different age distributions in

a groundwater system (Jurgens et al., 2012; Małoszewski & Zuber, 1982). While many advances have been made in groundwater dating in other parts of the world, little has been done in Africa (Lapworth et al., 2013). For instance, Kamtchueng et al. (2015) used multi tracers (CFCs, SF6, and Cl) to assess the origin and recharge mechanism in the Lake Nyos catchment, Northwest Cameroon. Masule (2019) used SF6 to date perched aquifers in the Okongo area, Northcentral Namibia. Apparent ages ranging between 1 and 17 years were measured in these aquifers. Tindimugaya (2008) employed SF6 and CFCs to determine the groundwater residence time of fewer than 22 years in a weathered crystalline aquifer system in Uganda.

The study area selected for this work is a transboundary basin of the White Volta River basin of Ghana and is being proposed as managed aquifer recharge (MAR) site. The MAR aims to make water available all year round to counteract the increasing water scarcity that occurs every dry season. There are reported cases of low groundwater yields and groundwater overdraft in the White Volta River basin (Martin & van de Giesen, 2005; SNC-Lavalin/INRS, 2011) In addition, the semi-arid nature of the area, coupled with the unfavourable weather condition (short rainfall season and high evapotranspiration), have had dire consequences on the available water resources (Ghana Statistical Service, 2013). Since groundwater is the only reliable water supply in the area for domestic and irrigation purposes, quantification of groundwater is needed to ensure a sustainable water supply. To achieve this, groundwater age dating is being investigated to obtain relevant hydrogeologic data for the MAR project and also to understand the hydrogeological processes of the catchment. In Ghana, groundwater age dating using tritium, and carbon-14 dating has so far been studied (Acheampong & Hess, 2000; Anornu et al., 2017; Bam & Bansah, 2020; SNC-Lavalin/INRS, 2011). When compiling this research, no available studies on CFCs and SF6 groundwater age dating were seen in the literature. This study is a first of its kind in using CFCs ad SF6 to date groundwater in Ghana. This study aims to investigate the residence time of the groundwater and recharge patterns in the granitic terrain of Northeastern Ghana using CFCs and SF6. Based on the fewer years of SF6 and the low total dissolved solids of the groundwater samples, it is hypothesized that a short residence time of young groundwater would exist along the topographical flow line. It is also hypothesized that groundwater recharge in the catchment will come primarily from precipitation. Therefore, stable isotopes ($\delta^{18}O$ and δD) were used complementarily to investigate the different sources of groundwater recharge in the area. In addition, a numerical groundwater flow model was developed to determine the groundwater flow and the key aquifer properties, such as hydraulic conductivity and recharge rate in the basin. Characterization of the groundwater using the groundwater flow model, gas tracer, and isotope techniques would go a long way to provide

comprehensive information on the aquifer for improved groundwater resources planning. The findings will also serve as a guide for future studies outside the region.

5.2 Geology and hydrogeology

The catchment is largely underlain by rocks of the Tamnean Plutonic Suite (about 80%). These are crystalline basement rocks that have intruded the Birimian rocks and were formed during the Eburnean Orogeny of the Paleoproterozoic era ca. 2150 –2070 ma (Feybesse et al., 2006). This deformational stress has resulted in various degrees of fractures and faults within the rocks. The Tamnean Plutonic Suites are mainly granitoids composed of biotite – tonalite, hornblende–biotite tonalite, minor granodiorite, and minor quartz diorite (SNC-Lavalin/INRS, 2011). The Voltaian supergroup (about 20%) lies in the southeastern part of the catchment and consists exclusively of fine-grained and locally bedded sandstones from the Tossiego formations (Fig. 5.1). There are small pockets of Mesozoic rocks that are typically rich in mafic dyke and dolerite (SNC-Lavalin/INRS, 2011).

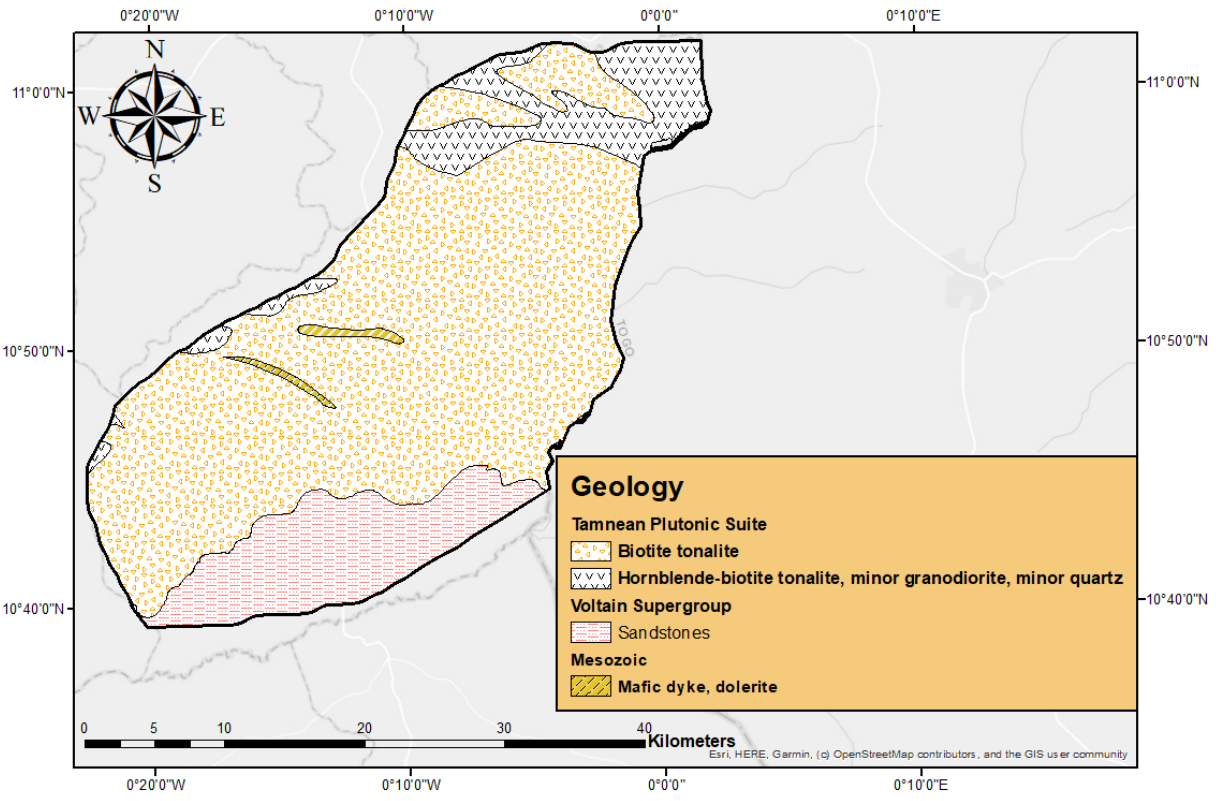

Fig. 5. 1. *The geological map of the area*

Hydrogeologically, the catchment belongs to Crystalline Basement Granitoid Complex Province and the Voltain Province. The Crystalline Basement Granitoid Complex Province are aquifers of the Tamnean Plutonic suite, while the Voltain Province are aquifers of the Voltaian Supergroup (Banoeng-Yakubu et al., 2011; Dapaah-Siakwan & Gyau-Boakye, 2000). The aquifers in the catchment are commonly semi-confined, and the mode of groundwater occurrence is controlled by structures such as faults and fractures developed from secondary permeability and porosity. The variability of the fractures within the rocks depends on the nature, aperture, degree of weathering, and interconnecting spaces. In the Voltaian Province, processes such as compaction and cementation have affected the primary porosity of the rocks, and thus, groundwater generally occurs in the fracture areas and bedding planes. (Carrier et al., 2008; SNC-Lavalin/INRS, 2011) Furthermore, the average regolith thickness of the Voltain Province aquifers is relatively thin, circa 9 m, due to the mixtures of clay, quartz, and mudstone materials in the area (Carrier et al., 2008).

Within the Crystalline Basement Granitoid Complex Province, groundwater occurs in the shallow aquifer, regolith aquifer, and fractured aquifer. The shallow aquifer is ephemeral that quickly dries up in the dry season. Figure 5.2 shows the available lithological data in the area that were used to construct multiple 3D strip logs. This consists of the topsoil (laterite, silt, sandy clay), saprolite (highly weathered granite), saprock (moderately to poorly weathered granite), and fresh granite. The saprolite and saprock layers are made up of the regolith aquifer. The fractured aquifer is made up of weathered granitic bedrock with fractures. The regolith thickness ranges from 7.8 m to 37m, with an average value of 25 m. High quantities of groundwater usually exist in coarse-grained granites and fractured quartz veins. Groundwater yield varies from 0.36 m^3/h to 37 m^3/h with a mean yield of 4.2 m^3/h (Banoeng-Yakubu et al., 2011). On average, the groundwater table in the catchment varies from 12 m to 25 m (Acheampong, 2017). Inflow to the aquifers is mainly through recharge from precipitation and, to some extent, from the White Volta River (Akurugu et al., 2020; Carrier et al., 2008) There is no established groundwater recharge and groundwater flow regime in the area. Generally, groundwater recharge in the White Volta Basin ranges between 3.4 % and 18.4 % of the mean annual precipitation of 980 mm (Obuobie, 2008). Groundwater flow in the crystalline basement complex is usually northeast to the southwest flow direction (Akurugu et al., 2020).

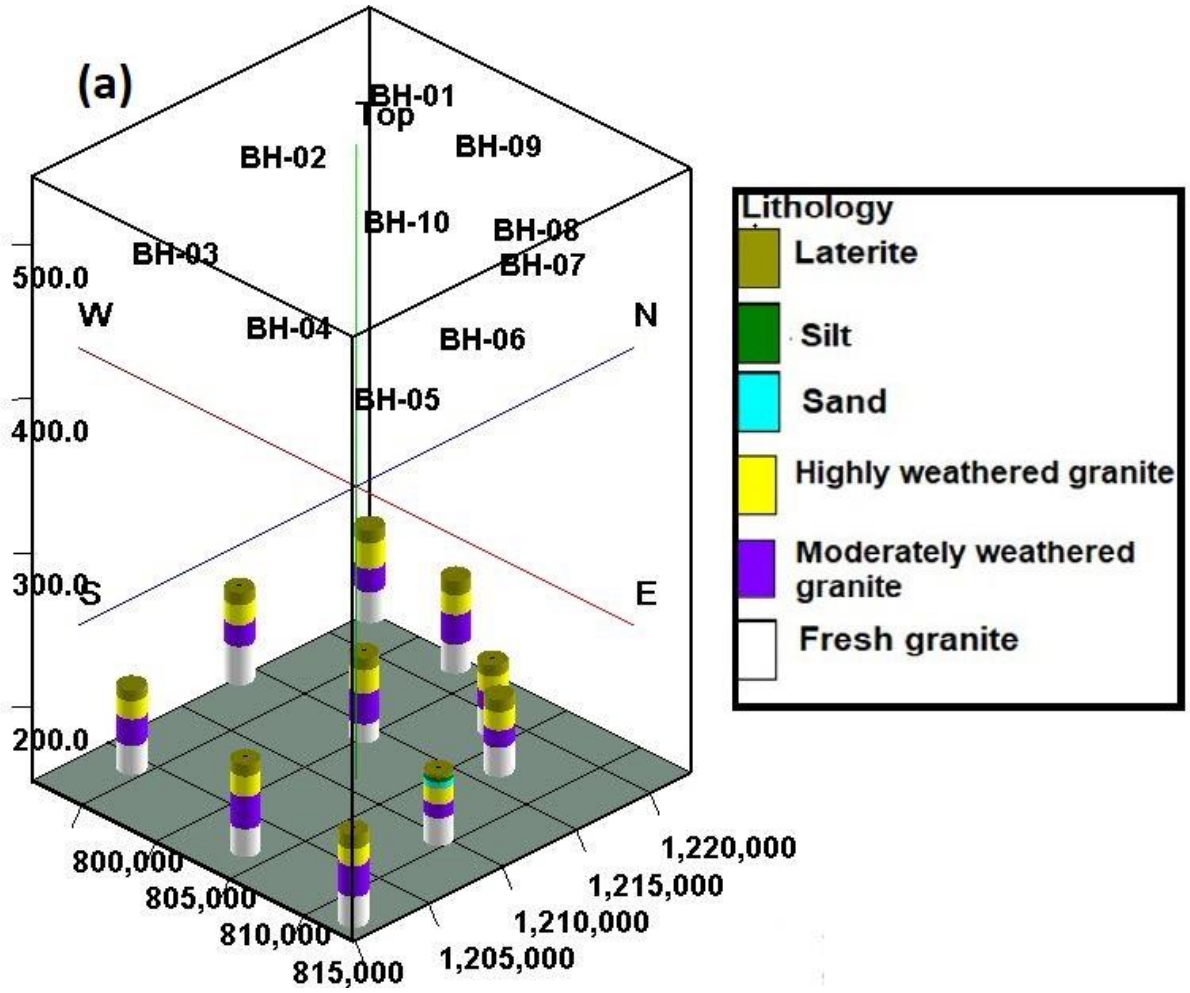

Fig. 5.2. *Hydrostratigraphy profile of the study area*

5.3. Theoretical background

SF6 and CFCs are purely synthetic compounds that have been introduced into the atmosphere in numerous ways. Industrial production of CFCs started in 1930 due to the constant use of CFCs in refrigerators, air conditions, aerosols propellants, and blowing agents for plastic foams (IAEA, 2006). The mixing ratios of CFCs are decreasing due to the ratification of the Montreal Protocol Treaty of 1987 designed progressively to halt the commercial use of CFCs and other substances that depletes the ozone. SF6 was introduced into the troposphere as gas-filled electrical switches in 1953 (Busenberg & Plummer, 2000; IAEA, 2006) Since then, the atmospheric mixing ratios of SF6 have risen steadily from a background value of 0.05 pptv (in 1953) to about 9 pptv at present (2020). The gradual increase of SF6 is due to its low solubility in water and high soil stability (Busenberg & Plummer, 2000; Mroczek, 1997) This makes SF6 an excellent tracer to date young groundwater because accurate dates would be obtained (Haase et al., 2014). CFC mixing ratios in populated urban areas are sometimes above the background atmospheric

concentrations, making dating problematic in these areas as the waters are contaminated with younger ages (IAEA, 2006). On the other hand, SF6 contamination of groundwater is rarely reported in urban areas. However, concentrations of SF6 in groundwater have been reported to be higher than atmospheric concentrations due to its natural terrigenous origin, frequently found in igneous and volcanic rocks (Busenberg & Plummer, 2000). Several processes can affect the apparent CFC ages of water to become either old or young if not adequately taken into consideration (Cook et al., 1995). Examples of the environmental processes that can make groundwater old are sorption, hydrodynamic dispersion, matrix diffusion, and microbial degradation (IAEA, 2006). Under anaerobic conditions, CFCs are affected by degradation, mainly by dechlorination reactions that yield hydrochlorofluorocarbons (HCFC) (IAEA, 2006). Laboratory work has proved that SF6 is highly resistant to degradation. Again, the octanol-water partition coefficient demonstrates that SF6 partitions into an aqueous solution more easily than CFCs, signifying that sorption of SF6 is limited and doesn't sorb easily onto aquifer materials (Plummer & Busenberg, 2000; Wilson & Mackay, 1996)

The global atmospheric mixing ratios of CFCs and SF6 have been historically measured and reconstructed by the National Oceanic and Atmospheric Administration Halocarbons (NAOO), as shown in Fig 5.3. By measuring the CFCs and SF6 concentrations in groundwater and comparing them with the historical dates at which the water was introduced into the saturated zone, it can be assumed that the solubility of the groundwater sample equilibrates with the atmospheric air at the time of recharge (IAEA, 2006).

Groundwater dating with SF6 and CFCs is governed by Henry's Law of solubility. The application required some basic assumptions to be made and important of this is the correction of recharge temperature, excess air, and the thickness of the unsaturated zone. The recharge temperature is usually determined by the concentrations of the dissolved gases in water such as N_2, Ar, Ne, and Xe (Aeschbach-Hertig et al., 1999; Vogel et al., 1981). Since these gases were not measured, the recharge temperature for this study was taken from the groundwater temperature, which is almost equal to the mean annual air temperature of the area. Uncertainties in recharge elevation can affect the apparent age of the water. The terrain in the study area is very flat, and therefore, the uncertainty in recharge elevation cannot introduce dating errors (IAEA, 2006). Furthermore, mostly fractured granites underlie the area where rapid diffuse recharge occurs across all sites (Bam & Bansah, 2020; Carrier et al., 2008). Therefore, an excess air of 5 cc/L was assumed and corrected for measured SF6 concentrations, suggested for fractured rocks (Wilson & McNeill, 1997). The average depth to the groundwater table is 9 m (Carrier et al., 2008). Based on this, the thickness of the unsaturated zone was not corrected because it is assumed the air in the thin

unsaturated zone has the same composition as the atmosphere (Cook & Solomon, 1997; Oster et al., 1996).

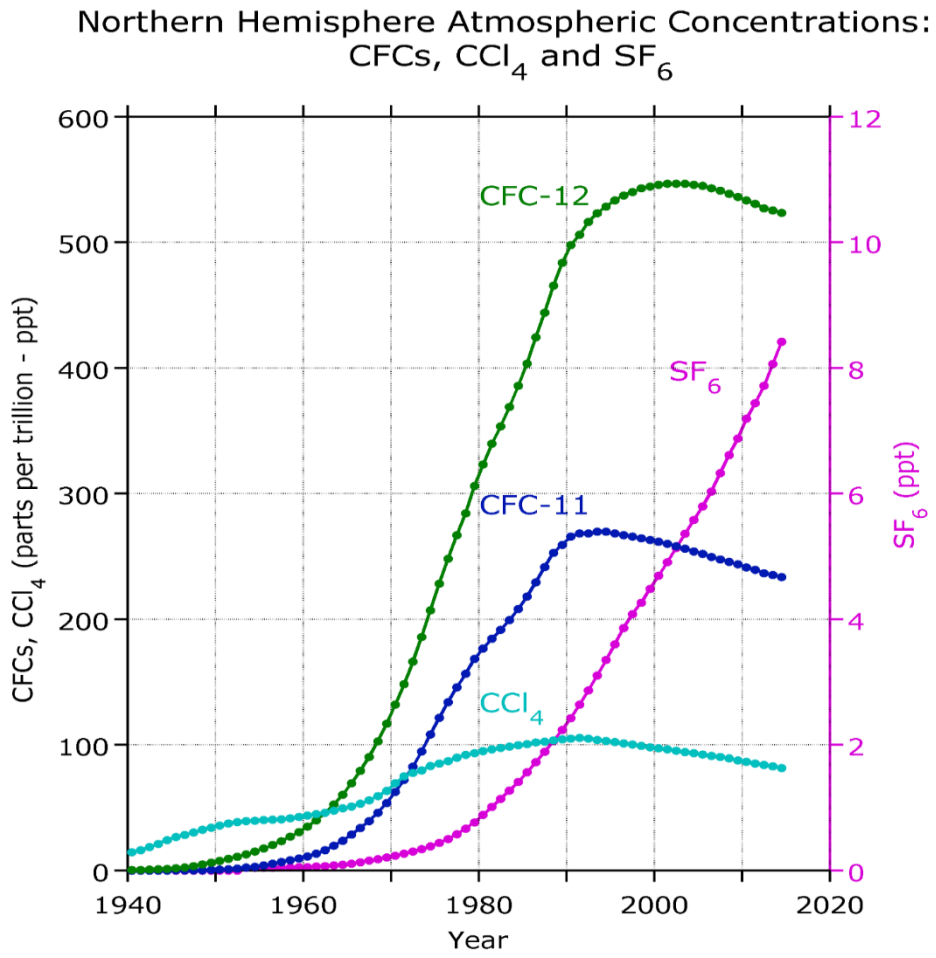

Fig. 5.3. *Northern Hemisphere Atmospheric Concentrations of the various tracers (https://www.pmel.noaa.gov/)*

5.3.1 Calculations

The concentrations of CFCs and SF6 obtained from the chromatography were converted to the atmospheric partial pressures (pptv) by employing a solubility function for a given temperature and salinity (Bu & Warner, 1995; Bullister et al., 2002; Warner & Weiss, 1985) The following sets of the equations (Eqn 5.1 to 5.7) were used to define the apparent age of the sample. In the first pace, the known mixing ratio of the gas injected into the GC was taken. The dry partial pressure (P) of the CFCs/SF6 in the headspace of the bottle was computed by subtracting the vapour pressure (PH_2O) from the total atmospheric pressure (Patm) and multiplying the results by the mixing ratio (MR)

$P = MR^* (Patm - PH_2O)$ 5.1

Subsequently, the concentration of CFCs/SF6 (X) in the water of the bottle was calculated using Henry's Law (KH).

$X = KH * P(atm)$ 5.2

In the next step, the number of moles of CFCs/SF6 in the water (Mw) was deduced by multiplying both the concentrations of CFCs/SF6 and the volume of water (V) in the bottle

$Mw = X * V$ 5.3

The number of moles (Mh) of the headspace gas was calculated using the ideal gas law.

$Mh = PV/RT$ 5.4

The concentration of CFCs/SF6 in the original sample (concentration in the aquifer) was calculated by dividing the total moles (Headspace + Water)/ mass of water.

$X(recharge) = (Mw + Mh)/V$ 5.5

Finally, the partial pressure at recharge was calculated using Henry`s Law

a. $P(recharge) = X(recharge)/KH$ 5.6
b. $MR(recharge) = (Precharge / Patm) *SR$ 5.7

Where SR is the scale ratio, i.e. 1E12 for parts per trillion

5.3.2 Lumped Parameter Models (LPMs)

Lump parameter models (LPMs) are pre-defined mathematical models of simplified flow geometry that describe the dispersion and mixing of waters in an aquifer (Jurgens et al., 2012; Małoszewski & Zuber, 1982). Groundwater sampled in a catchment may constitute different mixed ages, with the mean age and residence time considered as one entity. However, the apparent age of a sample will not be the same as the mean age because the tracers are non-linear functions of time (Cook & Herczeg, 2012). The lumped parameter models are thus used to compute the relationship between apparent age and the mean residence time. The age frequency distribution influences these in the groundwater sampled at a given time using a convolutional integral that adds up the tracer concentrations under a steady-state flow condition (Cook, P. G., & Herczeg, 2012; Małoszewski & Zuber, 1982)

$$C_{out}(t) = \int_{-\infty}^{t} C_{in}(t')\, e^{-\lambda(t-t')} g(t - t')dt' \quad 5.8$$

Where C_{out} = the output tracer concentration, C_{in} = the input tracer, t' = is the transit time of the tracer, t = sample date, $e^{-\lambda(t-t')}$ = decay of the radioactive tracers, g(t – t')= weighting function of the age frequency distribution.

The calculated mixing ratios (pptv) of the SF6 and CFCs and the tracer input history of northern hemisphere data contained in the TracerLPM software were used to model and investigate the age distributions of the samples (https://www.usgs.gov/software/tracerlpm). Three LPMs were selected for this study based on the basin hydrogeological characteristics: the piston-flow model (PFM), exponential mixing model (EMM), and the binary mixing model (BMM) (Małoszewski & Zuber, 1982). The PFM considers that a parcel of water moves from a recharge zone to a discharge zone in an aquifer neglecting hydrodynamic dispersion or mixing. This model is constrained to a catchment where the travel time of the water is short with a high average linear velocity. The EMM is characterized by a mixture of different water age distributions. A full penetrating aquifer with homogenous thickness and recharge that discharges into springs or rivers can be best represented by the exponential mixing model (EMM). The BMM, on the other hand, involves two models: the PFM and the EMM and is applicable for screens that traversed multiple aquifers (Jurgens et al., 2012).

5.4. Results and interpretation

5.4.1 Physicochemical parameters of the groundwater and surface waters

The groundwater temperature values range from 31.1°C to 32.9°C with an average value of 31.9°C whereas, the surface water temperature varies from 33.4°C to 35.1°C with a mean value of 34.7°C (Table 5.1). The groundwater temperature was higher than the recent average annual temperature (29°C) of the area, suggesting the local geothermal gradient influences the groundwater (Reiter, 2001). All the surface water temperatures were noticeably higher than the groundwater temperature. The electrical conductivity (EC) of the groundwater is within the range of 85.5 µS/cm - 593 µS/cm with an average value of 249.86 µS/cm suggesting a low to slightly mineralized water (Fig.5.4a). The EC values of the surface water were lower than that of the groundwater, with values ranging between 72 µS/cm and 192 µS/cm with an average value of 120.5 µS/cm.

The groundwater in the study area is moderately acidic to moderately alkaline, with pH values ranging from 6.25 to 7.93, with a mean of 7.09. The surface water exhibits alkaline conditions with values ranging from 7.58 to 8.65, with a mean value of 8.04. Dissolved oxygen concentrations of the groundwater are mostly anoxic, with values varying between 0.4 mg/L – 1 mg/L with a mean of 0.57 mg/L. The surface waters display oxic conditions due to direct exposure to the atmosphere. These values range from 4.0 mg/L to 5.4 mg/L with an

average of 4.6 mg/L. The total dissolved solids (TDS) as shown in (Fig 5.4b) have values less than 600 mg/L suggesting the water could be fresh and young (Freeze and Cherry,1979). The bicarbonate of the groundwater, which was measured as alkalinity in the field, ranges from 90.23 mg/L to 446.3 mg/L with a mean of 188.61 mg/L. The primary source of bicarbonate in groundwater is attributed to carbon dioxide in the atmosphere and in soil gases that dissolve in rain and surface water (Clark, 2015).

Table 5.1 Physicochemical parameters of groundwater and surface water in the study area

Communities	Eastings	Northing	Elev m	SWL m	Head m	pH	Temp °C	EC (µs/cm)	DO (mg/L)	HCO_3 (mg/L)	Cl (mg/L)	TDS (mg/L)
Garu Zongo 1	808746	1201053	263	-	-	6.25	31.6	348	0.47	195.1	42.22	313.23
Garu Zongo	808875	1200907	257	5.25	251.75	6.56	31.5	502	0.48	213.4	17.15	339.52
Garu Market	808451	1201182	239	9.10	229.90	6.57	31.4	154.1	0.57	181.7	0.52	193.23
Garu Central	807185	1205607	208	-	-	6.71	32.9	88.7	0.60	90.23	0.55	127.38
Napadi Yapa	806276	1206513	197	-	-	7.70	32.7	243	0.41	195.1	2.06	248.28
Pialugu	805279	1195367	221	10.28	210.72	7.51	31.4	256	0.49	221.9	1.33	269.55
Sigure Yapala	802781	1196108	230	4.60	225.40	7.42	32.2	229	0.55	197.5	5.74	237.87
Dusbuliga	802925	1190913	237	14.34	222.66	7.22	31.5	172.5	0.60	157.3	0.54	211.73
Senebaga	801737	1188297	215	12.02	202.98	6.93	31.4	262	0.43	197.5	10.13	250.35
Kogri	796280	1193112	232	3.80	228.20	6.54	32.1	212	0.61	242.6	0.97	272.50
Kogri 2	800847	1196178	225	8.77	216.23	6.42	31.1	137.2	0.50	112.2	1.97	155.84
Barboaka	810352	1200600	251	13.63	237.37	6.53	31.5	205	0.43	217	4.18	272.37
Busnatiga	8012363	1204210	207	5.71	201.29	7.12	31.8	244	0.48	175.6	0.91	210.82
Yabrago No.1	815266	1202988	233	11.13	221.87	6.91	31.7	157	0.83	219.5	1.00	252.34
Tindane Prim.	816918	1201899	237	1.58	235.42	7.69	32.4	346	0.60	217	3.19	274.74
Duadinyediga	817660	12106420	217	-	-	7.07	32.5	240	0.41	200	24.58	385.88
Kugashegu	817109	1208120	227	5.63	221.37	7.76	32.3	307	0.56	151.2	8.89	204.87
Pwalugu Nati.	817773	1209573	233	5.64	227.36	7.53	32.5	221	0.59	173.1	2.95	211.01
Baatiyok	815320	1209149	222	6.04	215.96	7.12	32.1	169.8	0.52	147.5	2.91	184.86
Abapusug	816275	1211889	241	4.95	236.05	7.39	32.2	206	0.52	143.9	4.46	188.77
Bugri Dam	814008	1214380	217	5.62	211.38	7.09	32.2	247	0.48	189	0.24	241.21
Zumandiga	813706	1215602	219	2.61	216.39	7.71	32.7	291	0.47	186.6	2.98	249.30
Bugri Central	812583	1215155	212	4.92	207.08	7.21	32	233	0.54	164.6	8.29	220.94

Sakparatinga	815060	1215407	230	5.88	224.12	6.99	32.1	283	0.45	201.2	8.16	266.81
Baranatinga	818511	1215991	230	3.04	226.96	7.23	32.8	356	0.42	251.2	16.95	398.18
Karateshie	819533	1213231	252	4.89	247.11	6.92	31.5	239	0.55	115.8	0.89	148.90
Winatinga	820385	1215102	245	3.97	241.03	7.21	32	295	0.56	191.4	2.80	253.26
Yaranatinga	821431	1215582	254	6.21	247.79	7.05	31.1	593	0.40	446.3	2.36	524.80
Garu D.A Pr.	808668	1200740	223	4.92	218.08	6.40	31.6	167	0.56	189	3.45	240.58
Garu Clinic	808487	1200819	229	-	-	6.71	31.2	85.5	0.86	153.6	0.49	179.42
Garu CBR	807989	1200737	231	6.99	224.01	6.41	31.7	171.5	0.64	256.1	15.66	306.63
Garu Belatek	807646	1201571	228	-	-	7.14	31.9	240	0.61	171.9	12.88	211.27
Garu Medina	808249	1201613	229	-	-	7.16	31.7	278	0.49	231.7	2.80	296.31
Holy E J.H.S	808608	1201996	226	-	-	7.09	32.1	373	1.0	206.1	2.36	324.92
Tanzugu	808782	1200400	239	5.39	233.61	7.33	32.3	455	0.96	151.2	13.99	249.29
Zumadori	808535	1199528	234	10.73	228.61	7.93	31.6	125.3	0.63	136.6	1.52	157.29
Nisbuligu	809375	1196172	246	9.85	235.27	7.41	31.6	250	0.52	164.6	0.82	193.66
Zaari	810567	1195197	262	-	-	7.16	31.6	112.2	0.68	111	3.83	151.76
RS1	810973	1209525	224			8.65	35.6	192	4.6			
RS2	797225	1187114	193			8.21	34.1	75	4.9			
RS3	804998	1181021	162			8.45	35.1	129	5.3			
RS4	805333	1201114	206			8	34.9	122	4.7			
RS5	825698	1217131	247			7.98	35.1	92	4.1			
RS6	822627	1219304	253			7.58	35.4	123	5.4			
RS7	811406	1216895	209			7.59	35.5	139	4.2			
RS8	819790	1198042	232			8.1	34.2	120	5.1			
RS9	816750	1193259	230			7.95	34.9	152	4.9			
RS10	816404	1206097	215			7.89	34.9	141	4.7			
White Volta 1	788261	1190484	157			8.04	33.7	79	4			
White Volta 2	787787	1185059	157			8.11	33.4	83	4.2			
Min						6.25	31.1	75	0.4			
Max						8.65	35.6	593	5.4			
Mean						7.31	32.6	218.8	1.55			
SD						0.58	1.33	110.1	1.79			

SWL(static water level), Head (hydraulic head), Elev (Elevation), RS1 – RS10 (surface water)

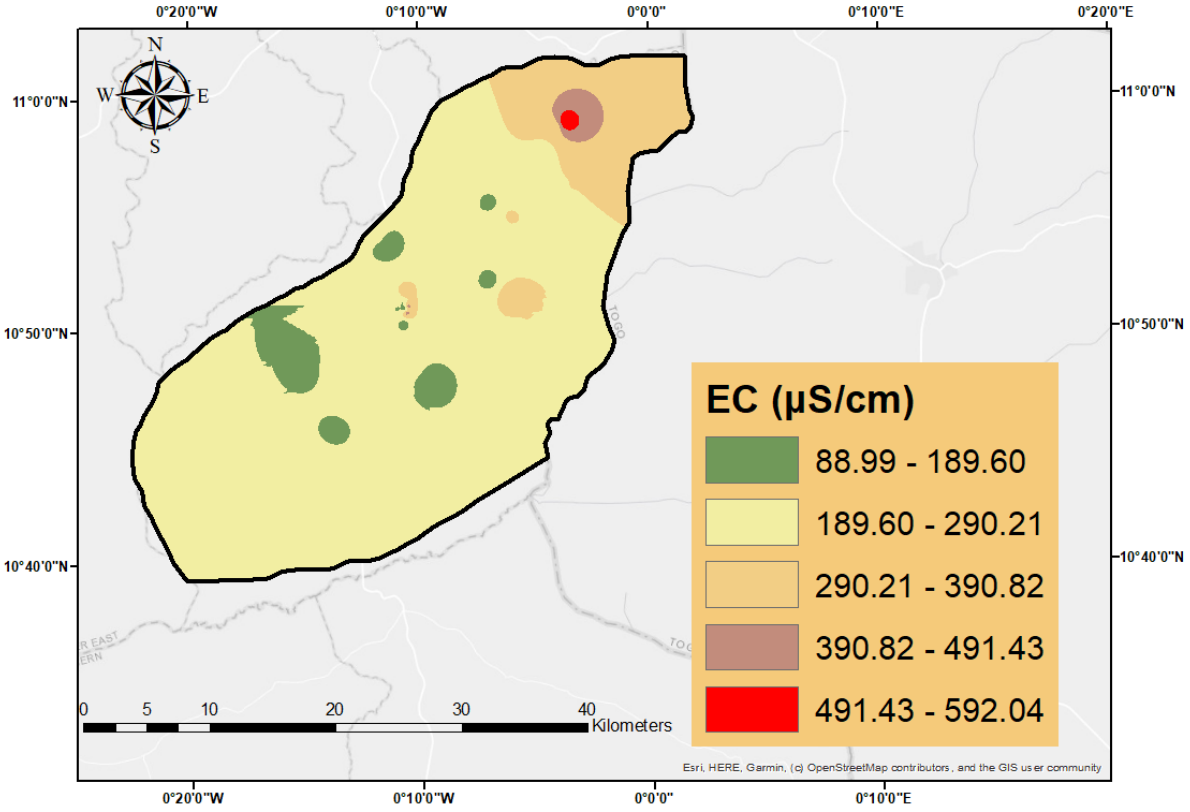

Fig. 5.4.a *Spatial distributions of EC concentrations in the groundwater*

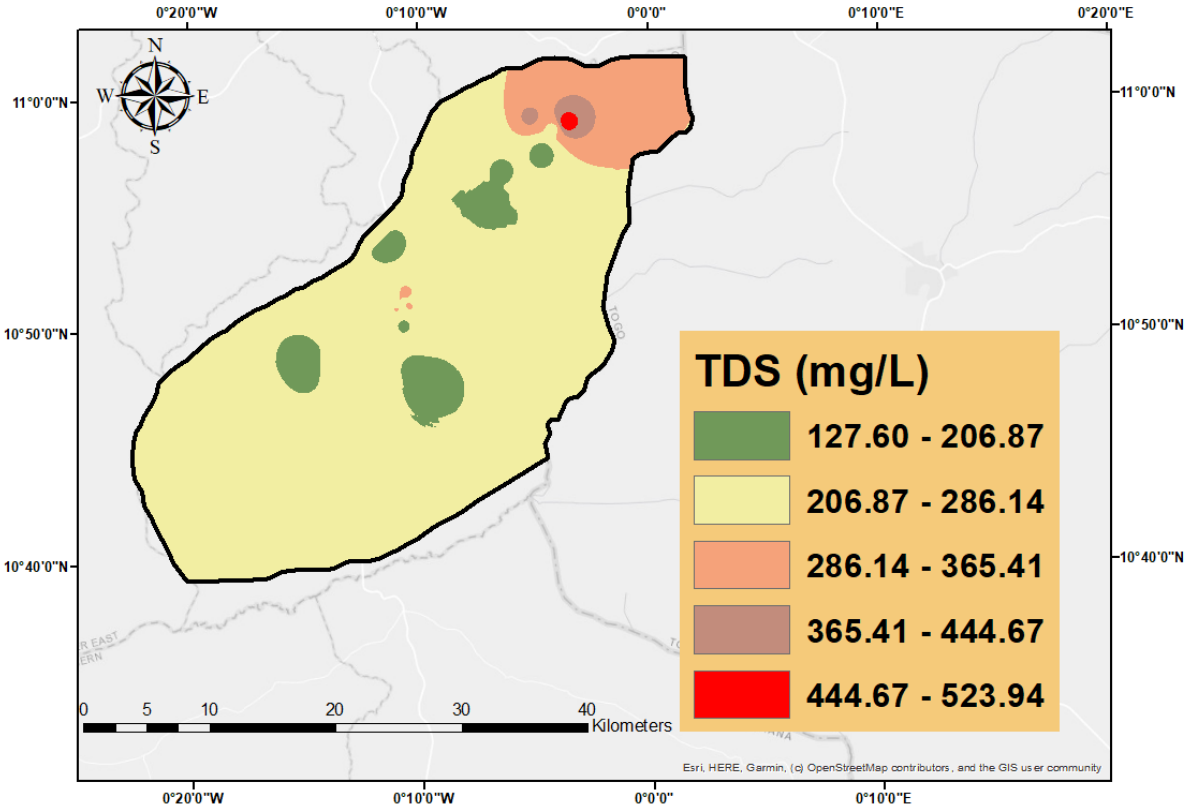

Fig. 5.4b *Spatial distributions of TDS concentrations in the groundwater*

5.4.2 Numerical groundwater flow model

A conceptual model has been developed based on groundwater chemistry, isotopes, and hydraulic heads data of the area. Conceptualization was done with the help of a map tool contained in the Groundwater Modeling System Software 10.4 (Aquaveo, 2020). The model domain was conceptualized as a single hydrogeological layer at which the model top was defined as a semi-confining condition to reflect the hydrogeological condition of the area. The bottom of the model was conceptualized as a confining condition since it is an inherently no-flow boundary with low permeabilities and hydraulic conductivities (Anderson et al., 2015). A general head boundary (GHB) was imposed in the model to simulate groundwater flow across the entire boundary. Coverages for recharge, hydraulic conductivity, hydraulic head, and abstraction were created and incorporated into the model.

In the next step, the conceptual model was converted into a 3D numerical model consisting of a cell-centred, finite difference USGS MODFLOW – 2000 simulation code (McDonald and Harbaugh, 1998). The model domain of 1200 km^2 was discretized into 1000 uniform cells using a finite-difference grid with 100 rows and 100 columns to achieve a good model output. The MODFLOW was then used to simulate groundwater flow only under steady-state conditions because there are no historical water level measurements of the area for transient simulation. The steady-state condition of the area represents the water levels taken in 2017, in which groundwater flow was assumed to be constant, and shows equilibrium condition after a long-term pumping. Thirty hydraulic head data (Table 5.1) were used for the steady-state simulation, and a calibration target of 1 m was set for all the wells. In the final step, calibration was performed in two parts: the manual trial-and-error and automated calibration using the automated parameter estimation (PEST) interface in GMS.

Figure 5.5a shows the spatial hydraulic head distribution of the steady-state model. Different groundwater flow paths are also observed due to the fractured nature of the rocks. Groundwater movement in the area is mainly dictated by secondary porosities and permeabilities developed from the weathering and fracturing (Dapaah-Siakwan & Gyau-Boakye, 2000). The groundwater contours mimic the geology and surface topography of the area where the highest and lowest hydraulic heads are seen in the northern and southern parts, respectively. This conforms to the assertion that hydraulic heads in aquifers are generally a subdued replica of the topography (Haitjema & Mitchell-Bruker, 2005). Simulated flow predominantly shows NE– SW preferred flow patterns. In Ghana, the NE– SW flow patterns have been reported in many studies (Kesse, 1985; Yidana et al., 2015) This is due to the tectonic and structural deformation of the rocks. Both local and regional flow systems controlled by structural entities are observed in the study area.

A plot of simulated and measured field groundwater heads (Fig. 5.5b) significantly correlates with a root mean square residual head of 1.11 m. This indicates a good match, and the simulated flow can be reliably used to represent the hydrogeological conditions of the area. The calibrated recharge values obtained range from 5.0 × 10^{-3} mm/day to 7.5× 10^{-2} mm /day, which corresponds to 0.19% and 2.9 % of the average annual precipitation in the area. The recharge values are consistent with values reported by (Akurugu et al., 2020). These low recharge estimates reflect the prolonged dry season and high evapotranspiration of the area.

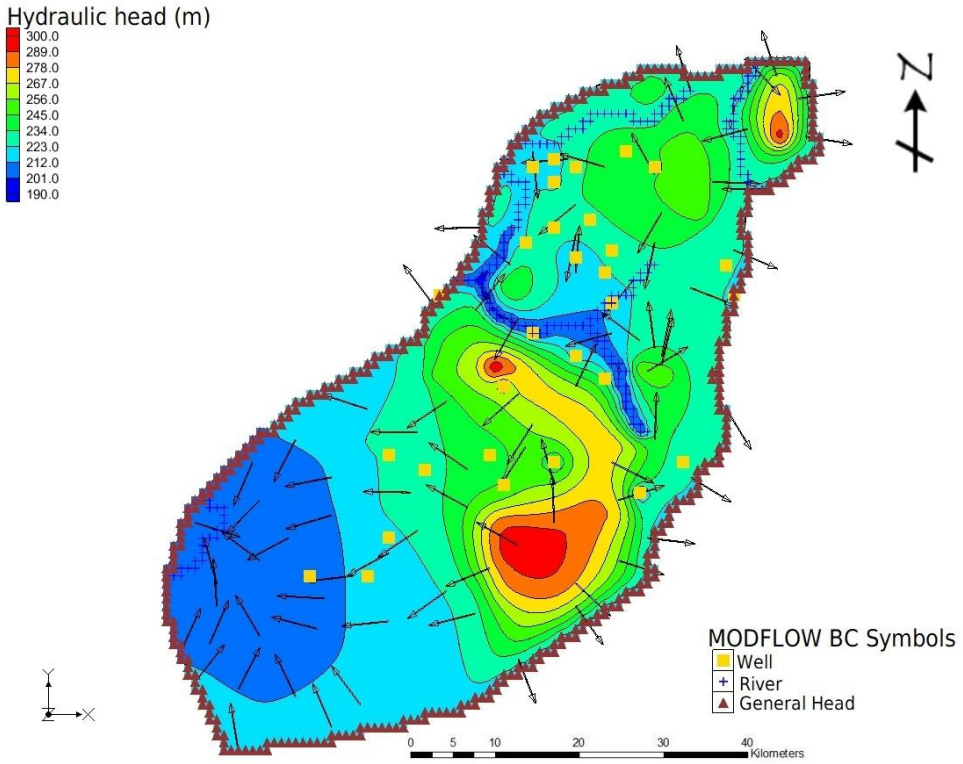

Fig.5.5a. *A steady-state model showing the simulated flow patterns of the area*

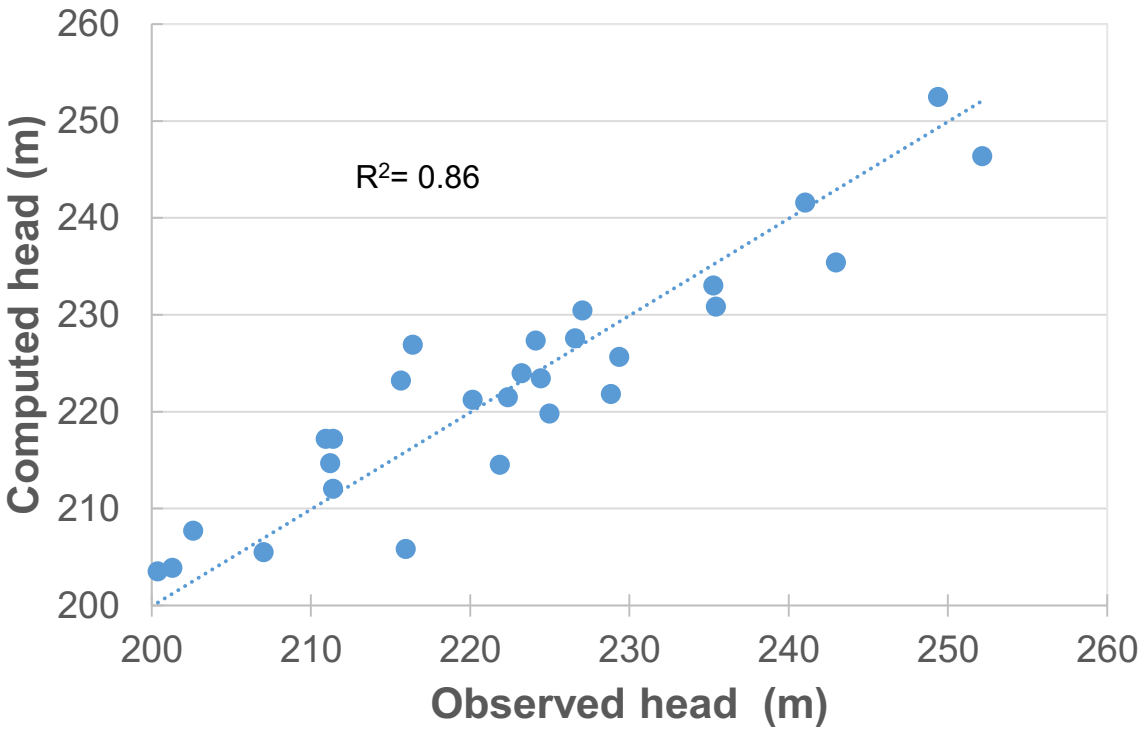

Fig.5.5b. *Relationship between observed and computed head*

The estimated hydraulic conductivity field shows values ranging from 0.2 m/day to 10 m/day (Fig. 5.6). The highest hydraulic conductivity values are found in the southwestern parts, and this can be explained as enhanced fractures of the rocks that permit rapid vertical groundwater recharge and enough groundwater storage. This development indicates a piston flow model with a short groundwater residence time (Kamtchueng et al., 2015). This also ties in with low EC and TDS values observed in the southwestern part of the area, as shown in Figures 5.4a and 5.4b. The surrounding terrains mostly have HK values less than 2 m/day, which is within the range of literature values for granitic rocks. These lowest hydraulic conductivities may be associated with massive rocks, and fine particles from the weathering processes, which might have filled the interconnecting spaces precluding free circulation of water and allowing rapid lateral flow (Addai et al., 2016; Lapworth et al., 2013). The groundwater chemistry in this terrain is characterized by varying EC values with the highest concentrations and enriched isotopic values occurring in the northern part. The weathered layers in this area may intercept high groundwater concentrations facilitating prolonged residence time, resulting in different groundwater ages.

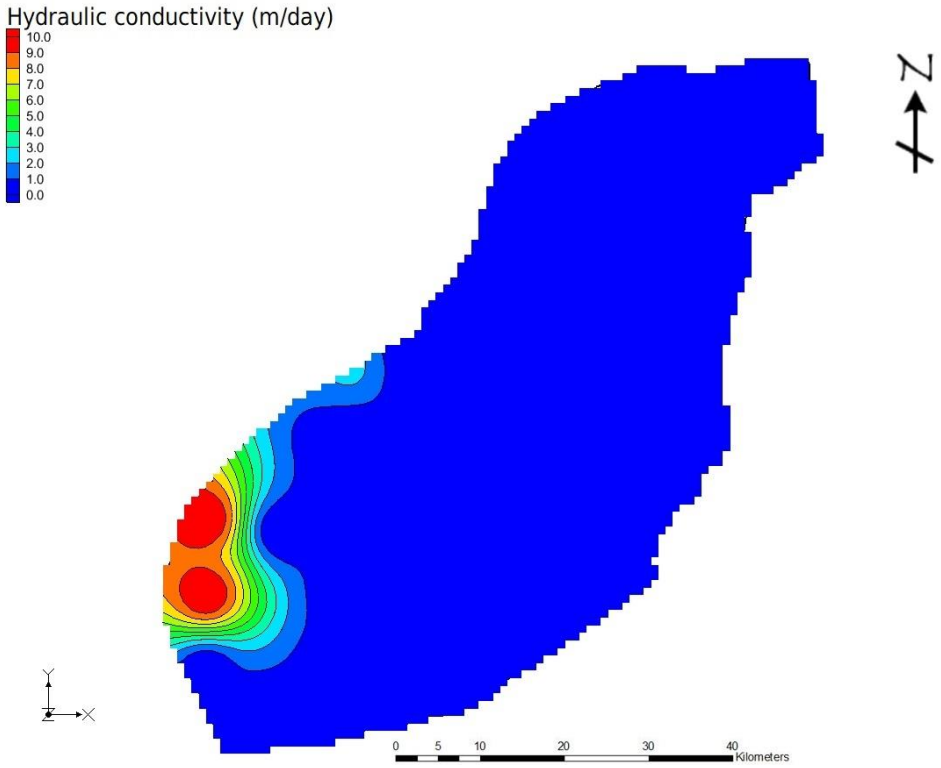

Fig.5.6. *Hydraulic conductivity field of the calibrated steady-state model*

5.4.3 Groundwater recharge estimate

The groundwater recharge estimation in the area was investigated from the chloride mass balance (CMB) approach. Several assumptions are made in using the CMB. These are (1) the area is under state (2) chloride does not change in composition (acts conservatively) in the groundwater along its flow path (3) chloride source is only from precipitation and (4) there is no surface runoff (Cook et al., 2017). If all the assumptions are satisfied, then groundwater recharge can be computed using the relation in Eqn 5.9.

$$\text{Recharge} = \frac{C_p}{C_{gw}} * P \qquad 5.9$$

Where C_p and C_{gw} are chlorides in precipitation and chloride in groundwater, respectively, and P is the average annual precipitation.

The average chloride content in precipitation (1.31 mg/L) was taken from the nearest basin in Northern Ghana, and this was used in the calculation. Chloride concentrations from 37 wells were used in the computation since one borehole (Bugri Dam View) was too low and not included in the analysis. Based on the annual average precipitation (938 mm/year) of the area, the computed percentage recharge ranges from 0.2 % to 24.8 %, with an average of 7

% (Fig 5.7). This suggests the fraction of precipitation that enters the unsaturated zone and reaches the groundwater system as effective recharge. These values are consistent with CMB values reported by different researchers in the White Volta River basin and Northern Ghana (Afrifa et al., 2017; Akurugu et al., 2020; Obuobie et al., 2012)

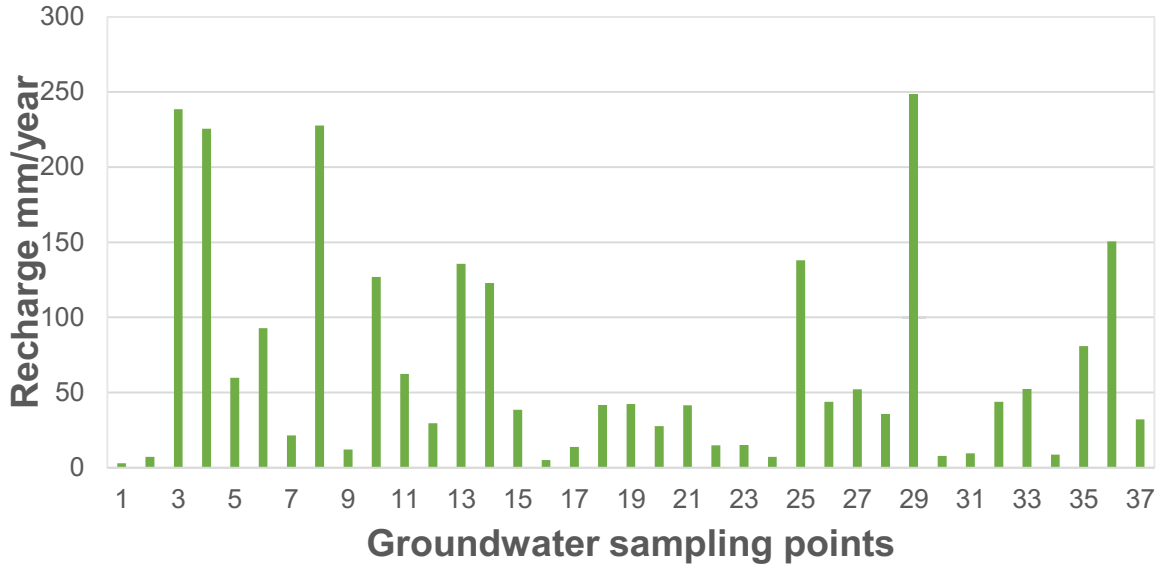

Fig. 5.7. *Groundwater recharge rate at each sampling location in the catchment*

5.4.4 Stable isotopes analysis

The monthly isotopic composition of precipitation (n=70) measured at Dapaong station in Northern Togo from 2015 to 2019 and integrated into the IAEA-GNIP database was adopted as a local meteoric water line (LMWL) due to its proximity and similar climatic conditions to the study area. The local precipitation has δ^2H and δ18O values ranging between -60.39 ‰ and 28.15‰ and -8.93‰ and 2.91‰, respectively. The positive and negative values recorded can be described as the seasonal changes in the isotopic composition of precipitation. This is mainly controlled by the temperature-dependent equilibrium fractionation effect, in which negative values are typically recorded in the rainy season (more negative in July) and positive values recorded in the dry season (Clark & Fritz 1997). The regression equation of LMWL is presented in (Eqn 5.10), which is consistent with the values obtained by different researchers in Northern Ghana (Addai et al., 2016; Akurugu et al., 2020; Oteng Mensah et al., 2014). The global meteoric water line (GMWL) after Craig (1961) is also presented in (Eqn 5.11)

$$\delta^2H = 7.45\delta^{18}O + 6.48 \quad (5.10)$$

$$\delta^2H = 8\delta^{18}O + 10 \quad (5.11)$$

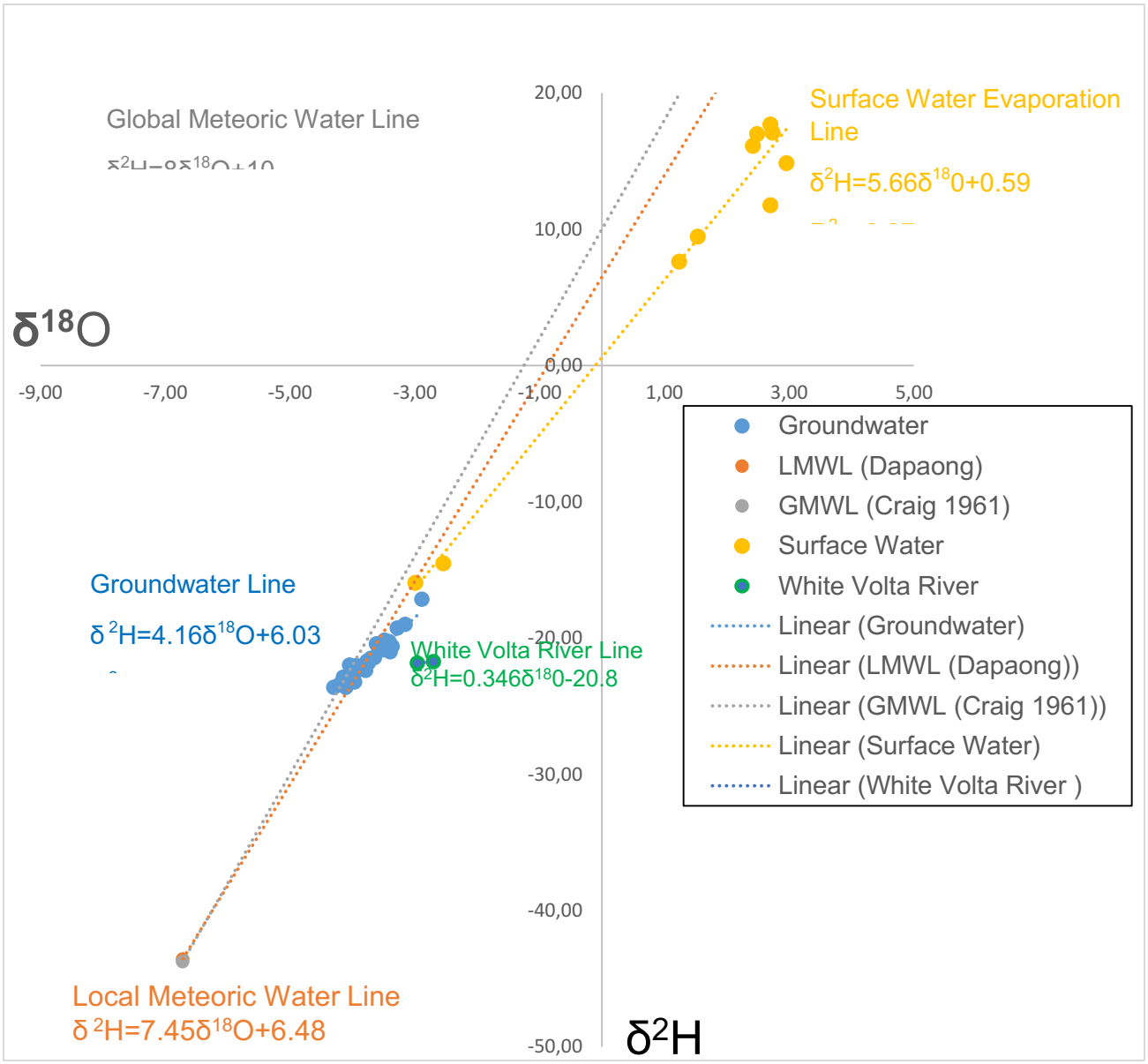

Fig. 5.8. *The relationship between $\delta^{2}H$ and $\delta^{18}O$ of groundwater and surface water*

The LMWL deviates slightly from the GMWL with a lower slope and intercept of 7.4 and 6.4, respectively. This indicates a slight enrichment in heavy isotopes of the LMWL, which is caused by the evaporation of the rain droplets at the local scale. During the dry season, low relative humidity coupled with high rising temperatures is recorded, leading to the secondary evaporation of rain droplets in the air. A consequence of this leads to a smaller slope less than 8, as observed in (Eqn 5.10) relative to the slope of GMWL (Leibundgut et al., 2009). Another factor for the modification of the LMWL is the differences in air masses, which is the dry continental air mass and maritime air mass from the Atlantic Ocean that bring seasonal variations in the isotopic composition of precipitation in the area. The air masses usually come from the sea and ocean, and as they move inland with increasing distance from the ocean, a progressive depletion in ^{18}O and ^{2}H is recorded (Clark & Fritz 1997).The area is

mainly flat in topography, and as such altitude effect has minimal or no consequences on the isotopic composition of precipitation (Aggarwal et al., 2005).

5.4.5 Stable isotopes of surface water, mixing, and evaporative enrichment

The ^{18}O composition of the surface waters ranges between -2.99 ‰ and 2.74 ‰ with an average of 1.33‰; whereas the δ^2H composition shows -15.96‰ and – 17.68‰ with an average of 8.10‰. Almost all the surface waters are below the GMWL and LMWL, indicating evaporation. The evaporation produces characteristic enrichment in heavier isotopes along the evaporation line at a lower slope and intercept than the GMWL and LMWL. The equation of the surface evaporation line is shown in Eqn 5.12

$$\delta^2H=5.66\delta^{18}0+0.59 \qquad 5.12$$

The surface waters were sampled in November at the driest time of the year and conform to the assertion that surface waters are subjected to modification by evaporative fractionation during the dry season (Clark & Fritz 1997). The effects of the evaporative enrichment of the surface waters tend to have a shallower slope under a high temperature and low relative humidity in the area (Darling et al., 2003). However, two of the samples are depleted in heavier isotopes relative to the other surface water samples. These are large rivers located in the northwestern part of the area and are tributaries of the White Volta, which is also depleted. As they flow naturally towards the White Volta River with trees and vegetation cover, they are subjected to minimal evaporation since they are not exposed much to sunlight (Gampson et al., 2017). The samples also fall on the LMWL, suggesting precipitation is the primary source of recharge for these surface waters. It might be possible that the two samples are affected by kinetic evaporation, but the infiltrating rainfall is enough to buffer the isotopic enrichment of the water that is caused by evaporation. The two samples are close to the groundwater samples and exhibit a similar pattern to the latter, indicating a groundwater discharge into the surface water. During summer, the surface waters are subjected to evaporation, making the surface waters' level much lower than the groundwater. The groundwater then serves as a baseflow that feeds the surface water (Leibundgut et al., 2009) Most surface water samples are positive and shifted to the right side of the evaporation line, which suggests significant enrichment in heavier isotopes than the two samples discussed above. This enrichment is because most of the samples are from ponds, dams, and ephemeral streams that are standing waters with slow discharge. These have more time to undergo considerable evaporation documented with low deuterium excesses (Table 5.2) than the other surface waters. Furthermore, the water from the dams is used for irrigation, and the available data suggest no interaction between the irrigated water and the groundwater.

The intersection points for the surface water evaporation line and the LMWL (Fig 5.8) correspond to -15.68‰ and -2.99‰ for $\delta^{2}H$ and $\delta^{18}O$, respectively. This indicates the source of the isotopic composition of surface water before undergoing kinetic fractionation. When compared to the intersection point values, the high variability of the isotopic composition of precipitation may suggest the mixing of diverse isotopic signatures (Afrifa et al., 2017). During evaporation, the water vapour in the atmosphere becomes depleted in heavy isotopes due to its low pressure, leaving the residual water on the land surface enriched in heavy isotopes. This pattern of fractionation processes in the hydrological cycle leads to global and local isotope effects (Leibundgut, et al., 2009). The point of intersection also indicates that the surface waters in the catchment are recharged by the precipitation (Bam & Bansah, 2020).

The isotopic composition of the White Volta River flowing in two communities (Kpinkpan Yug and Songo Guur) ranges from -21.84 ‰ to -21.75‰ for $\delta^{2}H$, and -2.96‰ to -2.76‰ for $\delta^{18}O$. These are depleted in heavier isotopes than the surface waters and near the LMWL, which could suggest minimal evaporation, and a hydraulic connection between the White Volta River and the groundwater.

5.4.6 Isotopic composition of groundwater

The stable isotope composition of the granitic aquifer in the area has ^{18}O values ranging between -4.30‰ and -2.89‰ with an average of -3.78‰ (Fig.5.9a), whereas the deuterium composition varies between -23.63 ‰ and -17.17‰ with an average of -21.76 (Fig.5.9b). The groundwater samples have relatively similar isotopic values with an average standard deviation of 0.30 and 0.05 for δ2H and $\delta^{18}O$, respectively. The seeming homogeneity of the aquifer samples suggests that groundwater recharge possibly comes from similar precipitation events (Addai et al., 2016). The groundwater produces an evaporation line with a regression equation as shown in Eqn 5.13.

$$\delta^{2}H = 4.16\delta^{18}O + 6.03 \qquad 5.13$$

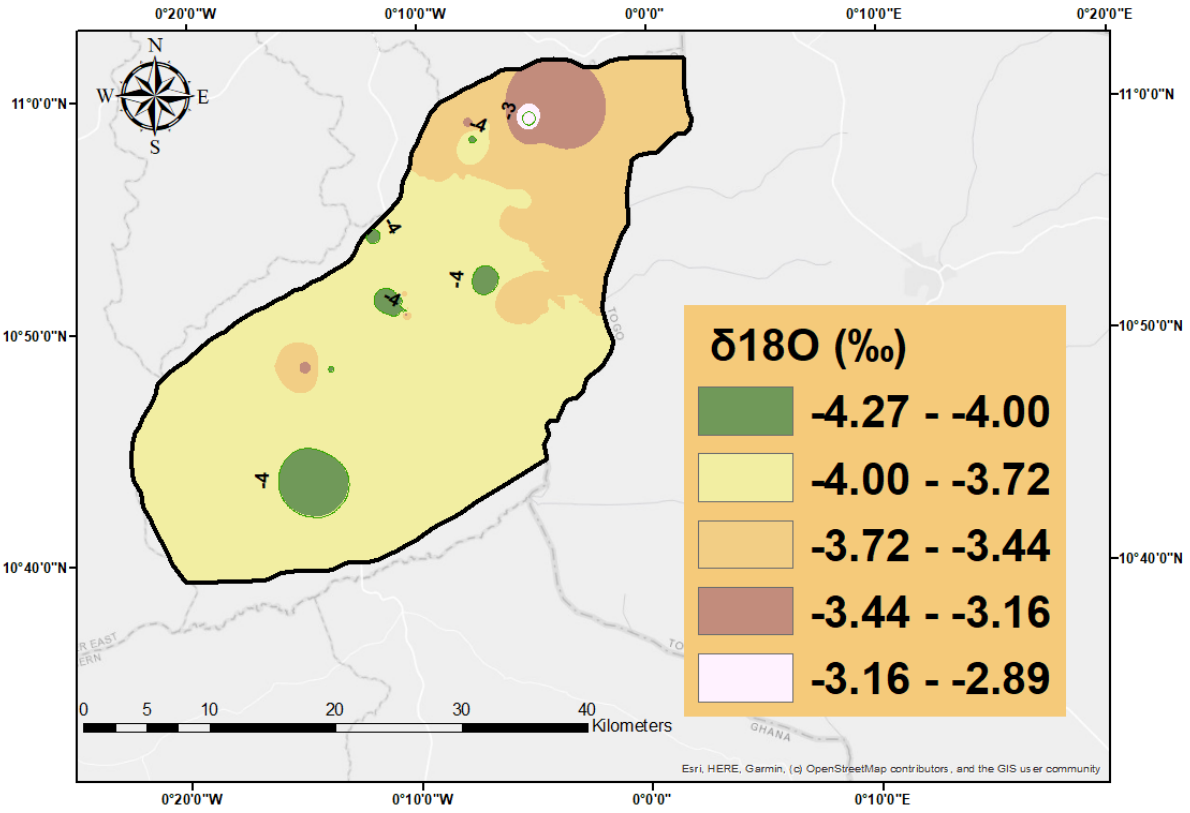

Fig.5.9a. *Spatial distribution of $\delta^{18}O‰$ of the groundwater*

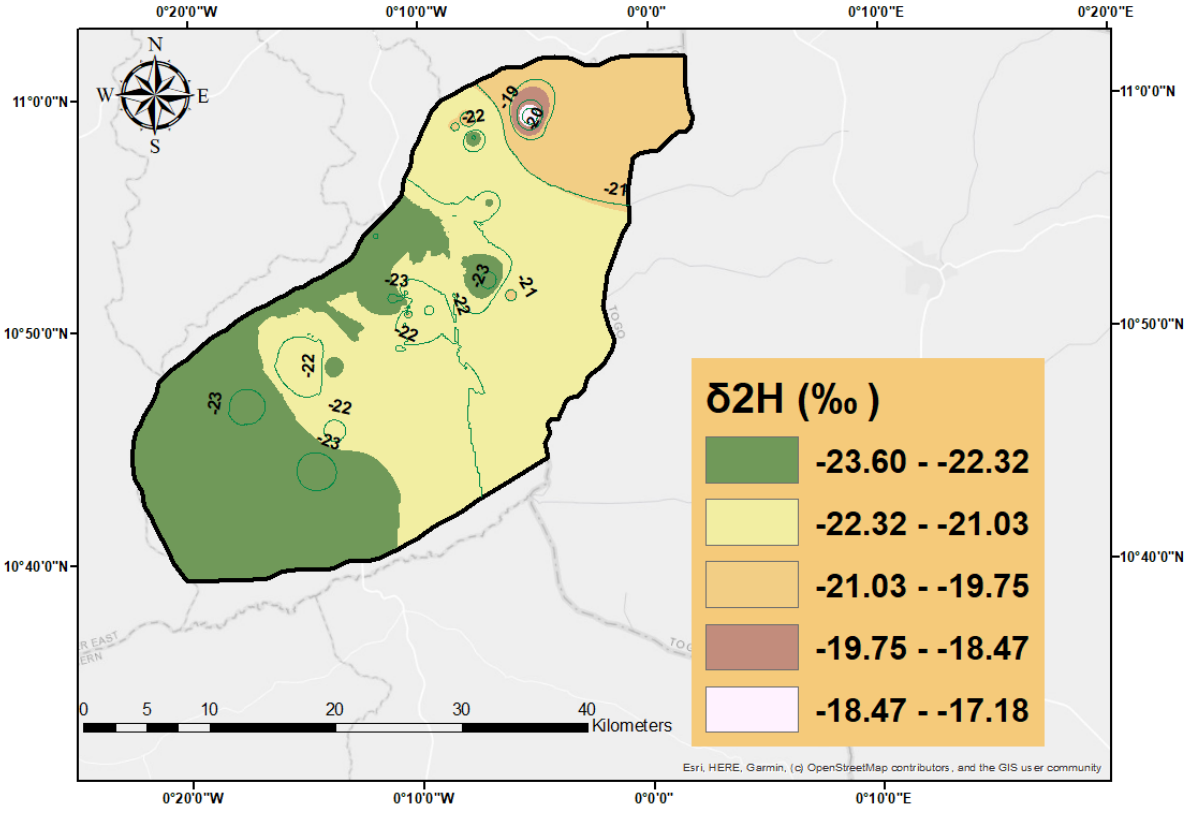

Fig.5.9b *Spatial distribution of $\delta^{2}H‰$ of the groundwater*

As illustrated in (Fig 5.8), almost all the groundwater samples are clustered close to the GMWL, and LMWL indicates the recharge source is of meteoric origin. In addition, this suggests that recharge is influenced by the local precipitation (Gat, 2010). The groundwater samples are depleted in heavier isotopes relative to the surface waters, implying that fractionation does not affect the recharge processes considerably. The area has a short rainy season between May to August, with virtually no or little rains in the dry season. The rains recharging the aquifer carry equilibrium isotope signals into the groundwater, thus explaining the closeness of the groundwater to the LMWL. The surface water inflows to the groundwater, which is much enriched due to evaporation, do not significantly affect the groundwater recharge. The data show that there is groundwater-surface water interaction, where groundwater discharges into the surface water. This is in line with the regional hydrogeology knowledge that the exchange is constrained to groundwater discharging into the surface waters because the aquifer samples do not plot substantially under the LMWL (Rey et al., 2018). Groundwater recharge occurs through joints and fractures in the weathered granitic rocks resulting from secondary porosity of the underlying bedrock (Carrier et al., 2008). These structures may receive high preferential flow from rainfall, thus precluding surface pounding, causing significant evaporation. Even though the area is found in a semi-arid dry climatic zone, where there are high evaporation and greater interception of plants before groundwater recharge, the isotopic data of the groundwater do not support this hypothesis (Jasechko et al., 2014).

5.4.7 Relationship between chloride and stable isotopes

The relationship between $\delta^{18}O$ and Cl^- was examined to understand the sources of groundwater salinity and recharge areas in the aquifer system. Chloride and Oxygen-18 are conservative tracers that aid in understanding the evaporation process before groundwater recharge (Bam & Bansah, 2020). In principle, evaporation occurs when chloride and $\delta^{18}O$ concentrations increase. An event where chloride ion increases without a corresponding enrichment in $\delta^{18}O$ will imply a dissolution of chloride salts such as halite in the unsaturated portion. The plot of $\delta^{18}O$ and Cl^- (Fig 5.10) follows this trend, in which most groundwater samples are clustered together without a significant increase in Cl^- concentration (from 0.3 mg/L to 16.98 mg/L), whereas the $\delta^{18}O$ values tend to increase slightly from -4.40 ‰ to -2.89‰. This trend cannot be related to halite dissolution since no halite salts have been reported to exist in the area. It is, therefore, suggested that the possible source of chloride is precipitation which carries an equilibrium chloride signal into the groundwater. The anomalous high chloride concentrations (25 mg/L and 42 mg/L) can be attributed to anthropogenic activities such as fertilizer application or cattle-rearing in the area that might contaminate the groundwater (Bam and Bansah, 20202)

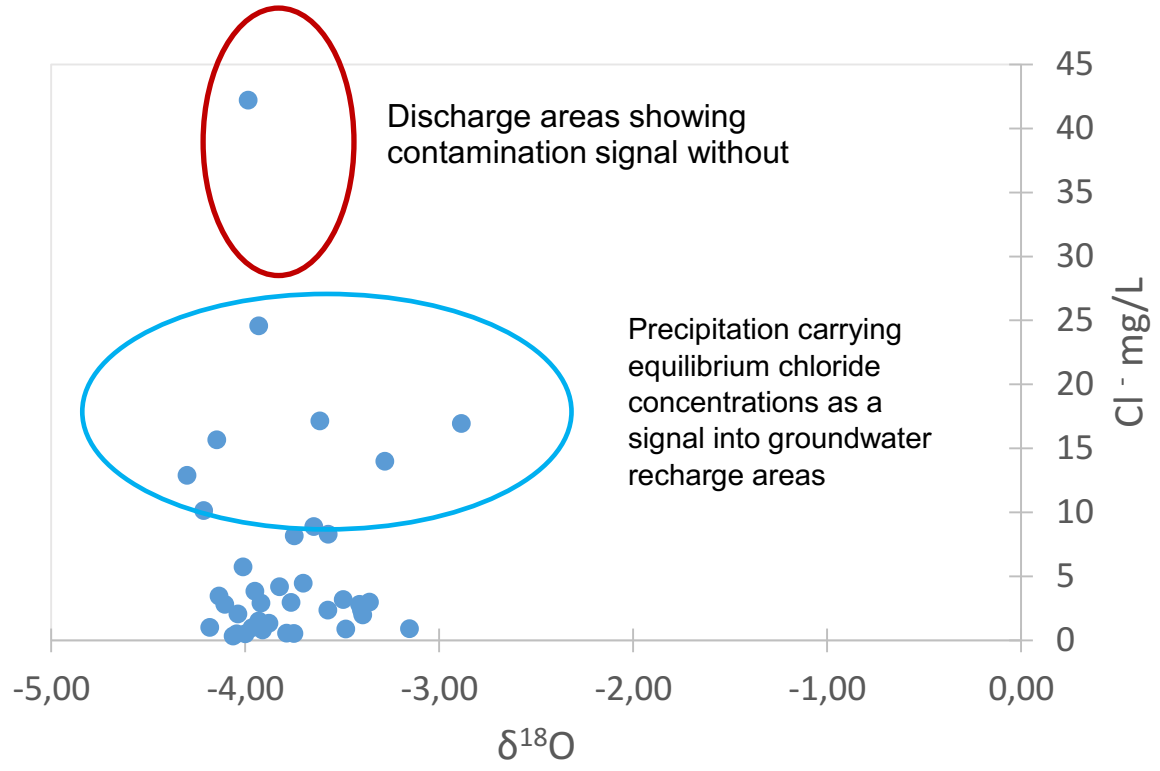

Fig.5.10. Relationship between $\delta^{18}O$ and Cl^- of the groundwater

5.4.8 Groundwater residence time and mixing

Sulphur hexafluoride (SF6) and chlorofluorocarbons (CFC-12, CFC-11) concentrations in the groundwaters are presented in part per trillion by volume (pptv), as shown in Table 5.2. This ensures that the measured concentrations are comparable with the northern hemisphere atmospheric curves and avoid local recharge variations (IAEA, 2006). The results show that most SF6 and CFCs samples are in equilibrium with the northern hemisphere air mixing ratios. Twenty-six percent of the samples have no concentrations or are below detection limits, and few samples exceed the recent air-water equilibrium concentrations, possibly indicating contamination (IAEA, 2006). Furthermore, the average ages of the groundwater modelled for piston flow (PFM), exponential mixing (EMM), and binary mixing (EMM) indicate modern waters are less than 30 years.

A plot of CFC-12 against CFC-11 shows that most of the samples agree with the piston flow model (Fig 5.11a). This indicates that infiltration in the catchment occurs in pronounced recharge sources and travels towards the discharge source (a well) without mixing or dispersion. Conversely, some samples are found around and on exponential mixing (EMM) curves suggesting water mixing within the borehole (Jurgens et al., 2012). The samples

found on the BMM line suggest a binary mixture of young waters diluted with old CFC-free waters. Samples plotted outside the model curves indicate degradation or contamination of CFCs.The low dissolved oxygen concentrations (< 0.5 mg/L) in most of the analyzed groundwater samples (Table 5.1) imply a degradation of CFCs, particularly CFC-11 under anaerobic conditions (IAEA, 2006; Oster et al., 1996). CFC-11 appears to be biased old relative to CFC-12 in almost all the analyzed samples (Table 2) and such instances indicate degradation. According to Deipser & Stegmann (1997), CFC-11 degrades almost 16-fold more than CFC-12. In addition, the study area is far from an urban area and landfill sites, and as such anthropogenic inputs may have little influence on the age determination. Therefore, the possible source of CFCs contamination may be introduced during sampling and the sampling materials in contact with the outside air (Reynolds et al., 1990). As shown in (Fig. 5.11a), almost all the samples are found between 1990 and 2007, representing modern recharge waters with few samples between the early and mid-1980s and one sample in the mid-1970s. Based on the analysis presented above, CFC-12 is considered more stable and reliable in the dating process showing age ranges between (5–42 years) with an average age of 24 years, whereas CFC-11 has age ranges between (14 – 44 years) with an average age of 28 years. It must be noted that the post - 1995 levelling of CFCs gases makes it largely uncertain to date groundwaters recharged in the last decades (Plummer et al., 1998).

A cross plot of SF6 versus CFC-12 and SF6 versus CFC-11 are presented in (Fig 5.11b and Fig. 5.11c), respectively. It can be seen that the majority of the samples are plotted outside the curve suggesting CFC reduction and contamination (Busenberg & Plummer, 2000; Lapworth et al., 2013) Again, few samples are scattered around the PFM, BMM, and EMM lines, and therefore, cannot represent any of the flow regimes. The modelled SF6 ages range from 5 years to 32 years with an average age of 15 years. These ages were younger than the modelled CFCs ages and can be explained as anoxic biodegradation at the discharge point (Oster et al., 1996). Another reason is the additional inputs of SF6 derived from the granitic rocks in the catchment (Busenberg & Plummer, 2000). Terrigenous enrichment of SF6 in granitic areas is usually invoked to account for the additional and high inputs of SF6 in groundwater. This is evident in some communities such as Napadi Yapala, Dusbuliga, and Kogri, which have elevated SF6 concentrations in the groundwater.

There is no agreement between the SF6 and CFCs model ages as the water in the catchment is characterized by different groundwater ages. The aquifer in the area is mainly fractured granite, where diffuse flow systems occur in all parts. Therefore, groundwater pumped from the aquifer may constitute apparent ages affected by the mixing (IAEA, 2006; Shapiro, 2002).

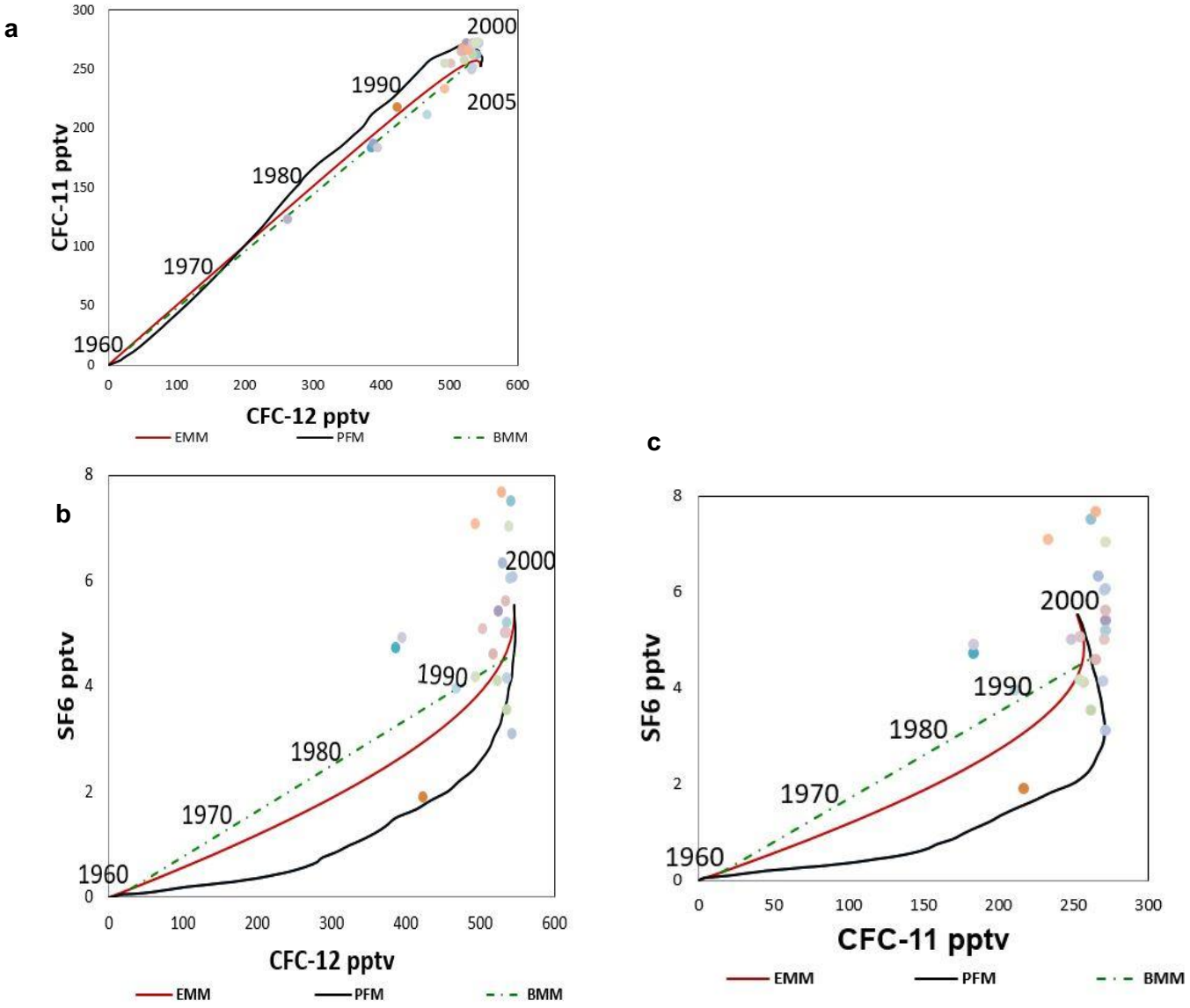

Fig. 5.11. *Cross-plots of (a) CFC-11versus CFC-12 (b) SF6 versus CFC-12 and (c)SF6 versus CFC-12*

Table 5.2. Isotopic composition of groundwater and surface water as well as the apparent recharge years of the groundwater

Community	δ 2H	δ 18O	d-excess	**SF6**	**CFC-12**	**CFC11**	SF6	CFC12	CFC-11	SF6	CFC12	CFC-11
				Equivalent air conc (ppt)			Recharge year			Residence Time (years)		
Garu Zongo1	-22.92	-3.98	8.96	4.72	386.92	183.69	2000	1984.5	1982	19	34.5	37
Garu Zongo	-20.44	-3.62	8.48	1.895	423.74	217.39	1987	1986.5	1986	32	32.5	33.5
Garu Market	-22.87	-4.00	9.13	8.26	389.97	187.25	2014	1984	1982	5	35	37

Garu Central	-22.38	-3.79	7.92	ND	522.85	265.8	-	1993	1990	-	26	29
Napadi Yapa	-23.03	-4.04	9.27	10.27	1185.44	354.87	Cont.	Cont.	Cont.	Cont.	Cont	Cont
Pialugu Tand	-22.28	-3.88	8.75	5.406	524.94	271.56	2003	2014	1992	16	5	27
Sigure Yapal	-22.52	-4.01	9.57	7.513	541.07	261.88	2011	2007	1989	8	12	30
Dusbuliga	-21.88	-3.75	8.12	10.39	909.34	ND	Cont.	Cont.	-	Cont.	Cont.	Cont.
Senebaga	-23.43	-4.21	10.28	6.331	530.06	267.32	2007	1995	1991	12	24	28
Kogri	-23.23	-3.96	8.49	9.056	528.06	266.5	2006	1994	1996	13	25	23
Kogri 2	-21.03	-3.39	6.12	3.542	535.24	262.3	1995	1996	1990	24	23	29
Barboaka	-22.05	-3.82	8.53	ND	262.94	122.77	-	1977	1975	-	42	44
Busnatiga	-19.02	-3.15	6.20	5.203	535.30	272.21	2002	1996	1993	17	23	26
Yabrago No.1	-23.35	-4.18	10.11	8.275	520.02	267.05	2014	1992	1990	5	27	29
Tindane Prim	-20.87	-3.50	7.09	3.098	543.60	272.15	1993	1998	1992	26	21	27
Duadinyediga	-22.08	-3.93	9.36	4.587	517.7	265.1	1999	1992	1990	20	27	29
Kugashegu	-21.46	-3.65	7.72	4.106	523.01	257.2	1997	1993	1989	22	26	30
Pwalugu Nati	-21.71	-3.76	8.40	ND	ND	ND	-	-	-	-	-	-
Baatiyok	-22.39	-3.92	8.97	6.039	539.96	271.4	2006	1997	1992	13	22	26
Abapusug	-21.49	-3.70	8.12	7.661	528.24	265.5	2011	1994	1990	8	25	29
Bugri Dam	-23.09	-4.06	9.41	ND	ND	ND	-	-	-	-	-	-
Zumandiga	-20.62	-3.36	6.26	5.612	534.42	268	2004	1995	1996	15	24	23
Bugri Central	-20.94	-3.57	7.64	8.541	542.2	272.5	2015	1998	1993	4	21	26
Sakparatinga	-21.85	-3.75	8.13	ND	ND	ND	-	-	-	-	-	-
Baranatinga	-17.17	-2.89	5.93	3.95	468.23	211.5	1997	1989	1985	22	30	34
Karateshie-N	-20.16	-3.48	7.70	7.08	493.5	233.5	2010	1990	1987	9	29	32
Winatinga	-20.27	-3.41	7.01	4.151	535.7	270.1	1998	1996	1991	21	23	28
Yaranatinga	-20.77	-3.40	6.44	5.072	503.45	254.4	2002	1991	1988	17	28	31
Garu D.APrim	-23.00	-4.13	10.08	4.176	494	254.5	1998	1990	1988	21	29	31
Garu Clinic	-22.00	-4.04	10.36	5.005	533.4	249.1	2002	2010	2005	17	9	14
Garu CBR	-22.89	-4.15	10.29	6.823	456.9	235.7	2009	1988	1987	10	31	32
Garu Belatek	-23.63	-4.30	10.76	ND	ND	ND	-	-	-	-	-	-
Garu Medina	-23.63	-4.11	9.21	8.25	534.9	251.2	2014	2010	2004	5	9	15
Holy Eng.Sch	-20.52	-3.57	8.07	4.998	536.24	271.2	2001	1996	1992	18	23	27
Tanzugu	-19.29	-3.28	6.95	7.023	539.3	272.2	2010	1997	1994	9	22	25

Zumadori	-22.03	-3.93	9.42	4.905	395.2	183.6	2001	1985	1982	18	34	37
Nisbuligu	-22.18	-3.91	9.11	ND	ND	ND	-	-	-	-	-	-
Zaari	-22.31	-3.95	9.28	ND	ND	ND	-	-	-	-	-	-
SW1	16.11	2.42	-3.25									
SW2	17.08	2.74	-4.84									
SW3	-14.54	-2.54	5.78									
SW4	-15.96	-2.99	7.96									
SW5	16.98	2.49	-2.94									
SW6	17.68	2.70	-3.92									
SW7	7.61	1.24	-2.31									
SW8	9.45	1.54	-2.87									
SW9	14.84	2.96	-8.84									
SW10	11.75	2.70	-9.85									
White Volta 1	-21.84	-2.96	1.84									
White Volta 2	-21.75	-2.70	-0.15									

Cont- Contamination ND- non-detectable

5.5. Conceptual model of groundwater recharge and flow mechanisms

The weathered granitic aquifer studied is largely heterogeneous and conditioned by different flow patterns. Multi-tracers investigations coupled with the steady-state flow model and EC of the groundwater collaborate with the data and study hypothesis. The similar isotopic signatures of the groundwater close to the LMWL support the hypothesis that recharge in the area is primarily from rainfall with little contribution from surface waters. Water infiltration from high elevations occurs diffusely and rapidly via fractures and pores in the shallow aquifer where low mineralized water (low EC and TDS) and short residence time are pronounced in recharge areas. As groundwater transits towards discharge areas, increasing residence time and high mineralized groundwater are observed. Based on the numerical model, surface topography dictates groundwater flow with preferred NE–SW flow directions.

In addition, It was hypothesized that young groundwater (less than 50 years) would travel along the topographical flow line. This is in good agreement with the results inferred from the modelled groundwater ages. Here, three groundwater flow regimes can be delineated (Fig 5.12). The first flow regime is the piston flow model that occurs in deep groundwater recharge zones. High CFCs and SF6 values are present, implying the circulation of young groundwater ages. In the middle of the basin, the exponential flow model occurs,

characterized by mixtures of old water and modern recharged water of different ages. The final flow regime is a local flow in a discharge area, where there are interactions between the surface water and groundwater over several years. This is supported by low SF6 and CFCs concentrations suggesting less recharge of young groundwater in the discharge area (Gooddy et al., 2006). The local flow occurs downstream of the catchment in the southern part where the White Volta River flows. The mixing process or interaction of the White Volta River with the groundwater is consistent with the results of the stable isotopes analysis (Fig. 5.8) and other studies in Northern Ghana (Afrifa et al., 2017; Bam & Bansah, 2020).

In summary, the findings presented in this study show a varying range of groundwater residence times in the granitic aquifer. This implies the aquifer has enough storage to accommodate different ages of water, which would be helpful for MAR water infiltration piloting in the area. A successful MAR scheme depends on an aquifer having enough storage capacity and hydraulic conductivity. The study area experiences water scarcity during the dry season due to the short unimodal rainfall season and high evapotranspiration (Ghana Statistical Service, 2013). These have led to the drying up of the surface waters, as evident in the enrichment of the heavy isotope of these water bodies. Even though modern recharged waters enter the catchment and can safeguard any short-term groundwater withdrawals, future water supply remains uncertain, mainly from population growth and increasing water demand. On this basis, managed aquifer recharge can be a good technique to increase agricultural water supply reliability in the region in the future looking at the promising aquifer hydraulic properties and young groundwater ages obtained from this study.

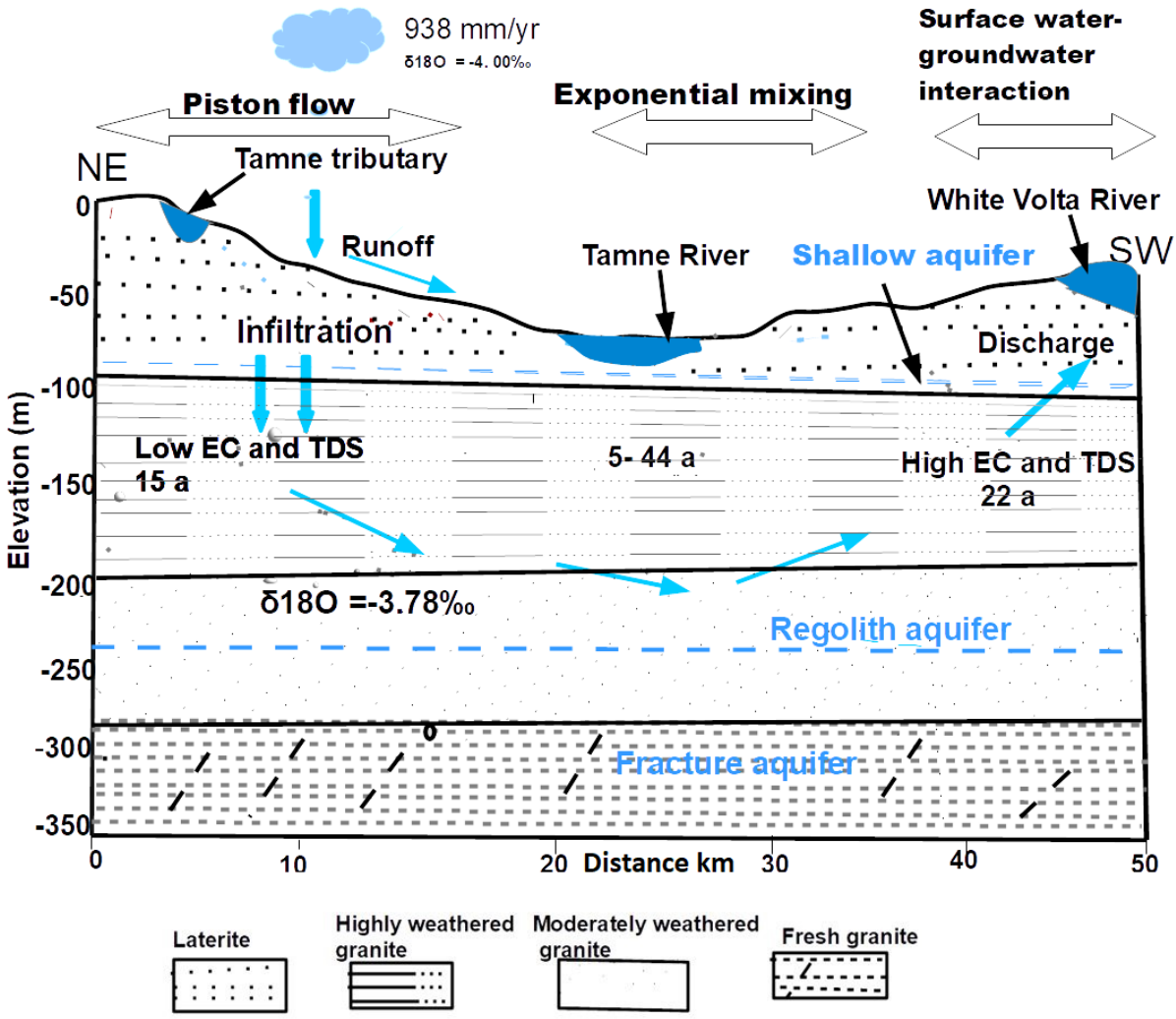

Fig.5.12. Conceptual groundwater flow in the study area

5.6. Conclusions

This study has underlined the importance of using multi tracers to understand groundwater residence time and recharge patterns of the shallow groundwater in Northeastern Ghana. The granitic aquifer receives diffuse recharge mainly from precipitation with little contribution from the White Volta river. There is no noticeable link between the groundwater, and the ephemeral streams and ponds as these show much enrichment in heavier isotopes. Groundwater recharge through chloride mass balance (CMB) ranges from 0.2 % to 24.8 % (average 7%) of the average annual precipitation of the area. The calibrated steady-state model reveals a preferred northeast-southwest flow direction, which is topographical driven. Aquifer hydraulic conductivity ranging from 0.2 m/day to 10 m/day exhibits many heterogeneity values attributed to the weathering and fracturing of the basement rocks.

The lump parameter model shows different age distributions of very young and old groundwater and some mixing processes. The results indicate younger biased ages of SF6 relative to the CFCs. This suggests terrigenous source enrichment and leaves much in question the effectiveness of using SF6 as a dating tool in the area. The conceptual groundwater model describing groundwater flow patterns reveals piston flow, exponential mixing, and local flow (surface water and groundwater interactions). Despite some uncertainties in the groundwater age interpretations and the methods applied, it is believed that this research could be a springboard for future-related research outside the region and the country as a whole.

CHAPTER 6

A three-dimensional numerical groundwater flow model to assess the feasibility of managed aquifer recharge in the Tamne River Basin of Ghana

Reproduced from: Okofo Boansi Louis and Martienssen Marion. A three-dimensional numerical groundwater flow model to assess the feasibility of managed aquifer recharge in the Tamne River Basin of Ghana: Journal of Hydrogeology (2022). https://doi.org/10.1007/s10040-022-02492-7

Abstract

Increasing population growth and global climatic changes threaten water security in semi-arid regions such as Northern Ghana. The Tamnean Plutonic Suite aquifer is the main source of water supply for the inhabitants of the Tamne River basin, which is a transboundary sub-basin of the White Volta Basin, Ghana. The basin is a flood-prone area where flooding occurs every rainy season, but there is water scarcity during the dry season, mainly due to poor groundwater resource planning. It is expected that the population will increase in the next 10 years, implying a greater water demand. A steady-state and transient groundwater flow model has been developed to understand the hydrogeological conditions and assess the feasibility of managed aquifer recharge (MAR) in the area. A single granitic aquifer formation was delineated from the three-dimensional lithology modelling. The calibrated aquifer recharge through precipitation is very low due to high evapotranspiration and low rainfall. A MAR injection scenario was tested using the available treated floodwater that is registered during the rainy season in the area. The results show the total volume of water injected at the end of the 4-month study period is 11,000 m^3/day (approximately 1.3×10^6 m^3), which significantly increases aquifer storage and groundwater levels. The volume of water recovered at the end of 8 months (1.4×10^6 m^3) is enough for domestic and irrigation purposes during the dry season. In general, MAR is feasible in augmenting the water levels in the area when combined with controllable irrigation and domestic withdrawals.

6.1 Introduction

Achieving water supply reliability through a well-developed engineering technology such as managed aquifer recharge (MAR) is a prerequisite to bolstering climate resilience with respect to social, environmental, and economic goals in arid and semi-arid regions (Dillon et al., 2020). Besieged by the inherently limited water resources in these regions, other factors, such as intensive use of groundwater for irrigation and increasing water demand from the ever-growing population, has led to water scarcity and adverse socio-economic issues (Kwoyiga & Stefan, 2019; Ray, 2019). For example, declining groundwater levels in most arid areas have caused the drying up of farmlands, especially in the dry season. The effect is that irrigation wells have to be deepened and abstracting water has become expensive. In the same vein, the depletion of groundwater resources due to excessive withdrawals has occasioned seawater intrusion in many arid coastal aquifers, such as the Jamma aquifer in Oman, deteriorating the quality of water (El-Rawy et al., 2019). It is imperative that these challenges are addressed so that water-sector stakeholders can enhance the availability and quality of water in water-scarce areas. As a response to this, MAR has become a unique technique for collecting and treating water and storing it in aquifers during availability and later using it when there is scarcity (Bouwer, 2002; Maliva and Missimer, 2012).

In recent years, the use of MAR to augment the supply of groundwater, especially in drought-prone areas of the world, has attracted considerable interest (Dillon et al., 2020; Gale, 2005a; Maliva and Missimer, 2012). For instance, in the quest to tackle growing water scarcity problems in the southern European countries and Mediterranean regions, due to the impact of climate change on the available water resources, a managed-aquifer-recharge solutions (MARSOL) project was set up in six European countries (Greece, Germany, Italy, Malta, Portugal, Spain) and Israel using different MAR methods and water sources, such as treated wastewater, desalinated water, and river water (Marsol, 2014). The objective of MARSOL was to augment the natural storage of aquifers and create market avenues for the European industry by applying low-tech and cost-effective MAR solutions. Dillon et al.(2009) documented that MAR has significantly improved irrigation water supply by 45 GL/yr and the supply of water to urban towns by 75 GL/yr in Australia as of the year 2008. Other advantages of MAR include the system providing a barrier to combat saline intrusion in overexploited aquifers, and sustaining environmental flows and phreatophyte vegetation in stressed surface-water or groundwater systems (Dillon et al., 2014).

In Africa, the development of MAR is taking shape, and about 44 MAR cases have been documented in the global MAR inventory web portal (Stefan & Ansems, 2018), with eight additional MAR cases in the literature reported by Ebrahim et al. (2020), making a total of 52 cases to date. According to the global MAR portal, most MAR sites can be found in South

Africa and Tunisia, with little-discussed sites also in West Africa — only two MAR sites in Nigeria. However, there are emerging MAR schemes in Ghana, where two schemes are found in the Jagsi and Kpasenkpe communities in Northern Ghana, and one scheme in the Weisi community in the Upper East Region of Ghana. These projects are being piloted by the International Water Management Institute (IWMI) and they employ Bhungroo Irrigation Technology (BIT; widely used in India for floodwater harvesting). BIT is akin to the artificial storage and recovery (ASR) method, which harvests excess floodwater, infiltrates it directly into the well as a means of storage, and recovers the water for use during the dry season (Owusu et al., 2017). According to Conservative Alliance, (2015), BIT can harvest and store approximately 40,000 m^3 of water in the unsaturated zone with a depth ranging between 8 m and 25 m. This total volume of water is considered sufficient to secure irrigation water during the prolonged seven months of the dry season, thus improving food security in these areas (Owusu et al., 2017).

Notwithstanding the significant progress of MAR schemes in Africa, Kwoyiga & Stefan (2019) argued that institutional guidelines for successful MAR implementation are lacking. Furthermore, there has been only a little insight gained from the groundwater modelling studies in Africa to assess the feasibility of managed aquifer recharge.

The Tamne River basin is a transboundary sub-basin of the White Volta River basin of Ghana (SNC-Lavalin/INRS, 2011). As high as 80 percent of the inhabitants are engaged in agriculture, which is heavily focused on onions, tomatoes, and watermelons. This serves as the main source of income for the people (Ghana Statistical Service, 2013). The main sources of water used for agricultural irrigation are rainwater, groundwater, and surface water from the Bugri and Gagbiri dams. The area experiences only one short rainy season between May and September and is accompanied by a long dry period from October to April (Issahaku et al., 2016). A large quantity of rainwater in the area is lost through evapotranspiration from open surfaces; according to the Ghana Statistical Service (2013), a rainwater volume of approximately 1.55 to 1.65 cubic metres per square metre of the area is lost annually. This causes drought and contributes to low groundwater recharge in the area.

In response to the problems mentioned above, the Bugri and Gagbiri dams, with canal lengths of 1.35 km and 2.9 km respectively, were constructed purposely to provide an alternative water source for irrigation farming during the dry season. However, challenges such as inadequate rainfall to fill up the dams, high water demand for irrigation, high evaporation losses, and broken and choked canals due to inadequate repairs have rendered the irrigation activities in the dry season ineffective and counter-productive (Jonah & Dawda, 2014b).

Furthermore, it is a flood-prone area, where instances of flooding have occurred every rainy season due to recorded high torrential rainfall combined with the release of excess water

from upstream of Bagre Dam in neighbouring Burkina Faso — located several kilometres from the study area (Armah et al., 2010). The seasonal flooding is also a result of the highly irregular seasonal flow patterns and poor drainage from the river basins of Tamne and Pawnaba-Kiyinchongo, as well as the tributaries of the White Volta in the study area. During the rainy season, these rivers flow excessively, followed by recession and low water levels during dry seasons (Ghana Statistical Service, 2013). These developments resulted in low and no water for use during the dry-season farming periods, causing a negative water balance. As part of measures to sustain their livelihoods, most farmers resorted to growing crops that consume less water in order to cope with the limited groundwater availability. However, these measures do not bring any substantial returns to them. This makes farming activities very difficult in the dry season and consequently affects livelihoods, and most of the farmers have abandoned their farms. Besides the problems described above in the study area, it has been reported that the population of Ghana rises annually by 2.5 % (Ghana Statistical Service, 2013). This would imply an increase in water demand in the future, coupled with climate-induced variability in the available water resources in the study area. There are calls for additional water sources to bolster agricultural activities in the dry season and beyond, which will ultimately increase the economic fortunes of the farmers and reduce poverty in the region.

On this basis, the study area is being considered as a potential MAR site, drawing inferences from other successful MAR applications in Africa and the pilot MAR schemes in Northern Ghana. The available floodwater that is registered every rainy season will be used as a source of water for this MAR feasibility study. A successful MAR scheme depends on the local hydrogeology, with the aquifer having sufficient storage capacity and hydraulic conductivity (Maliva and Missimer, 2012). Where floodwater is to be considered a source of water, the water must be treated before infiltrating into the aquifers. This is because floodwater contains a mixture of various contaminants from other areas, which might affect the water quality or clog the well when infiltrated. Modelling techniques such as MODFLOW are used to design, optimize and manage MAR schemes (Bekele et al., 2011; Lacher et al., 2014; Legg and Sagstad, 2002). Other modelling tools such as MT3DMS, PHREEQC, MARTHE, and CXTFTIT are also used to identify and evaluate the water quality changes and geochemical processes during MAR infiltration (Ringleb et al., 2016). Ebrahim et al. (2016) used MODFLOW in conjunction with a genetic optimization algorithm to obtain information on the maximum recharge and extraction rates for MAR feasibility studies in the Samail Lower Catchment in Oman. Russo et al. (2015) simulated MAR projects in the Pajaro Valley Groundwater Basin in California, USA. The modelling results demonstrated a reduction of saline water intrusion in the coastal aquifer, which suggested MAR is feasible and advantageous in the area. El-Rawy et al. (2019) developed a steady-state transport

model to evaluate MAR and its economic feasibility for the Jamma aquifer in Oman. The results indicated that MAR could be used only for a single aquifer within a specific time frame, and maintenance and investment costs are economically unfeasible. As already mentioned, groundwater flow modelling scenarios used to study MAR applicability in Ghana have not been studied. Thus, the focus here is to develop a numerical groundwater flow model under steady-state and transient conditions and to have a better comprehension of groundwater sustainability in the basin. The study is also intended to characterize the aquifer hydraulic properties, estimate recharge rates, and quantify water balance in the Tamne River basin. The second objective is the use of MODFLOW to evaluate the feasibility of MAR and test groundwater management scenarios, by injecting seasonal floodwater using the ASR technique. This is intended to reverse declining groundwater levels, improve aquifer storage, and increase agricultural water supply reliability in the Tamne River basin.

6.2 Study area

The Tamne River basin is a sub-basin that falls within the White Volta River basin of Ghana. It is located 80 km northeast of Bolgatanga (regional capital) with an approximate land size of 848 km^2 (SNC-Lavalin/INRS, 2011). The Tamne River basin comprises two administrative areas: the western part of the Garu-Tempane district and the southern part of Bawku municipality. The study area is bordered to the east by Togo, to the south by Garu-Tempane district and Bunkpurugu-Yunyoo district, to the west by Bawku West and Binduri districts; and the north by Bawku municipality. The basin is characterized by surface elevation ranging between 185 m to 350 m with an average elevation of 219 m above sea level (Fig. 6.1). The area is drained by small streams and rivers of which the dominant one is the Tamne River, which flows into the White Volta River (SNC-Lavalin/INRS, 2011).

The climate in the study area belongs to the inter-tropical convergence zone, which brings two major air masses: the Southwest Monsoon winds and the North East Trade winds. The Southwest Monsoon winds emanate from the Atlantic Ocean, and these often occur during the rainfall season (Monsoonal rains) between May and September. The highest rainfall peaks occur in June, July, and August. The rainfall amounts in the Tamne River basin range from 669.8 mm to 1339.4 mm with an average value of 935 mm per year (Asamoah & Ansah-Mensah, 2020). The dry season occurs between October and April, characterized by varying temperatures ranging from 17°C to 44°C with an annual average temperature of 29.9°C.

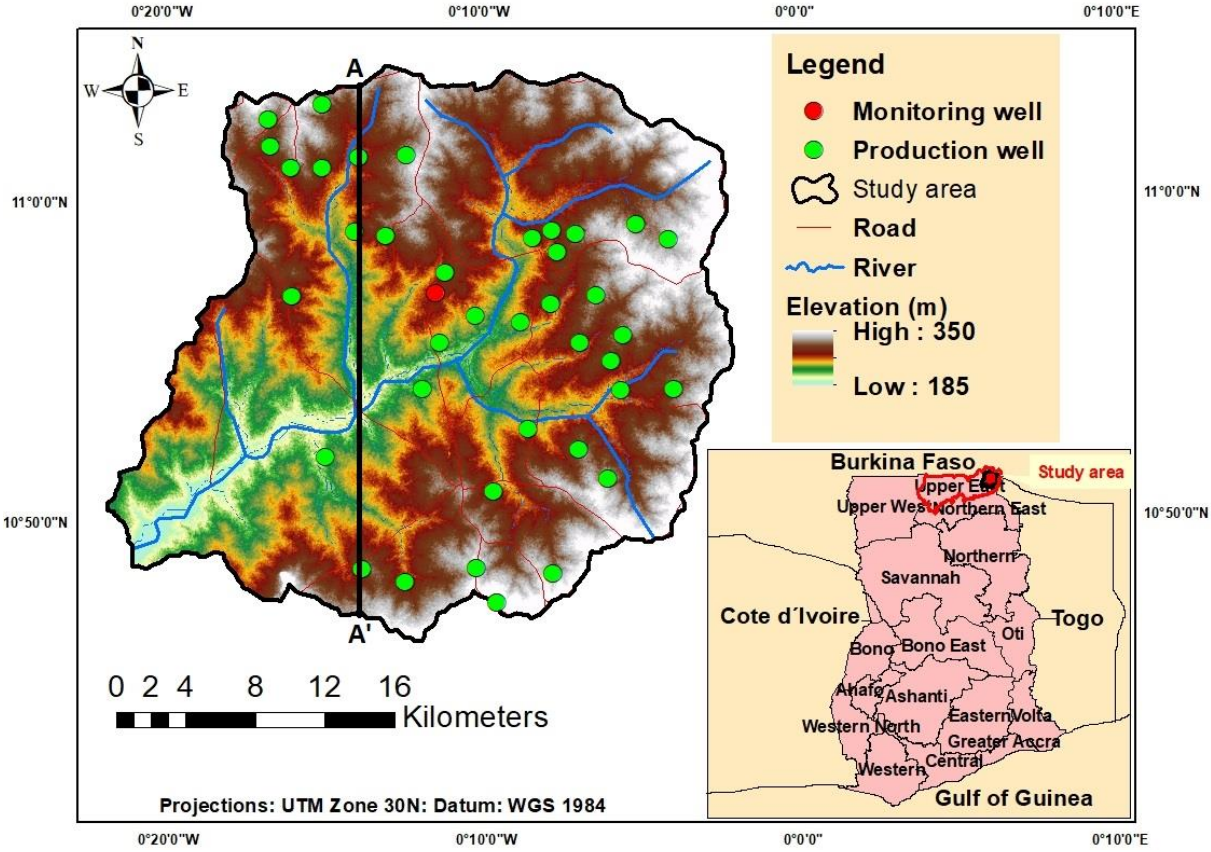

Fig. 6. 1 *Location map of the study area. A-A' shows the location of the hydrogeologic cross-section in Figure 6.4.*

6.2.1 Landuse and soil types

The vegetation of the basin belongs to the Sudanian savannah zone, which is characterized mainly by savanna woodland and grassland (SNC-Lavalin/INRS, 2011). The wide-open cultivated savannah woodland prevails in the study area and comprises trees such as baobabs, shea butter, and dawadawa trees, which are highly resistant to drought and fire. The grasslands are predominantly found in the northern part and scattered in the study area (Fig. 6.2). The grass and herbs are perennial plants that shed leaves and foliage and are affected by bush burning during the prolonged seven-month dry season. The open cultivated savannah woodland usually serves as an area for subsistence farming in which the inhabitants combine livestock rearing and crop farming. Common crops and vegetables grown in the area include sorghum, millet, maize, yam, groundnut, onion, and tomatoes (SNC-Lavalin/INRS, 2011). The open forest is a very good natural site for livestock rearing and serves as an essential source of income for about 80% of the inhabitants in the study area (Ghana Statistical Service, 2013).

The soils in the study area typically comprise lixisols, leptosols, gleysols, and fluvisols. These soils are formed from the weathering of the granitic bedrock that underlies the entire area.

The haplic lixisols dominate the area and are characterized by reddish-brown coarse-grained sandy loams and clay-rich content (Martin, 2006). The lithic leptosols are enriched in pale ash sandy loam with biotic granite and are found in the northern and southern parts of the basin. The eutric gleysols are found in waterways along the Tamne River and other streams in the area. The fluvisols are found in small quantities, usually in floodplains (SNC-Lavalin/INRS, 2011).

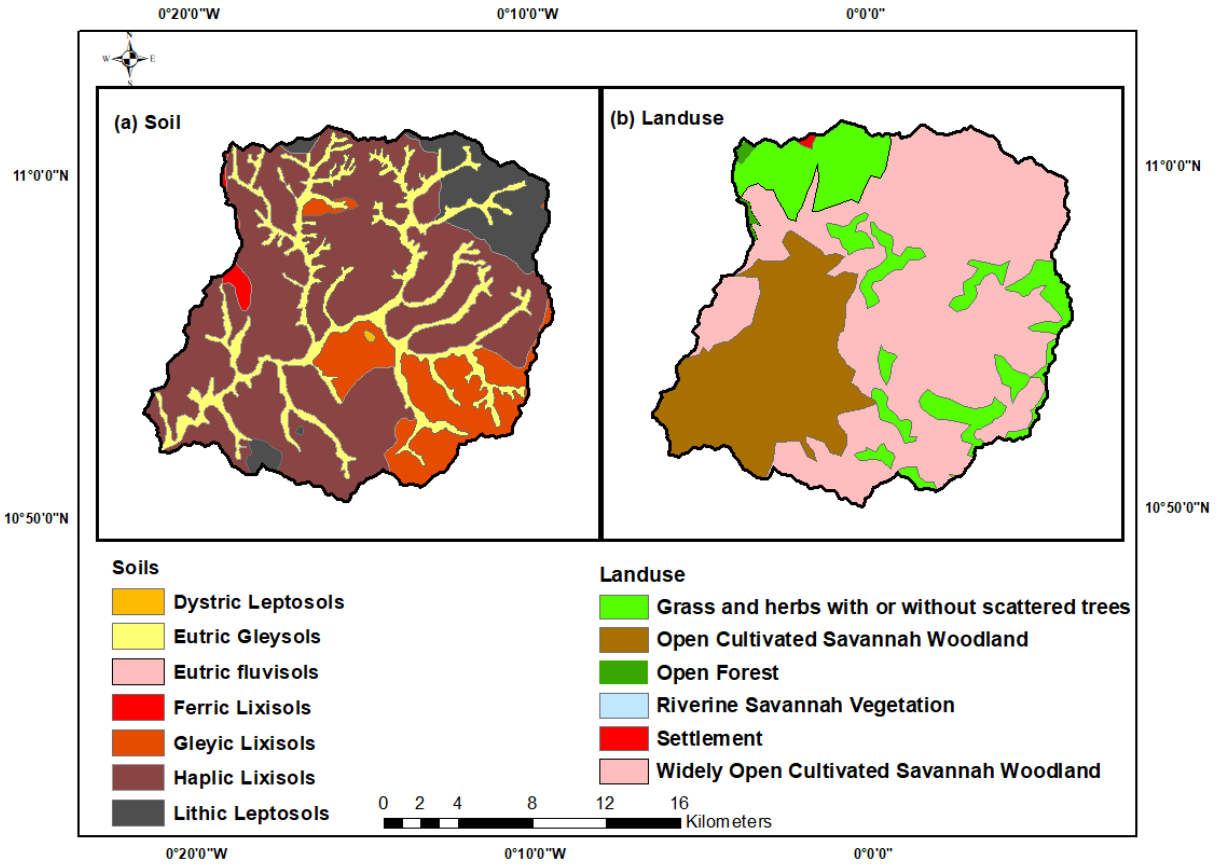

Fig. 6.2 (a) Landuse and (b) soil types of the study area

6.2.2 Regional and local geology

The Tamne River basin is predominantly underlain by rocks of the Tamnean Plutonic Suite and a few patches of Birimian Supergroup and Mesozoic rocks (Fig.6.3). The Birimian Supergroup belongs to the sub-province of the Precambrian basement complex and consists of metamorphosed sedimentary and igneous rocks that underlie 54% of Ghana (Dapaah-Siakwan & Gyau-Boakye, 2000). According to Bates (1955), the Birimian system is subdivided into Lower Birimian and Upper Birimian. The Lower Birimian are older metasedimentary rocks that consist of greywackes, phyllites, schists, tuffs, and sandstones. The Upper Birimian, on the other hand, are very young metavolcanic rocks typically of pyroclastic lava, andesites, and tholeiitic basalts. Most of the rocks in the Upper Birimian have undergone systematic metamorphism and have formed new grades of rock types such as hornblende, amphibolites (greenstones), and calcareous chlorite schist. The original

basaltic lavas that were subaqueous when erupted are now seen as pillow-like structures in the Upper Birimian (Banoeng-Yakubu et al., 2011).

The Birimian rocks are intruded by Tamnean Plutonic Suite, mainly granitoids formed during the Paleoproterozoic era circa 2150 –2070 Ma (Feybesse et al., 2006). The granitoids cover 95% of the study area and are rich in minerals such as hornblende-biotite tonalite, minor granodiorite, and minor quartz diorite. The Mesozoic rocks are non-metamorphic rocks composed of mafic dyke and dolerite, found in small portions of the area. The Birimian rocks in the area are metavolcanic rocks of basalt and minor interbedded volcaniclastics.

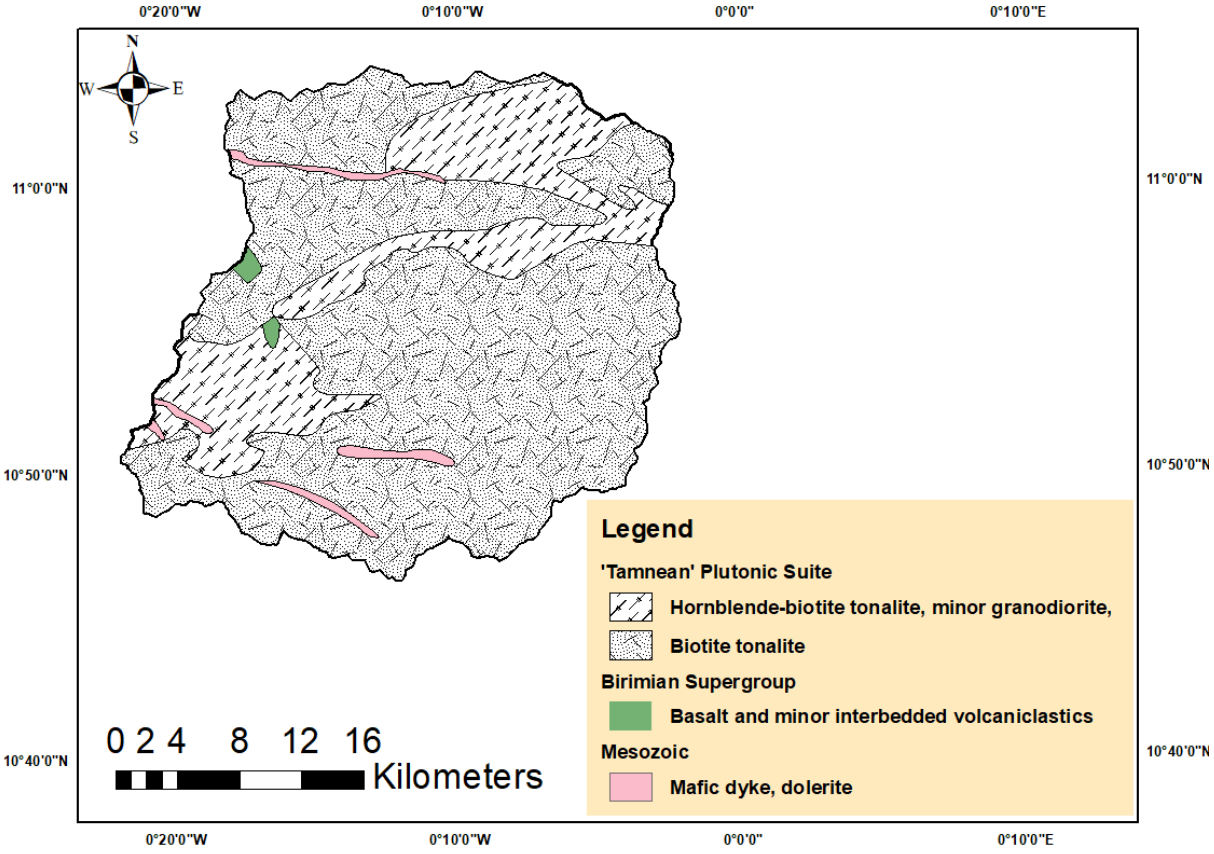

Fig. 6.3 *Geological map of the study area*

6.2.3 Hydrogeology

The hydrogeology of the Tamne River basin falls under two main provinces: the Birimian Province and the Crystalline Basement Granitoid Complex Province. The Birimian Province consists of the Birimian metasediments and metavolcanics. The Crystalline Basement Granitoid Complex Province also comprises the granitoids. The rocks in the basin contain little or no primary porosity, and thus, the mode of groundwater occurrence is mainly from secondary porosity arising from faulting and chemical weathering of the underlying rocks. (Dapaah-Siakwan & Gyau-Boakye, 2000). The groundwater development in the Tamne

basin occurs in three main aquifer formations: the shallow aquifer, the regolith aquifer, and the fractured aquifer, as seen in Fig 5.4. The shallow aquifer comprises coarse-grained lateritic and sandy units with an average thickness of 5 m. Most of the farmers have dug wells to tap water from this shallow aquifer for irrigation purposes. Unfortunately, the shallow aquifer is ephemeral and dries up in the dry season. The regolith aquifer is a weathered granitic unconfined aquifer that serves as the principal aquifer for the inhabitants. It comprises saprolite and saprock with an average thickness of 25 m (SNC-Lavalin/INRS, 2011). The saprolite consists of the topsoil, the lateritic soil, and the highly weathered bedrock, whereas the saprock consists of moderately weathered bedrock. The fractured aquifer is an unweathered confined granitic aquifer, contributing significant amounts of water to the basin. The occurrence of groundwater in the Birimian Province is more pronounced and productive in the saprolite and the upper part of the saprock since these two regolith profiles are hydraulically connected with respect to their storage and permeability (Carrier et al., 2008). The upper part of the saprolite usually has lower permeability and can form a semi-confining layer for the productive zone. In terms of weathering, rocks of the Birimian show a higher degree of weathering than the granitoid due to the lower jointing and fracturing contained in the granitoid. This has consequently resulted in lower groundwater yields and shallower water tables in some granitic terrains. In addition, the weathering and erosion have caused isostatic uplift of the overlying regolith materials resulting in the creation of sub-horizontal exfoliation or sheet fracturing in the upper portion of the fractured bedrock (Carrier et al., 2008).

The groundwater flow in the area is from N to S, mainly in the regolith aquifer but to some extent in the fractured aquifer (Fig. 6.4). A local groundwater flow (interflow) is also found within the subsurface towards the Tamne River as a discharge point. Groundwater recharge occurs mainly through direct infiltration of precipitation via rock matrices, crevices, and joints in the study area (Abdul-Wahab et al., 2021). There are no known recharge estimates in the Tamne River basin. However, various researchers have reported recharge estimates in the White Volta River Basin of Ghana. For instance, Obuobie (2008) used the water table fluctuation method to estimate the groundwater recharge, ranging from 3.4 % to 18.4 % of the mean annual rainfall (800-1140 mm/y). Oteng Mensah et al. (2014) estimated groundwater recharge using the chloride mass balance method in the White Volta Basin and ranged from 0.9% to 21% of the annual rainfall.

Borehole depth in the study area ranges between 14 m and 60 m, with an average of 37.2 m (SNC-Lavalin/INRS, 2011). The water level depth in the boreholes is between 1.63 m and 35 m, with an average of 15 m. The regolith thickness is between 7.8 and 37 m, with an average of 25 m. Groundwater yield varies from 0.36 m^3/h to 37 m^3/h with a mean yield of 4.2 m^3/h. Aquifer-specific capacity obtained from transmissivity measurements in the Tamne River

basin ranges from 1 to 27 l/min with an average of 7.1 l/min (SNC-Lavalin/INRS, 2011). The transmissivity values in granitoid formations have been reported in the range between 0.3 m^2/day and 114 m^2/day, with a mean value of 6.6 m^2/day (Carrier et al., 2008).

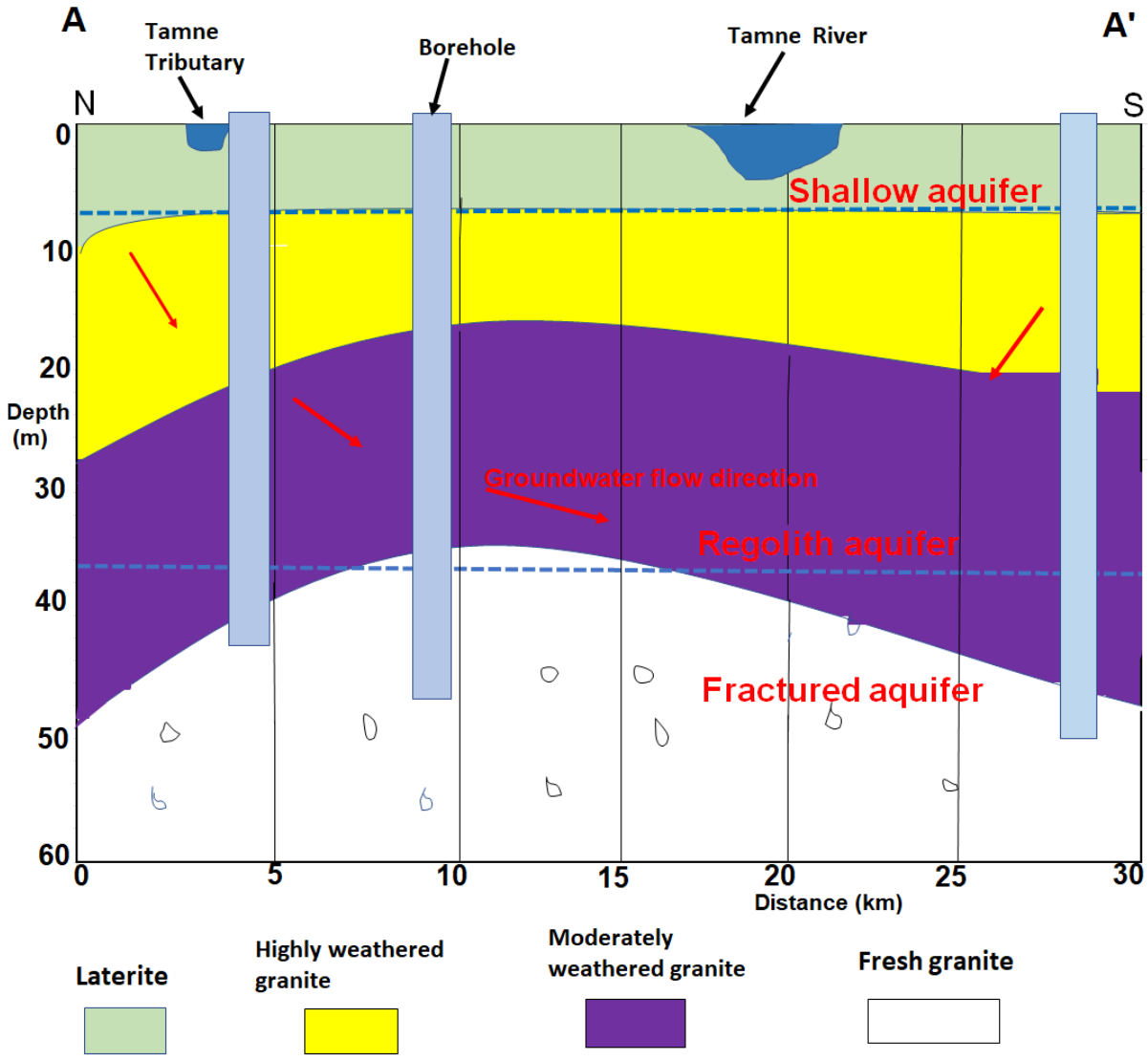

Fig. 6.4 *Hydrogeological cross-section through the Tamne River Basin*

6.2.4 Lithological modelling

Available drilling logs obtained from 10 wells, coupled with information from field campaigns and the literature, were compiled to develop multiple three-dimensional (3D) strip logs (Fig.6 5a), a 3D fence diagram (Fig6.5b), and a solid model (Fig.6.5c). The solid model was interpolated from borehole lithology intervals using the RockWorks Software Version 2020.9.3. The borehole logs indicate six major layers, of which the topmost layer comprises laterite soil, followed by silt and sand ranging between 0 – 9 m. The silt and sand are found only in small quantities in the study area. The fourth and fifth layers contain highly weathered

(10 m – 20 m) and moderately weathered grey granites (21 m – 40 m). These two weathered layers comprise the regolith profile: saprolite and saprock formed as a result of the in-situ chemical weathering of the granitic bedrock (SNC-Lavalin/INRS, 2011). The bottom layer consists mainly of unweathered fractured granite with an interval depth ranging between 41 and 60 m. The aquifer zone occurs within the highly weathered and moderately weathered granites. The lithology of the study area shows a cardinal direction from north to south, as shown in Fig.6.5. The SE direction comprises aquifer materials such as laterite, silt, and sand from the Birimian Supergroup and Mesozoic formations. From directions, NE to SW, the laterite, weathered granite, and fresh granite exclusively from the Tamnean Plutonic Suite are the main lithological materials.

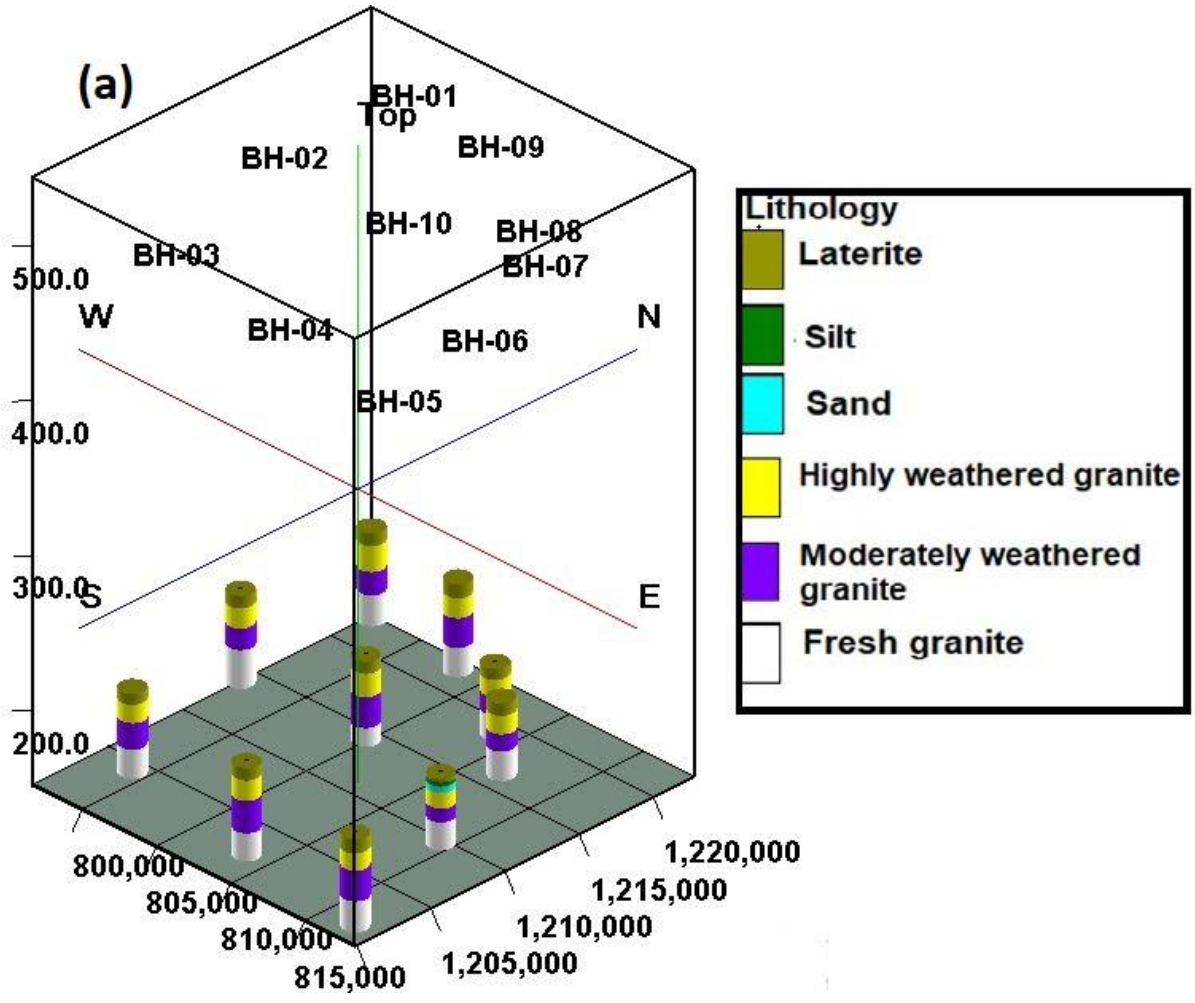

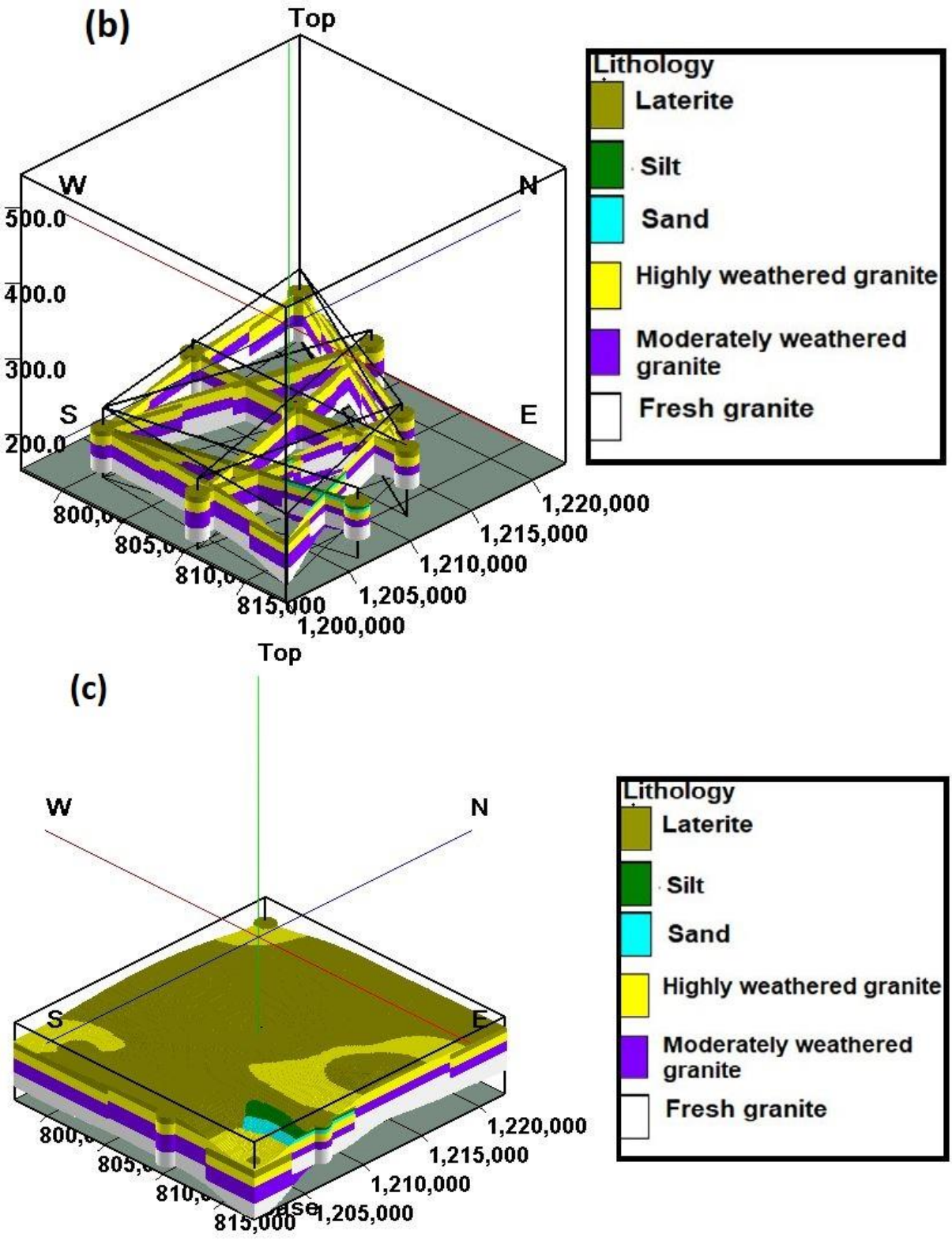

Fig. 6.5 *(a) Three-dimensional strip logs (b) fence diagram and (c) solid model of the study area. The horizontal axes are the latitude and longitude coordinates (UTM meters) and the vertical axis is elevation (meters).*

6.3 Materials and methods

Secondary data from sources such as borehole logs and pumping tests, and static water levels, were collected from the office of World Vision Ghana in Tamale. The monitoring well data were also taken from the Water Resource Commission of Ghana in Accra. The borehole logs obtained were analyzed, and these were used to develop the 3D lithological model and the conceptual framework. The aquifer hydraulic properties such as hydraulic conductivity and storativity were estimated using the Copper and Jacob (1944)) method.

6.3.1 Conceptual framework of the Tamne River Basin

A conceptual framework for numeric modelling of the hydrogeology of the region was developed based on the lithological data, hydrochemistry, groundwater level data (heads), and some previous studies that correspond to the hydrogeological and hydrologic settings of the study area (Anderson et al., 2015). The conceptualization was carried out with the Groundwater Modelling System (GMS) 10.4 Software (Aquaveo, 2020). In the initial stage of the conceptualization, the GIS map tool in GMS was used to import and register the geological map on the premise of creating a base map of the area. The model domain was delineated as a single hydrogeological layer because of the paucity of borehole logs, and the available well logs do not reveal any significant differences among the units. A general head boundary (GHB), which is the head-dependent flow boundary condition in GMS, was assumed and delineated for the Tamne basin. This was assigned because the analyzed hydraulic head distribution map, topographical map, digital elevation model (DEM), and field reconnaissance survey undertaken in October 2019 imply no existence of hydraulic or physical boundaries to preclude flow across the boundaries (Yidana et al., 2016). According to Anderson et al. (2015), the head-dependent boundary (HDB) allows the modeller to simulate volumetric flow rate (Q) across the boundary by using the assigned hydraulic head and conductance values of the aquifer material as illustrated in Eqn. 6.1.

$$Q = C\,\Delta h = C\,(h_B - h) \qquad 6.1$$

Where Q is the volumetric flow rate (L^3/T), C is the conductance (L^2/T), and Δh is the difference between the assigned boundary head (h_B) and the model computed head near the boundary (h). The borehole logs revealed spatial thickness, and these were used in the model conceptualization by adding the top and bottom elevations of the lithological materials. The top and bottom elevations (thickness) were then interpolated using the kriging method to cover the whole area of the basin (Yidana et al., 2015). Many studies have shown that kriging is an effective interpolation scheme when the data points are distributed in a regular pattern across the region (Anderson et al., 2015; Reilly & Harbaugh, 2004). The boundary condition at the top of the model is a semi-confining condition simulating partial infiltration from recharge. In contrast, the bottom boundary is a no-flow boundary because the

underlying granitic layers have a very low hydraulic conductivity (Yidana et al., 2016). The vertical aquifer boundaries were conceptualized as a head-dependent boundaries to allow flows from within and outside the basin. The basin has many river networks, including the Tamne River and its tributaries, and as such, the rivers were digitized to be included in the model together with their conductance, river stage, and elevation. Figure 6.6 shows a simplified 3D conceptual framework of the hydrogeology of the Tamne River basin with the input parameters. Even though five hydrostratigraphy layers (Fig.6.5) were delineated, the conceptual framework shows only two layers mainly due to a lack of detailed geological or geophysical investigations. According to Anderson et al. (2015), several geological formations may be lumped together to form a single stratigraphic unit, or geological formations may be subdivided into aquifers and confining layers.

In the Tamne basin, inflow to the aquifer occurs mainly as specified water flux in the form of precipitation, interflow, or induced river recharge and, to a lesser extent, seasonal flooding and irrigation water returns.

Based on this information, seven recharge zones were created. Each of the recharge zones was assigned values based on the land use patterns, the geology of the area, and information from previous studies (Anderson et al., 2015). Initial recharge values assigned were in the range between 5.1×10^{-5} m/day and 1.3×10^{-4} m/day (computed based on 2% and 5% of the mean annual precipitation of 935 mm/year) as espoused by Akurugu et al. (2020), who conducted similar research in the White Volta Basin of Ghana.

The zones in the model also included hydraulic conductivity, hydraulic heads, and pumping test data acquired from the well dataset. The values for hydraulic conductivity in the zones ranged between 0.01 m/day and 15 m/day. The values for hydraulic conductivity were selected according to the literature values and analysis from the pumping test (Fetter, 2001), and the hydraulic head values (difference between elevation and measured water levels) were included as 2D points and included in the model domain as observation heads.

The model domain of 848 km^2 was discretized into 10000 uniform cells using a finite-difference grid with 100 rows and 100 columns. The number of active cells was 6104, with the model domain-oriented in the north-south direction. All the applicable coverages of the conceptual model were mapped to a grid-based MODFLOW numerical model for steady-state and transient simulations.

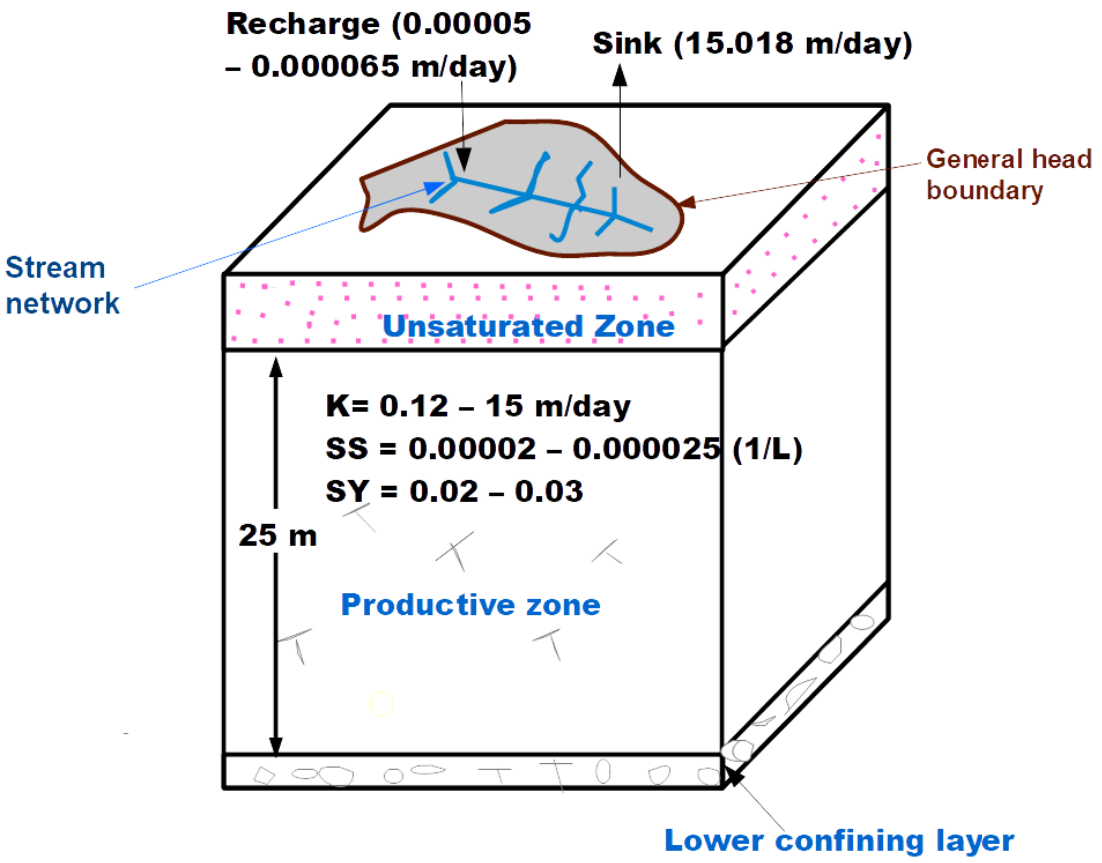

Fig. 6.6 *A 3D conceptual framework of the Tamne River basin. K= hydraulic conductivity, SS= specific storage, SY = specific yield*

6.3.2 Numerical simulation and model calibration

A 3D numerical groundwater flow model was set up using the US Geological Survey's cell-centered, finite difference MODFLOW-2000 incorporated in the GMS software (McDonald and Harbaugh, 1998). The MODFLOW model was first used to simulate groundwater flow with a steady-state condition based on the assumptions that the aquifer is heterogeneous, saturated, and anisotropic with Darcian flow. The steady-state groundwater condition for the basin represents the groundwater heads that were measured in 2017, in which groundwater flow was assumed to be constant and indicate an equilibrium condition after a lengthy pumping. In the steady-state model, the hydraulic properties together with the computed heads and flows never change with respect to time.

The measured groundwater heads were calibrated so that the simulated results approximate the natural conditions. Calibration was done in two stages: manual trial-and-error and automated calibration. Under the manual approach, the assigned initial aquifer hydraulic properties, such as hydraulic conductivity (*K*), recharge, and conductance of the GHB were

tuned to reduce the head residuals. The residual head is the difference between the computed head and the measured field head. After a reasonable head residual was achieved, the automated approach was refined. The automated calibration was performed with the help of the automated parameter estimation (PEST) module in GMS. PEST is a robust statistical tool that alters parameters within its defined space, and reruns the model several times until calibration can be achieved (Ryter et al., 2018). In addition, PEST can calibrate a large number of parameters efficiently within several minutes, depending on the speed of the user's computer. Before running the PEST program, an inverse model utility interface in PEST was set up by parameterizing the aquifer hydraulic inputs. The parameterization was done using the PEST pilot point method. Here, the inverse model was used to evaluate the pilot point values of the hydraulic conductivity, adjust the values, and interpolate the values providing an acceptable objective function to be achieved.

In GMS, PEST has options that enhance the parameterization process, and these are the single value decomposition (SVD) and Tikhonov regularization options. In the SVD dialog option, the parameter estimation process or calibration is enhanced by automatically removing parameters that have little effect on the predicted outcome while maintaining important parameters in the parameter estimation process. Similarly, with the Tikhonov regularization dialog option, there is a penalty applied to the objective function if parameters deviate from their original values. The method regularizes the results for a more stable and efficient parameter estimation and calibration (Doherty et al., 2010; Ryter et al., 2018). In this study, the SVD and the Tikhonov regularization were applied to the aquifer hydraulic values of the model.

Furthermore, in numerical modelling and calibration, a model layer (delimited by layer elevations top and bottom) is usually defined as a confined, convertible or unconfined layer used to simulate groundwater flow between cells (Anderson et al., 2015). The modelling problem arises when the MODFLOW code unwittingly converts the confined layer to an unconfined layer. This causes an unfeasible calculation of the saturated thickness. In confined layers, the transmissivity is time-invariant (constant), where the head rises above the top layer during simulation. Any change of head below the top layer will cause the above-stated problem to occur because the MODFLOW code recognizes the layer to be confined if specified by the modeller (Anderson et al., 2015). In GMS, the convertible and confined layers are the only possible layers in the Layer-Property Flow (LPF) package. The LPF package defines the horizontal and vertical hydraulic conductivity for each layer, and subsequently, MODFLOW uses the hydraulic conductivity values and layer geometry to calculate the cell-by-cell conductance. In this study, the convertible layer was chosen because the storage parameter can be simulated as specific storage or specific yield. In

addition, it can simulate dry and wet cells, which is not possible in the confined layer (Harbaugh et al., 2000).

6.3.3 Sensitivity analysis

Sensitivity analysis was carried out for both the calibrated steady and transient models to evaluate the response of the developed model when subjected to changes in some of the parameters. A model that deviates significantly after calibration (highly sensitive parameters) when some adjustments are made to the hydraulic properties is unstable and unfit to forecast future conditions (Anderson et al., 2015). Sensitivity analysis was done automatically using PEST in MODFLOW after calibration, where histograms showing the parameters were generated. For this study, hydraulic conductivity, recharge, and specific yield were not highly sensitive to the model and as such can be described as very stable parameters, suggesting a well-calibrated model.

6.4 Results and discussion

6.4.1 Steady-state model

The steady-state model was calibrated by using the hydraulic head measurements of 35 groundwater wells. The calibration was achieved by reproducing the field-measured hydraulic heads at a calibration target of ± 2 m. This implies that the difference between the simulated and the field measured heads should not be greater than 2 m (Yidana et al., 2016). The root mean square error (RMSE) values of the simulated hydraulic heads, as expected, are less than 10% of the difference between the highest and lowest field-measured groundwater levels (Ely et al., 2011; Lutz et al., 2007). The simulated and field-measured groundwater heads (Fig. 6.7) show a significant correlation with R^2 = 0.86, and a root mean square weighted residual of 6.91 m at a 95% confidence interval. The mean residual is -1.97 m, which indicates that the average simulated heads were higher than the field-measured groundwater levels by 1.97 m (Ryter et al., 2018). In general, the simulated model suggests a satisfactory match, and the model is deemed calibrated to represent the hydrogeological flow conditions of the area.

The spatial distribution of the hydraulic head in the steady-state model (Fig.6.8) ranges between 180 m and 330 m. The highest hydraulic heads are found in the northern and south-eastern parts of the study area. The groundwater-level contours of the steady-state model also show that the lowest hydraulic heads are seen in the southwestern sections of the area. These match the surface topography of the basin and conform to the assertion that hydraulic heads in aquifers are mostly a subdued replica of the topography (Haitjema & Mitchell-Bruker, 2005). The contour heads also show that the southern and northern parts are

hydraulically separated from the other areas due to the low transmissivity or stratigraphy settings of the area (Islam et al., 2017).

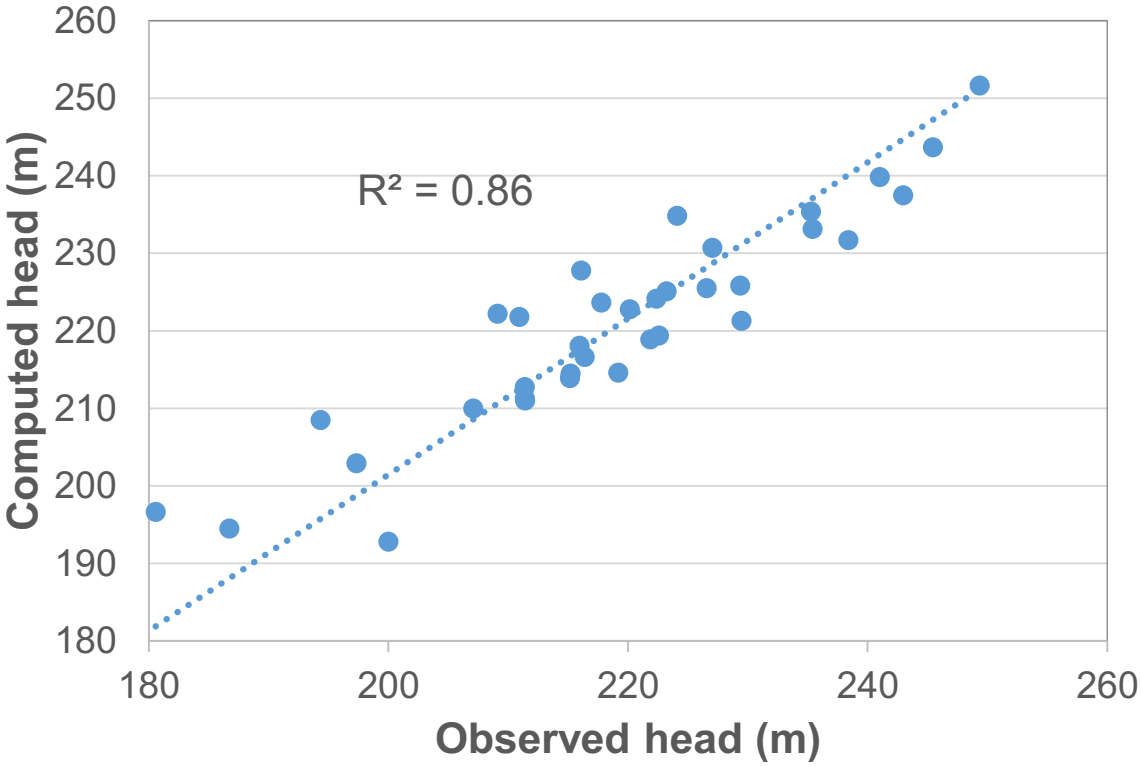

Fig. 6.7 *Plot of the observed head and computed for the steady-state model of the study area*

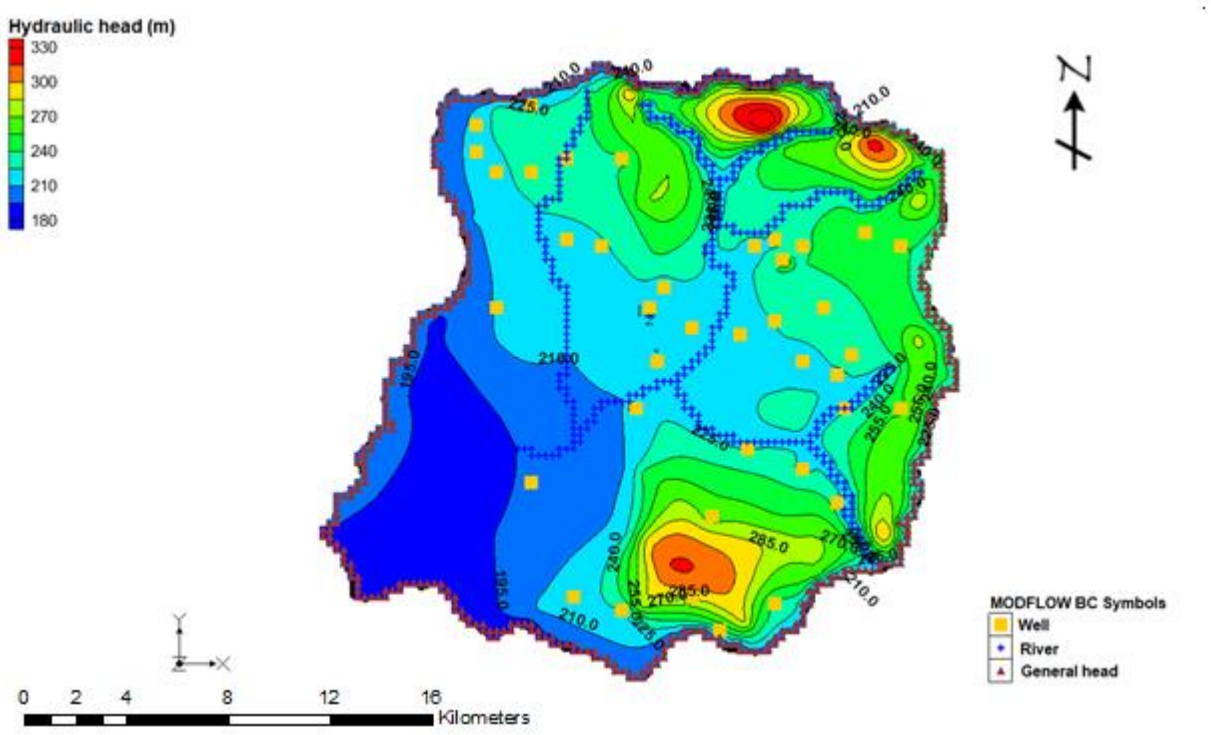

Fig. 6. *8 Calibrated steady-state model showing the hydraulic head distribution in the study area. BC= boundary condition*

6.4.2 Simulated groundwater flow

The calibrated steady-state model shows different flow paths in the Tamne River Basin due to the fractures and joints of the aquifer system. This interrupts continual groundwater flows and makes them move in different pathways. The flow paths were computed using velocity vector information from MODFLOW that shows the magnitude and direction of horizontal flow within each cell of the model layer. Conspicuously large magnitudes of flow are seen in the flow patterns of the southern part, where the Tamne River leaves the basin and joins the White Volta River. These flow patterns likely suggest that the highest amounts of groundwater discharge to streams and rivers occur in the southern section of the study area (Ryter et al., 2018). In the northern part of the basin, the vectors of groundwater flow are missing or absent in (area A in Fig. 6.9). Such instances indicate low hydraulic gradients and support the assertion that recharge to the northern section of the aquifer could be due to the ineffectiveness of the aquifer system at moving groundwater away from that portion (area A) (Ryter et al., 2018). In addition, the low or missing vectors could be attributed to highly weathered regolith materials that are thin, poorly permeable, and exposed to the land surface.

The simulated flow shows four distinguished groundwater flow patterns as observed from areas B to E in Fig.6.9. The spatial differences in the groundwater flow patterns in the Tamne River basin could be attributed to the structural entities, the surface topography, and the

drainage patterns (Yidana et al., 2015). In general, the groundwater flow directions in the Tamne River basin follow the surface topography with N – S preferred flow. This is consistent with the results obtained by Akurugu et al. (2020), who found similar flow directions in the crystalline basement rocks of Northern Ghana. The movement of groundwater in the study area can be defined as local and regional flow systems. Generally, under the local flow system, recharge areas coincide with topographic highs, whereas discharge areas are seen in topographic lows that are found adjacent to each other. For the regional flow system, recharge areas are generally located along the water divide, and discharge areas are found at the bottom of the basin (Tóth, 1963). It can be added that the recharge and discharge areas in regional flow systems are usually separated by several kilometres, and the aquifers can be partly or wholly confined, underlying a local flow system. It is noteworthy that potential regional recharge areas in the Tamne River basin are observed in the south-eastern and northern sections, where the highest hydraulic heads can be seen.

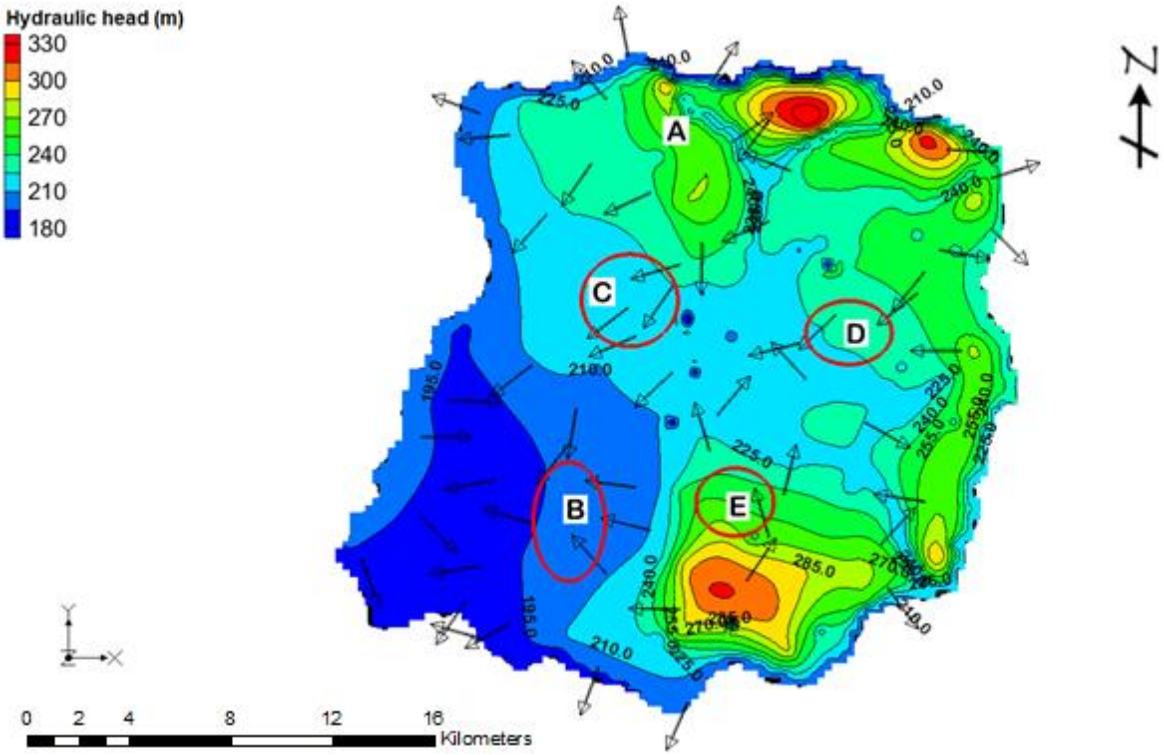

Fig. 6.9 *Simulated vector magnitudes of groundwater flow in the study area. Flow patterns are distinguished in areas A-D. Arrows indicate flow directions*

6.4.3 Mass water balance of the steady-state

The groundwater flows budget that quantifies the net inflow and outflow flow in the study area is shown in Table 6.1. Of the 312960.24 m^3/day of water that flows through the

Tamnean Plutonic Suite aquifer in the area, 55% (172461.964 m^3/day) represents recharge and contributes the most significant inflow to the model. The next contributor of inflow comes from the general-head-dependent boundary condition representing 41% of the water coming from neighbouring aquifers and basins. Forty-six percent of the water (141613.95 m^3/day) leaves the basin by virtue of the rivers and streams incorporated into the model as river coverage. Another significant outflow from the model (54% of the water) is from the general-head-dependent boundary condition that probably discharges into streams, rivers and ditches, or by means of evaporation. An amount of 4198.95 m^3 of water is abstracted daily from 35 groundwater wells. This value is very low and accounts for 1.34 % of the total water flowing out of the model. This would imply that wise management of groundwater resources could supply the current water needs. However, it is important to note that the total number of boreholes exceeds the number used in the study and cannot represent the actual abstraction rate. The baseflow obtained from the model is 128461.53 m^3/day — computed as the difference between the inflow and outflow river leakages. The resultant regional groundwater flow in the basin is the difference between the simulated recharge and the computed baseflow, which is 44000.43 m^3/day.

Table 6.1 Flow Budget of the Calibrated Steady-State Model

Flow budget component	Inflow (m^3/day)	Outflow (m^3/day)
Wells	0	4198.95
River leakage	13152.43	141613.95
Head-dependent boundary	127345.85	167147.31
Recharge	172461.96	0
Total	312960.24	312960.24

6.4.4 Hydraulic conductivity field

Hydraulic conductivity of earth materials is an important aquifer property used to determine the ease at which groundwater flows in porous media. It is by far a key hydraulic property that defines the transmissivity of an aquifer for the proper groundwater resources planning (C. Fetter, 2001). According to Fitts (2002), a promising and cheap way to estimate hydraulic conductivity can be through a good simulated groundwater flow model. This is because the standard estimation of hydraulic conductivity values using sieve analysis and permeameters in the laboratory, and also pumping tests in the field, are sometimes time-consuming and expensive. For this study, estimated hydraulic conductivity values from the pumping test supported by literature values were used to generate a hydraulic conductivity map by means of PEST pilot points in GMS. The simulated hydraulic conductivity distribution (Fig.6.10)

shows that a large portion of the study area has low hydraulic conductivity values, less than 3 m/day, possibly suggesting a homogeneous hydraulic conductivity field (Fetter, 2001).

The hydraulic conductivity values range between 0.01 m/day and 15 m/day, which is consistent with the works of various researchers who obtained similar hydraulic conductivities in similar geological terrains of Ghana (Lutz et al., 2007; Yidana et al., 2015). The highest hydraulic conductivity values occur in the southwestern part of the basin, suggesting an enhanced secondary permeability associated with features such as faults, joints, and fractures in the Tamnean Plutonic Suite aquifer, which could serve as good sources of groundwater delivery. In comparing the hydraulic conductivity with the geology of the area, the lowest hydraulic conductivity values are found in the granitic rocks of the Tamne Plutonic Suite. In contrast, the highest values occur in areas with patches of the Birimian Supergroup and Mesozoic rocks, and the Tamnean Plutonic Suite. This confirms the assertion made by Banoeng-Yakubu et al. (2011) that the best source of groundwater is found in the Birimian Supergroup of Ghana.

Three different methods are commonly used to determine groundwater flow through fractured rock (Anderson et al., 2015). A continuum approach is widely used to describe groundwater flow in a fractured bedrock, where the flow is analogous to porous media or unconsolidated flow. The second approach is the discrete approach, which describes the flow through individual fractures in the aquifer system. This requires sufficient data, and analysis is practically impossible and very expensive. The dual-porosity approach, the last approach, assumes that the flow through the media consists of a fracture system and a less permeable matrix block (Lee et al., 1999).

The computed hydraulic conductivity field suggests some degree of weathering and fracturing of the rocks and interconnected structures to allow continual flow. Based on the current analysis, the area can be represented by a combination of dual-porosity and continuum approaches.

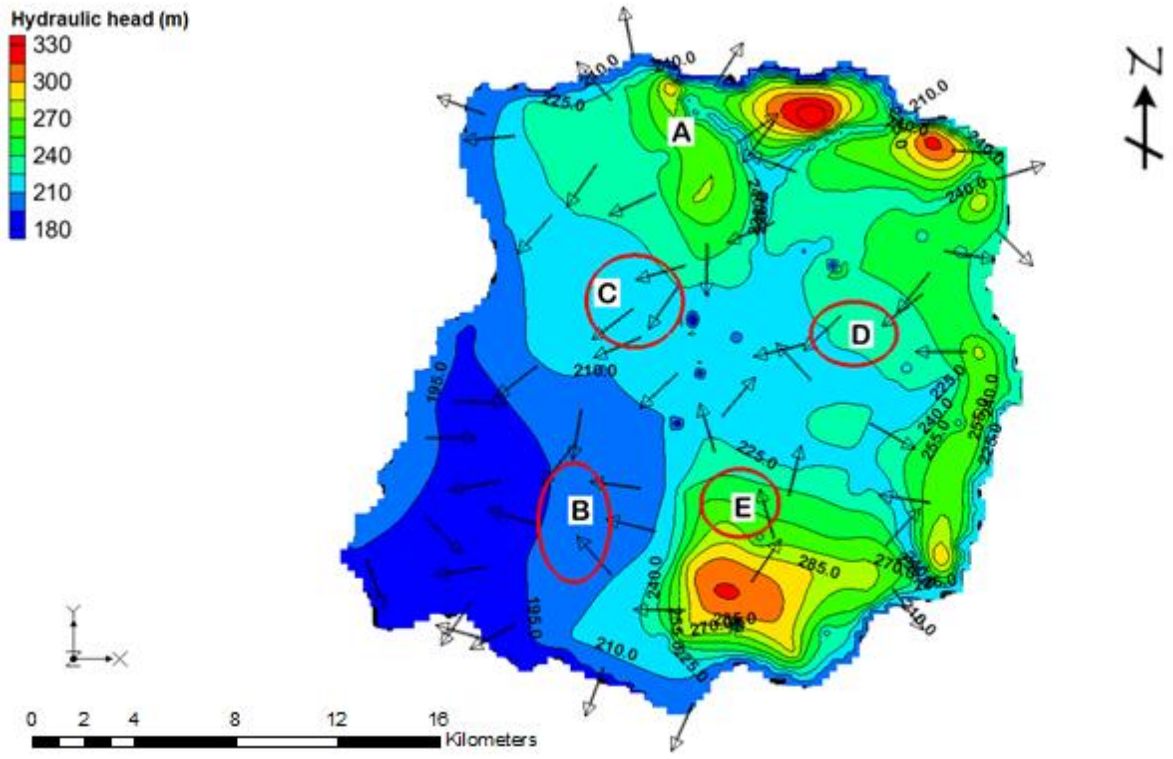

Fig. 6.10 Spatial distribution of hydraulic conductivity in the study area

6.4.5 Simulated groundwater recharge

One of the objectives of this study is to estimate and quantify groundwater recharge in the basin for efficient aquifer management. Scanlon et al. (2002) broadly discussed various techniques for estimating groundwater recharge; these include tracer techniques, numerical modelling, physical techniques (water-table fluctuation method, lysimeters), Darcy's law, and the zero-flux plane. For this study, the initially assigned recharge values imposed in the model ranged between 2% — 5% of the area's average annual rainfall, and this was adjusted during the calibration. The calibrated recharge values obtained range from 5.0×10^{-3} mm/day to 6.5×10^{-2} mm /day, corresponding to 0.19% and 2.5 % of the average annual precipitation in the basin. Low recharge values are found in the southwestern and central parts, where the hydraulic heads are the lowest. The low recharge rates obtained reflect the high evapotranspiration that reduces significant fractions of infiltrating rainfall in the semi-arid region of Northern Ghana. In addition, the low spatial recharge in the area is attributed to the nature of the topography or the unsaturated zone processes that preclude the vertical movement of rainfall into the aquifer (Anderson et al., 2015). The simulated recharge compared to the current groundwater abstraction rates would imply significant and sustainable water to meet the current needs. However, with a projected increase in water demand for agriculture and the expected global climatic changes in the future, there is a need for critical groundwater resources planning. The highest recharge rates in the Tamne

River basin occur in the southeastern and northwestern parts, where the topographic surface has a high elevation (Fig. 6.11). This observation can be attributed to the enhanced fractures and joints of the weathered granite rocks that facilitate the movement of groundwater in the basin.

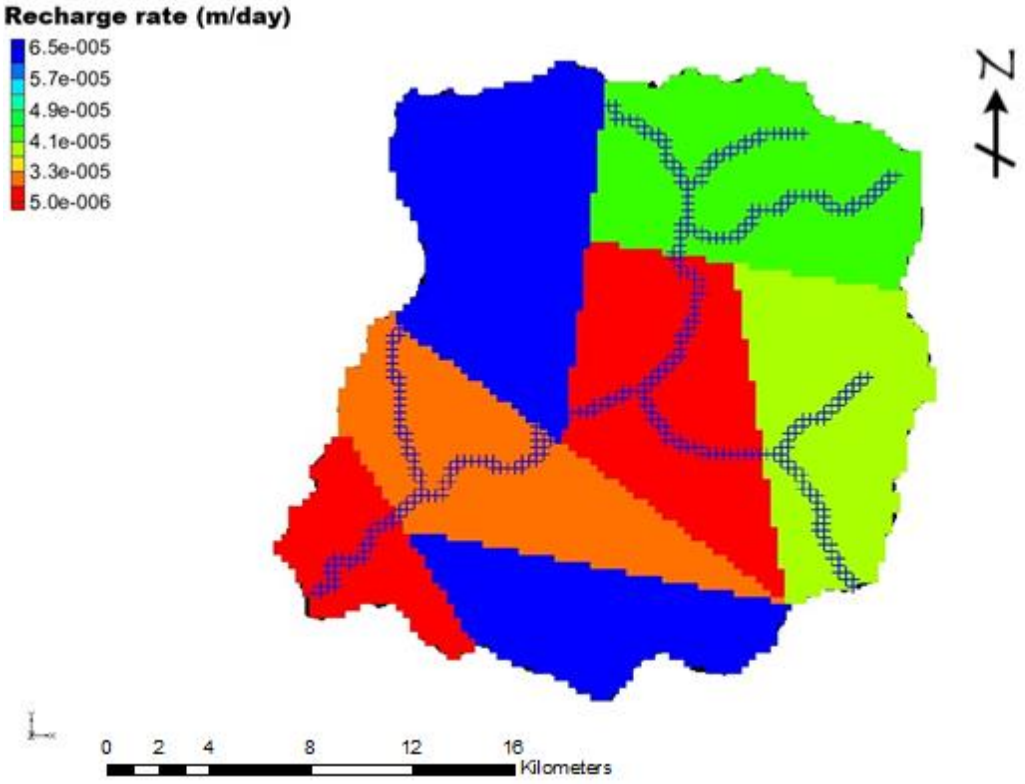

Fig. 6.11 *Simulated groundwater recharge in the study area.*

6.4.6 Transient simulations

In the study area, data from only one monitoring well with monthly water level measurements between November 2009 and April 2012 were available, and these were averaged and used for the transient simulation. Although monitoring well data are extremely limited, it is important to note that the developed transient model provides some insights into the seasonal pumping and recharge rates important for this baseline feasibility study. The hydraulic water heads produced from the steady-state model were used as initial conditions in the transient model. The transient model was developed based on the literature and pumping test values of 0.00002 m^{-1} — 0.000025 m^{-1} for specific storage, and 0.02 — 0.03 for specific yield. The simulated transient head distributions after 29 stress periods are presented in Fig.6.12. The stress periods represented the monthly time intervals between 2009 and 2012 that were used in the model to simulate transient stress parameters such as recharge rate, river stage, and pumping rate. These parameters, especially the recharge rate, varied according to the monthly seasons since recharge flux depends mostly on

precipitation in the catchment. Figure 6.12 represents the water-level conditions at the Kabingo well. The plot shows low groundwater levels between October and March, and high groundwater levels from June to August. These trends are in response to the seasonal rainfall patterns in the study area leading to different recharge regimes and corresponding groundwater levels.

In general, the simulated head changes and observed heads do not show any noticeable differences with regard to head and flow geometries. This might be because the groundwater abstraction over these years did not cause any significant stress and did not change the overall water levels and flows in the basin. It is noteworthy that where long-term hydraulic head measurements are available, the transient simulation can provide a thorough assessment of the seasonal pumping and recharge in the area. More data will therefore be needed to conduct a detailed transient simulation in subsequent works.

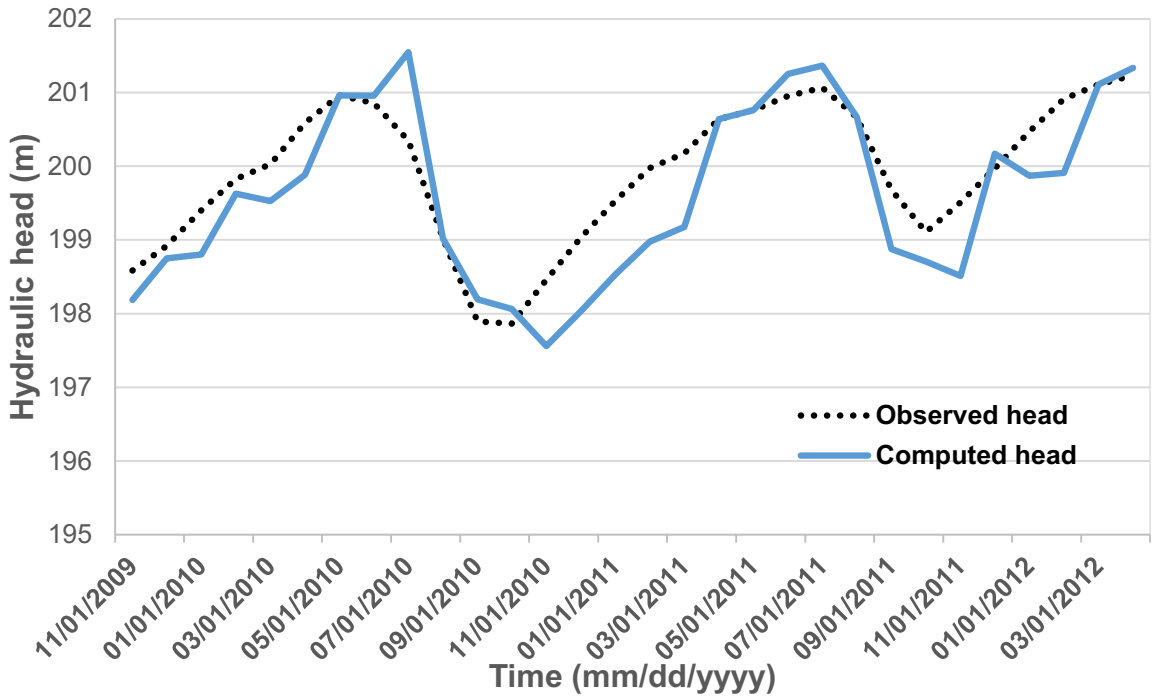

Fig. 6.12 *Transient head changes at the Kabingo monitoring well from 2009 to 2012*

The flow budget of the transient simulation shows a well balance between the inflows and the outflows (Table 6.2). The transient model shows that significant inflows come from recharge and the head-dependent boundary. The average lateral inflows (head-dependent boundary) arising from the neighbouring areas is 137203 m^3/day. An amount of 136487 m^3/ day was lost as outflows, suggesting an average of 716 m^3/ day was gained. The Tamne River basin forms part of the White Volta basin, and it is suggested that the lateral inflows and outflows are from the White Volta basin since the basins are interconnected (Yidana et al., 2016). More abstractions can cause significant lateral inflows into the aquifer with a corresponding

reduction of the hydraulic heads in the area. Transient storage is an important aquifer property used to investigate the sufficient volume of water that would be needed for successful aquifer storage and recovery (ASR) application. Figure 6.13 shows the monthly storage variations of the whole transient period.

Table 6.2 Monthly average of the calibrated transient flow model

Flow budget component	Inflow (m^3/day)	Outflow (m^3/day)
Wells	0	5982.08
River leakage	8320.54	154987.61
Head-dependent boundary	137203.45	136487.01
Recharge	173121.97	0.00
Storage	5786.60	26975.86
Total	324432.56	324432.56

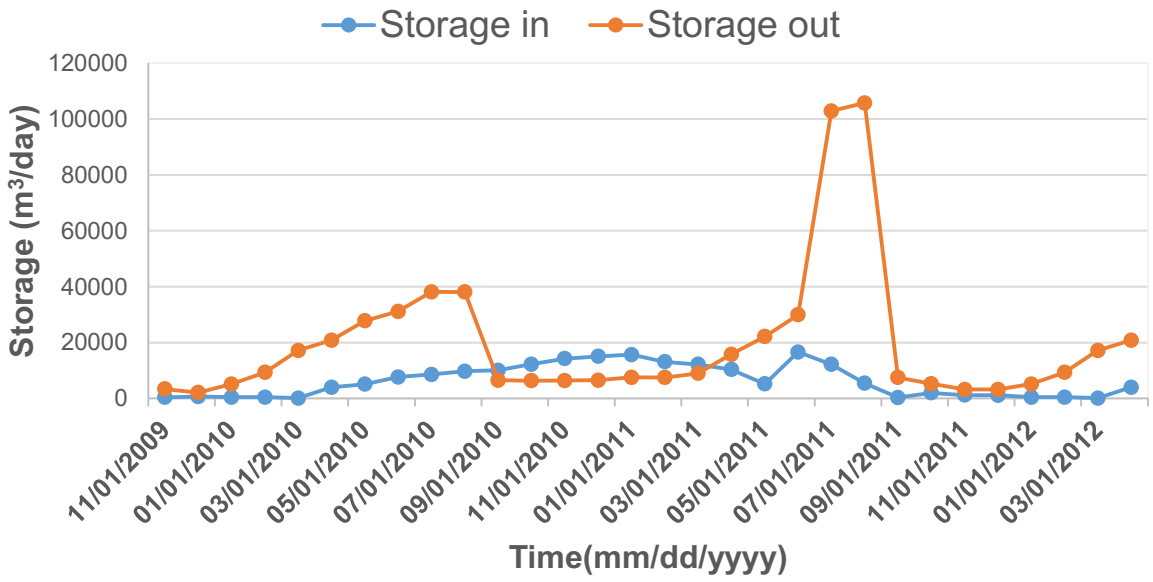

Fig. 6.13 *Monthly change in storage in the Tamne River Basin*

The storage fluctuations mimic the rainfall pattern in the area, where low storage values are recorded in the dry season and high storage values are recorded in the rainy season. The highest storage value was recorded in September, probably due to the time lag of rainfall and infiltration in the area. The average storage inflows and outflows are 5786 m^3/day and 26975 m^3/day, respectively.

6.5 MAR scenarios

The study aims to evaluate the feasibility of MAR through injection and abstraction scenarios using the ASR technique. The ASR method is usually suitable for confined and semi-confined aquifers because in unconfined aquifers groundwater velocities are usually higher,

a situation that can make some of the stored water move away from the well, thereby minimizing recovery efficiency (Pyne, 1995). In addition, the choice of the ASR method also depends on land suitability assessment; according to Owusu et al. (2017), land, soil, and subsurface characteristics in the Upper East region of Ghana are suitable for the ASR method. Based on this, 35 injection wells were used for the MAR scenarios, and their locations were selected based on land availability, proximity to existing wells, rivers, and potential sources of contamination. For instance, injection wells sited close to rivers or lakes might lose most of the storage discharging into the rivers (Ebrahim et al., 2016). The well spacings considered here are approximately 200 m, which is within the distance of 100 m – 300 m, as suggested by Pyne, (1995). Four scenarios were tested for groundwater management decisions and presented as follows:

1. The first scenario was simulated as a baseline scenario to investigate the extent of groundwater movement between November 2009 and December 2031, with 266 stress periods assuming recharge, abstraction, and climatic conditions remain the same.

2. Scenario 2 was considered as a MAR injection scenario; this was tested by injecting a volume of 325 m^3/day during a 4-month period every year, which was simulated until 2031. This volume of water injected is equal to the total available floodwater that is registered in every rainy season (40,000 m^3) in Northern Ghana as documented by Conservative Alliance, (2015).

3. The third scenario was simulated as a MAR abstraction scenario, which considered 8 months of abstraction after 4 months of MAR injection. This scenario intends to recover the same amount of water injected. Unfortunately, injection and abstraction rates do not occur simultaneously in MODFLOW. For this scenario, a per capita water demand was assumed to determine the actual domestic water and irrigation withdrawals in the area. The current aquifer abstraction obtained from the 35 wells during the steady-state and transient simulations cannot represent the actual abstraction rate of the basin because the boreholes in the area far exceed this number. The total water abstraction rate or demand from a population of about 150,184 people was considered; individual water consumption is 50 L/capita/day in the region (Ghana Statistical Service, 2013). This per-capita number was doubled to include additional use of domestic water, irrigation water withdrawals, and water for large-scale cattle production in the basin. A resultant abstraction rate of 15018 m^3/day was evenly spread among the 35 boreholes, and this was used as the actual daily abstraction rate for the third scenario.

4. For Scenario 4, the abstraction rate was increased by 50% after the MAR injection. The increased abstraction scenario intends to investigate the resilience of the aquifer in the face

of increased irrigation, population demand, and climate change in the future. The different MAR scenarios are presented in Table 6. 3.

Table 6.3 MAR injection and abstraction scenarios

Scenario	Description	Injection rate during the 4-month/8-month period (m^3/day)	Number of injection wells	Volume of water abstracted (m^3/day)
1	Baseline scenario	NA	NA	6591.4
2	MAR injection	325	35	6591.4
3	MAR abstraction	NA	35	12559.6
4	MAR abstraction increased by 50 %	NA	35	18829.34

NA means no injection/wells

Hydraulic head contours of the various scenarios (1-4) are shown in Fig. 6.14a-d. The results of the baseline scenario from the period 2012 to 2031 show no significant differences in the water balance with respect to the calibrated transient model. The projections do not excessively have an impact on the lateral inflows and outflows. The storage capacity follows the same pattern as the transient simulation, where dry season periods have little or zero flow. The average storage inflows increase slightly from 5786 m^3/day to 6201 m^3/day, whereas the average storage outflows increase from 26975 m^3/day to 28765 m^3/day. In general, this scenario has a minimal effect on the groundwater flow and the available water resources in the basin.

For the injection scenario, applying 325 m^3/day into the aquifer shows a resulting increase in groundwater levels in most parts of the aquifer, as expected. The total volume of water injected at the end of the 4-month period every year is 11 000 m^3/day, approximately 1. 3 X 10^6 m^3 — computed by multiplying the injection rate and the number of days in 4 months. There are significant gains in the storage inflows and outflows with respect to the baseline scenario. Figure 6.15 shows the hydraulic head changes in the different scenarios. The injection scenario shows that the groundwater levels rise by 1.05 m on average. This shows that MAR is feasible in augmenting the water levels in the area when combined with controllable irrigation and domestic withdrawals. More available floodwater will probably increase aquifer storage. However, the availability of floodwater is limited in the area.

In the third scenario, applying the ‘per individual water consumption rate of 100 L/capita/day in the model causes a slight increase of the lateral inflows to 147385 m^3/day with respect to the baseline scenario. The net river inflows and outflows also have a minimal increase. The average storage inflows increase slightly from 6186 m^3/day to 7186 m^3/day. However, the average storage outflows reduce from 26975 m^3/day to 22197 m^3/day, resulting in a minimal

reduction of the hydraulic heads in the south-eastern and northern parts of the area. The volume of water abstracted at the end of 8 months is 12559.57 m^3/day (3.1 X 10^6 m^3) as seen in Table 4. Subtracting this abstraction rate from the baseline abstraction rate (without MAR) gives a net abstraction rate of 5968.09 m^3/day (approximately 1.48 X 10^6 m^3).

In scenario 4, increasing groundwater abstraction by 50% after MAR injection shows a reduction of the hydraulic head. The lateral inflows and outflows increase as well as the river inflows. The volume of water recovered at the end of the simulation period is 18829 m^3.

Table 6.4 Water Budget of the MAR Scenarios

Scenario	Wells (m^3/day)		River Leakage (m^3/day)		Head-Dep Boundary (m^3/day)		Recharge (m^3/day)		Storage (m^3/day)	
	Inflow	Outflow	Inflow	Outflow	Inflow	Outflow	Inflow	Outflow	Inflow	Outflow
(1) Baseline	0	6591,4	89705	155068,1	141735,5	139589,2	173121	0	6186,6	287655
(2) Injection	11000	6591,4	22370,1	176168,5	176655,4	181589,0	199241.2	0	16366,7	61385,9
(3) Abstraction	0	12559,6	9220,5	158178,3	147385,0	144589,1	173621.9	0	7186,6	22197,3
(4) 50% Abstraction	0	18829,3	11710,1	161150,9	169238,77	164389,01	173621.9	0	8986,15	19187,66

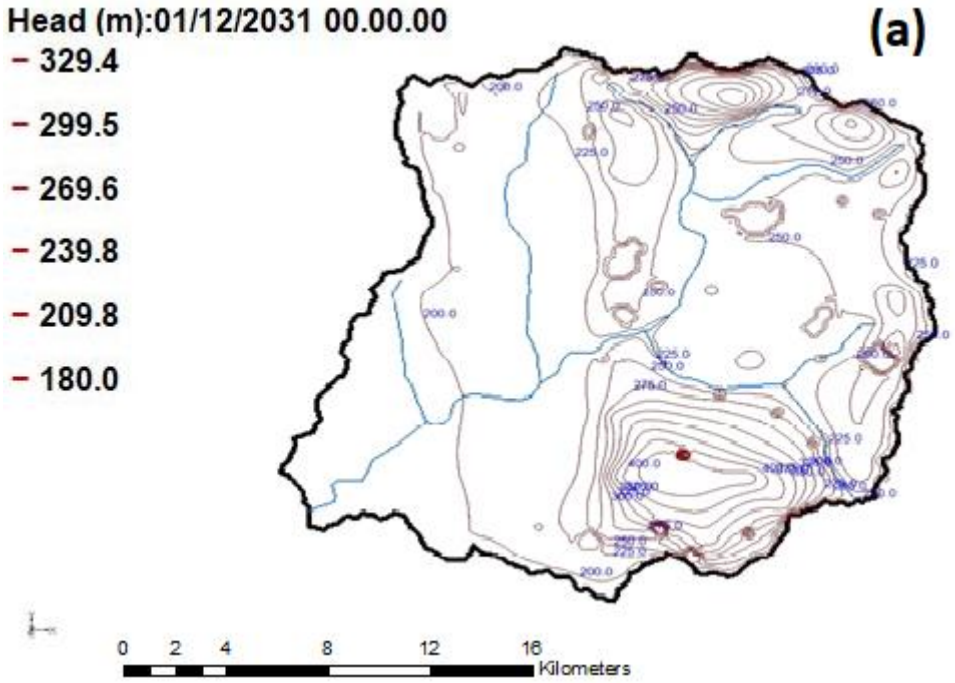
Head (m):01/12/2031 00.00.00
329.4
299.5
269.6
239.8
209.8
180.0
(a)
0 2 4 8 12 16
Kilometers

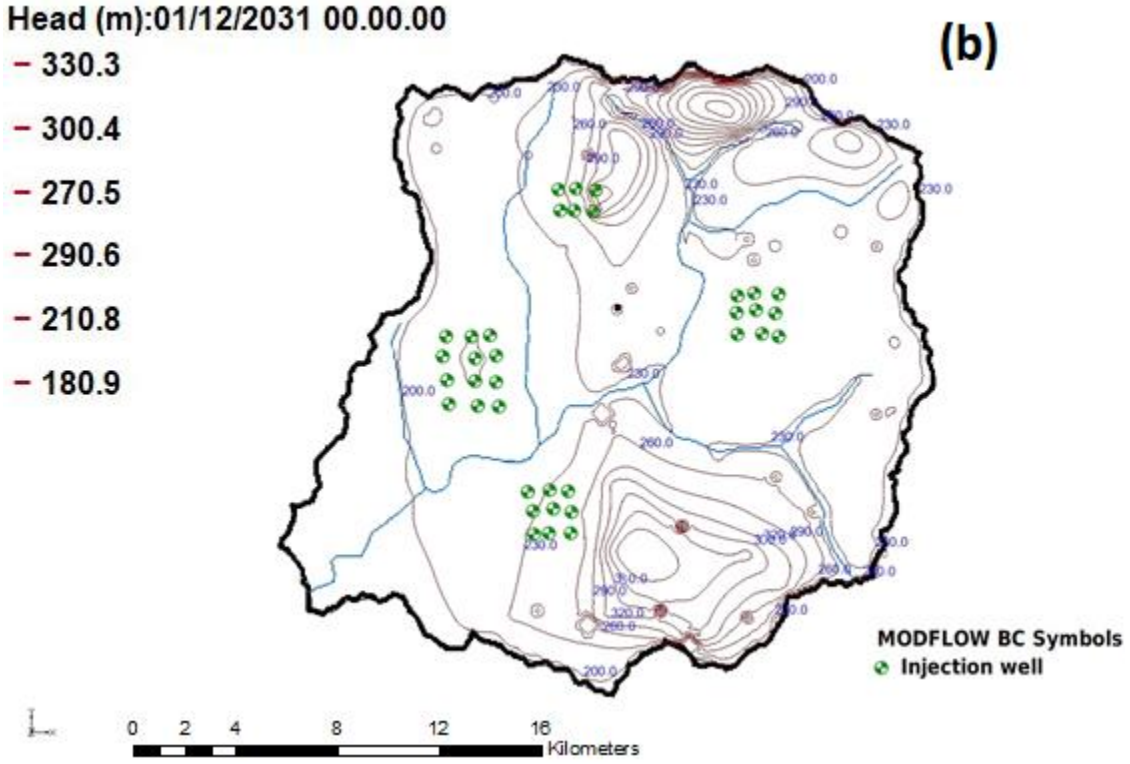
Head (m):01/12/2031 00.00.00
330.3
300.4
270.5
290.6
210.8
180.9
(b)
MODFLOW BC Symbols
Injection well
0 2 4 8 12 16
Kilometers

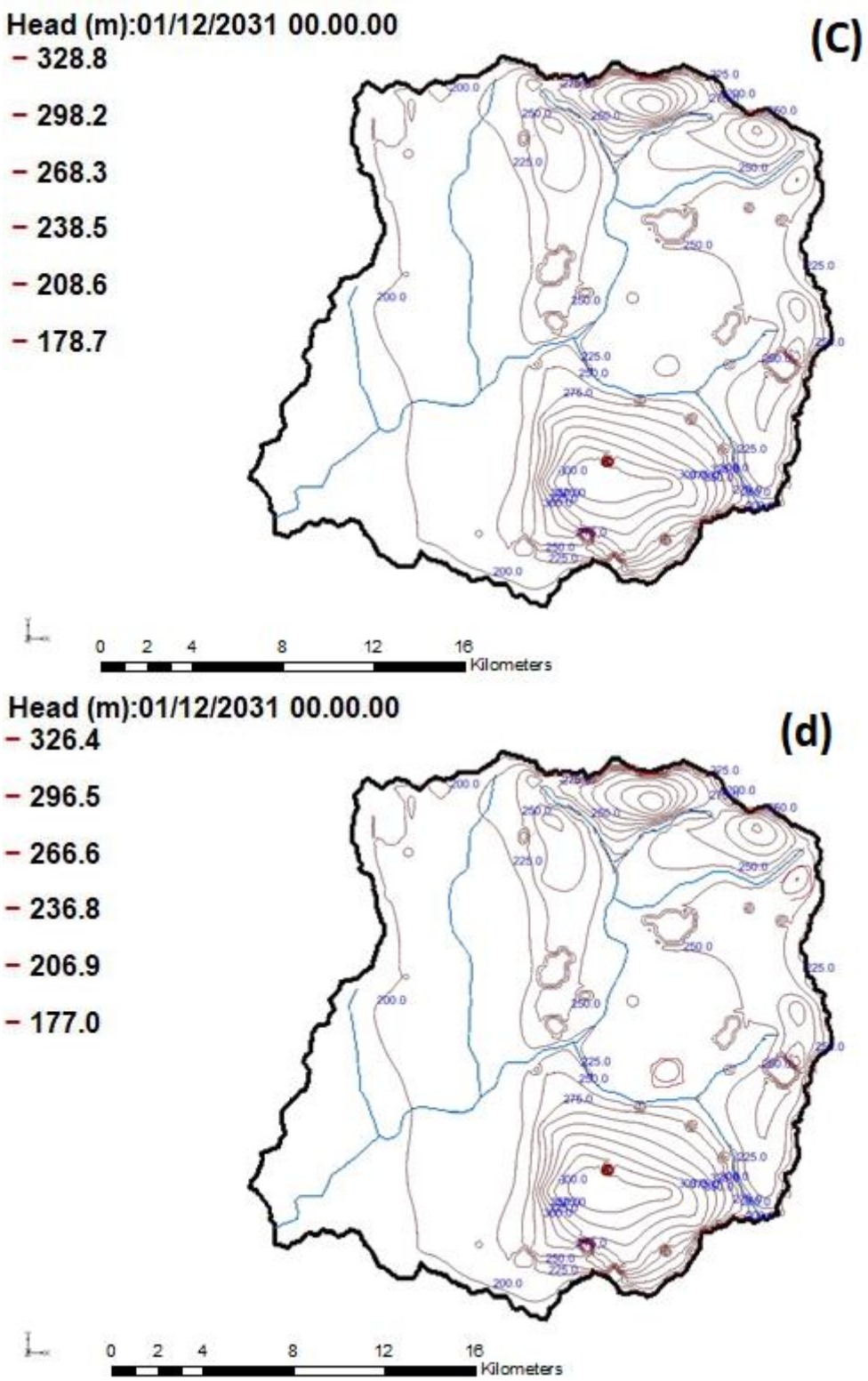

Fig. 6.14 *Hydraulic head elevation (m above sea level) for various MAR scenarios (see Table 3): (a) baseline, (b) MAR injection, (c) MAR abstraction, and (d) 50 % increase in abstraction*

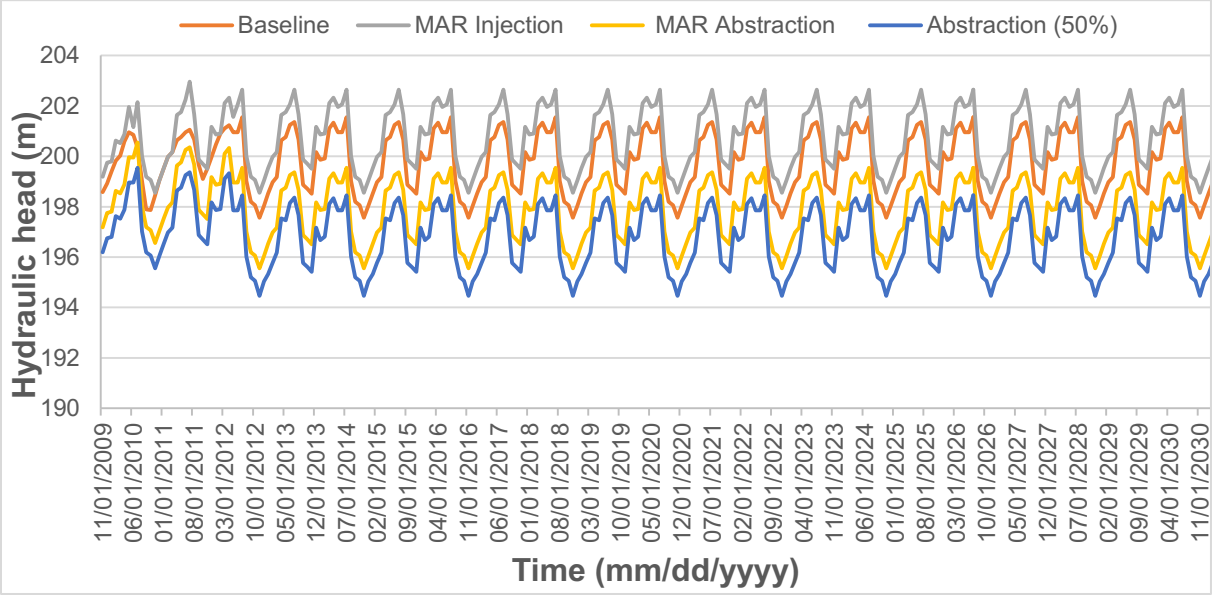

Fig.6.15 *Hydraulic head changes with the different scenarios*

A cross-section (distance) that runs through the zone of the injection wells (from the northern to the southern parts of the modelled area; Fig. 6.14b) is plotted against the simulated hydraulic heads as shown in Fig.6.16. The continuous injection shows a gradual build-up of the groundwater mound at a distance of 6 km and 14 km. This is reflected in the aquifer storage and shows that MAR is effective in restoring groundwater levels.

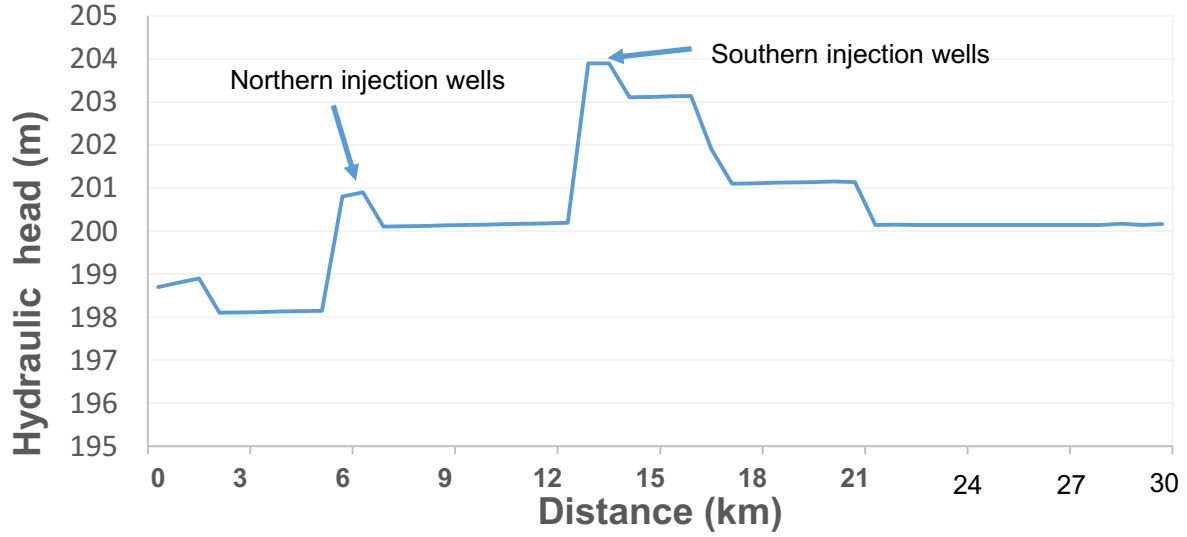

Fig.6.16 *Simulated head changes in the injection wells versus distance from the northern to the southern part of the modelled area shown in Fig 6.14b*

6.5 Importance of MAR as a source of water supply

MAR is being proposed as a feasible option to counteract the water scarcity in the area and make water available for dry-season irrigation farming. The study area is flood-prone and, as discussed earlier, the total floodwater available during the four months rainy season is 40,000 m^3 (Conservative Alliance, 2015). The water demand (domestic and irrigation water) in the area is approximately 15018 m^3/day considering the current population of 150,184 and a per water demand of 100 L/capita/day. The water demand is projected to go higher, considering the global climatic changes, urbanization, and population growth. For instance, applying the Ghana Statistical Service (2013) exponential annual growth rate of 2.5% and using the 2021 population, it is expected that the population will reach 187,730 by the year 2031. The resulting water demand would then be 18,773 m^3/day, assuming the same per capita water consumption. This calls for additional water to be provided for domestic and irrigation purposes (Ebrahim et al., 2016).

The MAR modelling scenarios show that the net volume of water that can be abstracted during the 8 months is 5968 m^3/day. Assuming the volume of water without MAR practice, which is 5982 m^3/day, remains the same, the total volume of water from the basin, including that of MAR, would then be 11950 m^3/day. This volume of water would provide for future domestic and irrigation water needs, particularly in the dry season. It would also improve the economic fortunes of the people, who will get all-year-round water to irrigate their farms.

However, the laws and legislation governing the implementation of MAR are not clear, as no policy either accepts or rejects MAR development in Ghana. This may affect the operation of MAR schemes that are currently gaining attention in Northern Ghana, due to a lack of legislative support. Furthermore, informal institutions operated through water leaders, and customs and traditions at the local scale, are entrenched within the existing culture and they play a significant role in the water development discourse in the country (Kwoyiga & Stefan, 2019). To achieve successful MAR goals, both formal and informal institutions must sanction a strong policy to enhance MAR implementation and operations in Ghana.

6.6 Conclusions and recommendations

This study presents a combined approach for understanding the hydrogeological conditions and for assessing the feasibility of managed aquifer recharge (MAR) in the Tamne River basin of Ghana. A groundwater flow model has been developed under steady-state and transient conditions using the available limited data. The steady-state model suggests that precipitation is the significant inflow in terms of the basin water budget. The calibrated recharge values obtained range from 5.0×10^{-3} mm/day to 6.5×10^{-2} mm /day, which correspond respectively to 0.19% to 2.5 % of the average annual precipitation in the area. This low recharge rate results from the low erratic rainfall and high evapotranspiration in

Northern Ghana. Groundwater flow in the basin is topography driven, in which the dominant flow pattern is north to south with local and regional flow regimes. Estimated hydraulic conductivity field values range between 0.01 m/day and 15 m/day, which is within the values obtained from the pumping test and literature covering the aquifer materials. The heterogeneous and anisotropic nature of the aquifer requires more careful consideration for the MAR site selection and implementation procedures.

The transient model shows that the aquifer has enough storage to accommodate MAR water infiltration. Here, different MAR scenarios were tested to investigate the aquifer response to injection and abstraction. Treated floodwater during the rainy season was used as a source of water for the MAR. The total volume of water injected by the end of the 4-month period every year is approximately 1.3 X 10^6 m^3. This shows a resultant increase in aquifer storage and groundwater levels and proves that MAR is feasible in the Tamne River basin. The volume of water that can be abstracted at the end of the 8 months is 5968.09 m^3/day (approximately 1.48 X 10^6 m^3). This volume of recovered water would be sufficient for the population during the prolonged dry-season months, in which there is water scarcity. The results imply that the farmers will get all-year-round water for irrigation if MAR is fully implemented in the region. This will eventually increase their incomes and reduce poverty. It will also help stakeholders and decision-makers to manage the limited water resources in the region. The developed model and the MAR scenarios are the first of their kind in Ghana and set a stage for more MAR projects. There are a lot of uncertainties in the model due to lack of data; therefore, it is recommended that more monitoring well data should be available in future research to reduce the model uncertainties in the transient simulation. A simulation-optimization groundwater model approach and water quality issues should be addressed to better understand the MAR conditions in the area.

CHAPTER 7

Synthesis

7.1 Conclusion

The hydrogeological catchment represents a typical case study to evaluate the feasibility of managed aquifer recharge (MAR). The region is a semi-arid area where surface waters are limited and the available water resources are usually under constant threat due to increasing population growth and global climatic changes. This pattern has resulted in water scarcity, which is prevalent, particularly during the dry season and has caused a decrease in agricultural food production and also affected the livelihoods of the people. There have been instances of flooding every rainy season, but no water for use during the prolonged dry season. To ensure sustainable all-year-round water for agricultural farming and domestic purposes, the available floodwater that is registered during every rainy season was used as source water for this MAR groundwater modelling feasibility study. There are emerging MAR schemes (PAVE and Bhungroo Irrigation technology) in northern Ghana where excess rainwater or floodwaters are captured, filtered and injected into the aquifers as means of storage and recovered for use during the dry season. However, these schemes are limited to only a few places and there is growing evidence of declining water levels and water scarcity during the dry season in Northern Ghana. Furthermore, groundwater modelling studies and detailed hydrogeological investigations have not been investigated to assess the feasibility of MAR in Ghana.

Therefore, this work aimed to evaluate the feasibility of MAR in northeastern Ghana using a numerical groundwater model, hydrochemistry and environmental tracers. The study was conducted in two administrative places (1) the Garu- Tempane areas and (2) the Tamne River, basin, which comprises parts of the Garu district and parts of Bawku Municipality. Groundwater modelling studies were done in the Tamne River basin due to the presence of long-term historic water levels for transient simulation. The areas are underlain by crystalline basement rocks mainly of granitoids, and small portions of Voltain sedimentary rocks and Mesozoic rocks. Groundwater occurrence is through secondary porosity developed as a result of weathering and faulting of the underlying bedrock. The PhD work was set for three objectives: (1) to characterize the groundwater from a hydrogeochemical perspective (2) to use multi- environmental tracers to understand groundwater residence times and recharge processes and (3) to assess the feasibility of managed aquifer recharge in the Tamne River basin using numerical groundwater flow model. Relevant conclusions taken from this study can be described as follows.

The literature review of managed aquifer recharge (Chapter 2) examined the state of the art information on managed aquifer recharge in Europe and Africa. It was found out that the

European MAR catalogue consists of 224 active MAR sites presently found in 23 countries. Induced bank filtration was the most used MAR type in Europe followed by the spreading method and lastly well injection method. In Africa, 46 MAR sites can be found in the global MAR inventory portal. The majority of MAR sites were found in South Africa, Kenya, Tunisia, Algeria and Egypt. In West Africa, only two MAR sites were found in Nigeria. In terms of MAR types, the spreading method was the commonest MAR type, followed by induced bank filtration and borehole recharge method. In addition, the predominant source of MAR water was river water and reclaimed wastewater. There was no recognized MAR site in Ghana in the global MAR portal. However, emerging MAR schemes such as PAVE irrigation technology and Bhungroo technology can be found in Northern Ghana. The few MAR sites in West Africa could be attributed to a lack of resources and experts to implement the MAR schemes. This is because the majority of the MAR schemes are found in the African richest countries. Furthermore, there has been little insight into groundwater modelling studies to evaluate the feasibility of MAR in Africa. Water quality issues about MAR have broadly not been discussed in Africa. These knowledge gaps formed the springboard of this PhD work and were addressed in the various chapters.

The study employed fieldwork, groundwater and tracer gas sampling, secondary data collection and comprehensive laboratory work (Chapter 3). The laboratory equipment used for this research includes Ion chromatography 882 Compact (IC), Atomic Absorption Spectrometry (AAS), Picarro L2130-I Cavity Ringdown Spectrometry and the Gas Chromatography (GC Shimadzu 2014).

In Chapter 4, multivariate statistical tools and conventional graphical methods were used to elucidate the natural baseline chemistry of the groundwater and the factors controlling groundwater chemistry in the area. The shallow groundwater was mainly taken from the Tamnean Plutonic Suite aquifers. The pH of the groundwater was moderately acidic and alkaline (pH < 7.93). The water was mostly anoxic and generally fresh with TDS less than 1000 mg/L. The cations composition were mixed characters of $Ca^{2+} > Na^{+} > Mg^{2+} > K^{+}$ with their average concentrations of 20.32 mg/L, 17.7 mg/L, 9.8 mg/L, 1.7 mg/L, respectively. It was concluded that calcium and magnesium originated from silicate mineral weathering and dissolution. The decreasing trends of the anions were $HCO_3^{-} > NO_3^{-} > Cl^{-} > S0_4^{2-} > F^{-}$ with resulting mean values of 188.61 mg/L, 21.8 mg/L, 6.23 mg/L and 0.59 mg/L, respectively. The HCO_3^{-} was attributed to carbon dioxide in the atmosphere and in soil gases that dissolve in rain and surface water. Some of the communities had nitrate levels in groundwaters exceeding the WHO acceptable drinking water and this could be attributed to the application of chemical or organic fertilizers in the area. The multivariate statistics revealed that the groundwater is influenced by silicate mineral weathering and the cation exchange process.

The water quality index (WQI) and the Wilcox plot showed that the groundwater is suitable for drinking and irrigation purposes.

In Chapter 5, multi-tracers (SF6, CFC-11, CFC-12, $\delta^{18}O$ and δD) were used to investigate the residence times and recharge patterns of the study area. It was revealed that the residence time of the groundwater was less than 50 years indicating young groundwater. The SF6 ages obtained were much younger than CFCs, an indication of terrigenous source enrichment. The young groundwater ages obtained were in line with the results obtained from the stable isotopes, in which modern precipitation recharged the groundwater. The main source of groundwater recharge can be concluded to originate from precipitation with little contribution from the White Volta River. A conceptual model describing groundwater flow indicated piston flow model, exponential model and local flow (surface water and groundwater interaction).

Chapter 6 examined the applicability of using a 3D numerical groundwater flow model to evaluate the feasibility of MAR in the Tamne River basin. In the first place, a steady-state and transient groundwater flow model was developed to understand the hydrogeological conditions of the area. MAR injection and abstraction scenario was applied further to test the resilience of the aquifer. The results showed the total volume of water injected at the end of the 4 months study period is 11000 m^3/day, which significantly increased aquifer storage and groundwater levels. The abstraction scenario suggested that the volume of abstracted water at the end of the 8 months after MAR injection is 5968. 09 m^3/day. This volume of water recovered, including the water without MAR practice, is enough for domestic and irrigation purposes during the dry season. In general, MAR is feasible in augmenting the water levels in the area when combined with controllable irrigation and domestic withdrawals.

7.2 Recommendations and future research needs

This PhD work is a first step toward enhancing the hydrogeological characterization of the Garu-Tempane areas. The numerical groundwater model was developed to understand the hydrogeological conditions of the area and also to evaluate the feasibility of managed aquifer recharge in the catchment. The models and MAR feasibility will help water managers, decision-makers and other water stakeholders in exploring other prospects for aquifer management. Due to limited data, this model is only fit for the available data used. This creates a lot of uncertainties and possibly significant errors. Therefore, several recommendations are needed to improve the model for future works.

Groundwater models are sometimes non-unique and do not always represent the actual site-specific conditions. Some of the factors that can result in model uncertainties include the right choice of code, errors in water levels measurement and sampling, and wrong geological

and hydrogeological data interpretations. In addition, there are uncertainties associated with the model forecasting for future stresses that are known and unknown such as future abstraction and recharge rates. Therefore, a holistic uncertainty analysis and post audits should be addressed in the future. In addition, in the study area, three hydrostratigraphy layers have been delineated. However, due to data paucity, the model was developed as a single aquifer layer. It is recommended that future work should include groundwater modelling in all three layers. Geophysical investigations such as GPR, electromagnetics and other methods should be used to delineate the vertical distribution of aquifer layers. More long-term groundwater levels should be measured for transient simulation since there is only a well with historic water levels between 2009- 2012. Obtaining this information will enable adequate determination of current groundwater storage and yield and also the proper forecasting of any future work.

For the MAR feasibility studies, several limitations are clearly stated in the thesis. Therefore, future work in the Garu-Tempane area should focus on the suitable areas where MAR can be piloted. With this, emphasis should be on site-specific GIS mapping to select feasible sites in the catchment. Also, field investigations including runoff measurements, analysis of long term rainfall and temperature, and estimation of potential evaporation and infiltration rate should be conducted to quantify the water balance and budget of the area. Furthermore, cost-benefit analysis involving the cost of acquiring the land, cost of source water, cost of hydrogeological investigations and the overall economic evaluation with stakeholders using social-environmental benefit indicators and profitability indicators such as Net Present Value (NPV) and Internal Rate of Return (IRR) should be addressed in future work to improve the MAR studies in Ghana. Lastly, qualitative and quantitative assessments using mixed interviews and observations should be done to enable comprehensive investigations of the importance of water availability in the dry season on the livelihoods and also the environmental feasibility of MAR.

Regarding the stable isotopes, SF6 and CFCs age dating and hydrochemical analysis, all these data were sampled just at the beginning of the dry season in November. It is recommended that another sampling campaign in the wet season should be taken to compare the seasonal trends of the hydrogeological parameters of the aquifer. Nitrate levels exceeded the WHO acceptable levels in some of the boreholes, it is therefore recommended to apply NO_3 isotopes to identify the main sources of elevated nitrate occurring in some of the wells.In general, the area under study has a great potential for groundwater resource development in terms of domestic and irrigation water supply. The MAR feasibility studies show that more water can be stored for dry season irrigation farming and this MAR study must be executed and managed accordingly.

Declaration of Authorship

Study 1

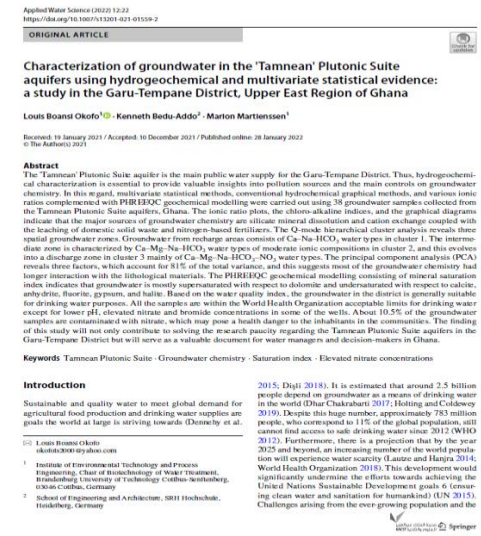

Applied Water Science (2022) 12:22
https://doi.org/10.1007/s13201-021-01559-2

ORIGINAL ARTICLE

Characterization of groundwater in the 'Tamnean' Plutonic Suite aquifers using hydrogeochemical and multivariate statistical evidence: a study in the Garu-Tempane District, Upper East Region of Ghana

Louis Boansi Okofo[1] · Kenneth Bedu-Addo[2] · Marion Martienssen[1]

Received: 19 January 2021 / Accepted: 10 December 2021 / Published online: 28 January 2022
© The Author(s) 2021

Abstract
The 'Tamnean' Plutonic Suite aquifer is the main public water supply for the Garu-Tempane District. Thus, hydrogeochemical characterization is essential to provide valuable insights into pollution sources and the main controls on groundwater chemistry. In this regard, multivariate statistical methods, conventional hydrochemical graphical methods, and various ionic ratios complemented with PHREEQC geochemical modelling were carried out using 38 groundwater samples collected from the Tamnean Plutonic Suite aquifers, Ghana. The ionic ratio plots, the chloro-alkaline indices, and the graphical diagrams indicate that the major sources of groundwater chemistry are silicate mineral dissolution and cation exchange coupled with the leaching of domestic solid waste and nitrogen-based fertilizers. The Q-mode hierarchical cluster analysis reveals three spatial groundwater zones. Groundwater from recharge areas consists of Ca–Na–HCO_3 water types in cluster 1. The intermediate zone is characterized by Ca–Mg_2–Na–HCO_3 water types of moderate ionic compositions in cluster 2, and this evolves into a discharge zone in cluster 3 mainly of Ca–Mg–Na–HCO_3–NO_3 water types. The principal component analysis (PCA) reveals three factors, which account for 81% of the total variance, and this suggests most of the groundwater chemistry had interaction with the lithological materials. The PHREEQC geochemical modelling consisting of mineral saturation index indicates that groundwater is mostly supersaturated with respect to dolomite and undersaturated with respect to calcite, anhydrite, fluorite, gypsum, and halite. Based on the water quality index, the groundwater in the district is generally suitable for drinking water purposes. All the samples are within the World Health Organization acceptable limits for drinking water except for lower pH, elevated nitrate and bromide concentrations in some of the wells. About 10.5% of the groundwater samples are contaminated with nitrate, which may pose a health danger to the inhabitants in the communities. The finding of this study will not only contribute to solving the research paucity regarding the Tamnean Plutonic Suite aquifers in the Garu-Tempane District but will serve as a valuable document for water managers and decision-makers in Ghana.

Keywords Tamnean Plutonic Suite · Groundwater chemistry · Saturation index · Elevated nitrate concentrations

Introduction

Sustainable and quality water to meet global demand for agricultural food production and drinking water supplies are goals the world at large is striving towards (Dennehy et al. 2015; Digli 2018). It is estimated that around 2.5 billion people depend on groundwater as a means of drinking water in the world (Dhar Chakrabarti 2017; Holting and Coldewey 2019). Despite this huge number, approximately 783 million people, who correspond to 11% of the global population, still cannot find access to safe drinking water since 2012 (WHO 2012). Furthermore, there is a projection that by the year 2025 and beyond, an increasing number of the world population will experience water scarcity (Lautze and Hanjra 2014; World Health Organization 2018). This development would significantly undermine the efforts towards achieving the United Nations Sustainable Development goals 6 (ensuring clean water and sanitation for humankind) (UN 2015). Challenges arising from the ever-growing population and the

Louis Boansi Okofo
okofols2000@yahoo.com

[1] Institute of Environmental Technology and Process Engineering, Chair of Biotechnology of Water Treatment, Brandenburg University of Technology Cottbus-Senftenberg, 03046 Cottbus, Germany

[2] School of Engineering and Architecture, SRH Hochschule, Heidelberg, Germany

Citation: Okofo, L.B., Bedu-Addo, K.& Martienssen,M(2022) Characterization of groundwater in the 'Tamnean' Plutonic Suite aquifers using hydrogeochemical and multivariate statistical evidence: a study in the Garu-Tempane District, Upper East Region of Ghana. *Appl Water Sci* **12,** 22 (2022). https://doi.org/10.1007/s13201-021-01559-2

Declaration of authorship: Okofo Louis wrote the manuscript, which was reviewed by all the authors.

Study 2

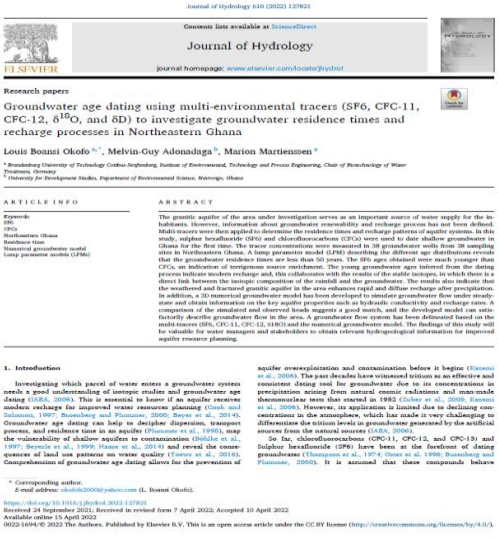

Journal of Hydrology 610 (2022) 127821

Contents lists available at ScienceDirect

Journal of Hydrology

journal homepage: www.elsevier.com/locate/jhydrol

Research papers

Groundwater age dating using multi-environmental tracers (SF6, CFC-11, CFC-12, $\delta^{18}O$, and δD) to investigate groundwater residence times and recharge processes in Northeastern Ghana

Louis Boansi Okofo [a,*], Melvin-Guy Adonadaga [b], Marion Martienssen [a]

[a] Brandenburg University of Technology Cottbus-Senftenberg, Institute of Environmental, Technology and Process Engineering, Chair of Biotechnology of Water Treatment, Germany
[b] University for Development Studies, Department of Environmental Science, Navrongo, Ghana

ARTICLE INFO

Keywords:
SF6
CFC
Northeastern Ghana
Residence time
Numerical groundwater model
Lump parameter models (LPMs)

ABSTRACT

The granitic aquifer of the area under investigation serves as an important source of water supply for the inhabitants. However, information about groundwater renewability and recharge process has not been defined. Multi-tracers were then applied to determine the residence times and recharge patterns of aquifer systems. In this study, sulphur hexafluoride (SF6) and chlorofluorocarbons (CFCs) were used to date shallow groundwater in Ghana for the first time. The tracer concentrations were measured in 38 groundwater wells from 38 sampling sites in Northeastern Ghana. A lump parameter model (LPM) describing the different age distributions reveals that the groundwater residence times are less than 50 years. The SF6 ages obtained were much younger than CFCs, an indication of terrigenous source enrichment. The young groundwater ages inferred from the dating process indicate modern recharge and, this collaborates with the results of the stable isotopes, in which there is a direct link between the isotopic composition of the rainfall and the groundwater. The results also indicate that the weathered and fractured granitic aquifer in the area enhances rapid and diffuse recharge after precipitation. In addition, a 3D numerical groundwater model has been developed to simulate groundwater flow under steady-state and obtain information on the key aquifer properties such as hydraulic conductivity and recharge rates. A comparison of the simulated and observed heads suggests a good match, and the developed model can satisfactorily describe groundwater flow in the area. A groundwater flow system has been delineated based on the multi-tracers (SF6, CFC-11, CFC-12, $\delta^{18}O$) and the numerical groundwater model. The findings of this study will be valuable for water managers and stakeholders to obtain relevant hydrogeological information for improved aquifer resource planning.

1. Introduction

Investigating which parcel of water enters a groundwater system needs a good understanding of isotopic studies and groundwater age dating (IAEA, 2006). This is essential to know if an aquifer receives modern recharge for improved water resources planning (Cook and Solomon, 1997; Busenberg and Plummer, 2000; Beyer et al., 2014). Groundwater age dating can help to decipher dispersion, transport process, and residence time in an aquifer (Plummer et al., 1998), map the vulnerability of shallow aquifers to contamination (Böhlke et al., 1997; Beyerle et al., 1999; Haase et al., 2014) and reveal the consequences of land use patterns on water quality (Travi et al., 2018). Comprehension of groundwater age dating allows for the prevention of aquifer overexploitation and contamination before it begins (Kazemi et al., 2006). The past decades have witnessed tritium as an effective and consistent dating tool for groundwater due to its concentrations in precipitation arising from natural cosmic radiations and man-made thermonuclear tests that started in 1952 (Zuber et al., 2005; Kazemi et al., 2006). However, its application is limited due to declining concentrations in the atmosphere, which has made it very challenging to differentiate the tritium levels in groundwater possessed by the artificial sources from the natural sources (IAEA, 2006).

So far, chlorofluorocarbons (CFC-11, CFC-12, and CFC-13) and Sulphur hexafluoride (SF6) have been at the forefront of dating groundwater (Thompson et al., 1974; Oster et al. 1996; Busenberg and Plummer, 2000). It is assumed that these compounds behave

* Corresponding author.
E-mail address: okofols2000@yahoo.com (L. Boansi Okofo).

https://doi.org/10.1016/j.jhydrol.2022.127821
Received 24 September 2021; Received in revised form 7 April 2022; Accepted 10 April 2022
Available online 15 April 2022
0022-1694/© 2022 The Authors. Published by Elsevier B.V. This is an open access article under the CC BY license (http://creativecommons.org/licenses/by/4.0/).

Citation: Okofo, L.B., Adonadaga Melvin-Guy, Marion Martienssen. Groundwater age dating using multi-environmental tracers (SF6, CFC-11, CFC-12, $\delta^{18}O$, and δD) to investigate groundwater residence times and recharge processes in Northeastern Ghana: Journal of Hydrology Vol 60 (2022) https://doi.org/10.1016/j.jhydrol.2022.127821

Declaration of authorship: Okofo Louis prepared and evaluated the data and wrote the manuscript, which was reviewed by all the authors,

Study 3

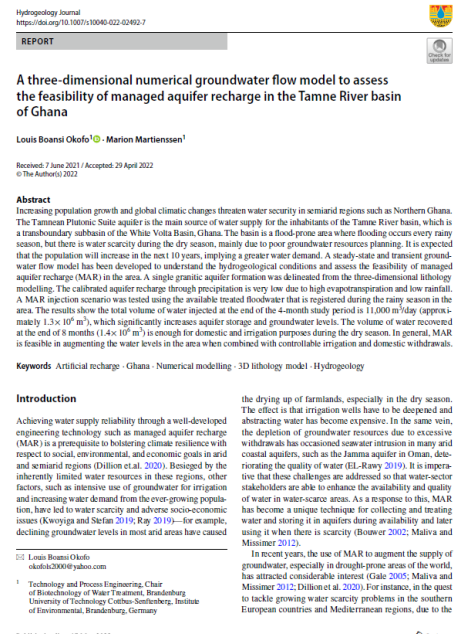

Hydrogeology Journal
https://doi.org/10.1007/s10040-022-02492-7

REPORT

A three-dimensional numerical groundwater flow model to assess the feasibility of managed aquifer recharge in the Tamne River basin of Ghana

Louis Boansi Okofo[1] · Marion Martienssen[1]

Received: 7 June 2021 / Accepted: 29 April 2022
© The Author(s) 2022

Abstract
Increasing population growth and global climatic changes threaten water security in semiarid regions such as Northern Ghana. The Tamnean Plutonic Suite aquifer is the main source of water supply for the inhabitants of the Tamne River basin, which is a transboundary subbasin of the White Volta Basin, Ghana. The basin is a flood-prone area where flooding occurs every rainy season, but there is water scarcity during the dry season, mainly due to poor groundwater resources planning. It is expected that the population will increase in the next 10 years, implying a greater water demand. A steady-state and transient groundwater flow model has been developed to understand the hydrogeological conditions and assess the feasibility of managed aquifer recharge (MAR) in the area. A single granitic aquifer formation was delineated from the three-dimensional lithology modelling. The calibrated aquifer recharge through precipitation is very low due to high evapotranspiration and low rainfall. A MAR injection scenario was tested using the available treated floodwater that is registered during the rainy season in the area. The results show the total volume of water injected at the end of the 4-month study period is 11,000 m^3/day (approximately 1.3×10^6 m^3), which significantly increases aquifer storage and groundwater levels. The volume of water recovered at the end of 8 months (1.4×10^6 m^3) is enough for domestic and irrigation purposes during the dry season. In general, MAR is feasible in augmenting the water levels in the area when combined with controllable irrigation and domestic withdrawals.

Keywords Artificial recharge · Ghana · Numerical modelling · 3D lithology model · Hydrogeology

Introduction

Achieving water supply reliability through a well-developed engineering technology such as managed aquifer recharge (MAR) is a prerequisite to bolstering climate resilience with respect to social, environmental, and economic goals in arid and semiarid regions (Dillion et al. 2020). Besieged by the inherently limited water resources in these regions, other factors, such as intensive use of groundwater for irrigation and increasing water demand from the ever-growing population, have led to water scarcity and adverse socio-economic issues (Kwoyiga and Stefan 2019; Raj 2019)—for example, declining groundwater levels in most arid areas have caused the drying up of farmlands, especially in the dry season. The effect is that irrigation wells have to be deepened and abstracting water has become expensive. In the same vein, the depletion of groundwater resources due to excessive withdrawals has occasioned seawater intrusion in many arid coastal aquifers, such as the Jammа aquifer in Oman, deteriorating the quality of water (EL-Rawy 2019). It is imperative that these challenges are addressed so that water-sector stakeholders are able to enhance the availability and quality of water in water-scarce areas. As a response to this, MAR has become a unique technique for collecting and treating water and storing it in aquifers during availability and later using it when there is scarcity (Bouwer 2002; Maliva and Missimer 2012).

In recent years, the use of MAR to augment the supply of groundwater, especially in drought-prone areas of the world, has attracted considerable interest (Gale 2005; Maliva and Missimer 2012; Dillion et al. 2020). For instance, in the quest to tackle growing water scarcity problems in the southern European countries and Mediterranean regions, due to the

Louis Boansi Okofo
okofols2000@yahoo.com

[1] Technology and Process Engineering, Chair of Biotechnology of Water Treatment, Brandenburg University of Technology Cottbus-Senftenberg, Institute of Environmental, Brandenburg, Germany

Citation: Okofo, L.B., Martienssen Marion. A three-dimensional numerical groundwater flow modelling to assess the feasibility of managed aquifer recharge (MAR) in the Tamne River Basin of Ghana. Journal of Hydrogeology (2022). https://doi.org/10.1007/s10040-022-02492-7

Declaration of authorship: Okofo Louis developed the numerical model and the review was done by all the authors

References

Abdul-Wahab, D., Adomako, D., Abass, G., Adotey, D. K., Anornu, G., & Ganyaglo, S. (2021). Hydrogeochemical and isotopic assessment for characterizing groundwater quality and recharge processes in the Lower Anayari catchment of the Upper East Region, Ghana. *Environment, Development and Sustainability*, *23*(4), 5297–5315. https://doi.org/10.1007/s10668-020-00815-w

Acheampong, A. (2017). *Borehole yield estimation from electrical resistivity measurement – A case study of Garu Tempane and Bawku West Districts, Upper East Region, Ghana By (BSc . Geological Engineering) A thesis submitted to the Department of Geological Engineering, Kwa*. *May*, 71.

Acheampong, S. Y., & Hess, J. W. (2000). Origin of the shallow groundwater system in the southern Voltaian Sedimentary Basin of Ghana: An isotopic approach. *Journal of Hydrology*. https://doi.org/10.1016/S0022-1694(00)00221-3

Acheampong, Stephen Y., & Hess, J. W. (1998). Hydrogeologic and hydrochemical framework of the shallow groundwater system in the southern Voltaian Sedimentary Basin, Ghana. *Hydrogeology Journal*. https://doi.org/10.1007/s100400050173

Addai, M. O., Yidana, S. M., Chegbeleh, L. P., Adomako, D., & Banoeng-Yakubo, B. (2016). Groundwater recharge processes in the Nasia sub-catchment of the White Volta Basin: Analysis of porewater characteristics in the unsaturated zone. *Journal of African Earth Sciences*. https://doi.org/10.1016/j.jafrearsci.2015.04.006

Aerts, J., Lasage, R., Beets, W., de Moel, H., Mutiso, G., Mutiso, S., & de Vries, A. (2007). Robustness of Sand Storage Dams under Climate Change. *Vadose Zone Journal*. https://doi.org/10.2136/vzj2006.0097

Aeschbach-Hertig, W., Peeters, F., Beyerle, U., & Kipfer, R. (1999). Interpretation of dissolved atmospheric noble gases in natural waters. *Water Resources Research*. https://doi.org/10.1029/1999WR900130

Afrifa, G. Y., Sakyi, P. A., & Chegbeleh, L. P. (2017). Estimation of groundwater recharge in sedimentary rock aquifer systems in the Oti basin of Gushiegu District, Northern Ghana. *Journal of African Earth Sciences*. https://doi.org/10.1016/j.jafrearsci.2017.02.035

Agarwal, A & Narain, S. (1997). Dying wisdom. Rise, fall and potential of India's traditional water harvesting systems. *New Delhi: India Centre for Science and Environment.*

Aggarwal, P. K., Froehlich, K. F., & Gat, J. R. et al. (2005). *Isotopes in the water cycle*.

International Atomic Energy Agency (IAEA).

Ahn, M. K., Chilakala, R., Han, C., & Thenepalli, T. (2018). Removal of hardness from water samples by a carbonation process with a closed pressure reactor. *Water (Switzerland)*. https://doi.org/10.3390/w10010054

Akurugu, B. A., Chegbeleh, L. P., & Yidana, S. M. (2020). Characterisation of groundwater flow and recharge in crystalline basement rocks in the Talensi District, Northern Ghana. *Journal of African Earth Sciences*, *161*, 103665. https://doi.org/10.1016/j.jafrearsci.2019.103665

Al-Turbak, A. S., & Al-Muttair, F. F. (1989). Evaluation of dams as a recharge method. *International Journal of Water Resources Development*. https://doi.org/10.1080/07900628908722423

Alfredo, K. A., Lawler, D. F., & Katz, L. E. (2014). Fluoride contamination in the Bongo District of Ghana, West Africa: Geogenic contamination and cultural complexities. *Water International*. https://doi.org/10.1080/02508060.2014.926234

Anderson et al., M. P., Woessner, W. W., & Hunt, R. J (2015). *Applied groundwater modelling simulation of flow and advective transport*. CRC press.

Anim-Gyampo, M., Anornu, G. K., Appiah-Adjei, E. K., & Agodzo, S. K. (2018). Hydrogeochemical evolution and quality assessment of groundwater within the Atankwidi basin: the case of northeastern Ghana. *Arabian Journal of Geosciences*. https://doi.org/10.1007/s12517-018-3753-6

Anornu, G., Gibrilla, A., & Adomako, D. (2017). Tracking nitrate sources in groundwater and associated health risk for rural communities in the White Volta River basin of Ghana using an isotopic approach (δ15N, δ18O[sbnd]NO3 and 3H). *Science of the Total Environment*. https://doi.org/10.1016/j.scitotenv.2017.01.219

Apambire, W. B., Boyle, D. R., & Michel, F. A. (1997). Geochemistry, genesis, and health implications of fluoriferous groundwaters in the upper regions of Ghana. *Environmental Geology*. https://doi.org/10.1007/s002540050221

Appelo, C. A. ., & Postma, D. (2005). Groundwater, geochemistry and pollution. In *Taylor & Francis Group plc*.

Aquaveo. (2020). *Groundwater Modelling System, Version 10.4. Provo, Utah, USA.*

Armah, F. A., Yawson, D. O., Yengoh, G. T., Odoi, J. O., & Afrifa, E. K. A. (2010). Impact of Floods on Livelihoods and Vulnerability of Natural Resource Dependent Communities in Northern Ghana. *Water*, *2*(2), 120–139. https://doi.org/10.3390/w2020120

Asamoah, Y., & Ansah-Mensah, K. (2020). Temporal Description of Annual Temperature and Rainfall in the Bawku area of Ghana. *Advances in Meteorology*. https://doi.org/10.1155/2020/3402178

Asano, T. (2016). *Artificial recharge of groundwater.* Butterworth Publishers. Stoneham, USA.

Ashraf, B., Aghakouchak, A., Alizadeh, A., Mousavi Baygi, M., Moftakhari, H. R., Mirchi, A., Anjileli, H., & Madani, K. (2017). Quantifying Anthropogenic Stress on Groundwater Resources. *Scientific Reports*. https://doi.org/10.1038/s41598-017-12877-4

Bam, E. K. P., & Bansah, S. (2020). Groundwater chemistry and isotopes reveal the vulnerability of granitic aquifer in the White Volta River watershed, West Africa. *Applied Geochemistry*. https://doi.org/10.1016/j.apgeochem.2020.104662

Banoeng-Yakubu B., Yidanna., S, Ajayi., JO. Yvonne., Y and Asiedu D (2011). *Hydrogeology and groundwater resources of Ghana: A review of the hydrogeology and hydrochemistry of Ghana. J.M. McMan*.

Barcelona, M. J., Gibb, J. P., Helfrich, john A., & Garske, E. E. (1985). *A practical guide for ground-water sampling*.

Bates, D. (1955). *Geological map of Ghana: Ghana Geological Survey Department, scale 1:1,000,000.*

Bekele, E., Toze, S., Patterson, B., & Higginson, S. (2011). Managed aquifer recharge of treated wastewater: Water quality changes resulting from infiltration through the vadose zone. *Water Research*. https://doi.org/10.1016/j.watres.2011.08.058

Beyer, M., Van Der Raaij, R., Morgenstern, U., & Jackson, B. (2014). Potential groundwater age tracer found: Halon-1301 (CF3Br), as previously identified as CFC-13 (CF3Cl). *Water Resources Research*. https://doi.org/10.1002/2014WR015818

Beyerle, U., Aeschbach-Hertig, W., Hofer, M., Imboden, D. M., Baur, H., & Kipfer, R. (1999). Infiltration of river water to a shallow aquifer investigated with 3H/3He, noble gases and CFCs. *Journal of Hydrology*. https://doi.org/10.1016/S0022-1694(99)00069-4

Bhattacharya, P., Sracek, O., Eldvall, B., Asklund, R., Barmen, G., Jacks, G., Koku, J., Gustafsson, J. E., Singh, N., & Balfors, B. B. (2012). Hydrogeochemical study on the contamination of water resources in a part of Tarkwa mining area, Western Ghana. *Journal of African Earth Sciences*. https://doi.org/10.1016/j.jafrearsci.2012.03.005

BMI. (1985). *Künstliche Grundwasseranreicherung: Stand der Technik und des Wissens in der Bundesrepublik Deutschland.*

Böhlke, J.K., Ericksen, G. E., & Revesz, K. (1997). Stable isotope evidence for an atmospheric origin of desert nitrate deposits in northern Chile and southern California, U.S.A. *Chemical Geology*, *136*(1–2), 135–152. https://doi.org/10.1016/S0009-2541(96)00124-6

Böhlke, John Karl. (2002). Groundwater recharge and agricultural contamination. *Hydrogeology Journal*. https://doi.org/10.1007/s10040-001-0183-3

Bouwer, H. (1991). Groundwater recharge with sewage effluent. *Water Science and Technology, 23, 2099–2108.*

Bouwer, Herman. (2002). Artificial recharge of groundwater: Hydrogeology and engineering. *Hydrogeology Journal*. https://doi.org/10.1007/s10040-001-0182-4

Bu, X., & Warner, M. J. (1995). Solubility of chlorofluorocarbon 113 in water and seawater. *Deep-Sea Research Part I: Oceanographic Research Papers*, *42*(7), 1151–1161. https://doi.org/10.1016/0967-0637(95)00052-8

Bullister, J. L., Wisegarver, D. P., & Menzia, F. A. (2002). The solubility of sulfur hexafluoride in water and seawater. *Deep-Sea Research Part I: Oceanographic Research Papers*, *49*(1), 175–187. https://doi.org/10.1016/S0967-0637(01)00051-6

Busenberg, E., & Plummer, L. N. (2000). Dating young groundwater with sulfur hexafluoride: Natural and anthropogenic sources of sulfur hexafluoride. *Water Resources Research*. https://doi.org/10.1029/2000WR900151

Busenberg, P. & E. (2000). *Environmental Tracers in Subsurface Hydrology*. P.G Cook, A.L Herczed Eds) Springer, Boston, MA.

Candela, L., & Morell, I. (2009). *Basic chemical principles of groundwater. Encyclopedia of Life Support Systems, 2, 43-55.*

Candela, L. and Morell, I. (1998). *Basic chemical principles of groundwater. UNESCO-EOLSS Sample chapters. Groundwater- Vol II.*

Carey, B. M. (2001). *Groundwater / Surface Water Interactions In the Sammamish River : a Preliminary Analysis*. *03*, 1–18. http://www.ecy.wa.gov/biblio/0303015.html

Carrier, M. A., Lefebvre, R., Racicot, J., & Asare, E. B. (2008). Northern Ghana hydrogeological assessment project. *Access to Sanitation and Safe Water: Global Partnerships and Local Actions - Proceedings of the 33rd WEDC International Conference*.

Chegbeleh, L. P., Akurugu, B. A., & Yidana, S. M. (2020). Assessment of Groundwater

Quality in the Talensi District, Northern Ghana. *Scientific World Journal*. https://doi.org/10.1155/2020/8450860

Clark, I. D., & Fritz, P. (1997). *Environmental isotopes in hydrogeology*. CRC press.

Clark, I. (2015). Groundwater geochemistry and isotopes. In *Groundwater Geochemistry and Isotopes*. https://doi.org/10.1201/b18347

Cloutier, V., Lefebvre, R., Therrien, R., & Savard, M. M. (2008). Multivariate statistical analysis of geochemical data as indicative of the hydrogeochemical evolution of groundwater in a sedimentary rock aquifer system. *Journal of Hydrology*, *353*(3–4), 294–313. https://doi.org/10.1016/j.jhydrol.2008.02.015

Cobbinah, P. B., Okyere, D. K., & Gaisie, E. (2016). *Population Growth and Water Supply*. https://doi.org/10.4018/978-1-5225-0187-9.ch012

Conservative Alliance. (2015). *Overview of Bhungroo. Conservation Alliance, Accra.* http://conservealliance.org/overview-of-bhungroo/. Accessed 10 Apr 2016

Cook, P. G., & Herczeg, A. L. (2012). *Environmental tracers in subsurface hydrology.* Springer Science+Business Media, LLC.

Cook, P., Dogramaci, S., McCallum, J., & Hedley, J. (2017). Groundwater age, mixing and flow rates in the vicinity of large open-pit mines, Pilbara region, northwestern Australia. *Hydrogeology Journal*. https://doi.org/10.1007/s10040-016-1467-y

Cook, P. G., & Solomon, D. K. (1997). Recent advances in dating young groundwater: chlorofluorocarbons, and 85Kr. *Journal of Hydrology*, *191*(1–4), 245–265. https://doi.org/10.1016/S0022-1694(96)03051-X

Cook, P. G., Solomon, D. K., Plummer, L. N., Busenberg, E., & Schiff, S. L. (1995). Chlorofluorocarbons as Tracers of Groundwater Transport Processes in a Shallow, Silty Sand Aquifer. *Water Resources Research*. https://doi.org/10.1029/94WR02528

Coralie, R., François, C., Daniel, V., Thierry, L., Yann, L., Jérôme, V. der W., Julien, A., & Luc, A. (2021). Characterization of groundwater circulations in a headwater catchment from an analysis of chemical concentrations, Sr-Nd-U isotope ratios, and CFC, SF6 gas tracers (Strengbach CZO, France). *Applied Geochemistry*. https://doi.org/10.1016/j.apgeochem.2021.105030

Craig, H. (1961). Isotopic variations in meteoric waters. *Science*. https://doi.org/10.1126/science.133.3465.1702

CWSA. (2021). *Community Water and Sanitation Agency*.

Dapaah-Siakwan, S., & Gyau-Boakye, P. (2000). Hydrogeologic framework and borehole yields in Ghana. *Hydrogeology Journal*. https://doi.org/10.1007/PL00010976

Darling, W. G., Bath, A. H., & Talbot, J. C. (2003). The O and H stable isotope composition of freshwaters in the British Isles. 2. Surface waters and groundwater. *Hydrology and Earth System Sciences*. https://doi.org/10.5194/hess-7-183-2003

Deipser, A., & Stegmann, R. (1997). Biological degradation of VCCs and CFCs under simulated anaerobic landfill conditions in laboratory test digesters. *Environmental Science and Pollution Research*. https://doi.org/10.1007/BF02986348

Dennehy, K. F., Reilly, T. E., & Cunningham, W. L. (2015a). Groundwater availability in the United States: The value of quantitative regional assessments. *Hydrogeology Journal*. https://doi.org/10.1007/s10040-015-1307-5

Dennehy, K. F., Reilly, T. E., & Cunningham, W. L. (2015b). Groundwater availability in the United States: The value of quantitative regional assessments. *Hydrogeology Journal*. https://doi.org/10.1007/s10040-015-1307-5

Dhar, Chakrabarti. (2017). *People, planet and progress beyond (2015). The Energy and Resources Institute (TERI), New Delhi, p 462*

Dillon P, Vanderzalm J, Sidhu J, Page D, and C. D. (2014). *A water quality guide to managed aquifer recharge in India.*

Dillon, P., Stuyfzand, P., Grischek, T., Lluria, M., Pyne, R. D. G., Jain, R. C., Bear, J., Schwarz, J., Wang, W., Fernandez, E., Stefan, C., Pettenati, M., van der Gun, J., Sprenger, C., Massmann, G., Scanlon, B. R., Xanke, J., Jokela, P., Zheng, Y., … Sapiano, M. (2019). Sixty years of global progress in managed aquifer recharge. *Hydrogeology Journal*. https://doi.org/10.1007/s10040-018-1841-z

Dillon, Peter. (2005). Future management of aquifer recharge. *Hydrogeology Journal*. https://doi.org/10.1007/s10040-004-0413-6

Dillon, Peter, Fernández Escalante, E., Megdal, S. B., & Massmann, G. (2020). Managed Aquifer Recharge for Water Resilience. *Water*, *12*(7), 1846. https://doi.org/10.3390/w12071846

Dillon, Peter, Gale, I., Contreras, S., Pavelic, P., Evans, R., & Ward, J. (2009). Managing aquifer recharge and discharge to sustain irrigation livelihoods under water scarcity and climate change. *IAHS-AISH Publication*.

Dişli, E. (2018). Evaluation of Hydrogeochemical Processes for Waters' Chemical Composition and Stable Isotope Investigation of Groundwater/Surface Water in Karst-

Dominated Terrain, the Upper Tigris River Basin, Turkey. *Aquatic Geochemistry*, *24*(5–6), 363–396. https://doi.org/10.1007/s10498-019-09349-8

Dişli, Erkan, & Gülyüz, N. (2020). Hydrogeochemical investigation of an epithermal mineralization bearing basin using multivariate statistical techniques and isotopic evidence of groundwater: Kestanelik Sub-Basin, Lapseki, Turkey. *Geochemistry*, *80*(4), 125661. https://doi.org/10.1016/j.chemer.2020.125661

Doherty JE, and Hunt, R. (2010). *Approaches to highly parameterized inversion: a guide to using PEST for groundwater-model calibration (Vol. 2010).*

Ebrahim, Girma Y, Lautze, J. F., & Villholth, K. G. (2020). Managed Aquifer Recharge in Africa: Taking Stock and Looking Forward. *Water*, *12*(7), 1844. https://doi.org/10.3390/w12071844

Ebrahim, Girma Yimer, Jonoski, A., Al-Maktoumi, A., Ahmed, M., & Mynett, A. (2016). Simulation-Optimization Approach for Evaluating the Feasibility of Managed Aquifer Recharge in the Samail Lower Catchment, Oman. *Journal of Water Resources Planning and Management*. https://doi.org/10.1061/(ASCE)wr.1943-5452.0000588

El-Rawy, M., Al-Maktoumi, A., Zekri, S., Abdalla, O., & Al-Abri, R. (2019). Hydrological and economic feasibility of mitigating a stressed coastal aquifer using managed aquifer recharge: a case study of Jamma aquifer, Oman. *Journal of Arid Land*, *11*(1), 148–159. https://doi.org/10.1007/s40333-019-0093-7

Ely DM, Bachmann MP, and V. J. (2011). *Numerical simulation of groundwater flow for the Yakima River basin aquifer system, Washington.*

Fetter, C. (2001). *Applied Hydrogeology, fourth ed.* Pearson Education Limited, Prentice-Hall, Upper Saddle River, N.J., 612 p.

Fetter, W. (2004). *Applied Hydrogeology*. Volume 1. Edition 3. Macmillan Press. ISBN 0023364904, 9780023364907.

Feybesse, J. L., Billa, M., Guerrot, C., Duguey, E., Lescuyer, J. L., Milesi, J. P., & Bouchot, V. (2006). The Paleoproterozoic Ghanaian province: Geodynamic model and ore controls, including regional stress modelling. *Precambrian Research*. https://doi.org/10.1016/j.precamres.2006.06.003

Fisher, R. S., & Mullican, W. F. (1997). Hydrochemical evolution of sodium-sulfate and sodium-chloride groundwater beneath the Northern Chihuahuan Desert, Trans-Pecos, Texas, USA. *Hydrogeology Journal*. https://doi.org/10.1007/s100400050102

Fitts, C. (2002). *Groundwater science.* Academic Press, New York.

Fox, P., Houston, S., & Westerhoff, P. (2001). *Soil aquifer treatment for sustainable water supply (203 pp).*

Freeze RA, & C. J. (1979). Groundwater. Prentice-hall, Englewood Cliffs, NJ, 604p. *Groundwater*.

Friedrich, R., Vero, G., von Rohden, C., Lessmann, B., Kipfer, R., & Aeschbach-Hertig, W. (2013). Factors controlling terrigenic SF6 in young groundwater of the Odenwald region (Germany). *Applied Geochemistry*. https://doi.org/10.1016/j.apgeochem.2013.03.002

Gale, I. (2005a). *Strategies for Managed Aquifer Recharge (MAR) in semi-arid areas. International Association of Hydrogeologists Commission on Management of Aquifer Recharge IAH-MAR, International Hydrological Programme (IHP)*.

Gale, I. (2005b). Strategies for Managed Aquifer Recharge (MAR) in semi-arid areas. In *UNESCO-IHP*.

Gampson, E. K., Nartey, V. K., Golow, A. A., Akiti, T. T., Sarfo, M. A., Salifu, M., Aidoo, F., & Fuseini, A. R. (2017). Physical and isotopic characteristics in peri-urban landscapes: a case study at the lower Volta River Basin, Ghana. *Applied Water Science*. https://doi.org/10.1007/s13201-015-0286-y

Gat, J. R. (2010). *Isotope hydrology: a study of the water cycle*. World scientific.

Gathuru, N. (1990). *Estimation of recharge from the exponential decline of base flow in the Upper East catchment of River Ewaso Ngiro' in Nairobi University Geological Magazine 1990'.*

Gerges, N. Z., Dillon, P. J., Sibenaler, X. P., Martin, R. R., Pavelic, P., Howies, S. R., & Dennis, K. (2020). The South Australian experience in aquifer storage and recovery. In *Management of Aquifer Recharge for Sustainability*. https://doi.org/10.1201/9781003078838-93

Ghana statistical service. (2010). Garu tempane district. *Garu Tempane District,*.

Ghana Statistical Service. (2013). 2010 POPULATION & HOUSING CENSUS. *2010 Population & Housing Census - National Analytical Report*.

Gibbs, R. J. (1970). Mechanisms controlling world water chemistry. *Science*. https://doi.org/10.1126/science.170.3962.1088

Gil-Márquez, J. M., Sültenfuß, J., Andreo, B., & Mudarra, M. (2020). Groundwater dating tools (3H, 3He, 4He, CFC-12, SF6) coupled with hydrochemistry to evaluate the hydrogeological functioning of complex evaporite-karst settings. *Journal of Hydrology*.

https://doi.org/10.1016/j.jhydrol.2019.124263

Gooddy, D. C., Darling, W. G., Abesser, C., & Lapworth, D. J. (2006). Using chlorofluorocarbons (CFCs) and sulphur hexafluoride (SF6) to characterise groundwater movement and residence time in a lowland Chalk catchment. *Journal of Hydrology*. https://doi.org/10.1016/j.jhydrol.2006.04.011

Güler, C., Thyne, G. D., McCray, J. E., & Turner, A. K. (2002). Evaluation of graphical and multivariate statistical methods for classification of water chemistry data. *Hydrogeology Journal*. https://doi.org/10.1007/s10040-002-0196-6

Gumma, M. K., & Pavelic, P. (2013). Mapping of groundwater potential zones across Ghana using remote sensing, geographic information systems, and spatial modelling. *Environmental Monitoring and Assessment*. https://doi.org/10.1007/s10661-012-2810-y

Haase, K. B., Busenberg, E., Plummer, L. N., Casile, G., & Sanford, W. E. (2014). Measurements of HFC-134a and HCFC-22 in groundwater and unsaturated-zone air: Implications for HFCs and HCFCs as dating tracers. *Chemical Geology*. https://doi.org/10.1016/j.chemgeo.2014.07.016

Haimerl, G., Zunic, F., & Strobl, T. (2002). An infiltration test to evaluate the efficiency of groundwater recharge dams in arid countries. In V. P. Singh, M. Al-Rashed & M. M. Sherif (Eds.). *Surface Water Hydrology (Pp. 313–322). Lisse: Swets & Zeitlinger*.

Haitjema, H. M., & Mitchell-Bruker, S. (2005). Are Water Tables a Subdued Replica of the Topography? *Ground Water*, 050824075421008. https://doi.org/10.1111/j.1745-6584.2005.00090.x

Hannappel, S., Scheibler, F., Huber, A., & Sprenger, C. (2014). Characterization of European Managed Aquifer Recharge (MAR) Sites - Analysis. *DEMEAU*.

Harbaugh AW, Banta ER, Hill MC, M. M. (2000). (2000). *MODFLOW-2000, the U.S Geological Survey modular ground-water-mode l— User guide to modularization concepts and the Ground-Water Flow Process.*

Helmisaari, H. S., Derome, J., Hatva, T., Illmer, K., Kitunen, V., Lindroos, A. J., ... & Reijonen, R. (2006). Artificial recharge in Finland through the basin and sprinkling infiltration: soil processes, retention time and water quality. In Recharge systems for protecting and enhancing groundwater resources. *Proceedings of the 5th International Symposium on Management of Aquifer Recharge, ISMAR5, Berlin, Germany, 11-16 June 2005. FR.*

Hem, J. D. (1985). Study and interpretation of the chemical characteristics of natural water.

US Geological Survey Water-Supply Paper.

Höllriegl, V., & München, H. Z. (2011). Strontium in the Environment and Possible Human Health Effects. In *Encyclopedia of Environmental Health*. https://doi.org/10.1016/B978-0-444-52272-6.00638-3

Hölting, B., & Coldewey, W. G. (2019). *Hydrogeology*. Springer Berlin Heidelberg. https://doi.org/10.1007/978-3-662-56375-5

Holzbecher, Grützmacher G, Amy G, Wiese B, & S. S. (2008). The Bank Filtration Simulator-a MATLAB GUI. *In EnviroInfo (Pp. 359-365).*

Homonnay, Z. (2002). Use of bank filtration in Hungary. In Riverbank Filtration: Understanding. *Contaminant Biogeochemistry and Pathogen Removal (Pp. 221-228). Springer, Dordrecht.*

Horton, R. K. (1965). An Index Number System for Rating Water Quality. *Journal of Water Pollution Control Federation*.

Hounslow. (1995). *Water quality data: analysis and interpretation. CRC press.*

Huisman, L., & Olsthoorn, T. N. (. (1983). *Artificial groundwater recharge*. Pitman Publ. Inc. 320p.

Hwang, J. Y., Park, S., Kim, H.-K., Kim, M.-S., Jo, H.-J., Kim, J.-I., Lee, G.-M., Shin, I.-K., & Kim, T.-S. (2017). Hydrochemistry for the Assessment of Groundwater Quality in Korea. *Journal of Agricultural Chemistry and Environment*. https://doi.org/10.4236/jacen.2017.61001

IAEA. (2006). Use of Chlorofluorocarbons in Hydrology: A Guidebook. *Use of Chlorofluorocarbons in Hydrology: A Guidebook*.

IDEP Foundation. (2007). *Bali Water Protection Program - Penyelamatan Air Tanah Bali – Annex 2 - Aquifer Recharge Technical Overview – Page 19*.

IGRAC. (2007). *Artificial groundwater recharge of the world*.

IGRAC. (2020). *Global MAR Portal. accessed 21st May 2020*. https://www.un-igrac.org/ggis/mar-portal

Islam, M. B., Firoz, A. B. M., Foglia, L., Marandi, A., Khan, A. R., Schüth, C., & Ribbe, L. (2017). A regional groundwater-flow model for sustainable groundwater-resource management in the south Asian megacity of Dhaka, Bangladesh. *Hydrogeology Journal*. https://doi.org/10.1007/s10040-016-1526-4

Issahaku, A.-R., Campion, B. B., & Edziyie, R. (2016). Rainfall and temperature changes and

variability in the Upper East Region of Ghana. *Earth and Space Science*, *3*(8), 284–294. https://doi.org/10.1002/2016EA000161

Jacob, C. and. (1944). *Notes on determining permeability by pumping test under water table conditions*.

Jasechko, S., Birks, S. J., Gleeson, T., Wada, Y., Fawcett, P. J., Sharp, Z. D., McDonnell, J. J., & Welker, J. M. (2014). The pronounced seasonality of global groundwater recharge. *Water Resources Research*. https://doi.org/10.1002/2014WR015809

Jiménez, B., & Asano, T. (2008). Water reclamation and reuse around the world. *Water Reuse: An International Survey of Current Practice, Issues and Needs, 14, 3-26*.

Jonah, A., & Dawda, T. D. (2014a). Improving the management and use of water resources for small-scale irrigation farming in the Garu Tempane District of Ghana. *Journal of Sustainable Development*. https://doi.org/10.5539/jsd.v7n6p214

Jonah, A., & Dawda, T. D. (2014b). Improving the Management and Use of Water Resources for Small-Scale Irrigation Farming in the Garu Tempane District of Ghana. *Journal of Sustainable Development*, *7*(6). https://doi.org/10.5539/jsd.v7n6p214

Jurgens, B. C., Böhlke, J. K., Eberts, S. M., & Survey, U. S. G. (2012). TracerLPM (Version 1): An Excel® workbook for interpreting groundwater age distributions from environmental tracer data. *Techniques and Methods*.

Kagabu, M., Matsunaga, M., Ide, K., Momoshima, N., & Shimada, J. (2017). Groundwater age determination using 85Kr and multiple age tracers (SF6, CFCs, and 3H) to elucidate regional groundwater flow systems. *Journal of Hydrology: Regional Studies*. https://doi.org/10.1016/j.ejrh.2017.05.003

Kaiser, H. F. (1960). *The application of electronic computers to factor analysis. Educational and Psychological Measurement, 20, 141–151. http://dx.doi.org/10.1177/001316446002000116*.

Kamtchueng, B. T., Fantong, W. Y., Wirmvem, M. J., Tiodjio, R. E., Fouépé Takounjou, A., Asai, K., Bopda Djomou, S. L., Kusakabe, M., Ohba, T., Tanyileke, G., Hell, J. V., & Ueda, A. (2015). A multi-tracer approach for assessing the origin, apparent age and recharge mechanism of shallow groundwater in the Lake Nyos catchment, Northwest, Cameroon. *Journal of Hydrology*. https://doi.org/10.1016/j.jhydrol.2015.02.008

Katko, T. S., Lipponen, M. A., & Rönkä, E. K. T. (2006). Groundwater use and policy in community water supply in Finland. *Hydrogeology Journal*. https://doi.org/10.1007/s10040-004-0351-3

Kawo, N. S., & Karuppannan, S. (2018). Groundwater quality assessment using water quality index and GIS technique in Modjo River Basin, central Ethiopia. *Journal of African Earth Sciences*. https://doi.org/10.1016/j.jafrearsci.2018.06.034

Kazemi G. A., Lehr, J. H., & Perrochet, P. et al., 2006). (2006). Groundwater age. *John Wiley & Sons.*

Kesse, G. O. (1985). *The mineral and rock resources of Ghana*. United States: N. p., 1985. Web.

Kharaka, Y. K., & Hanor, J. S. (2003). Deep Fluids in the Continents: I. Sedimentary Basins. In *Treatise on Geochemistry*. https://doi.org/10.1016/B0-08-043751-6/05085-4

Kirschke, S., Häger, A., Kirschke, D., & Völker, J. (2019). Agricultural nitrogen pollution of freshwater in Germany. The governance of sustaining a complex problem. *Water (Switzerland)*. https://doi.org/10.3390/w11122450

Koffi, K. V., Obuobie, E., Banning, A., & Wohnlich, S. (2017). Hydrochemical characteristics of groundwater and surface water for domestic and irrigation purposes in Vea catchment, Northern Ghana. *Environmental Earth Sciences*. https://doi.org/10.1007/s12665-017-6490-3

Kortatsi, B. K. (1994). *Groundwater utilization in Ghana. IAHS Publications-Series of Proceedings and Reports-Intern Assoc Hydrological Sciences, 222, 149-156.*

Kortatsi, B. K., & Jorgensen, N. O. (2001). The origin of high salinity waters in the Accra plains groundwaters. *First International Conference on Saltwater Intrusion and Coastal Aquifers - Monitoring, Modeling and Management. Essaouira, Morroco*.

Kurtzman D., Ganot Y., Russak A., Nitzan, I., Bernstein, A., Katz, Y., Guttman, Y. (2014). *Development of monitoring system, sampling & characterization of the Menashe demonstration site, Israel.*

Kwoyiga, L., & Stefan, C. (2019). Institutional Feasibility of Managed Aquifer Recharge in Northeast Ghana. *Sustainability*, *11*(2), 379. https://doi.org/10.3390/su11020379

Lacher, L. J., Turner, D. S., Gungle, B., Bushman, B. M., & Richter, H. E. (2014). Application of hydrologic tools and monitoring to support managed aquifer recharge decision making in the upper San Pedro River, Arizona, USA. *Water (Switzerland)*. https://doi.org/10.3390/w6113495

Lapworth, D. J., MacDonald, A. M., Tijani, M. N., Darling, W. G., Gooddy, D. C., Bonsor, H. C., & Araguás-Araguás, L. J. (2013). Residence times of shallow groundwater in West Africa: Implications for hydrogeology and resilience to future changes in climate.

Hydrogeology Journal. https://doi.org/10.1007/s10040-012-0925-4

Lautze, J., & Hanjra, M. A. (2014). Water scarcity. In *Key Concepts in Water Resource Management: A Review and Critical Evaluation*. https://doi.org/10.4324/9781315884394-12

Lee, J., Choi, S.-U., & Cho, W. (1999). A comparative study of dual-porosity model and discrete fracture network model. *KSCE Journal of Civil Engineering*. https://doi.org/10.1007/bf02829057

Legg C, and S. S. (2002). *Optimization and use of various recharge techniques for reclaimed wastewater at a sensitive site in Glendale, Arizona: In Management of Aquifer Recharge for Sustainability, Proceedings of the 4th International Symposium on Artificial Recharge of Groundwater*.

Leibundgut, A. C., Maloszewski, P., & Külls, C et al. (2009). *Tracers in hydrology*. Wiley-Blackwell Publishing Ltd.

Liu, C. W., Lin, K. H., & Kuo, Y. M. (2003). Application of factor analysis in the assessment of groundwater quality in a Blackfoot disease area in Taiwan. *Science of the Total Environment*. https://doi.org/10.1016/S0048-9697(02)00683-6

Loh, Y. S. A., Akurugu, B. A., Manu, E., & Aliou, A. S. (2020). Assessment of groundwater quality and the main controls on its hydrochemistry in some Voltaian and basement aquifers, northern Ghana. *Groundwater for Sustainable Development*. https://doi.org/10.1016/j.gsd.2019.100296

Lutz, A., Thomas, J. M., Pohll, G., & McKay, W. A. (2007). Groundwater resource sustainability in the Nabogo Basin of Ghana. *Journal of African Earth Sciences*. https://doi.org/10.1016/j.jafrearsci.2007.06.004

M.G. McDonald, A. W. H. (1998). *A Modular Three-dimensional Finite-difference Ground-water Flow Model*. U.S. Geological Survey Techniques of Water-Resources Investigations, 06eA.

MacDonald, A. M., Bonsor, H. C., Dochartaigh, B. É. Ó., & Taylor, R. G. (2012). Quantitative maps of groundwater resources in Africa. In *Environmental Research Letters*. https://doi.org/10.1088/1748-9326/7/2/024009

Maliva, R. G., & Missimer, T. M. (2010). Aquifer storage and recovery and managed aquifer recharge using wells: Planning, hydrogeology, design, and operation. *Houston, Schlumberger Water Services, Methods in Water Resources Evaluation Series No. 2*.

Maliva R and Missimer T. (2012). *Arid lands water evaluation and management*. Springer

Science & Business Media.

Mallick, J., Singh, C. K., Almesfer, M. K., Singh, V. P., & Alsubih, M. (2021). Groundwater quality studies in the kingdom of Saudi Arabia: Prevalent research and management dimensions. In *Water (Switzerland)*. https://doi.org/10.3390/w13091266

Małoszewski, P., & Zuber, A. (1982). Determining the turnover time of groundwater systems with the aid of environmental tracers. 1. Models and their applicability. *Journal of Hydrology*. https://doi.org/10.1016/0022-1694(82)90147-0

Marandi, A., & Shand, P. (2018). Groundwater chemistry and the Gibbs Diagram. In *Applied Geochemistry*. https://doi.org/10.1016/j.apgeochem.2018.07.009

Mariani, I. (2013). *Water stable isotopes in Alpine ice cores as proxies for temperature and atmospheric circulation.* A PhD dissertations University of Bern, Switzerland.

Marsol. (2014). *Demonstrating managed aquifer recharge as a solution to water scarcity and drought.* http://www.marsol.eu/6-0-Home.html. Accessed 5 July 2019%0A

Martin, N. (2006). Development of a water balance for the Atankwidi catchment, West Africa – A case study of groundwater recharge in a semi-arid climate. *Ecology and Development Series*.

Martin, N., & van de Giesen, N. (2005). Spatial distribution of groundwater production and development potential in the Volta river basin of Ghana and Burkina Faso. *Water International*. https://doi.org/10.1080/02508060508691852

Masule L., N. (2019). *Age dating of groundwater in perched aquifers Okongo Area, Ohangwena Region.* A master's thesis submitted at the University of Namibia.

Meybeck, M. (1987). Global chemical weathering of surficial rocks estimated from river dissolved loads. *American Journal of Science*. https://doi.org/10.2475/ajs.287.5.401

Mook, W. G. (2000). Environmental isotopes in the hydrological cycle: Principles and applications. In *Environmental Isotopes in the Hydrological Cycle - Principles and Applications*.

Mroczek, E. K. (1997). Henry's law constants and distribution coefficients of sulfur hexafluoride in Water from 25 °C to 230 °C. *Journal of Chemical and Engineering Data*. https://doi.org/10.1021/je960194r

Murray, EC and Tredoux G. (1998). *Artificial recharge: A technology for sustainable water resource development. Water Research Commission (WRC) Report no. 842/1/98. Pretoria, South Africa:*

Murray, R. (2017). *Managed aquifer recharge- An introductory guide for the SADC groundwater management institute including the Windhoek case study.*

Mutiso, S. (2002). *The significance of subsurface water storage in Kenya. In Seminar Proceedings, Wageningen, The Netherlands (pp. 18-19).*

NRMMC-EPHC-AHMC, N. (2006). *Australian guidelines for water recycling: managing health and environmental risks (phase 1).*

NRMMC, EPHC, N. (2009). *Natural Resource Management Ministerial Council, Environment Protection, and Heritage Council National Health, and Medical Research Council. "Australian guidelines for water recycling, managing health and environmental risks, volume 2C—Managed aquifer rec*.

Nyenje, P. M., Foppen, J. W., Uhlenbrook, S., Kulabako, R., & Muwanga, A. (2010). Eutrophication and nutrient release in urban areas of sub-Saharan Africa - A review. In *Science of the Total Environment*. https://doi.org/10.1016/j.scitotenv.2009.10.020

Obuobie, E. (2008). Estimation of groundwater recharge in the context of future climate change in the White Volta River Basin, West Africa. *Ecology and Development Series. No. 62*.

Obuobie, E., Diekkrueger, B., Agyekum, W., & Agodzo, S. (2012). Groundwater level monitoring and recharge estimation in the White Volta River basin of Ghana. *Journal of African Earth Sciences*. https://doi.org/10.1016/j.jafrearsci.2012.06.005

Okofo, L. B., Anderson, N. A., Bedu-Addo, K., & Armoo, E. A. (2021). Hydrochemical peculiarities and groundwater quality assessment of the Birimian and Tarkwaian aquifer systems in Bosome Freho District and Bekwai Municipality of the Ashanti Region, Ghana. *Environmental Earth Sciences*, *80*(24), 818. https://doi.org/10.1007/s12665-021-10081-2

Ortuño, F., Molinero, J., Custodio, E., Juárez, I., Garrido, T., & Fraile, J. (2010). *Seawater intrusion barrier in the deltaic Llobregat aquifer (Barcelona, Spain): performance and pilot phase results. In Proceedings of the 21st Salt Water Intrusion Meeting (SWIM21, San Miguel, Azores, Portugal) (pp. 135-138).*

Oster, H., Sonntag, C., & Münnich, K. O. (1996). Groundwater age dating with chlorofluorocarbons. *Water Resources Research*. https://doi.org/10.1029/96WR01775

Oteng Mensah, F., Alo, C., & Yidana, S. M. (2014). Evaluation of groundwater recharge estimates in a partially metamorphosed sedimentary basin in a tropical environment: Application of natural tracers. *The Scientific World Journal*.

https://doi.org/10.1155/2014/419508

Ounvichit, T. (2011). Equal water sharing in scarcity conditions: The case of the Chaisombat Muang Fai Irrigation System in Thailand. *Paddy and Water Environment*. https://doi.org/10.1007/s10333-010-0245-z

Owusu, S., Mul, M. L., Ghansah, B., Osei-Owusu, P. K., Awotwe-Pratt, V., & Kadyampakeni, D. (2017). Assessing land suitability for aquifer storage and recharge in northern Ghana using remote sensing and GIS multi-criteria decision analysis technique. *Modeling Earth Systems and Environment*. https://doi.org/10.1007/s40808-017-0360-6

Parkhust, DL and Appelo, C. (2013). *Description of input and examples for PHREEQC version 3: a computer program for speciation, batch-reaction, one-dimensional transport, and inverse geochemical calculations (No.6-A43).*

Plummer, L Neil, Bexfield, Laura M., Anderholm, Scott K., Sanford, Ward E., Busenberg, E. (2012). Geochemical Characterization of Ground-water Flow in the Santa Fe Group Aquifer System, Middle Rio Grande Basin, New Mexico. *USGS*, *1.2*, 1–414.

Plummer, L. N., Busenberg, E., McConnell, J. B., Drenkard, S., Schlosser, P., & Michel, R. L. (1998). The flow of river water into a Karstic limestone aquifer. 1. Tracing the young fraction in groundwater mixtures in the Upper Floridan Aquifer near Valdosta, Georgia. *Applied Geochemistry*. https://doi.org/10.1016/S0883-2927(98)00031-6

Ponsadailakshmi, S., Sankari, S. G., Prasanna, S. M., & Madhurambal, G. (2018). Evaluation of water quality suitability for drinking using drinking water quality index in Nagapattinam district, Tamil Nadu in Southern India. *Groundwater for Sustainable Development*. https://doi.org/10.1016/j.gsd.2017.10.005

Protonotarios, V., Firfilionis G., Kallioras, A., Pouliaris, C., Foglia, L., Perdikaki, M., Apostolo-poulos, G., V. T. (2016). *MAR to combat seawater intrusion and to apply SAT in alluvial and karstified aquifers, Lavrion, Greece.*

Pyne, R. (1995). *Groundwater recharge and wells: A guide to aquifer storage recovery,* Lewis Publishers, Boca Raton, FL.

Pyne, R. (2005). Aquifer storage recovery, a guide to groundwater recharge through wells. *Gainesville, FL: ASR Systems. (606 Pp).*

Rajmohan, N., & Elango, L. (2004). Identification and evolution of hydrogeochemical processes in the groundwater environment in an area of the Palar and Cheyyar River Basins, Southern India. *Environmental Geology*. https://doi.org/10.1007/s00254-004-1012-5

Ray, C., Melin, G., & Linksy, R. B. (2003). Riverbank Filtration Improving Source-water Quality. In *Environmental Science and Engineering (Subseries: Environmental Science)*.

Ray, S. (2019). *Ground Water Development - Issues and Sustainable Solutions* (S. P. S. Ray (ed.)). Springer Singapore. https://doi.org/10.1007/978-981-13-1771-2

Rees, D. D. (1995). Role of nitric oxide in the vascular dysfunction of septic shock. *Biochemical Society Transactions*. https://doi.org/10.1042/bst0231025

Reilly, T. E., & Harbaugh, A. W. (2004). *Guidelines for evaluating ground-water flow models.* US Department of the Interior, US Geological Survey. Report 2004-5038, 30 p.

Reiter, M. (2001). Using precision temperature logs to estimate horizontal and vertical groundwater flow components. *Water Resources Research*. https://doi.org/10.1029/2000WR900302

Rey, N., Rosa, E., Cloutier, V., & Lefebvre, R. (2018). Using water stable isotopes for tracing surface and groundwater flow systems in the Barlow-Ojibway Clay Belt, Quebec, Canada. *Canadian Water Resources Journal*. https://doi.org/10.1080/07011784.2017.1403960

Reynolds, G. W., Hoff, J. T., & Gillham, R. W. (1990). Sampling Bias Caused by Materials Used To Monitor Halocarbons in Groundwater. *Environmental Science and Technology*. https://doi.org/10.1021/es00071a017

Ringleb, J., Sallwey, J., & Stefan, C. (2016). Assessment of Managed Aquifer Recharge through Modeling—A Review. *Water*, *8*(12), 579. https://doi.org/10.3390/w8120579

Russo, T. A., Fisher, A. T., & Lockwood, B. S. (2015). Assessment of Managed Aquifer Recharge Site Suitability Using a GIS and Modeling. *Groundwater*, *53*(3), 389–400. https://doi.org/10.1111/gwat.12213

Rusydi, A. F. (2018). Correlation between conductivity and total dissolved solids in various types of water: A review. *IOP Conference Series: Earth and Environmental Science*. https://doi.org/10.1088/1755-1315/118/1/012019

Ryter DR, Kunkel CD, Peterson SM, and T. J. (2018). Numerical simulation of groundwater flow, resource optimization, and potential effects of prolonged drought for the Citizen Potawatomi Nation Tribal Jurisdictional Area, central Oklahoma. In *U.S. Geological Survey Scientific Investigations Report 2014–5167, 27 p.,* https://doi.org/https://doi.org/10.3133/sir20145167

Sahu, P., & Sikdar, P. K. (2008). A hydrochemical framework of the aquifer in and around East Kolkata Wetlands, West Bengal, India. *Environmental Geology*.

https://doi.org/10.1007/s00254-007-1034-x

Sahu, S., Gogoi, U., & Nayak, N. C. (2020). Groundwater solute chemistry, hydrogeochemical processes and fluoride contamination in the phreatic aquifer of Odisha, India. *Geoscience Frontiers*. https://doi.org/10.1016/j.gsf.2020.10.001

Sajedi-Hosseini, F., Malekian, A., Choubin, B., Rahmati, O., Cipullo, S., Coulon, F., & Pradhan, B. (2018). A novel machine learning-based approach for the risk assessment of nitrate groundwater contamination. *Science of the Total Environment*. https://doi.org/10.1016/j.scitotenv.2018.07.054

Salifu, A., Petrusevski, B., Ghebremichael, K., Buamah, R., & Amy, G. (2012). Multivariate statistical analysis for fluoride occurrence in groundwater in the Northern region of Ghana. *Journal of Contaminant Hydrology*. https://doi.org/10.1016/j.jconhyd.2012.08.002

Sami, K. (1992). Recharge mechanisms and geochemical processes in a semi-arid sedimentary basin, Eastern Cape, South Africa. *Journal of Hydrology*. https://doi.org/10.1016/0022-1694(92)90193-Y

Saravanakumar, K., & Ranjith Kumar, R. (2011). Analysis of water quality parameters of groundwater near Ambattur industrial area, Tamil Nadu, India. *Indian Journal of Science and Technology*. https://doi.org/10.17485/ijst/2011/v4i5/30071

Scanlon, B. R., Faunt, C. C., Longuevergne, L., Reedy, R. C., Alley, W. M., McGuire, V. L., & McMahon, P. B. (2012). Groundwater depletion and sustainability of irrigation in the US High Plains and Central Valley. *Proceedings of the National Academy of Sciences of the United States of America*. https://doi.org/10.1073/pnas.1200311109

Scanlon, B. R., Healy, R. W., & Cook, P. G. (2002). Choosing appropriate techniques for quantifying groundwater recharge. *Hydrogeology Journal*. https://doi.org/10.1007/s10040-001-0176-2

Schöeller H. (1965). *Geochemistry of groundwater. In groundwater studies–an international guide for research and practice. UNESCO, Chapter 15, Paris, pp 1-18*.

Schüth, C. (2014). *Technical University of Darmstadt Hydrogeology lecture notes*.

Shapiro, A. M. (2002). Cautions and Suggestions for Geochemical Sampling in Fractured Rock. *Groundwater Monitoring & Remediation*, *22*(3), 151–164. https://doi.org/10.1111/j.1745-6592.2002.tb00764.x

Sharma, L., Greskowiak, J., Ray, C., Eckert, P., & Prommer, H. (2012). Elucidating temperature effects on seasonal variations of biogeochemical turnover rates during

riverbank filtration. *Journal of Hydrology*. https://doi.org/10.1016/j.jhydrol.2012.01.028

Simonffy, Z. (2002). Enhancement of groundwater recharge in Hungary – 'Bank infiltration or drinking water supply. Management of aquifer and subsurface storage. *NNC-IAH Publication#4. Utrecht, The Netherlands.*

Skougstad, M. W., & Horr, C. A. (1963). Chemistry of strontium in natural water: Occurrence and distribution of strontium in natural water. *Geological Survey Water-Supply Paper*, *1496-D*, 55–97. https://pubs.er.usgs.gov/publication/wsp1496D

SNC-Lavalin/INRS. (2011). Hydrogeological Assessment Project of the Northern Regions of Ghana (HAP). *Final Technical Report*, *I*(December), 383–403. https://doi.org/10.1016/S1570-8705(03)00040-4

Sprenger, C., Hartog, N., Hernández, M., Vilanova, E., Grützmacher, G., Scheibler, F., & Hannappel, S. (2017). Inventory of managed aquifer recharge sites in Europe: historical development, current situation and perspectives. *Hydrogeology Journal*. https://doi.org/10.1007/s10040-017-1554-8

Srinivasamoorthy, K., Gopinath, M., Chidambaram, S., Vasanthavigar, M., & Sarma, V. S. (2014). Hydrochemical characterization and quality appraisal of groundwater from Pungar sub-basin, Tamilnadu, India. *Journal of King Saud University - Science*. https://doi.org/10.1016/j.jksus.2013.08.001

Stefan, C., & Ansems, N. (2018). Web-based global inventory of managed aquifer recharge applications. *Sustainable Water Resources Management*. https://doi.org/10.1007/s40899-017-0212-6

Steinel, A. (2012). *Guidelines for assessment and implementation of managed aquifer recharge (MAR) in semi-arid regions.*

Stuyfzand, P. J., Nienhuis, P., Anthonio, A., & Zuurbier, K. G. (2013). *Haalbaarheid van ondergrondse berging via A (S/T) R in Hollands kustduinen. in druk.*

Stuyfzand, P. J. (1989). Hydrology and water quality aspects of rhine bank groundwater in The Netherlands. *Journal of Hydrology*. https://doi.org/10.1016/0022-1694(89)90079-6

Suciu, N., Farolfi, C., Zambito Marsala, R., Russo, E., De Crema, M., Peroncini, E., Tomei, F., Antolini, G., Marcaccio, M., Marletto, V., Colla, R., Gallo, A., & Capri, E. (2020). Evaluation of groundwater contamination sources by plant protection products in hilly vineyards of Northern Italy. *Science of the Total Environment*. https://doi.org/10.1016/j.scitotenv.2020.141495

Sunkari, E. D., & Abu, M. (2019). Hydrochemistry with special reference to fluoride

contamination in groundwater of the Bongo District, Upper East Region, Ghana. *Sustainable Water Resources Management*. https://doi.org/10.1007/s40899-019-00335-0

Suthar, S., Bishnoi, P., Singh, S., Mutiyar, P. K., Nema, A. K., & Patil, N. S. (2009). Nitrate contamination in groundwater of some rural areas of Rajasthan, India. *Journal of Hazardous Materials*. https://doi.org/10.1016/j.jhazmat.2009.05.111

Thompson, G. M., Hayes, J. M., & Davis, S. N. (1974). Fluorocarbon tracers in hydrology. *Geophysical Research Letters*, *1*(4), 177–180. https://doi.org/10.1029/GL001i004p00177

Tindimugaya, C. (2008). *Groundwater flow and storage in weathered crystalline rock aquifer systems of Uganda: evidence from environmental tracers and aquifer responses to hydraulic stress.* The University of London.

Toews, M. W., Daughney, C. J., Cornaton, F. J., Morgenstern, U., Evison, R. D., Jackson, B. M., Petrus, K., & Mzila, D. (2016). Numerical simulation of transient groundwater age distributions assisting land and water management in the Middle Wairarapa Valley, New Zealand. *Water Resources Research*. https://doi.org/10.1002/2016WR019422

Tóth, J. (1963). A theoretical analysis of groundwater flow in small drainage basins. *Journal of Geophysical Research*, *68*(16), 4795–4812. https://doi.org/10.1029/JZ068i016p04795

Tran, T. Q., Banning, A., Wisotzky, F., & Wohnlich, S. (2020). Mine water hydrogeochemistry of abandoned coal mines in the outcropped Carboniferous formations, Ruhr Area, Germany. *Environmental Earth Sciences*. https://doi.org/10.1007/s12665-020-8821-z

Tredoux, G., Cavé, L. C., & Bishop, R. (2020). Long-term stormwater and wastewater infiltration into a sandy aquifer, South Africa. In *Management of Aquifer Recharge for Sustainability*. https://doi.org/10.1201/9781003078838-8

Tutmez, B., Hatipoglu, Z., & Kaymak, U. (2006). Modelling electrical conductivity of groundwater using an adaptive neuro-fuzzy inference system. *Computers and Geosciences*. https://doi.org/10.1016/j.cageo.2005.07.003

Tyagi, S., Sharma, B., Singh, P., & Dobhal, R. (2017). Water quality assessment in terms of Water Quality Index. *International Research Journal of Engineering and Technology(IRJET)*.

UN. (2015). The Human Right to Water and Sanitation Media brief. *UN-Water Decade Programme on Advocacy and Communication and Water Supply and Sanitation Collaborative Council*.

Van Haveren, B. P. (2004). Dependable water supplies from valley alluvium in arid regions. *Environmental Monitoring and Assessment*. https://doi.org/10.1007/s10661-004-4031-5

Vogel, J. C., Talma, A. S., & Heaton, T. H. E. (1981). Gaseous nitrogen as evidence for denitrification in groundwater. *Journal of Hydrology*. https://doi.org/10.1016/0022-1694(81)90069-X

Warner, M. J., & Weiss, R. F. (1985). Solubilities of chlorofluorocarbons 11 and 12 in water and seawater. *Deep-Sea Research Part A. Oceanographic Research Papers*, *32*(12), 1485–1497. https://doi.org/10.1016/0198-0149(85)90099-8

WHO. (2012). *(World Health Organization) UNICEF Millennium development goal drinking water target met p 58. Retrieved from the internet*.

WHO. (2017). *(World Health Organization) (2017) Guidelines for drinking-water quality: The fourth edition incorporating the first addendum 978-92-4-154995-0.*

Wick, K., Heumesser, C., & Schmid, E. (2012). Groundwater nitrate contamination: Factors and indicators. *Journal of Environmental Management*. https://doi.org/10.1016/j.jenvman.2012.06.030

Wilcox, L. V. (1955). *Classification and use of irrigation water (Circular 969). Washington, DC, USA.*

Wilson, G. B., & McNeill, G. W. (1997). Noble gas recharge temperatures and the excess air component. *Applied Geochemistry*, *12*(6), 747–762. https://doi.org/10.1016/S0883-2927(97)00035-8

Wilson, R. D., & Mackay, D. M. (1996). SF6 as a conservative tracer in saturated media with high intragranular porosity or high organic carbon content. *Ground Water*. https://doi.org/10.1111/j.1745-6584.1996.tb01884.x

World Health Organization. (2018). Who Water, Sanitation and Hygiene Strategy 2018-2025. *Who*.

WRC. (2008). *Water Resource Commission (WRC) Integrated Water Resource Management Plan (IWRMP). White Volta River Basin*. Water Resource Commission Document Ghana.

Wu, X., Zheng, Y., Zhang, J., Wu, B., Wang, S., Tian, Y., Li, J., & Meng, X. (2017). Investigating Hydrochemical Groundwater Processes in an Inland Agricultural Area with Limited Data: A Clustering Approach. *Water*. https://doi.org/10.3390/w9090723

Xanke, J., Ender, A., Grimmeisen, F., Goeppert, N., & Goldscheider, N. (2020).

Hydrochemical evaluation of water resources and human impacts on an urban karst system, Jordan. *Hydrogeology Journal*, *Lerner 2002*. https://doi.org/10.1007/s10040-020-02174-2

Yidana, S. M., Alo, C., Addai, M. O., Fynn, O. F., & Essel, S. K. (2015). Numerical analysis of groundwater flow and potential in parts of a crystalline aquifer system in Northern Ghana. *International Journal of Environmental Science and Technology*. https://doi.org/10.1007/s13762-015-0805-2

Yidana, Sandow Mark, Addai, M. O., Asiedu, D. K., & Banoeng-Yakubo, B. (2016). Stochastic groundwater modelling of a sedimentary aquifer: evaluation of the impacts of abstraction scenarios under conditions of reduced recharge. *Arabian Journal of Geosciences*. https://doi.org/10.1007/s12517-016-2718-x

Yidana, Sandow Mark, Banoeng-Yakubo, B., & Akabzaa, T. M. (2010). Analysis of groundwater quality using multivariate and spatial analyses in the Keta basin, Ghana. *Journal of African Earth Sciences*. https://doi.org/10.1016/j.jafrearsci.2010.03.003

Yidana, Sandow Mark, Banoeng-Yakubo, B., Aliou, A.-S., & Akabzaa, T. M. (2012). Groundwater quality in some Voltaian and Birimian aquifers in northern Ghana—application of multivariate statistical methods and geographic information systems. *Hydrological Sciences Journal*. https://doi.org/10.1080/02626667.2012.693612

Yidana, Sandow Mark, Bawoyobie, P., Sakyi, P., & Fynn, O. F. (2018). Evolutionary analysis of groundwater flow: Application of multivariate statistical analysis to hydrochemical data in the Densu Basin, Ghana. *Journal of African Earth Sciences*. https://doi.org/10.1016/j.jafrearsci.2017.10.026

Yidana, Sandow Mark, Ophori, D., Banoeng-Yakubo, B., & Samed, A. A. (2012). A factor model to explain the hydrochemistry and causes of fluoride enrichment in groundwater from the middle voltaian sedimentary aquifers in the Northern Region, Ghana. *ARPN Journal of Engineering and Applied Sciences*, *7*(1), 50–68.

Zaidi, F. K., Nazzal, Y., Jafri, M. K., Naeem, M., & Ahmed, I. (2015). Reverse ion exchange as a major process controlling the groundwater chemistry in an arid environment: a case study from northwestern Saudi Arabia. *Environmental Monitoring and Assessment*. https://doi.org/10.1007/s10661-015-4828-4

Zakaria, N., Anornu, G., Adomako, D., Owusu-Nimo, F., & Gibrilla, A. (2020). Evolution of groundwater hydrogeochemistry and assessment of groundwater quality in the Anayari catchment. *Groundwater for Sustainable Development*. https://doi.org/10.1016/j.gsd.2020.100489

Zango, M. S., Pelig-Ba, K. B., Anim-Gyampo, M., Gibrilla, A., & Sunkari, E. D. (2021). Hydrogeochemical and isotopic controls on the source of fluoride in groundwater within the Vea catchment, northeastern Ghana. *Groundwater for Sustainable Development*. https://doi.org/10.1016/j.gsd.2020.100526

Zango, M. S., Sunkari, E. D., Abu, M., & Lermi, A. (2019). Hydrogeochemical controls and human health risk assessment of groundwater fluoride and boron in the semi-arid North East region of Ghana. *Journal of Geochemical Exploration*. https://doi.org/10.1016/j.gexplo.2019.106363

Zhu, G. F., Li, Z. Z., Su, Y. H., Ma, J. Z., & Zhang, Y. Y. (2007). Hydrogeochemical and isotope evidence of groundwater evolution and recharge in Minqin Basin, Northwest China. *Journal of Hydrology*, *333*(2–4), 239–251. https://doi.org/10.1016/j.jhydrol.2006.08.013

Zuber, A., Witczak, S., Rózański, K., Śliwka, I., Opoka, M., Mochalski, P., Kuc, T., Karlikowska, J., Kania, J., Jackowicz-Korczyński, M., & Duliński, M. (2005). Groundwater dating with 3H and SF6 in relation to mixing patterns, transport modelling and hydrochemistry. *Hydrological Processes*. https://doi.org/10.1002/hyp.5669

Supplementary Material - Chapter 4

Table S1 physical and chemical parameters of the groundwater

Communities	Eastings	Northing	Elev	PH	Temp (°C)	EC (µs)	Alkalinity (mg/l)	Oxygen (mg/l)	Ca (mg/l)	Mg (mg/l)	Na mg/L	K mg/L
Garu Zongo	808746	1201053	263	6,250	31,6	348	160	0,47	34,014	13,025	20,228	0,909
Garu Zongo	808875	1200907	257	6,555	31,5	502	175	0,48	34,909	12,235	48,603	3,653
Garu Market	808451	1201182	239	6.566	31,4	154,1	149	0,57	4,311	1,548	4,057	0,397
Garu Central	807185	1205607	208	6,712	32,9	88,7	74	0,60	16,017	7,096	10,829	0,761
Napadi Yapala	806276	1206513	197	7,704	32,7	243	160	0,41	19,511	13,809	14,236	1,518
Pialugu Tandago	805279	1195367	221	7,508	31,4	256	182	0,49	19,02	8,779	15,09	1,608
Sigure Yapala	802781	1196108	230	7,42	32,2	229	162	0,55	13,012	4,353	14,819	0,999
Dusbuliga	802925	1190913	237	7,22	31,5	172,5	129	0,60	23,462	11,801	14,521	3,135
Senebaga Kpat	801737	1188297	215	6,934	31,4	262	162	0,43	17,829	5,635	15,178	1,388
Kogri	796280	1193112	232	6,54	32,1	212	199	0,61	5,936	6,342	13,401	1,884
Kogri 2	800847	1196178	225	6,419	31,1	137,2	92	0,50	14,781	7,428	16,291	1,362
Barboaka	810352	1200600	251	6,53	31,5	205	178	0,43	19,008	8,684	17,099	1,949
Busnatiga	8012363	1204210	207	7,117	31,8	244	144	0,48	12,584	3,928	14,528	2,215
Yabrago No.1	815266	1202988	233	6,911	31,7	157	180	0,83	13,22	4,675	9,649	1,213
Tindane Prim.	816918	1201899	237	7,69	32,4	346	178	0,60	21,72	12,134	13,573	1,824
Duadinyediga	817660	12106420	217	7,074	32,5	240	164	0,41	61,792	29,328	44,43	5,522
Kugashegu	817109	1208120	227	7,762	32,3	307	124	0,56	16,471	8,714	15,073	0,807
Pwalugu Nating	817773	1209573	233	7,531	32,5	221	142	0,59	12,132	7,278	12,451	1,472
Baatiyok	815320	1209149	222	7,124	32,1	169,8	121	0,52	11,799	7,113	12,271	1,521
Abapusug	816275	1211889	241	7,386	32,2	206	118	0,52	14,524	8,303	13,762	1,8
Bugri Dam View	814008	1214380	217	7,085	32,2	247	155	0,48	22,345	11,192	15,561	1,535
Zumandiga	813706	1215602	219	7,714	32,7	291	153	0,47	26,439	11,237	15,928	2,797
Bugri Central	812583	1215155	212	7,211	32	233	135	0,54	15,853	8,617	20,5	1,224
Sakparatinga	815060	1215407	230	6,992	32,1	283	165	0,45	25,498	12,274	14,929	2,134
Baranatinga	818511	1215991	230	7,231	32,8	356	206	0,42	46,07	22,054	47,173	2,935
Karateshie- Nat	819533	1213231	252	6,922	31,5	239	95	0,55	11,521	5,369	12,767	0,326
Winatinga	820385	1215102	245	7,205	32	295	157	0,56	22,742	9,612	22,894	1,013
Yaranatinga	821431	1215582	254	7,05	31,1	593	366	0,40	28,362	6,787	32,691	6,102
Garu D.A Prim	808668	1200740	223	6,401	31,6	167	155	0,56	19,095	13,309	12,779	0,909
Garu Clinic	808487	1200819	229	6,71	31,2	85,5	126	0,86	8,507	5,539	9,514	0,607
Garu CBR/Urban	807989	1200737	231	6,411	31,7	171,5	210	0,64	13,862	7,27	8,601	0,236
Garu Belatek	807646	1201571	228	7,135	31,9	240	141	0,61	10,153	6,365	5,706	0,163
Garu Medina	808249	1201613	229	7,155	31,7	278	190	0,49	26,006	15,578	15,681	2,266
Holy Eng J.H.S	808608	1201996	226	7,092	32,1	373	169	1,0	45,922	30,482	34,029	2,793
Tanzugu	808782	1200400	239	7,326	32,3	455	124	0,96	31,847	12,875	31,691	3,483
Zumadori	808535	1199528	234	7,925	31,6	125,3	112	0,63	4,631	1,182	10,352	1,744
Nisbuligu	809375	1196172	246	7,409	31,6	250	135	0,52	10,041	3,221	13,174	0,568
Zaari	810567	1195197	262	7,16	31,6	112,2	91	0,68	17,143	9,138	8,689	0,048

Communities	SO4	Cl	F	NO2	Br	NO3	PO4	Li	NH4	Sr	CU
	mg/L	mg/L	mg/L	mg/L	mg/L	mg/L	mg/L	mg/L	mg/L	mg/L	mg/L
Garu Zongo	7,175	42,216	0,575	0,016	0,689	77,888		0,049		0,393	0,037
Garu Zongo	8,159	17,146	1,435		2,014	68,362	4,146	0,06	0,105	0,668	0,038
Garu Market	0,493	0,516	0,227		0,448	2,58	0,843		0,033	0,151	0,038
Garu Central	1,375	0,546	0,53	0,006	0,805	3,866	1,083	0,016		0,3	0,038
Napadi Yapala	1,489	2,055	0,569	0,012	0,933	2,133	0,382	0,024		0,12	0,038
Pialugu Tandago	1,399	1,327	0,415		0,869	11,278	0,505	0,017		0,271	0,043
Sigure Yapala	0,909	5,743	0,504		0,392	21,77	1,597	0,022	0,073	0,193	0,041
Dusbuliga	0,526	0,541	0,455	0,003	1,018	0,591	0,299	0,036	0,035	0,215	0,041
Senebaga Kpatua	2,397	10,127	0,267	0,015	0,6	35,443	0,443	0,021		0,39	0,046
Kogri	0,995	0,97	0,33	0,025	0,722	0,518		0,021	0,122	0,073	0,041
Kogri 2	1,216	1,974	0,608	0,019	0,752	10,45	0,951	0,017	0,047	0,35	0,065
Barboaka	3,427	4,179	0,989	0,008	0,616	29,964		0,015	0,033	0,322	0,041
Busnatiga	0,69	0,908	0,383	0,009	0,748	5,897	0,748	0,022	0,055	0,243	0,054
Yabrago No.1	2,711	1,002	0,397	0,029	0,486	1,629		0,015	0,039	0,202	0,054
Tindane Prim Sch	4,681	3,189	0,579		1,147	0,08	0,674	0,035		0,343	0,047
Duadinyediga	18,991	24,577	1,279	0,284	1,461	147,633	0,94	0,068	0,146	0,89	0,046
Kugashegu	2,989	8,898	0,727	0,007	0,625	32,146	0,609	0,032	0,037	0,167	0,038
Pwalugu Natinga	1,147	2,954	0,434		0,674	12,408	1,367	0,022	0,027	0,197	0,043
Baatiyok	1,269	2,912	0,438		0,66	12,124	1,338	0,021	0,024	0,188	0,046
Abapusug	1,283	4,456	0,76		0,728	15,225	0,443	0,022		0,157	0,049
Bugri Dam View	0,754	0,342	0,488	0,006	0,988	0,729	0,325	0,024		0,268	0,048
Zumandiga	2,824	2,976	0,541	0,011	0,491	22,672	0,299	0,024		0,13	0,040
Bugri Central	1,452	8,295	0,391	0,02	0,705	30,333	0,608	0,022		0,265	0,035
Sakparatinga	2,211	8,156	0,424		0,787	26,543		0,026	0,027	0,166	0,039
Baranatinga	10,365	16,945	1,461	0,096	1,809	85,751		0,056	0,076	0,503	0,045
Karateshie- Natin	1,839	0,892	0,347	0,006	0,493	1,845	0,224	0,013		0,146	0,043
Winatinga	2,037	2,804	0,729	0,047	0,793	18,236		0,018	0,042	0,032	0,042
Yaranatinga	1,387	2,363	0,845	0,018	1,937	17,208	1,143	0,069	0,186	0,515	0,036
Garu D.A Prim Sch	1,599	3,452	0,447	0,008	0,853	8,695	0,25	0,023	0,081	0,108	0,039
Garu Clinic	0,691	0,496	0,436	0,01	0,651	0,95	1,038	0,021			0,044
Garu CBR/Urban	4,724	15,66	0,228	0,007	0,327	31,838	0,226			0,266	0,040
Garu Belatek	3,879	12,884	0,202	0,027	0,309	26,58		0,016		0,079	0,040
Garu Medina	1,776	2,802	0,534		1,117	0	0,292	0,029	0,031	0,103	0,035
Holy Eng J.H.S	1,661	2,356	1,614	0,067	2,538	4,457	0,557	0,062		0,142	0,039
Tanzugu	3,353	13,988	0,855	0,026	1,596	44,033	1,488	0,091		0,59	0,040
Zumadori	0,907	1,52	0,39	0,009	0,511	10,281	1,018	0,014			0,036
Nisbuligu	0,778	0,818	0,454	0,015	0,684	0	1,506	0,021		0,153	0,045
Zaari	1,759	3,835	0,189	0,007	0,54	6,467		0,015		0,346	0,049

Communities	Ni	Mn	Pb	Fe	Cr
	mg/L	mg/L	mg/L	mg/L	mg/L
Garu Zongo	0,030	0,011	0,652	0,090	0,019
Garu Zongo	0,001	0,049	0,198	0,051	0,023
Garu Market	0,021	0,010	0,537	0,051	0,023
Garu Central	0,068	0,012	0,487	0,474	0,025
Napadi Yapala	0,026	0,032	0,512	0,101	0,025
Pialugu Tandago	0,022	0,052	0,118	0,005	0,025
Sigure Yapala	0,079	0,004	0,392	0,323	0,024
Dusbuliga	0,026	0,007	0,424	0,049	0,026
Senebaga Kpatua	0,007	0,096	0,575	0,036	0,027
Kogri	0,015	0,009	0,425	0,016	0,035
Kogri 2	0,037	0,004	0,215	0,045	0,041
Barboaka	0,037	0,013	0,155	0,025	0,039
Busnatiga	0,034	0,003	0,699	0,152	0,041
Yabrago No.1	0,058	0,002	0,738	0,286	0,036
Tindane Prim. Sch	0,043	0,035	0,795	2,952	0,030
Duadinyediga	0,044	0,012	0,333	0,016	0,029
Kugashegu	0,050	0,025	0,674	0,010	0,029
Pwalugu Natinga	0,037	0,008	0,695	0,072	0,027
Baatiyok	0,018	0,008	0,447	0,046	0,037
Abapusug	0,036	0,009	0,390	0,029	0,032
Bugri Dam View	0,026	0,014	0,471	0,059	0,025
Zumandiga	0,038	0,012	0,376	0,489	0,027
Bugri Central	0,021	0,008	0,401	0,054	0,028
Sakparatinga	0,001	0,044	0,751	0,060	0,026
Baranatinga	0,033	0,036	0,383	0,071	0,024
Karateshie- Natin	0,013	0,004	0,370	0,036	0,031
Winatinga	0,007	0,018	0,424	0,057	0,026
Yaranatinga	0,004	0,000	0,512	0,120	0,035
Garu D.A Prim Sch	0,003	0,014	0,246	0,076	0,041
Garu Clinic	0,034	0,076	0,285	0,173	0,037
Garu CBR/Urban	0,051	0,018	0,392	0,284	0,053
Garu Belatek	-0,001	0,016	0,666	0,126	0,039
Garu Medina	0,012	0,013	0,493	0,083	0,040
Holy Eng J.H.S	0,031	0,010	0,264	0,848	0,041
Tanzugu	0,013	0,022	0,145	0,142	0,043
Zumadori	0,013	0,019	0,752	0,156	0,044
Nisbuligu	0,027	0,101	0,338	0,010	0,036
Zaari	0,018	0,018	0,568	0,058	0,034

Table 2 Saturation indices of the groundwater

No of samples	si_calcite	si_halite	si_gypsum	si_anhydrite	si_fluorite	si_goethite	si_dolomite	si_aragonite
1	-1,573	-7,622	-3	-3,133	-2,294	-0,68	-2,14	-1,718
2	-1,095	-7,636	-2,949	-3,082	-1,502	-0,09	-1,223	-1,24
3	-1,437	-10,204	-4,901	-5,034	-3,911	1,248	-1,899	-1,582
4	-1,534	-9,758	-3,931	-4,064	-2,619	1,505	-2,002	-1,679
5	-0,041	-9,079	-3,895	-4,028	-2,529	3,545	1,192	-0,186
6	-0,196	-9,243	-3,915	-4,048	-2,807	1,654	0,695	-0,342
7	-0,49	-8,609	-4,229	-4,362	-2,784	3,23	-0,034	-0,635
8	-0,557	-9,647	-4,249	-4,382	-2,627	1,89	0,01	-0,702
9	-0,901	-8,355	-3,684	-3,818	-3,204	0,876	-0,88	-1,046
10	-1,77	-9,418	-4,501	-4,634	-3,47	-0,642	-2,09	-1,915
11	-1,874	-9,024	-4,024	-4,157	-2,538	-0,394	-2,628	-2,02
12	-1,348	-8,688	-3,511	-3,644	-2,04	-0,454	-1,616	-1,493
13	-0,874	-9,414	-4,341	-4,474	-3,019	2,059	-0,832	-1,019
14	-1,002	-9,55	-3,733	-3,867	-2,972	1,689	-1,035	-1,147
15	0,028	-8,911	-3,356	-3,489	-2,473	4,945	1,226	-0,118
16	-0,279	-7,537	-2,446	-2,58	-1,418	0,899	0,543	-0,425
17	-0,155	-8,414	-3,635	-3,768	-2,374	2,779	0,838	-0,3
18	-0,458	-8,972	-4,161	-4,294	-2,942	2,933	0,285	-0,603
19	-0,969	-8,982	-4,114	-4,247	-2,933	1,598	-0,738	-1,115
20	-0,61	-8,75	-4,036	-4,17	-2,375	2,159	-0,042	-0,756
21	-0,651	-9,817	-4,114	-4,247	-2,59	1,533	-0,181	-0,796
22	0,092	-8,874	-3,491	-3,614	-2,452	4,318	1,241	-0,054
23	-0,699	-8,313	-3,961	-4,085	-2,932	1,937	-0,236	-0,844
24	-0,67	-8,464	-3,609	-3,733	-2,675	1,299	-0,23	-0,815
25	-0,101	-7,667	-2,793	-2,916	-1,413	1,996	0,907	-0,247
26	-1,289	-9,475	-3,934	-4,058	-3,133	1,007	-1,486	-1,434
27	-0,495	-8,74	-3,679	-3,803	-2,247	1,907	0,063	-0,64
28	-0,246	-8,673	-3,802	-3,925	-2,068	1,547	0,316	-0,391
29	-1,565	-8,897	-3,844	-3,968	-2,73	-0,259	-1,862	-1,711
30	-1,559	-9,856	-4,486	-4,61	-3,065	1,024	-1,88	-1,704
31	-1,56	-8,412	-3,491	-3,614	-3,451	0,28	-1,975	-1,705
32	-0,947	-8,672	-3,695	-3,819	-3,682	2,083	-0,671	-1,092
33	-0,42	-8,909	-3,714	-3,837	-2,476	1,88	0,365	-0,565
34	-0,328	-8,661	-3,587	-3,71	-1,314	2,724	0,594	-0,474
35	-0,336	-7,907	-3,357	-3,48	-1,984	2,702	0,363	-0,481
36	-0,531	-9,331	-4,615	-4,739	-3,426	4,495	-0,226	-0,676
37	-0,66	-9,501	-4,374	-4,497	-2,971	1,781	-0,387	-0,805
38	-0,875	-9,014	-3,818	-3,942	-3,507	1,906	-0,597	-1,02

Supplementary Material - Chapter 5

Table S3 Constants for calculations of K_H for CFC-11, CFC-12, CFC-13 and SF6

K_H in $mol.L^{-1.}$ $(1013.25\ hPa)^{-1}$

Mol.L^{-1}	a_1	a_2	a_3	b_1	b_2	b_3
CFC-11	-134,1536	203,2156	56,232	-0,144449	0,092952	-0,0159977
CFC-12	-122,3246	182,5306	50,5898	-0,145633	0,092509	-0,0156627
CFC-13	-134,243	203,898	54,9583	-0,02632	0,005874	-
SF6	-96,5975	139,883	37,8193	0,0310693	0,0356385	0,00743254

K_H concentrations for temperatures ranging between 273.3.3 - 313K and salinities of 0-40‰

$$\ln K_H = a1 + a2\left(\frac{100}{T}\right) + a3 \ln\left(\frac{T}{100}\right) + S\left[b1 + b2\left(\frac{T}{100}\right) + b3\left(\frac{T}{100}\right)^{2)}\right] \quad \text{S1}$$

Total Pressure (P) $\ln P = \frac{\_H}{8300}$ H is the recharge elevation S2

The vapour pressure of water (PH_2O)

$$PH_2O = \ln PH_2O = 24{,}4543 - 67{,}4509\frac{(100)}{T} - 4{,}8489 \ln\left(\frac{T}{100}\right) - 0{,}000544S \quad \text{S3}$$

Supplementary Material - Chapter 6

Table S4 Groundwater modelling data

Community	Eastings	Northings	Elev	SWL	Head	Drilled Depth (m)	Constructed Depth	Discharge (l/min)	Discharge (M3/day)	DWL (m)	Drawdown (m)	Top Elev	Bottom Elev
Bugri Dam View	814010	1214379	217	5,62	211,38	60	60	80	115,2	26,13	20,51	115,7	99,2
Kogri	813666	1211384	232	8,77	223,23	60	60	50	72	25,42	16,65	203	175
Baatiyok	815299,98	1209141,91	222	6,04	215,96	55	55	330	475,2	14,97	8,93	176	168
Sakparatinga	815061,34	1215405,88	230	5,88	224,12	60	60	35	50,4	28,14	22,26	130	99,2
Bugri Central	812580,64	1215151,53	212	4,92	207,08	60	60	70	100,8	23,7	18,78	133	129
Asaadabog	813782,01	1195910,62	230	3,42	226,58	46	46	200	288	28,62	25,2	191	179
Nisbuliga	809370,52	1196173,89	246	10,73	235,27	50	50	180	259,2	29,51	18,78	131	71,2
Kolburi Natinga	817768,58	1209569,68	235	5,64	229,36	46	46	90	129,6	21,43	15,79	124	90,2
Kolbore	816272,94	1211887,65	232	4,95	227,05	60	60	50	72	31,44	26,49	108,7	90,2
Kugashegu	817109,59	1208122,23	228	5,63	222,37	55	55	25	36	46,79	41,16	91,7	90,2
Senebaga	801740,22	1188294,32	215	3,8	211,2	60	60	30	43,2	29,33	25,53	185	161
Dusbuliga	802820,08	1190947,88	237	12,02	224,98	70	70	20	28,8	35,8	23,78	127,5	124,4
Duadinyediga	817656,64	1206416,97	217	6,07	210,93	60	60	20	28,8	38,49	32,42	151	147
Tindaanin	816953,84	1201334,08	237	1,58	235,42	80	80	10	14,4	57,1	55,52	134,2	131,2
Yabrago No.1	815265,58	1202987,91	233	11,13	221,87	60	60	80	115,2	27,51	16,38	170	167
Tambalugu	822499,17	1196023,19	215	4,21	210,79	55	55	60	86,4	26,51	22,3	203	191

Nabdug/ Sigure	819346,21	1193787,84	212	11,62	200,38	60	60	60	86,4	38,41	26,79	194	192
Napadi Yapala	806274,55	1206514,48	197	10,28	186,72	65	65	25	36	25,18	14,9	158	146,2
Kpalsako Chapini	825296,05	1208860,58	232	7,57	224,43	60	60	80	115,2	40,39	32,82	152	94
Kugrago/Zaari	810565,44	1194199,66	262	9,85	252,15	65	65	20	28,8	37,88	28,03	135,2	134,1
Sigure Yapala	802780,7	1196106,1	230	14,34	215,66	60	60	60	86,4	38,5	24,16	227	207
Pialugu Tandago	805273,65	1195366,81	221	4,6	216,4	60	60	60	86,4	30,39	25,79	130	123,9
Vambara	797777,86	1188262,67	208	5,4	202,6	70	70	20	28,8	44,99	39,59	192	144
Zumandiga	813704,89	1215599,55	214	2,61	211,39	70	70	70	100,8	37,27	34,66	131	107,5
Asaanda Kudug	818512,48	1215986,91	246	3,04	242,96	70	70	54	77,76	28,04	25	154	152,5
Baranatinga	811918,81	1210344,19	230	9,85	220,15	65	65	20	28,8	46,66	36,81	139	111,2
Barboaka	810369,05	1200600,33	251	1,63	249,37	60	60	50	72	24,12	22,49	133	131,5
Busnatinga	812361,48	1204209,61	207	5,71	201,29	65	65	25	36	43,76	50	152	149
Winatinga	820386,24	1215103,1	245	3,97	241,03	60	60	50	72	31,13	53	233	160
Bimpella No. 1	825451,59	1206954,03	243	14,17	228,83	60	60	250	360	19,41	53	151,1	129,6

Table S5 Kabingo monitoring well data

Time	water level (cm)	water level (m)	Elev	Hydraulic head	Simulated head
01.11.09	641,43	6,41	205	198,6	198,2
01.12.09	607,91	6,08	205	198,9	198,8
01.01.10	559,79	5,60	205	199,4	198,8
01.02.10	517,42	5,17	205	199,8	199,6
01.03.10	497,49	4,97	205	200,0	199,5
01.04.10	441,48	4,41	205	200,6	199,9
01.05.10	403,90	4,04	205	201,0	201,0
01.06.10	414,21	4,14	205	200,9	200,9
01.07.10	465,12	4,65	205	200,3	201,3
01.08.10	597,96	5,98	205	199,0	199,0
01.09.10	710,63	7,11	205	197,9	198,9
01.10.10	713,68	7,14	205	197,9	198,9
01.11.10	654,15	6,54	205	198,5	197,6
01.12.10	596,80	5,97	205	199,0	198,0
01.01.11	546,78	5,47	205	199,5	198,5
01.02.11	502,58	5,03	205	200,0	199,0
01.03.11	482,64	4,83	205	200,2	199,2
01.04.11	436,20	4,36	205	200,6	200,6
01.05.11	423,96	4,24	205	200,8	200,8
01.06.11	404,80	4,05	205	201,0	201,3
01.07.11	393,73	3,94	205	201,1	201,8
01.08.11	433,38	4,33	205	200,7	200,7
01.09.11	532,29	5,32	205	199,7	197,9
01.10.11	589,57	5,90	205	199,1	198,1
01.11.11	548,81	5,49	205	199,5	198,5
01.12.11	502,90	5,03	205	200,0	201,0
01.01.12	453,16	4,53	205	200,5	201,2
01.02.12	408,88	4,09	205	200,9	200,9
01.03.12	389,19	3,89	205	201,1	201,1
01.04.12	376,53	3,77	205	201,2	201,6